Loughborough University

This item was submitted to Loughborough University as a PhD thesis by the author and is made available in the Institutional Repository (https://dspace.lboro.ac.uk/) under the following Creative Commons Licence conditions.

creative commons

COMMONS DEED

Attribution-NonCommercial-NoDerivs 2.5

You are free:

- to copy, distribute, display, and perform the work

Under the following conditions:

Attribution. You must attribute the work in the manner specified by the author or licensor.

Noncommercial. You may not use this work for commercial purposes.

No Derivative Works. You may not alter, transform, or build upon this work.

- For any reuse or distribution, you must make clear to others the license terms of this work.
- Any of these conditions can be waived if you get permission from the copyright holder.

Your fair use and other rights are in no way affected by the above.

This is a human-readable summary of the Legal Code (the full license).

Disclaimer

For the full text of this licence, please go to:
http://creativecommons.org/licenses/by-nc-nd/2.5/

Loughborough University

University Library

Author/Filing Title ....DIXON, P.....

....

Class Mark ....

Please note that fines are charged on ALL overdue items.

0403110246

The Influence of the Sideslip Target on the Performance of Vehicles with Actively Controlled Handling

by

Philip John Dixon

A Doctoral Thesis

Submitted in partial fulfilment of the requirements
for the award of
Doctor of Philosophy of Loughborough University
on the 31st March 2004

Copyright Phil Dixon 2004

Acknowledgments

It is simply impossible for me to thank everyone who has helped me to finally complete the writing of this thesis.

However, I must acknowledge those who have encouraged and inspired me the most throughout the process. Without that encouragement, the process can at times be both daunting and depressing, and it is undoubtedly the continuing support of family, friends and colleagues that drove me to finish.

My parents David and Judith and my sister Ruth of course encouraged me throughout, despite never really understanding what on earth it was that I was actually doing, nor how it could possibly be taking so long.

My wife Gia has contributed in countless ways, and reciprocally, I have my time at Loughborough to thank for having met her. I also made some of best friends of my life whilst studying at Loughborough. Particular mention must go to Matt, Terry, Graham and Keith for their unfloundering encouragement.

Last but not least, my supervisors Tim Gordon and Matt Best continued to provide strong direction to the very end, despite my resistance to it. And to Björn Petersson, I thank you for driving me onto a less trodden path.

Thank you all.

Abstract

The influence of sideslip on the handling capability of a four wheeled vehicle is investigated. Both nonlinear, steady-state and linear, transient analyses are conducted on simple models in order to understand how the geometric and inertial effects of sideslip control influence the maneuvering capability of the vehicle.

Nonlinear performance analyses confirm the findings of the literature, that constant sideslip angle at the centre of mass is required if it is desired to maintain consistent vehicle 'balance' with increasing lateral acceleration, and the reason for this is explained using simple mathematics.

Analyses of energy flow between the power source and the various sinks of the vehicle show that for a typical modern vehicle, the power dissipated in a steady turn near the limiting lateral acceleration is approximately comparable in magnitude to that dissipated by aerodynamic drag near the maximum speed of the vehicle. Additionally, it shown that whenever brake control, rather than steering control, is employed to generate a yawing moment, the component of dissipated energy associated with this yaw demand is larger by at least an order of magnitude. It is concluded that whenever the required dynamic behaviour can be delivered by means of steering alone pure steering control should be preferred over the use of direct yaw control. This suggests that direct yaw control should only be used when the limit of the envelope of the steered vehicle has been reached.

Transient analyses of sudden turn-in events are then undertaken. The assumption is that the driver wishes to maximise the lateral displacement of the vehicle as quickly as possible. Vehicle handling models with AWS are linearised and discretised, and Linear Programming is used to identify the optimal turn-in maneuver. The objective is to understand how to make a vehicle perform well against such a target without any use of any energy-dissipating direct yaw control. It is observed that the optimal controls usually involve an immediate step to the limiting force that the front axle is able to deliver. It is shown that for vehicles with yaw dynamics where this input does not lead to saturation of the rear tyres, the transient performance is totally insensitive to changes in the enforced sideslip control.

The form of this optimal force input is then used in a further mathematical analysis of the optimal obstacle avoidance maneuver. It is shown that in the case mentioned above, where sufficient friction is available at the rear axle, the time taken to build up lateral acceleration and yaw rate for a turn is a simple function of the geometric and inertial properties of the vehicle, and unrelated to rear tyre cornering stiffness, rear camber or rear steering control.

It is shown also shown that for an equal level of limit over- or under-steer, 2WS vehicles that are limit over-steering are able to turn in more quickly than those which are limit under-steering, since the excess friction is available at the front axle, and can be used during the turn-in phase.

Further, it is shown that both commonly adopted sideslip targets for 4WS vehicles and responses that often result from 2WS vehicles can easily be 'incompatible' with the handling envelope of a steered vehicle from an optimal obstacle avoidance point of view. This means that for some vehicles, strict enforcement of such sideslip targets directly increases the time taken to transfer such a vehicle to the limiting lateral acceleration.

This limit of 'compatibility' of the sideslip target and vehicle envelope is confirmed analytically. It is then shown, that the zero sideslip target which is commonly adopted for AWS vehicles in the literature, and which was previously shown to be the ideal for consistent vehicle stability and 'balance', is only able to deliver the optimal turn-in behaviour when the underlying vehicle has a limit-neutral or limit under-steering balance. Further, the zero sideslip target requires a strongly limit under-steering balance if the sideslip target is to be maintained when the vehicle is maneuvered from turning quickly in one direction to turning quickly in the other without compromising the time taken to complete the maneuver.

However, it is also shown that either a controlled front differential, or front axle direct yaw-moment control are each able to extend the envelope of the vehicle in the necessary direction that maintaining zero sideslip throughout such transients may become feasible, albeit at an energy cost that increases as the vehicle is maneuvered more rapidly.

Additionally, an alternative sideslip target is presented, that allows optimal maneuvering to take place whilst the sideslip target is simultaneously maintained, without requiring the intervention of controlled differentials or direct yaw control.

Contents

1 Introduction and Literature Review 1
- 1.1 Review of Vehicle Dynamics Control 2
  - 1.1.1 Actuators that may be controlled 2
  - 1.1.2 Control Strategies for in-plane force control 6
  - 1.1.3 Target Trajectories 16
  - 1.1.4 Summary 25
- 1.2 Formulation of Hypotheses 26

2 Modelling the Vehicle and External Forces 29
- 2.1 Survey of Types of Dynamics Model 29
- 2.2 Coordinate Systems and Notation 34
- 2.3 Model Inputs (Controls) and Outputs (Response) 36
- 2.4 Measures of Sideslip 37
- 2.5 Equations of Motion 43
- 2.6 Externally Applied Forces 44
- 2.7 Tyre Slip 45
- 2.8 Suspension Modelling 46
- 2.9 External Aerodynamic Forces 47
- 2.10 Slip Velocities of Tyre Contact Patches 49
- 2.11 Quasi-static Wheel Rotation Model 50
- 2.12 Coordinate Transformations 51
- 2.13 Driveline Modelling 52
- 2.14 Tyre Modelling 53
- 2.15 Concluding Remarks 57

3 Steady-State Performance 58
- 3.1 Analysis Method 58
- 3.2 Choice of Model 63
- 3.3 Results and Discussion 65
- 3.4 Concluding Remarks 80

4 Energy Consumption 82
- 4.1 Choice of Model 82
- 4.2 Analysis Method 86
- 4.3 Results and Discussion 89
- 4.4 Concluding Remarks 99

5	Identification of Tyre Force Demands (Frequency Domain)	101
	5.1 Choice of Model	102
	5.2 Analysis Method	104
	5.3 Results and Discussion	106
	5.4 Limitations of Frequency Domain Modelling and Analysis	109
	5.5 Concluding Remarks	110
6	Identification of Tyre Force Demands (Time Domain)	111
	6.1 Analysis Method	112
	6.2 Results and Discussion	113
	6.3 Limitations of Linear Modelling and Analysis	119
	6.4 Concluding Remarks	119
7	Identification of Ideal Transient Behaviour (by Linear Programming)	121
	7.1 Modelling the Vehicle and Limits	122
	7.2 Analysis Method	124
	7.2.1 Optimisation Objective	124
	7.2.2 Expression as a problem in Linear Programming	128
	7.3 Results and Discussion	136
	7.4 Possible Extensions and Fundamental Limitations	146
	7.5 Concluding Remarks	149
8	Further Mathematical Analysis	151
	8.1 Limit 'Steering' Characteristics of Vehicles	151
	8.2 Limit Under-Steer, Well Damped Rear Tyre Slip	152
	8.3 Limit Over-Steer, Well Damped Rear Tyre Slip	159
	8.4 Transient Rear Slip or Force Saturation	162
	8.5 Lateral Displacement due to Rear Lateral Force	164
	8.6 Time Delays Introduced By Actuator Limits	165
	8.7 Concluding Remarks	168
9	The Transient Handling Envelope	169
	9.1 Simplified Modelling of the Vehicle Envelope	170
	9.2 Results and Discussion	174
	9.3 Limitations	185
	9.4 Concluding Remarks	186

10	Optimal Target Trajectories		188
	10.1	Objective	188
	10.2	Fundamentals of optimal transient response	189
	10.3	The second-order responses of a 2WS vehicle	190
	10.4	Reduction of dynamics to first order	194
	10.5	Concluding Remarks	203
11	Synthesis and Conclusions		205
	Glossary		205
	References		207

Chapter 1:
Introduction and Literature Review

The many thousands of lives that are lost on the roads each year show clearly that there may be benefit in improving the handling of road vehicles such that drivers are more easily able to avoid obstacles in their path.

It is well known that even when the vehicle has the capability to satisfy the driver's demand, modern vehicles can often be difficult to control - especially in situations where the driver either demands a high path curvature or demands changes in path curvature very suddenly - with the vehicle typically entering unusual dynamic states and exhibiting unusual response characteristics. This inconsistent behaviour makes it extremely difficult for the driver to identify the feedback action required to precisely control the path followed by the vehicle. The high levels of tyre saturation where this difficulty occurs is encountered by most drivers in only the rarely encountered critical conditions where perhaps the driver has misjudged the available friction, and thus the time when the driver most needs assistance from the vehicle is the time it is most likely to behave unpredictably.

For this reason, in recent years, much attention has been focused on the subject of ***Vehicle Dynamics Control***, in which mechanical suspension and steering systems are replaced or augmented by electronically controlled systems that can quickly modulate the in-plane forces delivered by the tyres to deliver a response that is both more consistent and suited to the needs of the driver and the environment.

This chapter presents a review of vehicle dynamics control (section 1.1). This review identifies some shortcomings in the literature that lead to the formation of hypotheses to be answered by the thesis (section 1.2).

1.1: Review of Vehicle Dynamics Control

At the time of writing, there already exists a wealth of literature on the subject of Vehicle Dynamics Control. Typical papers on the subject present an analysis of the performance of a particular vehicle plant fitted with a sets of actuators, controlled according to particular strategies and required to follow some target state trajectory, or to try to satisfy a particular combination of potentially conflicting demands in some 'optimal' manner. Their goal is normally to ensure that the vehicle behaves in a manner that is consistent, robustly stable and fast to respond in all circumstances.

1.1.1: Actuators that may be controlled

Definitions

In the following literature survey, and in the majority of work on the subject of Vehicle Dynamics Control, the following definitions apply to describe the actuators which are available for control:

- 4WS ('Four Wheel Steering') refers to a vehicle with an actively controlled ***rear*** steer angle and ***manual*** (driver-controlled) front steering;
- AWS ('All Wheel Steering') refers to a vehicle with actively controlled front and rear steering (also known as 'Steer By Wire', SBW, since the mechanical connection between the driver and the steering is removed);
- DYC ('Direct Yaw-Moment Control') refers to a system which is able to apply a foundation brake to an individual wheel (and perhaps accelerate the other at the same time), in order that the opposed longitudinal forces create a yawing moment on the vehicle. DYC may be applied either to the front wheels, the rear wheels, or both;
- A 'Controlled Differential' refers to a passive differential which has an internal brake acting on the ***difference*** in half-shaft speeds.

Note: The effect on the tyre forces of braking a controlled, single-clutch differential is equivalent to that of DYC control, since both generate equal and opposite tyre forces (by accelerating the inner wheel whilst braking the outer). However, the energy consumption and the limits of the authority of these two types of DYC differ, since the controlled differential acts only against a ***difference*** in half-shaft speeds. This means that a controlled clutch between left and right half-shafts is capable only of generating a yawing moment in a sense that ***reduces*** the current yaw rate, never one which increases it.

There are also authors who consider the advantages associated with active front steering alone [Sato, 1998]. However, in the analyses which follow in this thesis, the focus is on improving the handling capability of the vehicle, so it is usually assumed that all available control inputs are able to be optimally controlled, and it is not distinguished whether this control must be provided by the driver or by a controller. Therefore, from the point of view of this thesis, the performance of a vehicle with electronically controlled ('active') front steering is considered equivalent to that of a standard, driver-controlled '2WS' vehicle, and the performance of the electronically controlled AWS vehicle would be equal to that of the driver controlled 4WS vehicle.

Therefore, although it is acknowledged that active, front-steer-only systems may be able to make a contribution to the handling 'feel' and stability of a vehicle from the point of view of a typical driver, such 'active front steering' systems are not specifically reviewed in this survey.

2WS

The vast majority of vehicles developed since the invention of the automobile have adopted the same front-steer configuration. For many years, therefore, engineers have worked to improve consistency of the handling of vehicles of this configuration as far as possible, by understanding of the effects and optimising the design of passive components such as steering systems, suspension linkages, bushings and other components. Recent advances in computing power have helped considerably, as optimisers and multi-body simulation packages may be used to understand and optimise behaviour in a simulated environment.

However, there are limits to what can be achieved [Cann, 1995; Seok Kang, 1997]. For example, it is well understood that robust stability of a vehicle can be assured only at the expense of limit handling performance, since a level of understeer is required, and this demands that the vehicle is 'unbalanced' in yaw at the limit. Consistent handling behaviour in varying road conditions [Sakvoor, 1993], is even more difficult to achieve by passive means. In addition, the characteristics of tyres lead to handling behaviour that always changes significantly with the vehicle speed [Dixon, 1995].

4WS

Early attempts at improving vehicle handling beyond the limits imposed by the typical mechanical front-steer layout involved introducing mechanical rear wheel steering (4WS). It was shown that this provided an improvement in the time response of the vehicle in 'normal operating conditions' - in other words, while the tyre force-generation process remains approximately linear [Furukawa, 1998]. In order to improve the consistency of the vehicle's response over a wider range of conditions, feedback control of rear steering was also investigated. These closed-loop systems are able to compensate for the non-linearity in the tyre behaviour by applying additional steering as necessary to maintain a linear vehicle response, and thus ensure consistent behaviour.

However, it will be seen in the following section that closed-loop control of steering can cause a deterioration in vehicle stability in critical conditions. This is understood to be due to the fact that as the tyre reaches saturation, the sensitivity of the steering reduces to zero and then changes sign, such that when the controller steers to increase the tyre force, it may actually reduce. Although they do not specifically describe this effect, Shimada and Shibahata [Shimada, 1994] conclude that rear steer control is 'the most sensitive' of all available controls at small sideslip angle and limited deceleration, but that it is 'much less effective' in other situations.

AWS

Several authors, including Ahring and Mitschke [Ahring, 1995] and Komatsu et al [Komatsu, 2000] suggest augmenting rear steer control with additional front steer control (yielding "All-Wheel Steering", AWS). Such control can improve on the performance that is achievable by 4WS in achieving a rapid, well damped and consistent, speed-insensitive vehicle response to the driver's demand, at least within the linear region of the tyres, where steering control has been shown to be effective (and thus the use of energy-dissipating alternatives such as DYC may be undesirable).

It is interesting to note that in contrast to those reporting on closed-loop 4WS systems, neither author analysing the performance of AWS systems observes any problem in conditions of rear-axle saturation (i.e. where the sensitivity of the lateral force to changes in rear steer angle diminishes, and may even change sign). This is surprising, but it may be that when a stabilising moment is required, allowing the controller to ***reduce*** the destabilising force provided by the front axle (as well to try to increase the stabilising force provided by the rear axle) may mitigate the destabilising effect of applying closed-loop control to the rear steering (though this is as yet unproven).

DYC ('Direct Yaw-Moment Control')

In addition to the often-cited benefit of making use of the significant longitudinal forces which remain available even when a tyre is saturated laterally, Abe also cites a further benefit of DYC actuation - that the ability to generate a particular longitudinal force is "not influenced" by lateral motion of the vehicle. In other words, the sensitivity of changes in vehicle yaw acceleration to changes in the DYC control input (brake pressure, brake torque or brake force) changes very little with vehicle sideslip.

This second benefit of longitudinal force control is due to the fact that it is possible to directly demand a tyre ***force*** (by application of a braking and/or driving torque) whereas in the case of steering control, it is more usual to control steer angle, which has a highly indirect relationship to the lateral force, influenced by non-linearity and time-delays in both the tyre and vehicle dynamics. This difference has important implications for robustness of control, as the same DYC control strategy is likely to work quickly and effectively throughout the vehicle handling envelope – at least until the tyre is completely saturated, beyond which anti-lock or traction control algorithms may be required, but are already both well established both in the literature and proven in practical applications.

It should be noted, however, that the ability of DYC to provide a pure yaw moment, may be limited by available drive torque (engine power or driveline layout) and also by lateral load transfer (LLT). At high lateral acceleration (with significant LLT), the DYC forces are able to act only on the outer wheels - so the vehicle can either accelerate and 'turn-in' (increase the yaw rate), or decelerate and stabilise or 'turn-out' (reduce the yaw rate).

Despite having initially demonstrated clear benefits derivable from steer angle control alone (i.e. 4WS or AWS) in maintaining a consistent vehicle response [Abe, 1989], and showing that it is also possible, in controlled conditions, to extend this into the nonlinear region, Abe [Abe, 1999] acknowledges the sensitivity of the necessary steering control laws to environmental conditions (e.g. changes in friction, tyre temperature or pressure), and concludes that 'the superiority of DYC over 4WS or AWS has been clearly established in the literature'.

However, energy consumption of a DYC system must also be considered, as must the possibilities for improving the robustness of steering control by using modern control techniques [Gordon, 1998; Komatsu, 2000] or online monitoring of local tyre behaviour [Sugai, 1998; Yeh, 1998].

1.1.2: Control Strategies for in-plane force control

In assessing each author's approach to vehicle dynamics control, it is necessary to consider the exact combination of:

(i) actuators (e.g. front steering, rear steering, individual brakes, engine torque, differential torque)

(ii) control strategy

(iii) controlled variables

(iv) variation of the reference value(s) for (iii)

that have been adopted, since the choice of each of these components can affect the overall system performance. It will be seen that whilst certain combinations work very well, different permutations of the same components can perform very poorly. It can therefore be dangerous to draw conclusions about the suitability of a single component (e.g. 'the DYC control' or 'the zero sidelslip target') based on the performance of a closed-loop system that comprises several interacting components.

Feedback Control of Steering Actuators

It has already been noted that the variation of the sensitivity of the 4WS input is in stark contrast to the consistent sensitivity of the DYC input. Several authors attempt to offer solutions which could improve the robustness of the more energy-efficient 4WS [Pasterkamp, 1997; Wakamatsu, 1997; Lu, 1999; Abe, 1989] by continuous on-line identification of the tyre and road conditions, but most acknowledge the fact that when conditions change quickly, their controllers may not behave as intended. Since changes of friction are an example of a situation where a driver may particularly be in need of help rather than hinderance from a controller, a failure of a controller to deliver in these situations must be considered a major issue.

Abe reviews the control law of a classical ***feedback*** 4WS system, which improves response and body slip angle control well into the nonlinear region, but which lacks robustness and may aggravate vehicle instability in critical conditions, if the rear tyres become laterally saturated [Abe, 1996; Abe, 1999].

Ahring and Mitschke [Ahring, 1995] present results from a feed-forward steering system with and without "sideslip angle compensation" by an additional feedback term. The authors deem compensation to be the necessary approach "because the vehicle and tyres show a nonlinear characteristic" (and the feed-forward control they apply is purely linear). However, they also demonstrate that on an icy surface, the inclusion of this feedback term in the rear steering control law degrades the overall performance.

Komatsu et al [Komatsu, 2000] do not appear to encounter this problem with their application of optimal full-state-feedback control to an AWS vehicle, though whether or not the maneuver analysed actually saturates the rear tyre force is not mentioned. They show an impressive performance in a lane-change maneuver, suggesting that controlling both front and rear steering together may have potential in overcoming the problem.

Open-Loop/Feed-Forward or Mechanical Control of Steering Actuators

One approach to avoiding exacerbation of limit instability due to the sign change in steering control sensitivity is to take the conservative approach of applying a ***feed-forward*** strategy for all steer angle control. Mechanical 4WS systems with gains that are speed-sensitive [Allen, 1993] or front steer-angle-sensitive [Furukawa, 1989] fall into this category, and both have reached production, indicating manufacturers' confidence that dangerous characteristics are not present.

Furukawa [Furukawa, 1989] describes the goals of Honda to be improving lateral acceleration response time about the straight ahead, and reducing the decrease in the yaw rate response that normally occurs at higher lateral accelerations. Their solution, which was one of the first 4WS systems to reach production, employs a mechanical linkage which prescribes a rear steer angle that is a non-linear function of front steer angle only. There is no adaptation to speed or vehicle loading condition, and improved performance is observed only within a limited range of speed and vehicle parameters.

Electronic feed-forward systems that adapt to variations in vehicle parameters have been shown to offer improved performance in a much wider range of conditions. Many authors design such systems to operate effectively within the linear range of vehicle dynamics,because the linear-region handling behaviour of the vehicle remains reasonably consistent even as the road surface changes.

Abe [Abe, 1999] presents the typical control law adopted by speed-sensitive feed-forward systems that use additional rear steer to minimise (zero) the vehicle sideslip angle (except at low speed) - either:

- only in the steady-state (by either electrical or mechanical, 'deadbeat' control), or
- at all times, including in the transient state (by using a model inversion and therefore, always by electronic feed-forward control).

It has been shown that deadbeat control (i.e. control without transient compensation) is ineffective in controlling sideslip in transient maneuvering [Koresawa, 1994]. More critically, though, the performance of any purely linear feed-forward control strategy has been shown to be little better than that of the vehicle without control when the tyres operate in their nonlinear regions [Abe, 1989].

Non-linear feed-forward systems have been shown to perform better provided road and tyre conditions are either constant or change very slowly, and 'disturbances' due to longitudinal load transfer are somehow measured.

Combined Feed-forward and Feed-back Control of Steering

Nagai [Nagai, 1989] uses feed-forward control to improve transient performance, and feedback to reject aerodynamic disturbances. In the non-linear region of the vehicle, however, it is assumed that this approach would suffer from the same performance degradation as the pure feedback approach, as shown by Ahring and Mitschke [Ahring, 1995], since the feedback term will compensate for any error in the vehicle response to the feed-forward control.

Non-linear Feed-Forward Control of Steering

Abe [Abe, 1989] showed that adaptive, non-linear feed-forward systems have the greatest performance potential for improvement of vehicle response, stability and sideslip control. He demonstrates non-linear feed-forward control of both front and rear steering, acknowledging the difficulty, but assuming the success of continuous and effective on-line identification of non-linear vehicle characteristics. He explains that traditionally, open loop (feed-forward) control laws tend to be based on the linear behaviour of the vehicle. This is often considered to be the logical approach as non-linear effects vary considerably with environmental conditions, and are difficult to identify with sufficient speed and accuracy for use in control. However, Abe presents a general non-linear approach which adapts 4WS to longitudinal and lateral acceleration, and demonstrates significantly improved performance in maintaining low vehicle sideslip and consistent control sensitivity.

Abe's approach employs an identified "equivalent cornering stiffness" which (locally) varies linearly with the measured lateral and longitudinal acceleration. He then identifies the necessary changes in the control actions for front and rear steering by inversion of a simplified on-line dynamic model of the vehicle, such that it follows a reference yaw rate and sideslip velocity response (actually a first order time lag in yaw rate, and zero sideslip, with the commonly adopted [Komatsu, 2000] yaw rate gain from a reference 2WS vehicle). Due to the presence of additional dynamic effects and further non-linearities which are not included in the on-line simplified model of the vehicle, the application of the identified control to the real vehicle will not follow the demand exactly, so Abe gives simulation results showing the result of applying the control to a more complex, non-linear source model, intended to represent a real vehicle.

Abe shows frequency response functions (FRFs) from steering input to both lateral acceleration and yaw rate, around various steady-state trims, and shows, for one particular vehicle, how these change with increasing steady-state lateral acceleration.

For the 2WS vehicle, these show the typical increase in phase lag and reduction in gain due to non-linear tyre properties, for which only experienced drivers are able to compensate effectively. The traditional linear feed-forward 4WS (without lateral and longitudinal acceleration-based adaptation) shows a similar phase lag and gain reduction at high lateral acceleration. At low lateral accelerations, it is shown that the response of the 4WS vehicle with non-linear feed-forward control is extremely close to the target first order time lag, and remains speed-insensitive as the authors required. At higher lateral accelerations, the response remains very similar, demonstrating the effectiveness of the control (on an unchanging surface). Additionally, since the control is feed-forward, there should be no sudden reduction in vehicle stability.

The performance of the strategy in circumstances of sudden change in friction is not mentioned, and there remains an unsolved (and not easily soluble [Horiuchi, 1999]) need for robust and rapid identification of non-linear tyre characteristics if the performance in such conditions is to be properly controlled.

The performance in situations where the tyres are saturated is not shown - the simulations presented show only up to 0.6g cornering on an flat, dry surface.

DYC

So far, the literature has shown that:

(i) linear, feed-back control of rear steering may exacerbate vehicle instability as the rear tyres become saturated;

(ii) purely linear feed-forward control is largely ineffective in the non-linear region;

(iii) the difficulty and sensitivity of on-line estimation of non-linear tyre state is a crippling factor for any non-linear feed-forward control strategy [Horiuchi, 1999]

These factors have led to the increasing popularity of DYC over 4WS or AWS for the improvement of handling dynamics (i.e. performance, response and stability). As mentioned above, in addition to the clear advantage of improving tyre force utilisation by employing longitudinal force components, the vehicle response to any DYC input is rapid, and remains highly consistent [Abe, 1999], which eases the task of the controller.

However, the generation of DYC moments by braking consumes significant energy, such that most controllers so far proposed will DYC by braking only in critical situations. Because of this, DYC systems are often unpopular with enthusiastic drivers (and especially with motoring journalists), who find it difficult to predict when the system will deem the current vehicle sideslip and/or yaw rate to be excessive and apply control, such that although potentially capable of higher performance when DYC is fitted, the vehicle is often judged to be more difficult to drive quickly and precisely, compared with the same vehicle without DYC and a skilled driver at the wheel.

For example, Yoshioka et al [Yoshioka, 1998] present a sliding mode approach to vehicle sideslip control, employing a simple online tyre model to estimate the road friction, tyre slips and loads, and the sensitivity of the DYC control input. The derived longitudinal slip demand, to generate precisely the correct yaw moment, is then passed to their anti-lock brake controller. However, they state that in practice, the control must be applied "with threshold values" to prevent frequent occurrences of unnecessary intervention (e.g. due to incorrect state estimation) that disturb the driver and slow down the vehicle.

For this reason, actively controlled differentials have been considered by several authors [Harty, 2003] as being a possible alternative, since these are able to provide many of the benefits of DYC by braking, but with significantly lower energy consumption, such that smooth and continuous operation is possible.

Ad-hoc Integrated Control of 4WD and 4WS

Many somehow 'integrated' systems have been proposed, and some have reached production (e.g. Nissan's 'Super-HICAS').

Matsuo et al [Matsuo, 1993] propose an "intelligent" four wheel drive system, which simply attempts to increase the load on the axle that requires it by using longitudinal forces at the axle with more available grip. They apply a yaw rate model following control, but introduce an unspecified first order time lag to their controller reference 'to allow for time lags in the dynamics of the vehicle'. They also demonstrate the performance of their system in conjunction with 4WS where that 4WS uses simple yaw rate feedback and they propose "integration" of the systems by varying the feedback gain according to the current torque distribution in the 4WD system, which in turn is influenced by both wheel-spin (front-rear mean axle speed difference) and by yaw error. Whilst their system does seem 'reasonable', it is hard to draw any clear conclusions about handling control or the optimality of their controller from their ad-hoc approach to the integration of the systems.

Integration with Suspension Design

Abe [Abe, 1999] clearly acknowledges the reliance of any handling control strategy on the available tyre frictional forces and consequently on the distribution of the vehicle weight between the tyres. The logical conclusion from this is that suspension design (irrespective of whether it be active or passive) should be integrated with handling control design.

An example of failure to do this may be seen clearly in early production front-wheel-drive DYC vehicles. Most of these vehicles have the distribution of vertical loads on the tyres controlled by passive, twist-beam rear suspensions with a strong anti-roll effect, such that rear lateral load transfer dominates near the limit of dry friction. In these conditions, rear axle DYC (which would otherwise be able to make a positive contribution to preventing excessive under-steer) is unable to generate the necessary longitudinal force.

The conclusion which must be drawn from this is that in assessing a new handling control strategy, the engineer should also consider the influence of changes in the vertical load control (regardless of whether it be active or passive).

A more even distribution of the lateral load transfer between front and rear axles (or, if the CG is not central, a bias towards the more lightly loaded axle) will improve the distribution of the available tyre forces to match the tyre force demands associated with steady-state turning. This in turn is likely to improve the controllability and cornering performance. However, a well-balanced vertical load distribution increases the changes in yaw moment that occur due to changes in longitudinal acceleration (brake or throttle inputs) as the vehicle enters the non-linear region, since in this condition, all four tyres are strongly sensitive to vertical load changes. Shimada and Shibahata [Shimada, 1994] show that when the vehicle's roll moment distribution is varied, a vehicle with even front to rear weight distribution (and thus tyre vertical load distribution) that is likely to perform well in steady-state handling, is the most sensitive in this respect. This contrasts with the throttle-sensitivity of the handling in the linear region, which is almost always near-zero, since the linear characteristics of tyres are only mildly influenced by vertical load changes [Milliken and Milliken, 1995]. Such changes in control sensitivity during a maneuver are generally undesirable as they make the driver's task more difficult. Whilst it might be possible to counter these changes by controlling a passive differential, frequently or continuously correcting diversions of vehicle behaviour away from the reference by means of the cheaper solution of individual brake intervention is both inefficient and disturbing to the driver. This yields an additional challenge in the implementation of 'optimal' vehicle dynamics control. One possibility to overcome this would be to employ an adaptive steering control strategy such as that proposed by Abe [Abe, 1989] that strives to invert the non-linear characteristics and maintain consistent sensitivity to driver inputs, regardless of the underlying passive chassis characteristics. However, the issue of sensitivity to errors in parameters or curves derived from noisy transducers and simple models remain to be adequately resolved, especially as the level of available road friction can change quickly. The fact that friction is limited is the most significant source of non-linearity in road vehicle dynamics, and is therefore the single 'disturbance' over which it is both most important and most difficult to exercise effective control.

The approach of Komatsu et al [Komatsu, 2000] to the control of an AWS vehicle considers the changes in available friction caused by transient lateral load transfer and camber change due to the suspension, and proposes a controller which reduces roll excitation by filtering the lateral tyre forces. An improvement in the lateral acceleration response for a typical lane-change maneuver is shown when this filtering is implemented, although the reason is not explained.

Integrated vs Non-Integrated Control

Abe [Abe, 1996] has compared the performance of pure steering control, direct yaw moment control and combined, integrated control, with the conclusion that strict cooperative control is not the best solution (possibly due, once again, to the change in sensitivity of the rear steer input). Horiuchi [Horiuchi, 1999] later uses model-following non-linear predictive control to compare 4WS, DYC and DYC + AWS with more positive conclusions regarding integrated control. However, of course, each author is able to simulate only a tiny subset of the vehicles and scenarios that may be encountered by the system.

The above review of the application of classical control in vehicle handling dynamics indicates that all problems have not yet been solved. Linear feed-forward steering control provides only minimal benefit (more rapid response about the straight-ahead);

fixed-structure linear feed-back controllers tend to become non-robust in the most critical operating conditions, non-linear approaches either perform poorly, or perform unpredictably whenever the parameters of which they require knowledge - such as friction - change quickly compared with the time constant of the system's learning. Most approaches to implementation of the easier-to-control DYC by means of brake control tend to disturb the enthusiastic driver, waste energy and slow down the vehicle (such that many skilled drivers simply switch the systems off).

Modern Control Techniques and Non-Linear Stability Analysis

Whenever trying to prove the stability of a strategy, it is important to consider the limitations of linear stability theory. In showing the destabilising effect of vehicle sideslip, Shimada et al [Shimada, 1994] present the standard vehicle stability criterion, which is based on linearisation of the dynamics (where these dynamics may be extended to include the effect of control if required). However, such an analysis hides the fact that despite a vehicle possibly being instantaneously stable, it is always possible, for example, for the body sideslip or rear tyre slip angle to increase over time, such that an unstable condition can be reached at a later time. This illustrates the limit of the applicability of linear stability theory to non-linear systems; a system can only be shown to be globally stable if it is stable at every reachable point within the state-space.

Free-control phase-plane analyses such as that of Inagaki [Inagaki, 1994] can show these conditions, provided a two-degree of freedom vehicle model provides a sufficiently good representation of the vehicle behaviour (e.g. with yaw and sideslip properly considered, but with roll motions and tyre load transfer assumed to occur near-instantaneously, as they would with the stiff suspension or roll excitation filtering described above). Free-control stability is one possible reason that many authors strive to ensure that the yaw rate, sideslip, and perhaps roll angle transfer functions have no overshoot following an impulsive driver input. This may be the reason that many authors adopt a first order time lag as a target transfer function between steering and yaw rate, and between steering and sideslip [Koresawa, 1994], since both states contribute to the rear tyre slip angle, any increase of which can lead to a reduction in vehicle stability. In addition, it is well known that the response of systems which have a first order response tends to be easier to predict and therefore to control (by either a driver or a predictive controller).

Other non-linear stability criteria (e.g. ensuring global system energy reduction, as provided by Lyapunov control) may be employed to guarantee system convergence towards the desired equilibrium point at all times [Gordon, 1998]. In this work, it is shown that by controlling the ***directions*** of the tyre slip vectors, it is possible to ensure that the vehicle response is always convergent towards the reference.

Robust and adaptive control

The term "adaptive control" applies to systems that use the values of some slowly varying measured state(s) of the vehicle in order to compute more appropriate controller parameters (such as gains or time constants). In this sense, "slowly varying" implies that the dynamics of these variations is of significantly lower bandwidth than the dynamics being controlled.

Conservative adaptation of system parameters can be an effective way to cater for non-linearities with lower risk of exacerbating instability. However, the accuracy of the identification of any dynamic state may be poor if the inputs to the system remain small for an extended period of time, or do not excite the important regions of the vehicle handling envelope (although it is possible to design a system which will constantly excite the vehicle and measure the response, in order to track the sensitivity of each control).

Neural networks can be used to identify non-linear vehicle dynamics, but controllers based on Neural Network models have uncertain robustness when the vehicle enters a region of the handling envelope for which little training data has been provided.

An alternative to on-line identification and adaptive control is to employ Robust Control, where the controller commonly has a fixed structure and gains, but where those gains are selected such that the performance and stability of the closed loop system remains acceptable for all possible variations in system parameters. Robust controllers are thus insensitive to identification errors, but often yield a compromised (or at best very conservative) performance. In addition, when applied to vehicle steering control, changes in control sensitivity can be so great that robust control is insufficient – the only "safe" feedback control applied to steering may be no feedback control at all, unless the current tyre condition can be identified.

Sliding Mode Control

In a joint paper, Abe, Kano, Shimada and Furukawa [Abe, 1999] apply sliding mode DYC control such that the vehicle body sideslip angle follows that of a notional purely linear vehicle. By using model-following control, they successfully prevent erroneous intervention of DYC due to natural sideslip overshoots caused by the passive dynamics of the vehicle, and thus intervene to control the vehicle only when the sideslip becomes excessive due to non-linearity (though they also state that the system is implemented with a 'threshold', such that once again it may be found to be disturbing to enthusiastic or skilled drivers).

Lyapunov Control

Gordon [Gordon, 1998] proposes an online force demand management strategy which assumes equal available friction front and rear (and thus requires no on-line friction estimation), and uses a Lyapunov approach to stabilise a vehicle that in practice sees variations in front to rear friction. The stability of the system on a surface with randomised friction is demonstrated, although this assumes an as yet undeveloped inner control loop that is able to deliver a certain lateral force, provided the tyre is capable of generating it, and the optimality of the response time in conditions where the available friction departs from the assumption of perfect balance - is not discussed. The significant advantage of the strategy is that it always guarantees convergence towards the desired states, even with uncertain road friction. However, in the form presented, the approach requires sufficient actuation and engine power to control the force directions from all of the tyres.

1.1.3: Target Trajectories

The 'target' or 'reference' of a controller refers to the manner in which the controller strives to get the vehicle to behave. In the case of sideslip control, it can be seen that both the choice of reference and the performance of the control strategy in getting the vehicle to follow the reference can influence the performance of the overall system. In this section, attention is directed at the author's choice of reference rather than the control strategy - although, as indicated earlier, there is always some coupling between the components of (i) target, (ii) control strategy and (iii) actuators being controlled.

The Target Trajectory

So many possibilities exist for how vehicles might respond to a steering input that the 'ideal' handling behaviour has not yet been clearly defined. Therefore, typically, particular controller targets are often presented only as example test-cases for controllers or actuator combinations, such that it can be shown that more 'consistent' behaviour can be assured when control is implemented.

However, it does seem that answering the question of what the system should do in response to driver demands should be answered (in addition to the question of how to make it behave well, against an arbitrary target), especially since it may be found that some of the capabilities of controllers may be of limited utility once the ideal target behaviour has been identified.

Certain simple targets, (controller references) have been presented many times, the most common of which being ***zero sideslip*** [Sano, 1986; Lin, 1992; Higuchi, 1992; Wang, 1993; Abe, 1996; Gordon, 1998; Horiuchi, 1999; Komatsu, 2000]). However, in most cases, this is proposed and used as a target without formal justification. In addition, since the vehicle 'plant' is always non-linear (i.e. friction-limited) in its behaviour, the choice of target certainly has an influence on the difficulty of the control task, and the performance of the proposed control structure with alternative targets is rarely presented or discussed.

Notably few authors [Hurdwell, 1992; Koresawa, 1994)] consider alternative sideslip targets than zero. However, Hurdwell and Koresawa each proposed the possibility of a fixed 'motion centre', of which 'zero sideslip' is a special case (where this 'motion centre' coincides with the centre of mass).

The justification for zero sideslip

Recently, Hac [Hac, 2002] reviewed the basic justification for targeting zero sideslip, concluding simply that "it is well known that in emergency lane change maneuvers both objective task performance measures and driver's subjective ratings of handling quality improve when the phase lags between the steering angle input and lateral acceleration and yaw rate responses are kept small". On this basis, Hac concludes (as does much of the literature) that zero sideslip should be the target, since the tracking of this minimises the time lag between lateral acceleration and yaw rate. However, it is not clear from the literature which lag (steering to yaw rate, steering to lateral acceleration, or yaw rate to lateral acceleration) is most important. Since in critical situations the available friction must be shared between the generation of lateral acceleration and yaw acceleration (i.e. yaw rate), the relative importance is an important question, as a faster lateral acceleration response could be achieved at the expense of yaw rate, or vice versa.

The Physical Influence of the sideslip Angle

The sideslip angle which is followed during the maneuver clearly has some influence on the obstacle avoidance and energy consumption performance of the vehicle. This influence might be separated into the following effects:

(i) **geometry** – the effects that arise due to the changes in the positions of the tyres, and thus the lines of action and moments of each of the forces, as the vehicle is rotated through the sideslip angle, β (relative to the instantaneous path)

(ii) **tyre loading** – the influence that those changes in position has on vertical load distribution, and thus the maximum frictional force $\hat{F}$ available from each tyre

(iii) **inertial** – the tyre forces that are demanded to yield a desired sideslip (β or V) and therefore sideslip rate $\left(\dot{\beta} \text{ or } \dot{V}\right)$, or in other words, to maintain a desired relationship between the lateral acceleration $\left(a_y\right)$ and yaw rate (r) of the vehicle.

In an often-referenced paper, Shimada and Shibahata [Shimada, 1994] concluded that vehicle stability always reduces with increasing body sideslip angle, by showing that the restoring yaw moment provided by the lateral tyre forces, per unit increase in vehicle sideslip angle reduces as the rear tyres enter their non-linear region. This was shown for both 2WS and 4WS vehicles, and is generally agreed upon as the most significant motivation for adoption of some form of vehicle dynamics (i.e. sideslip) control. This non-linearity also influences the sensitivity of the vehicle to control inputs, potentially also making the driver's control task more difficult as the vehicle becomes less stable. Abe [Abe, 1999] concurs with this conclusion that increasing vehicle sideslip angle degrades the vehicle stability, even for a 4WS vehicle.

It is important to note that both authors conclude that it is the increasing vehicle sideslip that angle degrades stability, ***not*** simply the increasing rear tyre slip angle. In fact, it can be shown that there are two components to this degradation of stability, depending on how the rear steering is controlled – (i) the increase in rear tyre slip, such that it may enter the non-linear region where the local cornering stiffness decreases, and (ii) the forward motion of the two outer tyres which, in circumstances of high lateral load transfer, generate the greatest cornering forces.

The majority of the open-loop (feed-forward) rear steer control strategies which have been proposed to date, including that analysed by Shimada, choose to adopt only small, same-sense rear steer angles at high speed [Furukawa, 1989; Sano, 1986], but there does exist the possibility for controllers to command larger, outward rear steer angles as necessary to reduce the direct connection between this loss of stability and the vehicle sideslip angle (i.e. to remove rear steer angle in circumstances where the controller had identified that such an action would improve, rather than reduce vehicle stability). However, the fact remains that the vehicle stability would tend to degrade with increasing sideslip, for any condition of nonzero load transfer and tyre non-linearity.

However, most authors to date have adopted minimisation of vehicle sideslip angle as the target for their vehicle dynamics controllers [Abe, 1996; Gordon, 1998; Horiuchi, 1999; Komatsu, 2000; Sano, 1986; Wang, 1993]. As mentioned above, in addition to the natural destabilising effect of increasing sideslip (which could perhaps be otherwise controlled), human performance in vehicle control has been cited as a further reason for targeting zero sideslip. However, whether the improvement in human performance is due directly to the more consistent stability is not shown.

Adopting the target of zero sideslip across the whole of the handling envelope, however, eliminates the possibility of deriving any advantages that may exist in allowing higher body sideslip angles in certain circumstances (e.g. to reduce aerodynamic drag, tyre vertical load transfer, or yaw moment demand). Therefore, these benefits will be analysed in this thesis, in order to clarify whether the adoption of zero sideslip as the target is likely to impair or improve the performance relative to other possible targets (motion centre locations).

Estimation of the current sideslip (for use in sideslip control)

The difficulty of estimating vehicle sideslip angle is a further complication of the problem of vehicle dynamics control (and the reason that many authors choose to control only the directly measurable vehicle yaw rate, or the simpler-to-identify sideslip rate). Many production vehicles which implement sideslip control use simple resetting integrators to identify sideslip. This approach exploits the fact that vehicles are often driven in straight lines in between turns in order to repeatedly correct any integration drift. However, these vehicles also employ large thresholds on their control intervention. In academic papers, and on some vehicles, Kalman Filtering or extended (non-linear) Kalman Filtering is employed [Venhovens, 1998; Best, 1998; Best, 2000], and whilst many authors show reasonable results, a known-robust approach has yet to be demonstrated.

The approach that Abe, Kano, Shibahata and Furukawa [Abe, 1999] apply to sideslip estimation employs an on-board tyre model and forces from this in the sideslip estimation – thus, if the sideslip predicted is excessive, then large restoring forces are predicted and thus the subsequent sideslip error is reduced – but as ever, this relies on the continuous updating of an on-board tyre model, and is therefore potentially prone to significant error.

Zero sideslip by DYC

Both Horiuchi and Abe [Horiuchi, 1999; Abe, 1996] show that the performance of DYC in maintaining zero sideslip is poor, and that this control strategy makes much less effective utilisation of tyre forces than the uncontrolled vehicle. This is an unsurprising conclusion given that the ability of the rear tyres to contribute to lateral force and thus moment generation is significantly compromised when zero sideslip is adopted as the target, especially at high speeds, because the rear tyre slip angle is equal to:

$$\alpha_r = \frac{V - cr}{U} - \delta_r$$

and thus when both the rear steer angle δ_r and the sideslip velocity, V are forced to zero, the vehicle yaw rate r becomes the only contribution to the rear tyre slip angle and thus the contribution of the rear tyres (to both the lateral acceleration to balancing the yaw moment balance generated by the front axle) is dramatically reduced, such that very large DYC moments are required if the lateral acceleration performance of the vehicle is to be restored.

Wang et al [Wang, 1993] also suggest minimisation of the sideslip angle for a vehicle without rear steer control. These approaches were clearly targeting maintenance of consistent vehicle stability and consistency of response at the expense of both efficiency and limit performance, but their poor performances primarily serve as examples of the fact that the controller target and the available actuation must be considered together.

In a further example of this same issue, Horiuchi [Horiuchi, 1999] concludes that combined DYC and AWS performs better than DYC alone for the case of maximising deceleration during a split-mu stop, but he does not consider that his controller target of zero sideslip inhibits the possibility for the vehicle that is equipped with DYC only (no rear steering) to employ rear lateral tyre forces. Had the zero sideslip target not been enforced, these lateral forces (which might be generated by rotating the vehicle to a small sideslip angle) would provide an opposing yaw moment and thus allow higher braking forces from the high-mu side.

Therefore, great care must be taken in drawing conclusions about the effectiveness of particular actuators or actuator combinations based on isolated studies - as described above, the actuator's effectiveness should always be considered in combination with the target and control strategy applied to it.

All of this work clearly shows the unsuitability (or at best, inefficiency) of the zero sideslip target for vehicles without rear steer control.

Nonzero sideslip by 4WS (with and without DYC)

Abe [Abe, 1989] suggests the use of pole placement (also known as eigenvalue assignment), or optimal control for finding an appropriate transfer function from the driver's steer input to the yaw rate and sideslip responses, acknowledging that zero sideslip should not necessarily be the target.

Nagai suggests the use of a first-order time lag as a reference for each of the (yaw and sideslip) transfer functions [Nagai, 1997], but without justification or suggestion of an appropriate value for that time lag. Conversely, yaw inertia data from historical (thus mostly subjectively tuned) 2WS vehicles [Crolla, 1996] suggests that for those vehicles, an attempt has been made to ***minimise*** rather than maximise the yaw damping (refer to Chapter 7 for an explanation of this). This suggests that there may be reasons that a first order response is undesirable - perhaps because it removes any possibility for the driver to use transient inputs to exercise control of the sideslip independently of the yaw rate and lateral acceleration, and thus yaw damping reduces the driver's authority over the vehicle stability or 'balance'. Therefore, if the system that is implemented is able to ensure optimal balance of the vehicle, then a first order target may be acceptable. However, if it is not able to ensure optimal balance (for instance, in the case of a vehicle with only feed-forward steering control), then the over-damping of the yaw motion may in fact reduce the controllability and performance capability of the vehicle (at least in the hands of a skilled driver).

Koresawa [Koresawa, 1994] specifically acknowledges that it may be desirable to target a nonzero sideslip angle, and whilst he does not present any specific reason that a nonzero sideslip angle might be a good target, he presents a number of strategies for tracking such a reference. His approach centres around maintaining a speed-invariant fixed 'centre of motion' (whose location relative to the vehicle CG is equal to the sideslip velocity divided by the yaw rate, and is thus the point on the vehicle where the sideslip is zero - equivalent to the 'perceived motion centre' of Hurdwell). Once again, this translates to targeting a first-order response in both states, but with some freedom over the choice of the time constant. The author cites an advantage of this strategy as being that for the same path followed, the vehicle sideslip angle versus distance (and thus the whole geometry of a maneuver) is invariant with speed, though he does not explain why this is an 'advantage'.

However, it should be noted that such a strategy implies that the ratio of sideslip to lateral acceleration (often referred to as the 'sideslip gain') changes with speed, such that for tail-out sideslip, the vehicle would be more stable for the same lateral acceleration at higher speed (where the path curvature and thus the sideslip and its destabilising effect is smaller).

Sideslip Rate Control (by AWS, and by DYC)

Komatsu et al [Komatsu, 2000] propose control of their on-line linear reference model such that a strong correlation between the lateral acceleration and yaw rate is maintained. Since a perfect correlation is possible only when zero sideslip is achieved, this effectively amounts to another attempt to target zero sideslip. However, Komatsu acknowledges that in order to maintain yaw rate and lateral acceleration in phase, the cost should be introduced onto the sideslip ***rate*** rather than onto the sideslip angle itself or the sideslip velocity. In other words, a small disturbance in the absolute value of the sideslip angle would not be corrected for. A secondary benefit of this approach is that it eases implementation (since only lateral acceleration, yaw rate and forward speed need be measured). There being no need for a potentially non-robust online sideslip angle observer [Best, 1998; Fukada, 1998; Kaminaga, 1998; Best, 2000] is one reason that a sideslip ***rate*** may be a very wise choice of target. In addition, this target permits some nonzero steady-state sideslip to occur if this happens to have positive implications on other terms in the cost function.

Alberti also proposed minimisation of the sideslip rate, but applying no control when the product of sideslip angle and rate is negative, i.e. when the sideslip is already reducing. This decision is made because DYC input is extremely 'expensive' in terms of energy consumed. It is anticipated that this controller would be both less efficient and less consistent than the AWS-based implementation proposed by Komatsu, and additionally it is partially reliant upon a sideslip ***angle*** observer.

Nonzero sideslip Target from a Reference Model, by DYC

In considering the appropriate strategy for DYC control, Abe [Abe, 1999] shows that for an uncontrolled vehicle, the transfer function from yaw rate to sideslip depends on rear tyre cornering stiffness, and thus if sideslip angle is not controlled, the steady-state sideslip increases as the rear tyre cornering stiffness deteriorates. Abe therefore concludes that since sideslip degrades vehicle stability, it is better to adopt side slip control (and have yaw rate control happen as a side-effect) rather than adopt yaw rate control alone, since this might allow the sideslip angle to increase slowly. Given the demonstration of Shimada and Shibahata - that the stabilising yaw moment due to the lateral forces reduces with increasing sideslip angle (due to lateral load transfer), this would seem to be a logical conclusion, but it is at odds with the sideslip ***rate*** control suggested by Komatsu and Alberti.

Abe & Kano [Abe, 1999] present a sideslip following control with the objective of ensuring that no control need be applied in the linear region of passive vehicle behaviour. As the control input is DYC, this seems to be logical, for the reasons of energy efficiency described earlier - if the vehicle is not near the limit of available friction, then efficiency is maintained; otherwise, stability and balance are controlled at the expense of some energy efficiency.

However, similarly to the case of zero sideslip control by DYC, this approach may become highly inefficient (in terms of both friction utilisation and energy) as the vehicle enters the non-linear region of rear tyre force, since the system would begin to choose to use front axle DYC (rather than fully utilise the rear tyre force) to provide some of the stabilising yaw moment.

Yaw Rate Control

Yaw rate control is straightforward to implement, and effectively controls the under-steer angle (that is, the difference between front and rear slip angles) by ensuring that the yaw rate is appropriate for the steer angle. However, despite the implementation of under-steer control, since the reference is the demand lateral acceleration and yaw rate, rather than the actual vehicle lateral acceleration (as in the case of sideslip rate control), the vehicle sideslip may still slowly increase in non-linear region of the rear tyres (since this increases the slip at both tyres), and beyond the saturation point of the rear tyres, a constant but excessive steer demand can lead to a terminally increasing sideslip angle [Abe, 1996].

Axle cornering stiffness control

Dreyer [Dreyer, 1992] proposes an approach that ensures full utilisation of tyre forces at the limit of lateral performance, by monitoring the instantaneous cornering stiffnesses of the tyres. However, this is a non-linear control method and thus requires online identification of tyre slip curves, or at least the instantaneous cornering stiffnesses. However, as a strategy for ensuring optimal performance from the vehicle at all times (steady-state and unsteady-state), it shows significant promise. A similar strategy formed the basis of the Mercedes '4-Matic' Four Wheel Drive system of the late 1980s.

Optimal Target Identification

Blank and Margolis showed that the optimal input for obstacle avoidance invariably involves a combination of braking and steering, and maximisation of the lateral acceleration at the expense of making zero speed reduction yields the best path for obstacle avoidance only in exceptional circumstances [Blank, 2000]. They optimised the controls for a very simple (particle) model, and demonstrated that the result was near-optimal for a single test case of a more complex non-linear vehicle model. The result showed for a long time horizon, an approximately ***balanced*** distribution of the tyre friction between the conflicting demands of braking and lateral acceleration is ***usually***, if not always, the optimal input (indicated in this work by a force vector at 45 degrees to the path). However, it was also shown that for ever shorter time horizons, the optimal input involves progressively ***less braking***, and therefore greater cornering forces. Although he makes no suggestion of how such a condition could be determined, Blank proposes the adoption of the balanced braking and cornering force target whenever 'both steering and braking inputs are saturated'. This seems reasonable, since the maximum obstacle avoidance performance for very near objects (short time horizons) could still be achieved by the driver simply saturating the steering without braking (or with light braking). This is considered appropriate, since it would probably be clear to most drivers that braking (which would compromise the lateral displacement for such short time horizons) would have little influence on the avoidance of an object that was only a very short distance from the vehicle.

1.1.4: Summary

In the literature, we see an acknowledged shift away from steering control stategies that ensure zero sideslip, due to (i) the difficulty of applying effective control to steering, and (ii) the inefficiency of the DYC input for controlling sideslip. However, it was seen that modern control techniques [Komatsu, 2000; Gordon, 1998] and the more efficient actuation provided by controlled passive differentials [Harty, 2003] may offer partial solutions, such that controlling sideslip to a reference value may indeed be feasible.

It was also observed that zero sideslip control has been shown to yield both the highest subjective ratings and the best objective performances from human drivers during emergency lane-changes (compared with alternative sideslip behaviour), and Shimada [Shimada, 1994] showed that changes in side-slip at the centre of mass lead directly to a negative change in vehicle stability. Therefore, constant (and therefore, usually zero) sideslip appears to offer an advantage in both a closed-loop (i.e. driver-in-the-loop) sense and in a purely objective, open-loop sense (since with constant sideslip, the balance of force demands between the front and rear tyres does not change as the path curvature increases, and the vehicle may then remain well balanced in yaw at both low and high path curvatures).

Also, the physical feasiblity of following a particular sideslip reference was not studied in detail, nor was the relationship between physical feasibility and controller success. Also, there were no attempts to assess whether zero sidslip is important only in the steady-state or also at high frequency, nor how precisely the sideslip must be controlled in order to provide sufficiently consistent vehicle balance. These questions are considered important, because it is possible that variations in the target (such as a 'softening' of the constraint, the choice of a non-zero refernce, or the enforcement of the zero reference only at low frequency) may place lower demands on the tyres during transients, thus easing the job of the controller, and still yielding the desirable consistent steady-state balance as path curvature is slowly increased.

This thesis therefore seeks to identify the importance of and the sensitivity to side-slip control in a fundamental sense. Simple definitions of good vehicle performance and simple models are combined in an attempt to quantify the effect that sideslip control and reference variation have on the handling capability of a typical vehicle, and consequently on the likely success of sideslip control.

1.2: Formulation of Hypotheses

Introduction

A review of application of in-plane tyre force control for the improvement of vehicle dynamics has been conducted, and a large number of studies have demonstrated that the introduction of control can effect improvements in the response times and consistency of the dynamic behaviour of vehicles.

However, it was also seen that many of the available control strategies for steering control can be ineffective or even detrimental in certain conditions (such as on changes of friction, or when tyre forces become saturated). It was also seen that there are important interactions between the chosen actuator set and the appropriate target yaw-sideslip behaviour that can have a significant influence on the performance.

This thesis will focus on addressing the latter point - how to make an appropriate choice of yaw-sideslip target for a particular actuator set. This was selected as the primary focus, because this is normally given secondary consideration in the literature.

In addition, the few observations about appropriateness of target that are presented in the literature are limited in their generalisibility, since the vehicle plant-controller-target-maneuver tested in each paper tends to be quite different, and most analysis is numerical such that any direct relationships between the system design and the performance are usually not clearly identified.

Hypotheses

A set of hypotheses was constructed, including hypotheses related to both (i) the choice of sideslip target and its effect on vehicle performance, and (ii) the proposed new approaches to analysis which, it is hoped, will lead to greater understanding of the problem of identifying an appropriate sideslip target. These hypotheses are:

H1: The maximum acceleration that a vehicle is able to generate in a particular direction in ${}^{P}a_x$–${}^{P}a_y$ space is influenced by the side-slip angle at the centre of mass, since a rotation of the vehicle relative to its path leads to changes in the tyre locations and thus vertical loads.

H2: The sideslip angle at the centre of mass during transient maneuvering influences the energy dissipated by the tyres, and the (related) sideslip angle at the aerodynamic reference point influences energy dissipation due to the influence on aerodynamic drag.

H3: If a particular sideslip behaviour is rigidly enforced, then the choice of that sideslip behaviour will have a direct influence on transient tyre forces required to turn the vehicle.

H4: Due to H3, certain sideslip targets may be more compatible with the forces that are able to be generated by certain vehicle configurations (i.e. depending on limits imposed by friction and the available controls).

Analysis Plan

In Chapter 2 (Modelling), the linear and non-linear vehicle dynamics models used throughout the thesis are presented. These models are use in a dynamic or quasi-static sense as appropriate in the analyses that follow.

In Chapter 3 (Steady-State Performance), the yaw-plane, non-linear model with quasi-static load transfer is used to investigate the influence of the sideslip angle on the tyre loading, contact patch positions and thus on the steady-state acceleration performance of the vehicle, in cornering and braking.

In Chapter 4 (Energy Consumption), both linear and non-linear yaw plane models are used to identify the energy-optimal combination of controls to satisfy a certain ${}^{P}a_x$–${}^{P}a_y - \alpha_z$ acceleration vector demand.

In Chapter 5 (Identification of Tyre Force Demands, Frequency Domain), the linear, yaw plane model (with sideslip constraints such as zero rear steer, or zero sideslip enforced) is used to determine transfer functions between critical quantities of interest, such as the relationship between the front and rear tyre force demand for following an oscillatory path with varying sideslip constraint. Note that if feedback control of steering is assumed, then the assumption of linear tyre behaviour does not affect the tyre force demands, provided an ideal (fast-responding) controller is assumed.

In Chapter 6 (Identification of Tyre Force Demands, Time Domain), Inverse Fourier Transforms the same frequency response functions are taken in order to identify the forces necessary to follow a sudden change in path curvature vehicle in the time domain (since any transient is a sum of phased frequency components), and it is the time-domain demands which must remain within the available friction.

In Chapter 7 (Identification of Ideal Transient Behaviour), the technique of Linear Programming is applied in a discrete-time, transient sense in order to identify the optimal controls and response to maximise the lateral displacement of the vehicle as soon as possible, within the constraints enforced by the limited available friction.

In Chapter 8 (Further Mathematical Analysis), the results from Chapter 7 are analysed analytically, leading to new analytical results in optimal handling behaviour.

In Chapter 9 (Transient Handling Envelope), another view of the tyre-friction constraints on optimal transient handling is utilised in order to better understand results from Chapters 8.

In Chapter 10 (Optimal Target Trajectories), the compatibility between these envelopes and the possible response trajectories in a_y-α_z space is considered in further detail. The set of trajectories which are completely compatible with envelope of the vehicle (and thus allow the driver to make optimal utilisation of the available friction) are identified and described as 'force-optimal'. Also, the yaw damping behaviour of 2WS vehicles is further investigated.

It is proposed that the results and improved understanding gained from these physical analyses could be used to guide the choice of sideslip target for future controlled vehicles.

Chapter 2: Modelling the Vehicle and External Forces

Throughout this work, it is assumed that control will be applied to the tyre slip in order to influence the in-plane tyre forces, which in turn control the motion the vehicle. It is therefore necessary to understand and model both the tyre and vehicle at an appropriate level of detail such that conclusions about control that are based on modelling are transferrable into the real world.

Therefore, the various types of vehicle and tyre model that might be adopted are discussed, and the actual models which are used in the subsequent analyses are presented.

2.1: Survey of Types of Dynamics Model

Particle and Quasi-Static Models

Particle models of vehicles have long been used for predictions of lap times on motor-racing circuits [Various, 1971; Gadola, 1996; Thomas, 1996] and for some fundamental analyses of optimal maneuvering [Blank, 2000]. Particle models neglect the yaw inertia of the vehicle, assuming that it is able to yaw instantaneously, and that any rapid yawing that occurs due to rapid changes in path curvature does not change the demands on the tyres. The particle model therefore simply represents the handling capabilities of the vehicle in terms of a limit on path-lateral and longitudinal accelerations.

Particle models, therefore, are not capable of representing the fine details of transient handling behaviour, since they neglect the degrees of freedom of primary importance, such as roll and sideslip. They are therefore considered unsuitable for assessment of controllers whose goals are to improve transient response and yaw stability.

Linear Models

Linear models are useful for the simulation of many dynamic systems, provided sufficiently small perturbations from a reference dynamic state are assumed. It is common, therefore, to use linearisations of complex non-linear vehicle models to analyse stability in response to small perturbations about specific conditions, such as during straight line driving or constant radius cornering [Gillespie, 1992; Charek, 1984; Huston, 1979; Milliken, 1995; Dixon 1996], but not for extreme cornering maneuvers.

The linearisation of a model enables identification of eigen-information, such as natural frequencies, damping ratios and mode shapes. This is useful in confirmation of the closed-loop stability of the system, and analysis in the frequency domain becomes possible. Linearisation of the governing equations can sometimes also provide analytical descriptions of the system behaviour that make it easy to see and understand the effect of system parameters [Watari, 1974], although such descriptions rapidly become prohibitively complicated for systems with many states.

When using linear models, it must always be remembered results are reliable only whilst the states remain within a limited region of the state-space. It is also well understood that the results from a time-invariant linear model have limited validity when important components of the real system (such as tyres, bushings or suspension) respond in a manner which is strongly non-linear with respect to the variation of an important state. Common phenomena such as saturation, dead-zones and dry friction all fall into this category, and must be treated with caution.

Due to these restrictions, the use of linearised models in vehicle handling dynamics - apart from in straight-line stability analysis - has historically been limited to texts which attempt to educate the reader in respect of those mechanisms which can lead to changes in vehicle response or stability.

Describing Function and Volterra Series Component Models

A 'Describing Function' is a description of a strongly non-linear component (such as those mentioned above) that is compatible with linear analysis techniques. It is assumed that the behaviour of the non-linear system, when excited by a continuous sinusoidal input, will be dominated by its response at the frequency of the input. This implies that the system response must be periodic with the excitation frequency, and additionally assumes that any response at the harmonics of the excitation frequency (known as 'harmonic distortion') is small enough to be neglected. Thus the non-linearity in any component of the system may be described as an amplitude-dependent gain and phase. For a given input amplitude, a linearisation can be identified that provides an ***indication*** of the likely large-scale behaviour of the system. Volterra developed an extension of this approach that also models the output at each harmonic of the excitation frequency.

Simplified non-linear models

Simplified non-linear models are commonly used in attempting to understand a system where it is not possible to capture important aspects with a linear model.

For instance:

- in the analysis of braking or ride behaviour, perhaps only pitch-plane dynamics will be modelled (and any yaw or roll response will be neglected), but the full non-linearity of the suspension (e.g. bump-stops) and the saturation of longitudinal tyre forces with respect to slip might be included;
- for rollover analysis, it is common to neglect yaw and pitch dynamics [Gillespie, 1992], but it is necessary to include the non-linearity which occurs when a wheel leaves the ground.
- for handling dynamics, it is common to assume a perfectly flat road, and sometimes only yaw-plane (or yaw and roll) vehicle motion.

It is, however, extremely important that critical effects are not excluded by adopting an oversimplified model. Therefore, rigorous scientific analyses that are based on modelling normally also show the result which is obtained from a model of increased complexity, to provide an indication of the likely error introduced by the modelling simplifications. However, since the important phenomena might in some cases only be captured in a model of yet further complexity, engineering judgment must always be exercised to ensure that the assumptions which are made are reasonable [Wade Allen, 1994].

Complete non-linear simulations

A complete or 'exact' model attempts to simulate the whole system behaviour in sufficient detail to capture all of the phenomena of interest, with little emphasis on simplification. However, fast dynamics may still be approximated in order to avoid problems with numerical stability and/or long computer simulation times. Also, no component is ever properly understood or modelled in every detail, and observed non-linear behaviour is frequently modelled using low-order functions or lookup tables that do not necessarily correctly represent higher-order coupling or take into account details or component to component variabilities.

A good comparison between a carefully simplified non-linear model and an "exact" model is presented in [Sayers, 1996] showing that there are significant benefits in computation time, and often little accuracy is lost when a model is carefully simplified.

Tyre Modelling

The component that has the dominant influence on vehicle motion is the tyre. Thus, if dynamics control is to be exercised, the tyres must be somehow controlled, and the factors that influence the forces that tyres generate must be well understood if they are to be controlled successfully.

The tyre is normally required to perform three functions:

(i) it enables the vehicle to roll over the surface (thus reducing the rolling resistance, provided the tyre is aligned in the direction of travel);

(ii) through its' vertical stiffness and limited damping, it generates a force that maintains the wheel (and ultimately the vehicle body) suspended a distance above the surface;

(iii) it exploits this load, together with friction between the rubber of the tyre and the ground plane, to enable the generation of in-plane forces and moments at the contact patch.

It should be noted that due to the need to maximise use of the available friction (and thus the vertical loading of the tyres), it is not useful to assign the functions of vehicle suspension and in-plane force generation to different tyres. The load supported by the tyres, and the location of their contact patches relative to the vehicle CG, is critically important for yaw-plane control of the vehicle, and all of the vertical load must be exploited if optimal handling performance is to be achieved.

The process by which frictional forces are generated by tyres is complex, because the force generation process is influenced by a complex structural design, by the chemistry of the material (usually a natural rubber), by the road surface conditions (including any lubrication and micro-texture), and by the vertical vibration of the tyre in response to rolling over the non-smooth road surface.

Schieschke and Hiemenz [Schieschke, 1993] describe "the decisive role the quality of tyre approximation plays in vehicle dynamics simulations", providing a description of the tyre modelling problem and advantages and disadvantages of analytical, numerical and physical approaches to tyre modelling. They conclude that low order analytical models of tyres often neglect to include important effects. However, where understanding is important, simple non-linear models such as the Pacejka Magic Formula model [Bakker, 1987] are usually considered to be of significant value, since the variation of a small number of parameters facilitates an approximate description of the aggregate characteristics of a wide range of tyres.

However, many simplified models neglect effects such as pneumatic trail and lateral offset of the longitudinal force. These effects can have a significant influence on steering feel, since as a tyre begins to lose lateral grip, the pneumatic trail reduces, leading to a significant loss in the slip-resisting steering torque that can be a warning to the driver of an impending loss of adhesion. However, these moments have limited influence on the vehicle behaviour apart from their effect on the forces in the steering system – so the analysis that will be performed (and, for instance, whether such steering system forces are important) should be considered when choosing an appropriate model.

In many handling situations, longitudinal and lateral forces are simultaneously demanded of the tyre. Notably, in validating vehicle dynamics models for the National Advanced Driving Simulator (NADS) at the University of Iowa, Garrott [Garrott, 1997] suggests that commonly used 'combined-slip' tyre models ***do not*** provide accurate simulations. Hirschberg [Hirschberg, 1993] suggests that this may be due to the fact that tyres tend to be measured only for "pure slip" conditions, i.e. pure lateral slip or pure longitudinal slip. Noronha [Noronha, 1999] explains that the difference between the cornering stiffness and longitudinal slip stiffness influences the co-linearity of the directions of the slip and force vectors. In many models, such as that built into the software package CarSim [Sayers, 1999], and that of Gim and Nikravesh [Gim, 1990], exact co-linearity of slip and force is assumed, though the accuracy of the resulting tyre model in combined-slip conditions is not discussed.

A number of papers employ low-order, physics-based phenomenological models for the frictional forces generated by tyres, such as the popular "brush" model [Fujioka, 1996; Svendenius, 2003]. These models sacrifice precisely capturing the exact behaviour of a particular measured tyre in favour of describing the tyre based on the actual physical processes which occur. One significant benefit of this is that it becomes possible to relate vehicle performance metrics directly to understandable and fundamental aspects of the tyre design, or the properties of the constituent materials.

Where intermediate objects such as particles of snow, sand or gravel exist between the tyre and the solid ground, tyre mechanics become much more complicated. This is the domain of Terramechanics, since the response of the surface is also significant. Also, the hydroplaning of tyres (where a fluid layer exists between tyre and road) is an extremely complex, and therefore left to specialist tribological analyses.

Transient Tyre Dynamics

It is well understood that tyres do not generate forces immediately in response to changes in slip. The delay, known as relaxation, is often modelled as a first order lag between the kinematic slip and the resulting force generation, where this relaxation time is dependent upon the rotational velocity of the wheel, such that it is normally expressed as a (near-constant) relaxation length.

Sayers and Han [Sayers, 1996] assert that whilst the lag for ***lateral*** slip can interact with the vehicle dynamics at low speed, the lag for longitudinal slip is "usually neglected".

Palkovics [Palkovics, 1994] discusses the variation of tyre relaxation with vertical load, and Higuchi [Higuchi, 1996] describes the variation with wheel slip and camber. Bernard and Clover [Bernard, 1996] mention that the lag should be on the slip experienced by the tyre and not on the force generated, such that changes in vertical load and camber yield a near-instantaneous response from the tyre, whereas the response to changes in slip is delayed.

2.2: Coordinate Systems and Notation

The right-handed, standard SAE axis systems [Gillespie, 1992] are used ***throughout*** this thesis. The coordinate system in which a quantity is expressed is represented by an uppercase letter (V, W, P or A, for *Vehicle, Wheel, Path* or *Aerodynamic*) above and to the left of the quantity. For instance, ${}^{V}\underline{\omega}$ represents the angular velocity vector of the vehicle centre of mass, expressed in the ***Vehicle***-fixed coordinate system.

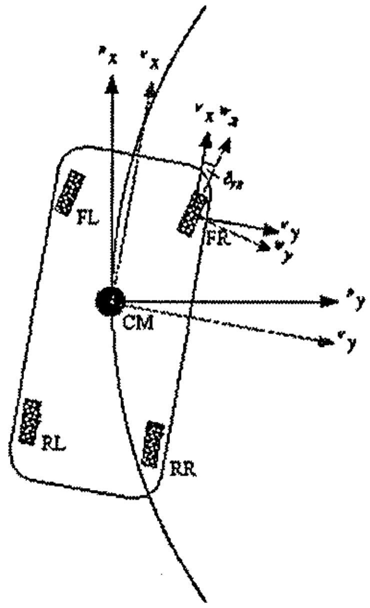

Figure 2.1
SAE Vehicle-fixed, Wheel-fixed and Path-fixed coordinate systems

The vehicle-fixed coordinate system, V is centred on the centre of mass of the vehicle, the x axis points forwards, y to the right and z vertically downwards. The wheel-fixed coordinate system, W, is centred on the wheel centre, with the axis directions being coincident when the wheel is un-steered ($\delta = 0$).

Vector quantities are expressed using an underscore (so $\underline{r}$ is a vector, r is not). The directed components of a vector are denoted with a subscript x, y or z (e.g. r_y).

Quantities related to individual wheels are denoted by the ***uppercase final subscripts*** (or sub-subscripts) FL, FR, RL, RR (such that $\underline{F}_{FL}$ represents the total force vector applied to the vehicle by the front left wheel, $F_{x_{FL}}$ represents the force in the x direction component of the force applied to the vehicle by the front left wheel).

In contrast, quantities related to individual ***axles*** are denoted with ***lowercase final subscripts*** f or r (so that, for example, M_{z_r} represents the z component of the (DYC) moment applied by the rear axle, and the angular velocity across the front differential is w_{diff_f}). For consistency, a lowercase c is used to represent the ***centre*** differential (e.g. w_{diff_c}).

2.3: Model Inputs (Controls) and Outputs (Response)

The inputs to be considered in the subsequent analyses include:

- Front steer angle, δ_f, or the total front axle lateral force, F_{y_f}
- Rear steer angle, δ_r, or the total rear axle lateral force, F_{y_r}
- Front axle direct yaw control (DYC) moment, ΔM_{z_f}, or the difference in longitudinal forces, ΔF_{x_f}
- Rear axle direct yaw control (DYC) moment, ΔM_{z_r}, or the difference in longitudinal forces, ΔF_{x_r}

And the outputs of interest include:

- sideslip (see below for measures of sideslip)
- yaw rate, r
- roll angle, ϕ (assumed zero for yaw-plane models)
- total front axle lateral force, F_{y_f}
- total rear axle lateral force, F_{y_r}
- total front axle longitudinal force, F_{x_f}
- total rear axle longitudinal force, F_{x_r}
- acceleration lateral to the path, ${}^P a_y$
- acceleration along the path, ${}^P a_x$
- roll angular velocity, p (also assumed zero for yaw-plane models)
- tyre vertical loads, F_z^k

2.4: Measures of Sideslip

Sideslip angle and velocity

Since vehicles tend to behave in a linear manner at low lateral acceleration, many analysis approaches require linear models, and it is generally agreed that a linear response in yaw-sideslip is desirable from a human control point of view, the steady-state sideslip behaviour of a vehicle is often expressed as a ratio between the sideslip state and one of the other fundamental handling states - for instance $\frac{{}^{V}V}{r}$.

However, some authors choose to discuss sideslip velocity, V, and others choose sideslip angle, $\beta = \tan^{-1}\left(\frac{V}{U}\right)$. Some relate sideslip velocity to yaw rate, r, others relate sideslip angle to lateral acceleration, others to path curvature, ρ.

Depending on the choice, the ratio may have different implications in terms of the influence of forward speed, U, or in terms of the phase angle between the quantities during transient maneuvering (such that the ratio may only be an expression of the steady-state relationship).

The appropriate choice is a question of 'horses for courses' - for instance, in Chapter 3, when it is clear that the sideslip angle at the centre of mass has a direct influence that is the same at all speeds (and the influence of the sideslip velocity, therefore, is speed-dependent), the sideslip angle is assumed the reference.

Also, depending on the effect of sideslip that is being discussed, different coordinate systems are appropriate. For instance, if geometric off-tracking or aerodynamic sideslip are of interest, then it is the sideslip at mid-wheelbase (i.e. in the standard Aerodynamic coordinate system) that is of interest, since zero sideslip at this point gives zero off-tracking, or zero aerodynamic sideslip. If moment balance or yaw motion is of interest, then it is the sideslip at the centre of mass (i.e. in the Vehicle coordinate system) which is important.

Since all of these quantities are related by some transformation, however, the conclusions drawn from each point of view must be combined into some general understanding of sideslip. If a certain behaviour relative to one coordinate system appears to be optimal but something different is optimal relative to another, this may suggest some ideal relationship between the centres of two coordinate systems (e.g. between mid-wheelbase and centre of mass, or between driver and centre of mass) that might influence the vehicle design.

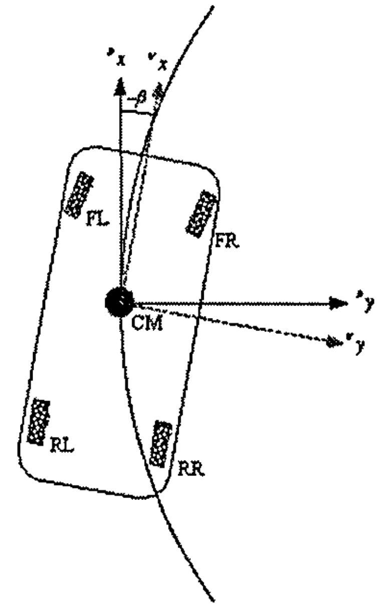

Figure 2.2a
Right Turn with Tail-Out Sideslip Angle at the Centre of Mass
(negative sideslip angle ${}^{V}\beta$ and sideslip velocity ${}^{V}V$)

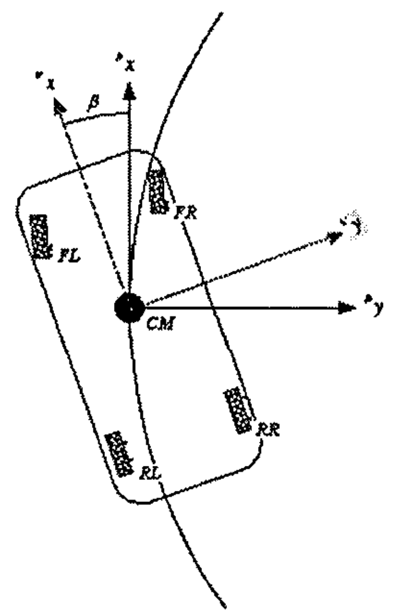

Figure 2.2b
Right Turn with Nose-Out Sideslip Angle at the Centre of Mass
(positive sideslip angle ${}^{V}\beta$ and sideslip velocity ${}^{V}V$)

Motion Centre

For the purposes of discussion of alternative sideslip targets, the term 'motion centre' is sometimes used. The 'motion centre' of a vehicle (or 'perceived motion centre' as Hurdwell describes it [Various, 1992]) is an alternative measure of the sideslip, and is defined here as the point on the vehicle centreline about which the vehicle is perceived to rotate. Mathematically, this is the point ${}^{V}x = d$ on the centreline of the vehicle at which the lateral velocity (which comprises contributions from the sideslip at the centre of mass and the yaw rate):

$$ {}^{V}v_y(x) = {}^{V}V + rx $$

is zero:

$$ \left. {}^{V}v_y(x) = 0 \right\} \quad x = d $$

$$ {}^{V}V + dr = 0 $$

where

${}^{V}V$ is the sideslip velocity at the mass centre

d is the distance from the centre of mass to the motion centre

r is the yaw rate of the vehicle

A positive value of d indicates a motion centre a distance d ***ahead*** of the centre of mass. In a right-turn, where the yaw rate, r is positive, this implies ***negative*** ('tail-out') sideslip angle and a corresponding ***negative*** sideslip velocity ${}^{V}V$ at the centre of mass.

The diagram below shows how the the yaw rate and the sideslip velocity at the centre of mass each contribute to the lateral velocity at different points along the centreline of the vehicle, ${}^{V}v_y(x)$:

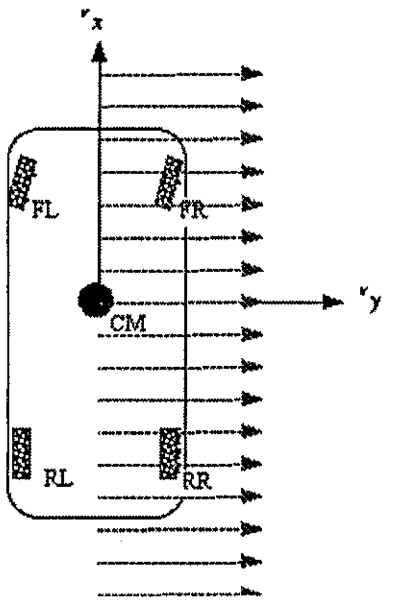

Figure 2.3a
${}^{V}v_y(x)$ **due to sideslip**
$= {}^{V}V$

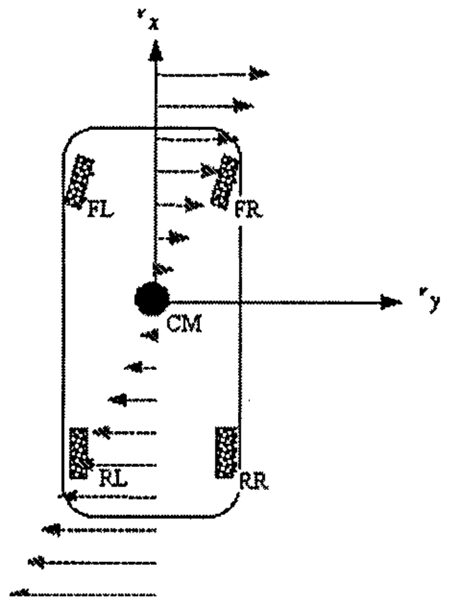

Figure 2.3b
${}^{V}v_y(x)$ **due to yaw**
$= rx$

These components sum to give the total ${}^{V}v_y(x)$:

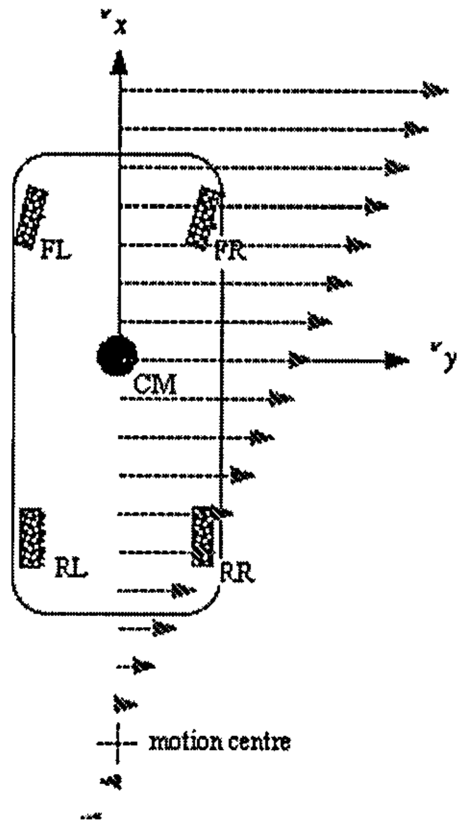

Figure 2.3c
Lateral velocity along the centreline of the vehicle
$$^{V}v_y(x) = {}^{V}V + rx$$
showing the motion centre $x = d$ **where** $^{V}v_y(x) = 0$

When the constraint of a ***fixed*** motion centre is applied, yaw rate r and sideslip velocity ^{V}V at the centre of mass remain ***in phase*** at all times (with a constant of proportionality of $-d$), and the constant speed yaw-sideslip model of the vehicle is reduced from second to first order. This is because one state - either the sideslip V or β, or the yaw rate r - may be removed since the relationship between V and r, and β and r remains proportional at all times, even during severe transients if ideal control is assumed.

A further geometric relationship which is maintained is that the steady-state ***centre of turn*** (as distinct from the 'motion centre') will always lie on the line through the motion centre, parallel to the lateral y axis of the vehicle.

Costing sideslip rate at the Motion Centre

One of the potential benefits of the cost function that is minimised by the controller proposed by Komatsu [Komatsu, 2000] is that the cost may be identified by measuring lateral acceleration, yaw rate and forward speed alone - the body sideslip angle is not required.

At first glance, it appears that there is a limitation to this strategy - that the cost J may ***only*** minimise the rate of change of the sideslip at the centre of mass:

$$\begin{aligned} J &= {}^{V}a_y - Ur \\ &= {}^{V}\dot{V} \end{aligned}$$

and this is the form of the cost function that is most commonly presented. However, it will be shown in this thesis that it may be desirable to instead minimise the rate of change of sideslip at another point ${}^{V}x \neq 0$ on the longitudinal axis of the vehicle.

The sideslip velocity at such a general point ${}^{V}x = e$ ahead of the centre of mass on a yaw-plane model is:

$${}^{V}V_e = {}^{V}V + er$$

The rate of change of the sideslip at this point is:

$${}^{V}\dot{V}_e = {}^{V}\dot{V} + e\dot{r}$$

such that the modified cost function to minimise the sideslip rate at this point would be:

$$\begin{aligned} J' &= {}^{V}\dot{V} + e\dot{r} \\ &= {}^{V}a_y - {}^{V}Ur + e\dot{r} \end{aligned}$$

The lateral acceleration measured at this same general point a distance e ahead the centre of gravity (on a yaw plane model) is:

$${}^{V}a_{y_e} = {}^{V}a_y + e\dot{r}$$

Therefore, the difference between this measured or estimated acceleration ${}^{V}a_{y_e}$ and the product of yaw rate and forward speed is costed, this cost becomes:

$$\begin{aligned} J' &= {}^{V}a_{y_e} - {}^{V}Ur \\ &= {}^{V}a_y - {}^{V}Ur + e\dot{r} \end{aligned}$$

which is that required to minimise the sideslip at this point.

Therefore, it is possible to adapt the cost functions employed by those authors proposing sideslip rate control such that the sideslip rate at a point other than the centre of mass (i.e. the desired motion centre) is minimised.

2.5: Equations of Motion

All models used in this thesis focus on the motion of the vehicle as a single rigid mass. Secondary inertial effects due to motion of the engine, occupants, load, wheels or axles relative to the body are neglected throughout.

Therefore, the equations of motion are derived directly from Euler's equations for the rate of change of momentum of a rigid body, expressed in the vehicle body-fixed coordinate system V:

$$\frac{{}^{V}d\underline{L}}{dt} = M\underline{a} = M\left(\begin{bmatrix}\dot{U}\\ \dot{V}\\ \dot{W}\end{bmatrix} + \begin{bmatrix}qW - rV\\ rU - pW\\ pV - qU\end{bmatrix}\right)$$

$$\frac{{}^{V}d\underline{H}}{dt} = \begin{bmatrix}I_{xx}\dot{p} - I_{xy}\dot{q} - I_{xz}\dot{r}\\ I_{yy}\dot{q} - I_{yx}\dot{p} - I_{yz}\dot{r}\\ I_{zz}\dot{r} - I_{zx}\dot{p} - I_{zy}\dot{q}\end{bmatrix} + \begin{bmatrix}(I_{zz}r - I_{zx}p - I_{zy}q)q - (I_{yy}q - I_{yx}p - I_{yz}r)r\\ (I_{xx}p - I_{xy}q - I_{xz}r)r - (I_{zz}r - I_{zx}p - I_{zy}q)p\\ (I_{yy}q - I_{yx}p - I_{yz}r)p - (I_{xx}p - I_{xy}q - I_{xz}r)q\end{bmatrix}$$

where

- ${}^{V}\underline{L}$ is the linear momentum vector of the vehicle (expressed in the vehicle-fixed coordinate system, V)
- ${}^{V}\underline{H}$ is the angular momentum vector of the vehicle (expressed in the vehicle-fixed coordinate system, V)
- ${}^{V}\underline{V} = {}^{V}\begin{bmatrix}U\\ V\\ W\end{bmatrix}$ is the velocity vector of the centre of mass (expressed in the vehicle-fixed coordinate system, V)
- ${}^{V}\underline{\omega} = {}^{V}\begin{bmatrix}p\\ q\\ r\end{bmatrix}$ is the angular velocity vector of the centre of mass (in roll, pitch and yaw, expressed in the vehicle-fixed coordinate system, V)

The following simplifying assumptions are then made:

(i) there is no pitch-plane motion (i.e. the vertical velocity, $\dot{w}$, and the pitch rate, q, and all of their derivatives are always negligible);

(ii) all second order terms *except* those involving the forward velocity, U are negligible (and U will be assumed large but constant);

(iii) the vehicle is symmetric about a vertical plane normal to the lateral axis of the vehicles, such that $I_{yz} = I_{zy} = I_{xz} = I_{zx} = 0$.

Making these assumptions yields much simpler expressions for the change of linear momentum in the lateral, y and longitudinal, x directions (with motion in the vertical, z direction remaining unmodelled):

$$^{V}\frac{dL_x}{dt} = Ma_x = M\left({}^{V}\dot{U}\right)$$
$$^{V}\frac{dL_y}{dt} = Ma_y = M\left({}^{V}\dot{V} + {}^{V}Ur\right)$$

and for the change of angular momentum of the vehicle body in roll and yaw:

$$^{V}\frac{dH_x}{dt} = I_{xx}\dot{p} - I_{xz}\dot{r}$$
$$^{V}\frac{dH_z}{dt} = I_{zz}\dot{r} - I_{zx}\dot{p}$$

2.6: Externally Applied Forces

The changes in the momentum of the vehicle body occur only in response to externally applied forces. For a rubber-tyred, four-wheel vehicle, these forces arise at (i) the contact patches of the four tyres, (ii) at the centre of mass (due to gravitational acceleration) and and (iii) at the aerodynamic reference (due aerodynamic forces and moments).

These forces are expressed in the vehicle-fixed coordinate system, V, in order that the vehicle response (rate of change of momentum, and thus ***acceleration***) may be determined:

$$^{V}\frac{d\underline{L}}{dt} = \sum {}^{V}\underline{F}_{ext} = {}^{V}\underline{F}_{aero} + \sum_{k=1}^{4} {}^{V}\underline{F}_k$$
$$^{V}\frac{d\underline{H}}{dt} = {}^{V}\underline{M}_{ext} + {}^{V}\underline{r} \times {}^{V}\underline{F}_{ext} = {}^{V}\underline{M}_{aero} + \sum_{k=1}^{4} {}^{V}\underline{r}_k \times {}^{V}\underline{F}_k + {}^{V}\underline{r}_{aero} \times {}^{V}\underline{F}_{aero}$$

In yaw,

$$^{V}\frac{d\underline{H}_z}{dt} = {}^{V}F_{y_f}b - {}^{V}F_{y_r}c + M_{z_f} + M_{z_r} + M_{z_{aero}}$$

where, for four-wheel models, the total lateral axle forces are

$$^{V}F_{y_f} = {}^{V}F_{y_{FL}} + {}^{V}F_{y_{FR}}$$
$$^{V}F_{y_r} = {}^{V}F_{y_{RL}} + {}^{V}F_{y_{RR}}$$

and the direct yaw control (DYC) moments due to the longitudinal tyre forces are

$$M_{z_f} = t_f\left({}^V F_{x_{FR}} - {}^V F_{x_{FL}}\right)$$
$$M_{z_r} = t_r\left({}^V F_{x_{RR}} - {}^V F_{x_{RL}}\right)$$

2.7: Tyre Slip

The lateral slip angle α_k and the longitudinal slip ratio, s, may be determined from the motion of the ground relative to the tyre contact patch, when viewed from the wheel coordinates. For non-linear models,

$$\tan(\alpha_k) = \frac{{}^W V_k}{{}^W U_k}$$

and

$$s_k = \frac{{}^W U_k - R_k \omega_k}{{}^W U_k}$$

and for linear models,

$$\alpha_k = \frac{{}^W V_k}{{}^W U_k}$$

Where a lateral relaxation lag is to be modelled, this lag is introduced as a first order lag on the tyre slip, so that the above is replaced by:

$$\left.\frac{\partial \tan(\alpha_k)}{\partial t} = \frac{1}{\tau_k}\left(\frac{{}^W V_k}{{}^W U_k} - \alpha_k\right)\right\} \quad k = FL, FR, RL, RR$$

where

$\left.\tau_k = \frac{l_k}{{}^W U_k}\right\}$ $k = FL, FR, RL, RR$ is the relaxation time for tyre k

l_k is lateral the relaxation length of tyre k

${}^W V_k$ is the lateral velocity of the hub of wheel k, in wheel co-ordinates

${}^W U_k$ is the longitudinal velocity of the hub of wheel k, in wheel co-ordinates

2.8: Suspension Modelling

Tyre Vertical Load

The vertical loads on the tyres include terms due to:

- static load on the tyre, $F_{z_{k,static}}$, including the weight of the vehicle and static aerodynamic loads according to the current vehicle speed;
- in-plane forces F_{x_k} and F_{y_k} due to suspension geometry where the 'effective trailing arm' or 'effective radius arm' of the suspension are inclined relative to the horizontal, $x-y$ plane (by the angles ε_{x_k} and ε_{y_k} respectively), such that the contact patch is constrained to follow a locus which is not vertical - this is the influence of the roll axis location and anti-pitch or anti-dive geometry;
- suspension (spring and damper) forces due to the current suspension deflection and the total vertical stiffness or flexibility measured at the contact patch (commonly described as the wheel rate), and the associated damping and damper inertia.

$$\begin{aligned} F_{z_k} = F_{z_{k,static}} \\ +F_{x_k}\tan\left(\varepsilon_{x_k}\right)+F_{y_k}\tan\left(\varepsilon_{y_k}\right) \\ -k_k d_k - c_k \dot{d}_k - m_k \ddot{d}_k \end{aligned}$$

For the purposes of this research, the effects of dry friction in the suspension, and the phenomenon of wheel lift are neglected.

Note 1: Although cross-coupling between wheel suspensions (e.g. by means of anti-roll bars) is commonly used, this cross-coupling is evident only when the vehicle is subject to pitch and heave motions. For yaw plane models or models with only a roll degree of freedom, stiffnesses which occur due to interconnections (such as due to anti-roll bars) may be lumped into the wheel rate, since whenever one left side wheel is displaced, the other left wheel is equally displaced, and both right-side wheels experience an equal and opposite displacement:

$$d_{FL} = d_{RL} = -d_{FR} = -d_{RR}.$$

Note 2: The zero of suspension deflection is therefore defined as the deflection with the vehicle statically loaded due to both its own weight (i.e. the action of gravity) and the static aerodynamic force vector for the current forward speed.

Therefore, changes in the suspension deflections d_k occur only due to body roll (with $\phi = p = \dot{p} = 0$ for pure ***yaw-plane*** models, and $p = \dot{p} = 0$ for models with ***quasi-static*** roll motion):

$$\left.\begin{aligned} d_k &= \phi r_{z_k} \\ \dot{d}_k &= p r_{z_k} \\ \ddot{d}_k &= \dot{p} r_{z_k} \end{aligned}\right\} \quad k = FL, FR, RL, RR$$

Due to the axle locations and suspension geometry (roll axis height and anti-dive) effects discussed earlier, the locations of the tyre contact patches, relative to the vehicle-fixed coordinate system V, are a function of the suspension deflection:

$$\begin{aligned} {}^V r_{x_{FL}} &= b + \varepsilon_x d_{FL} & {}^V r_{y_{FL}} &= -t_f + \varepsilon_y d_{FL} \\ {}^V r_{x_{FR}} &= b + \varepsilon_x d_{FR} & {}^V r_{y_{FR}} &= t_f + \varepsilon_y d_{FR} \\ {}^V r_{x_{RL}} &= -c + \varepsilon_x d_{RL} & {}^V r_{y_{RL}} &= -t_r + \varepsilon_y d_{RL} \\ {}^V r_{x_{RR}} &= -c + \varepsilon_x d_{RR} & {}^V r_{y_{RR}} &= t_r + \varepsilon_y d_{RR} \end{aligned}$$

2.9: External Aerodynamic Forces

Aerodynamic coordinate system

The following transformation (actually a simple translation) is required to convert from SAE aerodynamic to vehicle-fixed coordinate systems (i.e. a translation in x from mid-wheelbase to centre of mass and in z, from ground level to centre of mass) [Various, 1993]:

$${}^V r = {}^A r + \begin{bmatrix} \dfrac{b-c}{2} \\ 0 \\ h \end{bmatrix}$$

Since this transformation is only a translation (no rotation), forces expressed in each coordinate system remain the same. However, the force locations change and thus they have a different influence on the total moment:

$$\begin{aligned} {}^V \underline{F}_{aero} &= {}^A \underline{F}_{aero} \\ {}^V \underline{M}_{aero} &= {}^A \underline{M}_{aero} + \left({}^V \underline{r} - {}^A \underline{r}\right) \times \underline{F}_{aero} \end{aligned}$$

where $\left({}^V \underline{r} - {}^A \underline{r}\right)$ is the vector from the centre of mass to the centre of the aerodynamic coordinate system (where F_{aero} is applied), at mid-wheelbase at ground level.

The aerodynamic forces are computed from a simple model that allows investigation of the dependence of aerodynamic forces on the vehicle sideslip angle. However, the correct approach for computation of the aerodynamics sideslip angle in turning is undefined. In this work, the aerodynamic sideslip angle in turning is computed at the centre of the aerodynamic coordinate system (i.e. at mid-wheelbase):

$$\tan(\beta_{aero}) = \frac{{}^{A}V}{{}^{A}U} = \frac{{}^{V}V + r\cdot\left(\frac{b-c}{2}\right)}{{}^{V}U}$$

However, it was confirmed (see Chapter 4) that the forces generated have little sensitivity to the precise location of the sideslip angle reference point (e.g. whether the sideslip at the centre of mass, or at the aerodynamic reference point is used). This is because the vehicle yaw rate is always low when the aerodynamic forces are significant (i.e. at high forward speed, ${}^{P}U$), such that

$$\tan(\beta_{aero}) \approx \frac{{}^{V}V}{{}^{V}U} \approx \tan(\beta)$$

was shown to yield very similar results.

Aerodynamic Force Model

The aerodynamic force model employed is coefficient based (only up to second order), and therefore representative only for small angles of sideslip. Note that for ***linear*** models, ***only*** the terms in $\beta_{aero}(=\beta)$ remain.

$${}^{A}\underline{F}_{aero} = \frac{1}{2}\rho_a A\left({}^{P}U\right)^2\left(\begin{bmatrix} C_D|_{\beta=0} \\ C_Y|_{\beta=0} \\ C_L|_{\beta=0}\end{bmatrix} + \begin{bmatrix} \left.\frac{\partial C_D}{\partial\beta}\right|_{\beta=0} \\ \left.\frac{\partial C_Y}{\partial\beta}\right|_{\beta=0} \\ \left.\frac{\partial C_L}{\partial\beta}\right|_{\beta=0}\end{bmatrix}\beta_{aero} + \begin{bmatrix} \left.\frac{\partial^2 C_D}{\partial\beta^2}\right|_{\beta=0} \\ \left.\frac{\partial^2 C_Y}{\partial\beta^2}\right|_{\beta=0} \\ \left.\frac{\partial^2 C_L}{\partial\beta^2}\right|_{\beta=0}\end{bmatrix}\beta_{aero}^2\right)$$

$${}^{A}\underline{M}_{aero} = \frac{1}{2}\rho_a AE\left({}^{P}U\right)^2\left(\begin{bmatrix} C_{RM}|_{\beta=0} \\ C_{PM}|_{\beta=0} \\ C_{YM}|_{\beta=0}\end{bmatrix} + \begin{bmatrix} \left.\frac{\partial C_{RM}}{\partial\beta}\right|_{\beta=0} \\ \left.\frac{\partial C_{PM}}{\partial\beta}\right|_{\beta=0} \\ \left.\frac{\partial C_{YM}}{\partial\beta}\right|_{\beta=0}\end{bmatrix}\beta_{aero} + \begin{bmatrix} \left.\frac{\partial^2 C_{RM}}{\partial\beta^2}\right|_{\beta=0} \\ \left.\frac{\partial^2 C_{PM}}{\partial\beta^2}\right|_{\beta=0} \\ \left.\frac{\partial^2 C_{YM}}{\partial\beta^2}\right|_{\beta=0}\end{bmatrix}\beta_{aero}^2\right)$$

where

- A is the frontal area of the vehicle
- ρ_a is the density of the atmosphere
- E is the wheelbase of the vehicle ($E = b + c$)
- $C_D, C_Y, C_L, C_{RM}, C_{PM}$ and C_{YM} are the standard SAE aerodynamic coefficients for drag, lateral force, lift, rolling moment, pitching moment and yawing moment respectively.

2.10: Slip Velocities of Tyre Contact Patches

The slip velocities of the tyres relative to the ground are first determined in the ***vehicle*** coordinate system, V. The velocity at the contact patch comprises terms due to the velocity of the mass centre, the yaw rate of the vehicle and the rate of change of suspension deflection. This is because (as seen above), the in-plane position of the contact patch is a function of the suspension deflection.

Generally, in 3D, relative to the vehicle, the velocity of the tyre contact patch

$$\left.{}^{V}\underline{V}_k = {}^{V}\underline{V} + \left(\underline{\omega} \times {}^{V}\underline{r}_k\right) + {}^{V}\dot{\underline{r}}_k\right\} \quad k = FL, FR, RL, RR$$

which will have zero component in the direction normal to the ground plane, since the suspension velocity $\dot{d}_k$ is always determined such that this component is zero:

$$\left.{}^{V}\underline{V}_k \bullet {}^{V}\underline{n}_k = 0\right\} \quad k = FL, FR, RL, RR$$

Here:

d_k is the deflection of the suspension associated with wheel k

${}^{V}\underline{n}_k$ is the effective normal to the ground plane beneath the contact patch of the tyre k

${}^{V}\underline{r}_k(\delta_k)$ is the location of the contact patch of tyre relative to the vehicle centre of mass

For pure yaw plane models, where there is no roll motion and no suspension deflection, the above reduces to:

$$
\begin{aligned}
{}^{V}V_{FL} &= {}^{V}V_{FR} = {}^{V}V + br \\
{}^{V}V_{RL} &= {}^{V}V_{RR} = {}^{V}V - cr \\
{}^{V}U_{FL} &= {}^{V}U_{RL} = {}^{V}U + tr \\
{}^{V}U_{FR} &= {}^{V}U_{RR} = {}^{V}U - tr
\end{aligned}
$$

2.11: Quasi-static Wheel Rotation Model

The necessary tyre longitudinal forces are computed by assuming zero wheel spin inertia, i.e. that the tyre immediately generates the necessary force to balance the applied drive, brake and active differential torques:

$$\left. {}^{W}F_{x_k} = \frac{\left(T_{brake_k} + T_{drive_k} + T_{diff_k}\right)}{R_k} \right\} \quad k = FL, FR, RL, RR$$

Note: This model does not support wheel-spin or wheel-lock. The assumption is made that since (due to the shape of tyre force maps) for any force the tyre may generate within its unstable regime, the ***same*** force may be delivered with the tyre remaining within the stable operating regime (and thus at lower slip), optimal maneuvering need never demand the unstable (wheel-spin or wheel-lock) solution. In addition, in many conditions, only handling maneuvers, or steady-state longitudinal accelerations are considered - transient braking and acceleration events are not considered.

2.12: Coordinate Transformations

To facilitate large sideslip analysis (at least where non-linear models are employed), the proper trigonometric relationships are used in transforming between tyre-, vehicle- and path- coordinate systems.

The tyre forces expressed in the wheel-fixed coordinate system, W, may be transformed into the vehicle-fixed coordinate system, V by rotation through the steer angle of the wheel, δ:

$$\left.\begin{aligned} {}^{V}F_x &= {}^{W}F_{x_k}\cos(\delta_k) - {}^{W}F_{y_k}\sin(\delta_k) \\ {}^{V}F_y &= {}^{W}F_{x_k}\sin(\delta_k) + {}^{W}F_{y_k}\cos(\delta_k) \end{aligned}\right\} \quad k = FL, FR, RL, RR$$

The slip velocities computed in vehicle-fixed coordinates may be transformed into wheel-fixed coordinates by rotating them through the same steer angle, δ:

$$\left.\begin{aligned} {}^{W}U_k &= {}^{V}U_k\cos(\delta_k) + {}^{V}V_k\sin(\delta_k) \\ {}^{W}V_k &= -{}^{V}U_k\sin(\delta_k) + {}^{V}V_k\cos(\delta_k) \end{aligned}\right\} \quad k = FL, FR, RL, RR$$

The path-relative velocities of the vehicle centre of mass are also transformed between the vehicle-fixed coordinate system V and the path-centred coordinate system P, by rotation through the sideslip angle β (noting that the velocity lateral to the path, $V^P = 0$ ***always***):

$$\begin{aligned} {}^{V}U &= {}^{P}U\cos(\beta) - {}^{P}V\sin(\beta) \\ &= {}^{P}U\cos(\beta) \\ {}^{V}V &= {}^{P}U\sin(\beta) + {}^{P}V\cos(\beta) \\ &= {}^{P}U\sin(\beta) \end{aligned}$$

The vehicle-relative accelerations are converted to path-relative accelerations by the following transformation:

$$\begin{aligned} {}^{P}a_x &= {}^{V}a_x\cos(\beta) + {}^{V}a_y\sin(\beta) \\ {}^{P}a_y &= -{}^{V}a_x\sin(\beta) + {}^{V}a_y\cos(\beta) \end{aligned}$$

For ***linear*** models, this simplifies to:

$$\begin{aligned} {}^{P}a_x &= {}^{V}a_x + {}^{V}a_y\beta \\ {}^{P}a_y &= -{}^{V}a_x\beta + {}^{V}a_y \end{aligned}$$

2.13: Driveline Modelling

The driveline is assumed infinitely light and rigid, and no distinction is made between vehicle and wheel coordinate systems for shaft angular velocities (i.e. constant velocity joints are assumed). The four half-shaft speeds are therefore equal to the wheel rotation speeds, which may be computed directly from the tyre longitudinal slip:

$$w_k = \frac{{}^{W}U_k\left(s_k - 1\right)}{R_k} \Bigg\} \quad k = FL, FR, RL, RR$$

The engine speed and the angular velocities across the differentials may be computed from these half-shaft speeds, again taking into account the differential ratios:

$$w_{engine} = \sum_{k=1}^{4} w_k \cdot R_{d_k}$$

The 'differential speeds' against which a controlled clutch might act are simply equal to the difference in the speeds of the output shafts:

$$w_{diff_r} = w_{RR} - w_{RL}$$

$$w_{diff_f} = w_{FR} - w_{FL}$$

The proportion of the engine torque that is routed at each of the four wheels is determined by the differential ratios (with $R_{d_c} = 1$ giving pure front wheel drive, and $R_{d_c} = 0$ giving pure rear wheel drive):

$$R_{d_{FL}} = R_{d_c} \cdot \left(1 - R_{d_f}\right)$$

$$R_{d_{FR}} = R_{d_c} \cdot R_{d_f}$$

$$R_{d_{RL}} = \left(1 - R_{d_c}\right) \cdot \left(1 - R_{d_r}\right)$$

$$R_{d_{RR}} = \left(1 - R_{d_c}\right) \cdot R_{d_r}$$

The drive torque routed to each wheel is:

$$T_{drive_k} = R_{d_k} \cdot T_{engine} \Big\} \quad k = FL, FR, RL, RR$$

The torque contribution due to any controlled differentials is:

$$T_{diff_{FL}} = T_{diff_c} - T_{diff_f}$$

$$T_{diff_{FR}} = T_{diff_c} + T_{diff_f}$$

$$T_{diff_{RL}} = T_{diff_c} - T_{diff_r}$$

$$T_{diff_{RR}} = -T_{diff_c} + T_{diff_r}$$

2.14: Tyre Modelling

Transient tyre dynamics are modelled separately from the steady-state force generation (as a simple lag on the slip angle).

Linear Tyre Model

For the ***linear tyre model***, the longitudinal slip is related directly to the longitudinal force and similarly for the lateral direction (note that the force opposes the slip):

$$\left. {}^{W}s_k = -\frac{{}^{W}F_{x_k}}{C_{s_k}} \right\} \quad k = FL, FR, RL, RR$$

$$\left. {}^{W}F_{y_k} = -C_{\alpha_k} \tan(\alpha_k) \right\} \quad k = FL, FR, RL, RR$$

Note that for the ***linear*** tyre model, the force delivered at a given slip angle is independent of the vertical load F_{z_k} on the tyre (although the ***maximum*** force, in some linear analyses, is constrained by a ***non-linear*** function of the vertical load).

For the ***non-linear tyre model***, the relationship between slip and force requires a multidimensional lookup table (see the plots from the non-linear tyre model below).

Non-linear tyre model

For some of the analyses, a non-linear tyre model is required, since this captures some important phenomena in vehicle dynamics that a linear model does not. The non-linear tyre model implemented is based on the first and simplest version of the Pacejka Magic Formula. Generic force vs slip curves are generated off-line and stored in a lookup table. These are scaled according the the vertical load on the tyre, and the current value of the coefficient of friction. The tyre model is isotropic, such that the same slip curve exists for the longitudinal direction as for the lateral direction.

The tyre model employed is combined-slip, such that the in-plane forces ${}^{W}F_x$ and ${}^{W}F_y$ which are delivered is a function of:

- the tangent of the lateral slip angle, $\tan(\alpha)$
- the longitudinal slip ratio, s
- the lateral slip stiffness at zero slip, C_α (which is the stiffness assumed in the linear tyre model described below),

- the longitudinal slip stiffness at zero slip, C_s
- several parameters B, C, D, E which describe the non-linear shape of the force versus slip curve,
- the effective coefficients of friction in the lateral and longitudinal directions, μ_x and μ_y
- the vertical load on the tyre, F_z

The model is the following:

$$^{W}F_y = \overline{F_y}\hat{F}_y$$
$$^{W}F_x = \overline{F_x}\hat{F}_x$$

where

$$\overline{F_x} = \begin{cases} R\dfrac{s}{\sqrt{s^2 + n^2\tan(\alpha)^2}} & s^2 + n^2\tan(\alpha)^2 \neq 0 \\ 0 & s^2 + n^2\tan(\alpha)^2 = 0 \end{cases}$$

$$\overline{F_y} = \begin{cases} nR\dfrac{\tan(\alpha)}{\sqrt{s^2 + n^2\tan(\alpha)^2}} & s^2 + n^2\tan(\alpha)^2 \neq 0 \\ 0 & s^2 + n^2\tan(\alpha)^2 = 0 \end{cases}$$

where

$$n = \begin{cases} \dfrac{1}{2}(1 + n_0) - \dfrac{1}{2}(1 - n_0)\cos\left(\dfrac{k}{2}\right) & k < 2\pi \\ 1 & k \geq 2\pi \end{cases}$$

with

$$n_0 = \frac{C_\alpha \mu_x}{C_s \mu_y}$$

and the normalised slips are

$$\overline{\alpha} = \frac{C_\alpha \tan(\alpha)}{\mu_y F_z}$$

$$\overline{s} = \frac{C_s s}{\mu_x F_z}$$

yielding the normalised combined slip magnitude

$$k = \sqrt{\bar{s}^2 + \bar{\alpha}^2}$$

and the non-linear shape of the slip curve is defined by:

$$R = D\sin(\theta)$$

where

$$\theta = C\tan^{-1}(B\phi)$$

and

$$\phi = (1-E)k + \frac{E}{B}\tan^{-1}(Bk)$$

Dependence of tyre friction on vertical load

The model of vertical load dependence of tyre friction that was used for the analyses presented in this thesis is that of Gordon [Gordon, 1998]:

$$\hat{F}_{x_k}\left(F_{z_k}\right) = \frac{\mu_{x_k} F_{z_k}}{1 + \left(\dfrac{2F_{z_k}}{Mg}\right)^3}$$

$$\hat{F}_{y_k}\left(F_{z_k}\right) = \frac{\mu_{y_k} F_{z_k}}{1 + \left(\dfrac{2F_{z_k}}{Mg}\right)^3}$$

This model exhibits the typical 'diminishing returns' characteristic that is normally observed in real tyre data [Milliken, 1995], where the available frictional force doesnot quite increase linearly with the vertical load. **Note:** Alternative models of this vertical load dependence, all of which exhibit a similar characteristic, were also implemented. It was confirmed that all led to results of similar orders of magnitude and with similar trends (depending on the values of the parameters). Therefore, for the sake of consistency, a single model was used throughout the thesis.

It should be noted that many analyses undertaken in this thesis require a knowledge ***only*** of the maximum frictional forces, $\hat{F}_x(F_z)$ and/or $\hat{F}_y(F_z)$ that are available, and do not require specific knowledge of the variation of the force with slip up to this limit.

Rolling resistance

Rolling resistance forces vary with vehicle speed [Various, 1992]. However, rolling resistance is omitted from the tyre model here, since its influence on vehicle sensitivity to sideslip is considered to be minimal.

Example Output

The following plots give an example of the output from the tyre model, with the following parameters:

$$C_\alpha = 100000, C_s = 250000,$$
$$\hat{F} = 2700,$$
$$\mu_x = 1.3, \mu_y = 1.0,$$
$$B = 0.714, C = 1.40, D = 1, E = -0.2$$

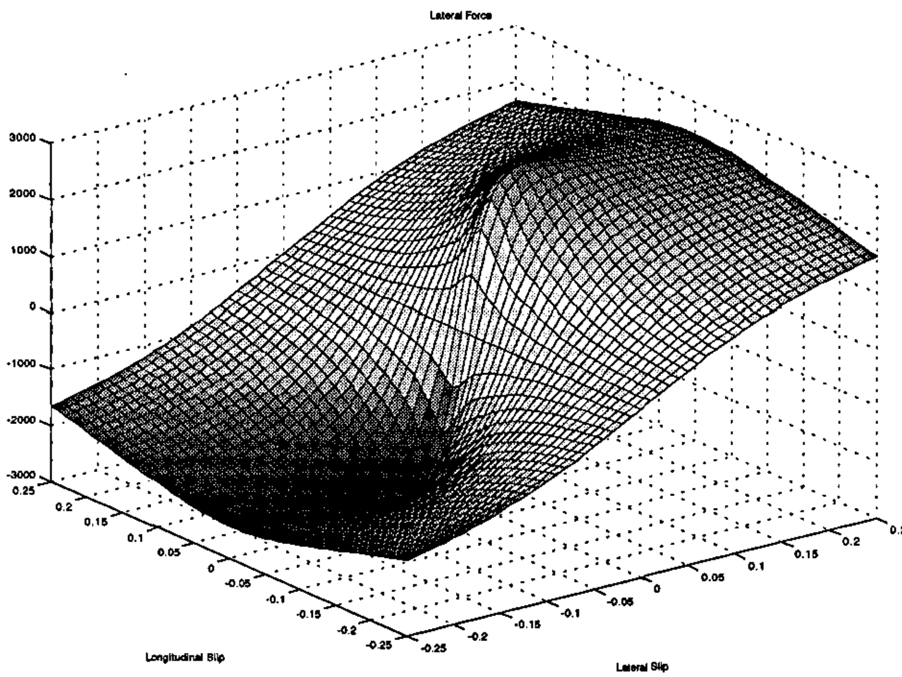

Figure 2.1:
Output from non-linear tyre model, showing lateral force against lateral and longitudinal slip, for fixed vertical load

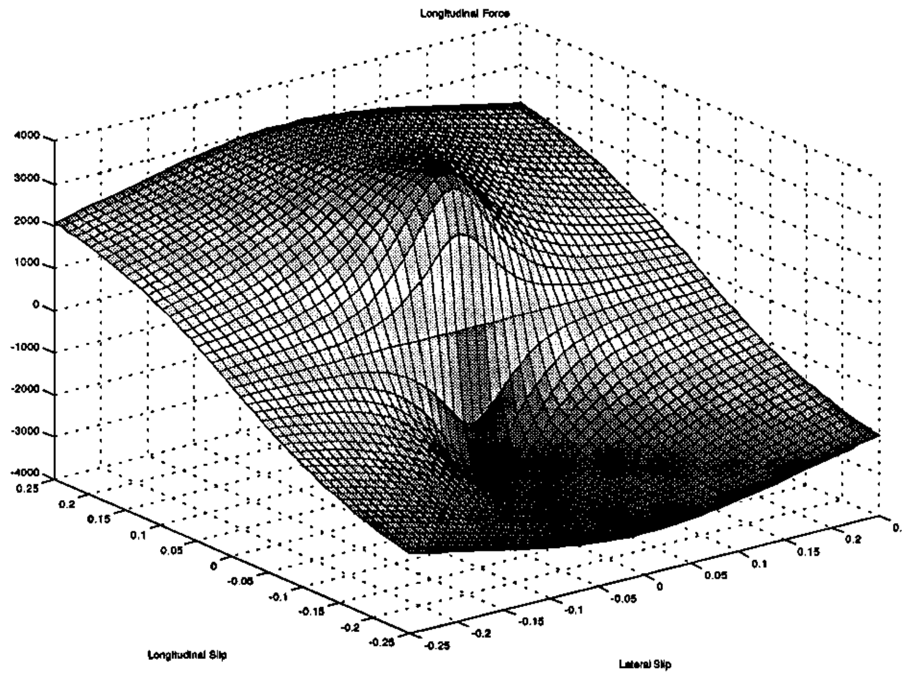

Figure 2.2
Output from non-linear tyre model, showing longitudinal force against lateral and longitudinal slip, for fixed vertical load

2.15: Concluding Remarks

In this section, all of the component models which are used throughout this thesis have been presented. In each analysis chapter, a subset of these equations is utilised, and combined as necessary to create a complete model of the vehicle dynamics.

The level of fidelity of the models, in general, is low. This is because the focus of this thesis is on the understanding of the very basic influences of fundamental design parameters and not, for instance, on the tuning of those performances using details such as suspension kinematics and compliances.

However, it is recognised that factors such as neglected degrees of freedom and the assumed form of non-linearities does mean that it is possible that different conclusions could be reached with alternative models. For this reason, for instance, various models of tyre non-linearity with respect to vertical load were implemented, and it was confirmed that the same phenomena and sensitivities of similar orders of magnitude were observed.

Chapter 3

Steady-State Performance

In this first chapter of analysis, the effect of sideslip on the ***steady-state*** performance of the vehicle is studied. Subsequent chapters consider the detail of the transient sideslip trajectory and the effect that this has on the forces which are required to maneuver the vehicle and effect changes in the sideslip state.

Here, the ***performance*** limit of the vehicle is identified - that is, the maximum acceleration which may be generated in the desired direction, whilst simultaneously satisfying the imposed constraints. It is assumed that whatever controller were fitted to the vehicle would be able to identify and apply whatever combination of controls turns out to be necessary in order to deliver the desired acceleration vector. Therefore, the limits of capability are identified ***without*** making reference to any control strategy, such that any control or identification errors which might occur with certain control strategies are deliberately excluded.

The goal is to identify the optimal sideslip angle and the sensitivity of the performance limits (i.e. the envelope of capability) to the sideslip angle, for different operating conditions. An optimisation approach is used to identify the optimal magnitudes and directions of the tyre forces. The acceleration of the vehicle is ultimately limited by maximum forces which fit inside the circles of friction of the tyres.

The hypothesis being tested here is H1.

3.1: Analysis Method

Problem specification

Constrained optimisations of several variables are carried out in order to determine the maximum acceleration that the vehicle (model) is able to generate along a given vector direction, with varying vehicle parameters, sideslip state and constraints on the vehicle acceleration.

In all cases, ***full authority*** over the in-plane tyre forces is assumed, such that there are eight variables (the 'controls'):

$$ {}^{P}F_{x_k}, {}^{P}F_{y_k} \quad k = FL, FR, RL, RR $$

all of which are available for optimisation in the range $-\infty < F < \infty$.

The scalar ***objective function*** of each optimisation is to maximise the magnitude of the ***projection*** of the vehicle acceleration vector onto a particular target direction $\underline{k}$ in ${}^{P}a_x - {}^{P}a_y - \alpha_z$ space:

$$ f = k_1 {}^{P}a_x + k_2 {}^{P}a_y + k_3 \alpha_z $$

where the values of k_1, k_2 and k_3 are the components of the vector $\underline{k}$, the direction in which the maximum acceleration is required. Note that the linear accelerations which are maximised are ***path-relative, not vehicle-relative***, since it is desired to distinguish performance in cornering from ability to change linear velocity.

Simultaneously, two basic types of constraint are enforced:

(i) ***equality constraints on the vehicle acceleration*** - to force the acceleration along one or both of the directions ***orthogonal*** to $\underline{k}$ either to zero, or to a required value.

For instance, to require a solution that is sustainable in steady-state, the equality constraint,

$$ \alpha_z \equiv 0 $$

is imposed, such that there is no acceleration in yaw (and thus the yaw rate of the vehicle would remain constant).

To require the centre of mass follow a particular path curvature ρ whilst accelerating or braking, a constraint

$$ {}^{P}a_y \equiv U^2 \rho $$

is enforced.

(ii) ***inequality constraints on friction utilisation*** - to ensure that the magnitudes of all of the in-plane tyre forces remain inside the friction circle for that tyre. This means that the magnitude of the in-plane frictional force must be ***less than or equal to*** the maximum frictional force available from that tyre:

$$ \sqrt{{}^{P}F_{x_k}^2 + {}^{P}F_{y_k}^2} \le \hat{F}_k\left(F_{z_k}\right) \quad k = FL, FR, RL, RR $$

Note that these are ***hard*** constraints, which are imposed by requiring that the optimisation absolutely reject solutions that do not satisfy the constraints. This is in contrast to other approaches which may simply modify the objective function such that violations of the constraints are 'costed' by an additional term.

The constrained maximum is identified using a standard ***gradient search*** optimisation method. In most cases, the starting point for the optimisation was chosen where the maximum force available from each tyre is generated in the same direction as the objective function. The optimisation routine iterates potential solutions by progressively moving in a direction that increases the objective function until one is found that is ***either*** limited by a constraint, or is a minimum of the objective function:

$$\frac{\partial f(\underline{x})}{\partial x_i}=0\ ,\ \frac{\partial^2 f(\underline{x})}{\partial x_i^2}<0\ \text{, for all } x_i$$

where $\underline{x}=\left[{}^PF_{x_{FL}}\,{}^PF_{y_{FL}}\,{}^PF_{x_{FR}}\,{}^PF_{y_{FR}}\,{}^PF_{x_{RL}}\,{}^PF_{y_{RL}}\,{}^PF_{x_{RR}}\,{}^PF_{y_{RR}}\right]$ is the vector of values ('controls') to be optimised, which is the same in all cases.

Note that in this Chapter, no attempt is made to find the optimal sideslip angle, since it was anticipated that the optimum would lie at an impractical value, and that it would therefore be necessary to impose an additional arbirtary constraint on the sideslip angle in order to find a 'practical' optimum angle, with the value of this user-specified constraint being returned as the identified optimum in most cases.

Instead, the influence of sideslip angle is identified and presented for a number of common scenarios where performance optimisation might be desirable (for instance, to facilitate successful obstacle avoidance [Blank, 2000]):

(i) Limit braking performance ***without*** any yaw motion constraint:

- $f=-{}^Pa_x$, such that ${}^Pa_x$ is minimised towards minus infinity
- α_z is unconstrained (so the optimal solutions which are identified may actually be unsteady-state - in any case where $\alpha_z\neq 0$ at the optimal solution).
- ${}^Pa_y$ is unconstrained (though it was confirmed that ${}^Pa_y=0$ at the optimal solution, such that the same solutions would be obtained with ${}^Pa_y=0$ as an imposed constraint)

The sideslip angle, β at the centre of mass is varied over the full range of possibilities -

from $-\pi$ (-180 degrees) to π ($+180$ degrees). This allows the influence of both small and large sideslip in either sense to be seen, and the continuity of the plot shows that the same (hopefully the global) extremum has been identified at $-\pi$ (-180 degrees) as has been identified at $+\pi$ ($+180$ degrees).

It is possible to identify the limit braking, acceleration ***and*** cornering performance from the same plot, since the solutions for these targets simply correspond to the same plot shifted by $\pm\pi$ (for acceleration, rather than braking) or by $\pm\pi/2$ (for cornering). This is because a certain change in sideslip angle is equivalent to an equal and opposite change in the direction of the desired acceleration vector . This is because the direction of the vehicle ***velocity*** vector does not influence the forces and accelerations which may be generated when full authority over the tyre forces is available:

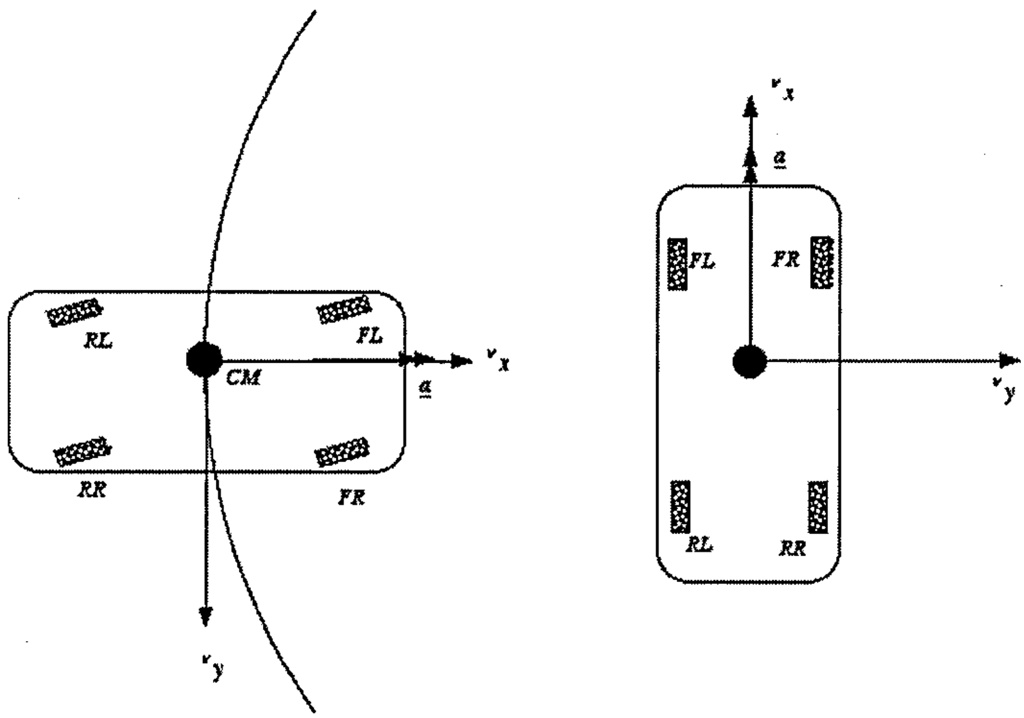

Figure 3.1a **Figure 3.1b**

Diagrams showing the *equivalence* of:

(a) cornering at 90 degrees of sideslip

(b) straight-line acceleration at zero sideslip

The absence of any constraint on yaw moment means that the plot will show only the influence of the distribution of vertical loads on the sum of the forces which can be generated by the tyres. Therefore, in this first plot, the fact that as the sideslip varies, the moment of those forces changes is not considered. Therefore, these accelerations could only be generated if the vehicle were allowed to simultaneously accelerate in yaw.

(ii) Limit braking, acceleration or steady-state cornering (with yaw motion constrained)

- $f = -{}^{P}a_x$, such that ${}^{P}a_x$ is minimised towards minus infinity
- ${}^{P}a_y$ and α_z are constrained to zero

Again, the sideslip angle, β is varied from $-\pi$ (-180 degrees) to π ($+180$ degrees). In this case, since the yaw motion is constrained, the optimal solution is a sustaniable steady-state. Again, the limit acceleration and cornering performance may be identified by shifting the same plot.

(iii) 'Split-mu' braking or acceleration, with yaw motion constraint

- $f = -{}^{P}a_x$, such that ${}^{P}a_x$ is minimised towards minus infinity
- ${}^{P}a_y$ and α_z are constrained to zero
- the friction coefficients of the left wheels $\mu_{FL} = \mu_{FR}$ and those of the right wheels $\mu_{RL} = \mu_{RR}$ differ

Again, the sideslip angle, β is varied from $-\pi$ (-180 degrees) to π ($+180$ degrees). However, the validity of the results for large sideslip angle is questionable, since the coefficients of friction are fixed with the tyres. Again, the limit cornering performance may also be identified from the same plot with a shift of $\pm\pi/2$ (± 90 degrees).

(iv) Braking or accelerating in a turn

- $f = -{}^{P}a_x$, such that ${}^{P}a_x$ is minimised towards minus infinity
- ${}^{P}a_y$ is constrained to a ***nonzero*** value

This final, more complex scenario generates a lateral load transfer and thus a left to right difference in available frictional forces that is similar to that which occurs on the split-mu surface. Again, the sideslip angle, β is varied between zero and 360 degrees.

3.2: Choice of Model

For this analysis, a quasi-static, yaw-plane, model with non-linearities (due to sideslip angle and with respect to tyre vertical load) was derived from the equations presented in Chapter 2, with assumptions of:

- steady-state roll motion: $p = 0, \dot{p} = 0$
- negligible roll compliance (and thus roll angle): $\phi = 0$
- non-zero sideslip: $\beta = \frac{V}{U} \neq 0$
- negligible influence of aerodynamic and rolling resistance forces

These assumptions were selected such that the fundamental influence of sideslip on steady-state and instantaneous performance, including effects due to geometric and tyre non-linearities, could be identified ***without*** any influence of transient dynamics or roll motion.

Additionally, it could be seen that if aerodynamic and rolling-resistance forces were neglected, then neither the forward speed U nor the yaw rate state r appear in the equations of motion. This was a benefit, since the identified results were applicable over a range of vehicle speeds.

For this analysis, the in-plane tyre forces are ***not*** expressed in the wheel coordinate system W. Instead, it is assumed that all control over the tyre slip and thus force is available, and therefore, the optimal in-plane tyre forces, F_x and F_y are simply identified ***directly*** in the vehicle coordinate system, V, rather than being identified in the wheel coordinate system W and then rotated into the vehicle system. However, it is necessary to transform the forces in the vehicle co-ordinate system into the path co-ordinate system, since accelerations relative to the path are of interest in terms of maneuvering, but accelerations relative to the vehicle are important for load transfer.

As described above, each of the four in-plane tyre force vectors is subject to a single constraint, that $\sqrt{{}^{P}F_{x_k}^2 + {}^{P}F_{y_k}^2} \leq \hat{F}_k\left(F_{z_k}\right) \quad k = FL, FR, RL, RR$.

The available frictional force $\hat{F}_k\left(F_{z_k}\right)$ is defined by the tyre model:

$$\hat{F}_k\left(F_{z_k}\right)=\frac{\mu_k F_{z_k}}{1+\left(\frac{2F_{z_k}}{\mathrm{Mg}}\right)^3}$$

and the vertical load is determined from a quasi-static vertical load transfer model. This load transfer model assumes a fixed ratio of roll compliances between front and rear suspension, and neglects any mass centre shift relative to the wheel base, contact patch shift relative to the vehicle or wheel lift, all of which are effects that might occur due to roll compliance, but which are fundamentally unconnected with the influence of sideslip.

The vehicle model utilised is therefore simply:

$$\begin{bmatrix} 1 & 1 & 1 & 1 \\ \text{-b} & \text{-b} & \text{c} & \text{c} \\ t & -t & t & -t \\ 1 & \text{-1} & -\lambda & \lambda \end{bmatrix}\begin{bmatrix} F_{z_{FL}} \\ F_{z_{FR}} \\ F_{z_{RL}} \\ F_{z_{RR}} \end{bmatrix}=\begin{bmatrix} Mg \\ h\sum_{k=1}^{4} {}^{V}F_x \\ h\sum_{k=1}^{4} {}^{V}F_y \\ 0 \end{bmatrix}$$

where the four equations represent the quasi-static force and moment balances for the vertical, pitch, roll and warp degrees of freedom, and

$\lambda=\frac{\Delta F_{z_f}}{\Delta F_{z_r}}$ is the ratio of front lateral load transfer to rear lateral load transfer

$$\begin{aligned}\Delta F_{z_f} &= \left(F_{z_{FL}} - F_{z_{FR}}\right) \\ \Delta F_{z_r} &= \left(F_{z_{RL}} - F_{z_{RR}}\right)\end{aligned}$$ are the lateral load transfer at each axle

Kinematic and compliant effects in the suspension that might cause changes in camber or steer angles are also omitted, since the optimisation is given full control over the tyre forces. The ability of a controller to control steering and therefore to cancel any kinematic or compliance effects is implicit in this assumption. The objective of these assumptions is to separate the fundamental influence of sideslip from other possible confounding influences such as additional load transfer due to excessive roll compliance, or forces arising due to the specific aerodynamic characteristics of a particular vehicle.

The controls which are optimised are the forces in the vehicle co-ordinate system, but the translational accelerations that are optimised are those in the path co-ordinate system $\left({}^{P}a_x,\ {}^{P}a_y\right)$, such that the vehicle performance as a result of the controls is found from:

$$
\begin{aligned}
{}^{P}a_x &= {}^{V}a_x\cos(\beta) + {}^{V}a_y\sin(\beta) \\
{}^{P}a_y &= -{}^{V}a_x\sin(\beta) + {}^{V}a_y\cos(\beta)
\end{aligned}
$$

where

$$
\begin{aligned}
{}^{V}a_x &= \frac{1}{M}\sum_{k=1}^{4}{}^{V}F_x \\
{}^{V}a_y &= \frac{1}{M}\sum_{k=1}^{4}{}^{V}F_y
\end{aligned}
$$

and

$$\alpha_z = \frac{1}{I_{zz}}\left[b\left({}^{V}F_{y_{FL}} + {}^{V}F_{y_{FR}}\right) - c\left({}^{V}F_{y_{RL}} + {}^{V}F_{y_{RR}}\right) + t\left({}^{V}F_{x_{FL}} - {}^{V}F_{x_{FR}}\right) + t\left({}^{V}F_{x_{FL}} - {}^{V}F_{x_{FR}}\right)\right]$$

Note that the yaw acceleration, α_z is computed directly from the forces in the vehicle co-ordinate system, since $\alpha_z = {}^{P}\alpha_z = {}^{V}\alpha_z$ and the moment arms remain constant if the forces are expressed in the vehicle co-ordinate system, which simplifies the mathematics.

3.3: Results and Discussion

Local and Global Extrema

In certain circumstances, the results exhibited trends which suggested that the routine was becoming trapped in different, local extrema. Therefore, each result was analysed critically before accepting it. The approach taken to try to achieve global optimality was to begin with a condition where the globally optimal combination of tyre forces was straightforward to identify (such as straight-line braking on equal friction). From this condition, the variables were ***slowly*** varied until the condition of interest was reached, and the solution was accepted if and only if the optimal solutions varied continuously with the changes in the demand, indicating that the same optimum was being tracked. Where the solution changed discontinuously at any point, the result was rejected. Although this approach does not absolutely guarantee that the global optimum has been found, the application of engineering judgment to each of the results suggested strongly that the optimal solution had indeed been found.

(i) Limit performance without any yaw motion constraint

First, it was desired to understand the effect that sideslip, centre of mass location and roll-stiffness distribution have on the tyre vertical loads ($F_{z_{FL}}, F_{z_{FR}}, F_{z_{RL}}, F_{z_{RR}}$), and what the effect of this is on the basic acceleration and deceleration performance of the vehicle. In order to understand this, the maximum translational acceleration was identified without placing any constraint on the yaw acceleration, α_z. The implication of this is that the acceleration which is generated could not be generated continuously in steady-state; only during a transient, but it allows the separation of the effect that sideslip has on tyre loading from the effect that it has on the yawing moment, since the yaw acceleration has no direct contribution to changes in tyre vertical load, but constraining the yaw acceleration to zero (as in the following simulation) may cause the lateral acceleration performance degrade, since lateral force must be compromised in order to use the same friction for the balancing of yaw moments.

In the results, a practically feasible region of sideslip is indicated using dotted lines at ±15 degrees, though results are shown across the full range of possible sideslip angles, since this can help with understanding of the plots.

The hypothesis being investigated here is **H1** - that by varying the vehicle sideslip angle, it may be possible to influence the tyre loading and thus improve the acceleration performance envelope of the vehicle.

The focus of the first plots, figures 3.2 and 3.4 to 3.6 is on braking performance, because it is considered that a reduction (rather than an increase) of speed is normally the better strategy for accident avoidance.

Figure 3.2 therefore shows the maximum stopping deceleration (maximum negative acceleration in the ${}^{P}x$ direction) performance of a vehicle travelling along a straight path (i.e. with zero yaw rate r and lateral acceleration ${}^{P}a_y$), with yawing moments ***unconstrained.***

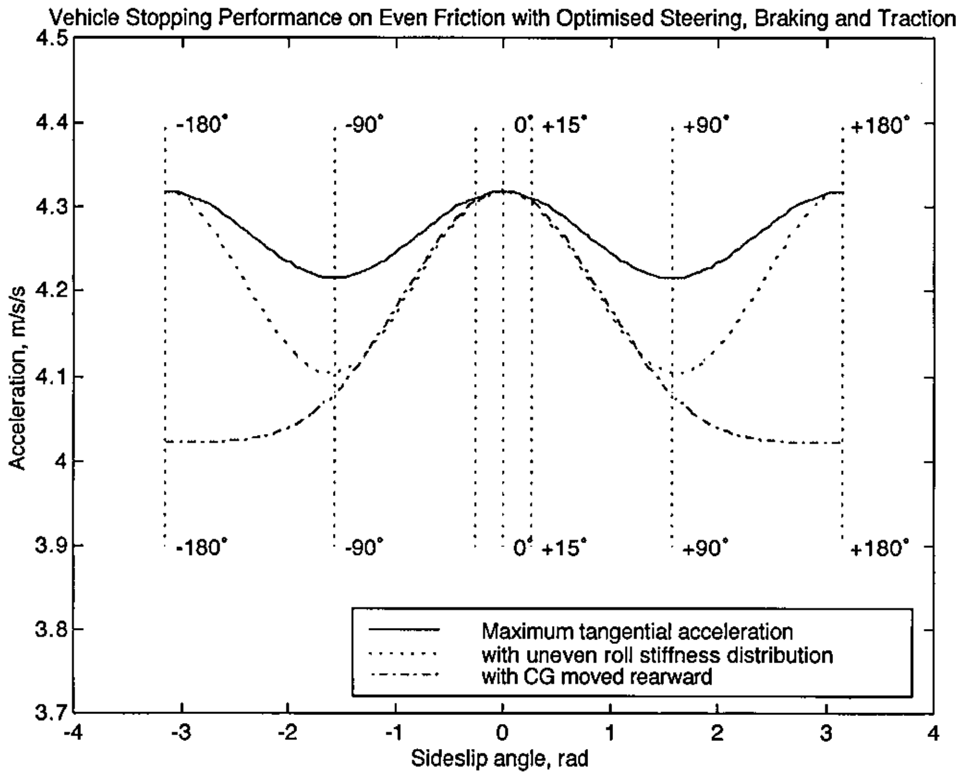

Figure 3.2

Vehicle Stopping Performance $\left(f = -{}^{P}a_x\right)$ **with varying tyre load distribution**

$$\mu_{FL} = \mu_{FR} = \mu_{RL} = \mu_{RR} = 0.5, M = 1400, h = 0.4, t_f = t_r = 0.7$$

(i) baseline $(b = c = 1.35, \lambda = 1)$

(ii) uneven roll stiffness distribution $(b = c = 1.35, \lambda = 0.7)$

(iii) rearward centre of mass (CG) $(b = 1.7, c = 1.0, \lambda = 1)$

For the centre CG vehicle, it can be seen that even when there is no requirement for zero yaw moment, peak performance is achieved at either zero or 180 degrees of sideslip (where the load transfer due to the acceleration vector occurs about the vehicle y axis).

By shifting the plot 180 degrees, the straight-line acceleration performance can also be identified. The solid line shows a vehicle where the centre of mass is located exactly in the centre of the wheelbase $(b = c)$, and it can be seen that the performance at zero sideslip in acceleration is equal to the performance at zero sideslip in braking (i.e. at 180 degrees of sideslip in acceleration).

The peak performance is seen at these sideslip angles because the overturning moment due to the height of the centre of mass above the tyre contact patches is reacted across the (longer) wheelbase, rather than across the (narrower) track of the vehicle. This reduces the magnitude of the load changes on the tyres:

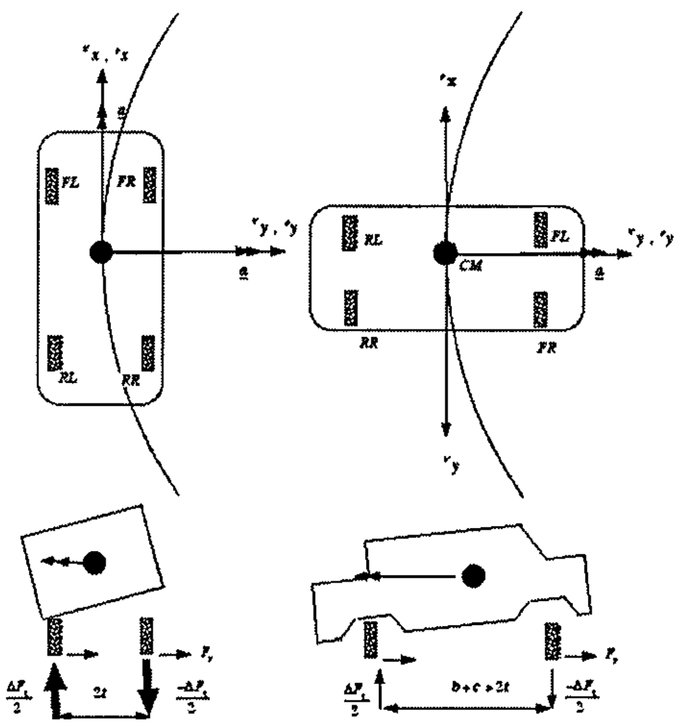

Figure 3.3a **Figure 3.3b**

Diagrams showing rolling moment reacted:
(a) across the typically narrow track (zero sideslip)
(b) across the typically longer wheelbase (90 degrees of sideslip)
and showing the lower load transfer in the latter case

Note: since all available controls are assumed (i.e. there is no limit on engine power or on steering angles) the best-case acceleration performance is equal to the best-case deceleration performance. This can be seen by making a 180 degree shift in the plot (i.e. a 180 degree shift in the sideslip angle ***relative*** to the acceleration vector). It can therefore be seen that for a vehicle with a centre of mass located mid-wheelbase, the acceleration performance at zero sideslip is (unsurprisingly) equal to the deceleration performance.

The worst performance can be seen to occur at –90 or +90 degrees of sideslip, where this pitching/rolling moment is reacted purely about the vehicle x axis, i.e. across the narrow track, rather than across the long wheelbase of the vehicle.

At 90 degrees of sideslip, with this tyre model, however, ***only 5% of the optimal deceleration is lost.*** Within the broadly practical range of –15 to +15 degrees, the change in performance is negligible.

For the vehicle with the CG moved rearwards, such that the tyre loading is more even in deceleration, it can be seen that the improvement in deceleration performance is negligible, yet the deterioration in acceleration performance (or equivalently, the braking performance at 180 degrees of sideslip) is significant. Between 0 and 180 degrees is can be seen that performance deteriorates progressively, with limited sensitivity to small changes in sideslip around 0 and 180 degrees. This finding is typical of the 'diminishing returns' character of the performance of tyres. For the vehicle with an uneven roll stiffness distribution, it can be seen that the performance at 0 and 180 degrees is equal, since the roll stiffness does not affect either the braking or acceleration performance. Performance is worst (similar to the offset CG vehicle) at 90 degrees (i.e. in cornering).

It can be seen that all of the vehicles exhibit the same region of near-zero sensitivity to sideslip angle around 0 and 180 degrees. This indicates that variation of the sideslip is having little beneficial or detrimental influence on the tyre loads.

For the rearward CG vehicle, it can be seen that there is some sensitivity to sideslip in cornering, with nose-out sideslip improving the lateral acceleration performance. This is due to the fact that nose-out sideslip in cornering causes some of the pitching moment to be reacted along the wheelbase (i.e. about the vehicle pitch axis, y), and forward-transfer of load evens out the uneven loading caused by the rearward centre of mass.

(ii) Limit braking, acceleration or cornering with yaw motion constrained

The results from the above analysis showed clearly the influence of sideslip, roll stiffness distribution and mass centre location on the maximum forces that the tyres are able to generate. However, these results have strongly limited validity in the real world, where the yawing moment that is generated must also be controlled (i.e. constrained to that required to keep the yaw motion and thus the future sideslip of the vehicle under control). Figure 3.3 indicates the influence of the ***yaw moment constraint*** on the vehicle deceleration performance.

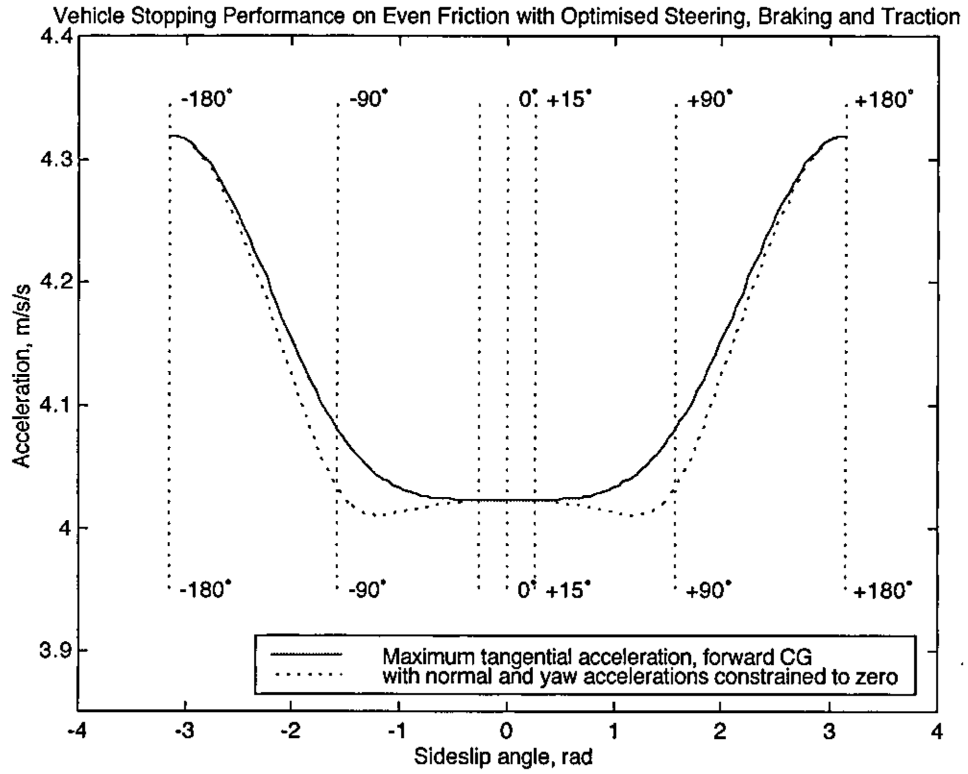

Figure 3.4

Influence of Yaw Moment Constraint

$$\mu_{FL} = \mu_{FR} = \mu_{RL} = \mu_{RR} = 0.5, M = 1400, h = 0.4, t_f = t_r = 0.7, b = 1.0, c = 1.7, \lambda = 1$$

(i) without yaw moment constraint $\left(f = -{}^P a_x\right)$

(ii) with yaw moment constraint $\left(f = -{}^P a_x, \alpha_z = 0\right)$

Here, the performance is shown for a vehicle with a forward CG, since this is typical of modern passenger cars, and the best-case performance with unconstrained yaw moments $(\alpha_z \neq 0)$ has been contrasted to the best-case performance with constrained yaw moments - in this case, the yaw acceleration has been constrained to zero $(\alpha_z = 0)$ since this represents the requirement for the common, steady-state cornering scenario.

It can be seen that the introduction of this constraint causes performance to be lost (rather than gained) at every sideslip angle, as expected. However, it shows that this loss occurs only when the sideslip angle is relatively large (outside the region of interest). This indicates that small sideslip angles (e.g. due to aerodynamic disturbances, or the end of a cornering transient) have negligible influence on the stopping performance of the vehicle.

However, ***in cornering*** - i.e. with the acceleration vector and thus the plot or the region of interest once again shifted 90 degrees, it is clear that the performance is worsened by the introduction of the yaw moment constraint. This is due to the need for the optimisation to compromise the force directions in order to balance the yawing moments acting on the vehicle - in this case, the forces ***do not*** act precisely lateral to the path they have some longitudinal component that serves to balance the total yaw moment on the vehicle. Therefore, since the lateral force must be compromised in order to generate the longitudinal component, the maximum lateral force and thus the maximum lateral acceleration is reduced.

In addition, there is a slightly ***greater sensitivity*** of the performance to the sideslip angle when the yaw moment is constrained, since it is not only the tyre loading which is influenced by the sideslip angle, but the ***moments*** of the tyre forces about the centre of mass.

For the vehicle shown, with a ***forward*** centre of mass, it can be seen that tail-out sideslip ***improves the performance***. This would have been expected based on the results from the previous analyses with unconstrained yaw moments since this sideslip causes some of the rolling moment to be reacted across the wheelbase, increasing the loads on the rear tyres and thus evening out the vertical loads and allowing the tyres to work more effectively. However, the sensitivity to sideslip is ***greater*** in this case. This is due to the fact that as the vehicle is rotated in sideslip relative to the path, the more heavily loaded outer tyres move forwards relative to the centre of mass, and each is therefore able to generate a greater turn-in moment at the same time as generating a lateral force.

Mechanism of sensitivity of yaw moment to sideslip

The mechanism by which the moments of the forces changes as the sideslip angle at the centre of mass is varied can be seen from a simple model of the yawing moments which would occur due to purely path-lateral forces.

The yawing moment due to a path-lateral force ${}^{P}F_{y_{FL}}$ acting at the front left tyre is

$$M_{z_{FL}} = {}^{P}F_{y_{FL}} r_f \cos(\theta_f - \beta)$$

and for the other tyres, the yaw moments are:

$$M_{z_{FR}} = {}^{P}F_{y_{FR}} r_f \cos(\theta_f + \beta)$$
$$M_{z_{RL}} = -{}^{P}F_{y_{RL}} r_r \cos(\theta_r + \beta)$$
$$M_{z_{RR}} = -{}^{P}F_{y_{RR}} r_r \cos(\theta_r - \beta)$$

where

r_f is the magnitude of the vector distance from the centre of mass to the front tyre contact patch, when projected into the vehicle $x-y$ plane

θ_f or θ_r is the magnitude of the angle between the longitudinal $\left({}^{V}x\right)$ axis of the vehicle and a line through both the centre of mass and the tyre contact patch

Such that the total yaw moment is:

$$M_z = M_{z_{FL}} + M_{z_{FR}} + M_{z_{RL}} + M_{z_{RR}}$$

and the change in total yaw moment due to a change in sideslip angle β is:

$$\frac{\partial M_z}{\partial \beta} = \frac{\partial M_{z_{FL}}}{\partial \beta} + \frac{\partial M_{z_{FR}}}{\partial \beta} + \frac{\partial M_{z_{RL}}}{\partial \beta} + \frac{\partial M_{z_{RR}}}{\partial \beta}$$

where, again taking the example of the ***front left*** corner,

$$\frac{\partial M_{z_{FL}}}{\partial \beta} = \lim_{\Delta\beta \to 0}\left\{\frac{M_{z_{FL}}(\beta - \Delta\beta) - M_{z_{FL}}(\beta + \Delta\beta)}{2\Delta\beta}\right\}$$
$$= {}^{P}F_{y_{FL}} r_f \lim_{\Delta\beta \to 0}\left\{\frac{\cos(\theta_f - (\beta - \Delta\beta)) - \cos(\theta_f - (\beta + \Delta\beta))}{2\Delta\beta}\right\}$$

employing compound angle identities yields

$$\frac{\partial M_{z_{FL}}}{\partial \beta} = {}^{P}F_{y_{FL}} r_f \lim_{\Delta\beta \to 0}\left\{\frac{1}{2\Delta\beta}\begin{pmatrix}\cos(\theta_f)\cos((\beta - \Delta\beta)) + \sin(\theta_f)\sin((\beta - \Delta\beta)) \\ -\cos(\theta_f)\cos((\beta + \Delta\beta)) - \sin(\theta_f)\sin((\beta + \Delta\beta))\end{pmatrix}\right\}$$
$$= {}^{P}F_{y_{FL}} r_f \left(\cos(\theta_f)\sin\beta - \sin(\theta_f)\cos\beta\right)$$

Applying the same identities for the front right corner yields:

$$\frac{\partial M_{z_{FR}}}{\partial \beta} = \lim_{\Delta\beta \to 0}\left\{\frac{M_{z_{FR}}(\beta - \Delta\beta) - M_{z_{FR}}(\beta + \Delta\beta)}{2\Delta\beta}\right\}$$
$$= {}^{P}F_{y_{FR}} r_f \left(\cos(\theta_f)\sin\beta + \sin(\theta_f)\cos\beta\right)$$

and similarly for the rear tyres,

$$\frac{\partial M_{z_{RL}}}{\partial \beta} = -{}^{P}F_{y_{FR}} r_r \left(\cos(\theta_r)\sin\beta + \sin(\theta_r)\cos\beta\right)$$

$$\frac{\partial M_{z_{RR}}}{\partial \beta} = -{}^{P}F_{y_{FR}} r_r \left(\cos(\theta_r)\sin\beta - \sin(\theta_r)\cos\beta\right)$$

such that

$$\begin{aligned}\frac{\partial M_z}{\partial \beta} = {}&{}^{P}F_{y_{FL}} r_f \left(\cos(\theta_f)\sin\beta - \sin(\theta_f)\cos\beta\right)\\ &+{}^{P}F_{y_{FR}} r_f \left(\cos(\theta_f)\sin\beta + \sin(\theta_f)\cos\beta\right)\\ &-{}^{P}F_{y_{RL}} r_r \left(\cos(\theta_r)\sin\beta + \sin(\theta_r)\cos\beta\right)\\ &-{}^{P}F_{y_{RR}} r_r \left(\cos(\theta_r)\sin\beta - \sin(\theta_r)\cos\beta\right)\end{aligned}$$

and therefore for small sideslip angle at the centre of mass, β,

$$\begin{aligned}\frac{\partial M_z}{\partial \beta} = {}&\left(\left({}^{P}F_{y_{FL}} + {}^{P}F_{y_{FR}}\right) r_f \cos(\theta_f) - \left({}^{P}F_{y_{RL}} + {}^{P}F_{y_{RR}}\right) r_r \cos(\theta_r)\right)\beta\\ &+\left({}^{P}F_{y_{FR}} - {}^{P}F_{y_{FL}}\right) r_f \sin(\theta_f) + \left({}^{P}F_{y_{RR}} - {}^{P}F_{y_{RL}}\right) r_r \sin(\theta_r)\end{aligned}$$

or

$$\begin{aligned}\frac{\partial M_z}{\partial \beta} = {}&\left(\left({}^{P}F_{y_{FL}} + {}^{P}F_{y_{FR}}\right) b - \left({}^{P}F_{y_{RL}} + {}^{P}F_{y_{RR}}\right) c\right)\beta\\ &+\left({}^{P}F_{y_{FR}} - {}^{P}F_{y_{FL}}\right) t_f + \left({}^{P}F_{y_{RR}} - {}^{P}F_{y_{RL}}\right) t_r\end{aligned}$$

It can be seen from the first term that sensitivity of the yaw moment to sideslip angle at the centre of mass ***increases*** with increasing sideslip in situations of large yawing moment $\left({}^{P}F_{y_{FL}} + {}^{P}F_{y_{FR}}\right) b - \left({}^{P}F_{y_{RL}} + {}^{P}F_{y_{RR}}\right) c$ (e.g. during turn-in).

The second component in the sensitivity is more important since it exists even in steady-state cornering, and even around $\beta = 0$. This term is due to the difference in lateral forces generated by the left and right tyres (due, for instance to load transfer or Ackerman steering geometry), and corresponds to the additional turning-in moment caused by the 'forward shift' of the outer tyres mentioned above:

$$\begin{aligned}\left.\frac{\partial M_z}{\partial \beta}\right|_{\beta=0} &= \left({}^{P}F_{y_{FR}} - {}^{P}F_{y_{FL}}\right) r_f \sin(\theta_f) + \left({}^{P}F_{y_{RR}} - {}^{P}F_{y_{RL}}\right) r_r \sin(\theta_r)\\ &= \left({}^{P}F_{y_{FR}} - {}^{P}F_{y_{FL}}\right) t_f + \left({}^{P}F_{y_{RR}} - {}^{P}F_{y_{RL}}\right) t_r\end{aligned}$$

It is also worthy of note than this sensitivity to sideslip angle increases directly with ***both*** t_f and t_r, indicating that vehicles with wide track are more sensitive to changes in sideslip angle. This is consistent with the observations of professional drivers, that 'square' vehicles with a low ***wheelbase-to-track ratio*** feel 'twitchy', i.e. inconsistent in their sensitivity to the controls.

This increase in turn-in moment as (nose-out) sideslip angle at the centre of mass increases allows the rear tyres to generate a greater stabilsing moment and thus generate greater cornering forces, and contributes to a net improvement in the performance of the vehicle. In other words, the steady-state cornering performance of the vehicle is ***significantly influenced*** by the sideslip angle, with tail-out improving the performance of a naturally under-steering vehicle.

Speed-dependence of the motion centre location of a 2WS vehicle

One further question which should be considered is whether the motion centre location need be speed-dependent. In this sense, an interesting result and some understanding can be derived from the analysis of the steady-state turning of a 2WS vehicle.

Speed-dependence of motion centre location, d, is an effect which occurs in the steady-state behaviour of a 2WS vehicle. In steady-state turning at constant forward speed U, for a vehicle guided only by lateral (steering) forces F_{y_f} and F_{y_r}, yaw moment balance is required:

$$F_{y_f} = \frac{c}{b} F_{y_r}$$

such that the lateral acceleration is

$$a_y = \frac{F_{y_f} + F_{y_r}}{M} = F_{y_r}\left(\frac{E}{b}\right)$$

If the rear tyre force (and thus the sideslip) is controlled by a tyre then

$$F_{y_r} = -C_{\alpha_r}\alpha_r$$

and if the tyre is un-steered (i.e. 2WS, not 4WS or AWS), then the slip angle is generated only by the lateral slip of the rear axle:

$$\alpha_r = \frac{V - cr}{U}$$

therefore,

$$a_y = -C_{\alpha_r}\left(\frac{V - cr}{U}\right)\left(\frac{E}{b}\right)$$

In steady-state, the lateral acceleration is directly related to the yaw rate

$$a_y = Ur$$

thus

$$r\left(1 - \frac{cC_{\alpha_r}E}{bU^2}\right) = -V\left(\frac{C_{\alpha_r}E}{bU^2}\right)$$

such that

$$d_{2WS,ss} = -\frac{V}{r} = -c + \frac{b}{C_{\alpha_r}E}U^2$$

It can quickly be seen that at zero speed, this collapses to the expected result of zero sideslip at the rear axle $d_{2WS}\big|_{U=0} = -c$. However, the second term indicates that the motion centre moves ***forwards*** as the speed increases, in proportion to the square of the forward speed.

Note: this change in motion centre location due to cornering compliance is the reason that 2WS vehicles always have a forward speed at which they exhibit zero sideslip in steady-state, (when $U = \sqrt{\frac{c}{b}C_{\alpha_r}E}$).

Since the sideslip angle β (rather than the sideslip velocity V) is the primary influence on steady-state stability and cornering performance, as shown in Chapter 3, and the tyre force vectors $\underline{F}$ remain approximately the same for the same lateral acceleration $a_y = Ur$ as the speed changes, the influence of the motion centre location on steady-state stability at a given lateral acceleration is:

$$\frac{\beta}{a_y} = \frac{V}{U^2 r} = -\frac{d}{U^2}$$

such that the stability influence of the 2WS sideslip characteristic, comprising terms due to (i) kinematics and (ii) cornering compliance - is:

$$\frac{\beta}{a_y} = \frac{V}{U^2 r} = -\frac{d}{U^2} = \frac{c}{U^2} - \frac{b}{C_{\alpha_r}E}$$

The striking thing about this is that it is ***not*** the change in position of the motion centre as speed increases that leads to any reduction in stability of a vehicle as speed increases (for the same lateral acceleration); it is the reduction of the ***influence*** of nose-out kinematic sideslip on stability as speed increases. This suggests that a simple proportional 4WS $\left(\delta_f = \frac{b}{E}\rho,\ \delta_r = \frac{-c}{E}\rho\right)$ that removes the term in U^{-2} should have a positive effect in removing changes in the stability influence of sideslip as forward speed changes. According to this simple model, sideslip angle (and the associated destabilisation) would then change only with increasing lateral acceleration.

The Initial Motion Centre of a 2WS Vehicle

At higher speed, the response of typical of 2WS vehicles is dominated by a second-order pole pair so that the motion centre location will generally shift during a transient. It can however, be shown that the ***initial motion centre*** location for a 2WS vehicle is always behind the centre of mass, at a point known as the ***centre of percussion*** [Den Hartog, 1984] of the vehicle with respect to forces applied laterally at the front axle:

$$d_{initial,2WS} = -\frac{k^2}{b}$$

This is due to the fact that for a 2WS vehicle, the initial rear axle lateral force $F_{y_r}(0)$ is always zero. Therefore, the motion centre will move from $d_{initial,2WS}$ to the steady-state location identified above during the transient, such that the stability influence of the sideslip angle will vary throught the transient.

(iii) Split-mu braking or acceleration with yaw motion constraint

Figure 3.4 shows a further case where the performance of the vehicle is significantly sensitive to the sideslip angle – that of stopping on a split-mu surface (i.e. where the available friction under left and right wheel tracks differs) ***with*** the yaw moment constraint that is required to prevent the vehicle from spinning. It can be seen that the sensitivity to sideslip angle is in strong contrast to the insensitivity found for the even-mu surface.

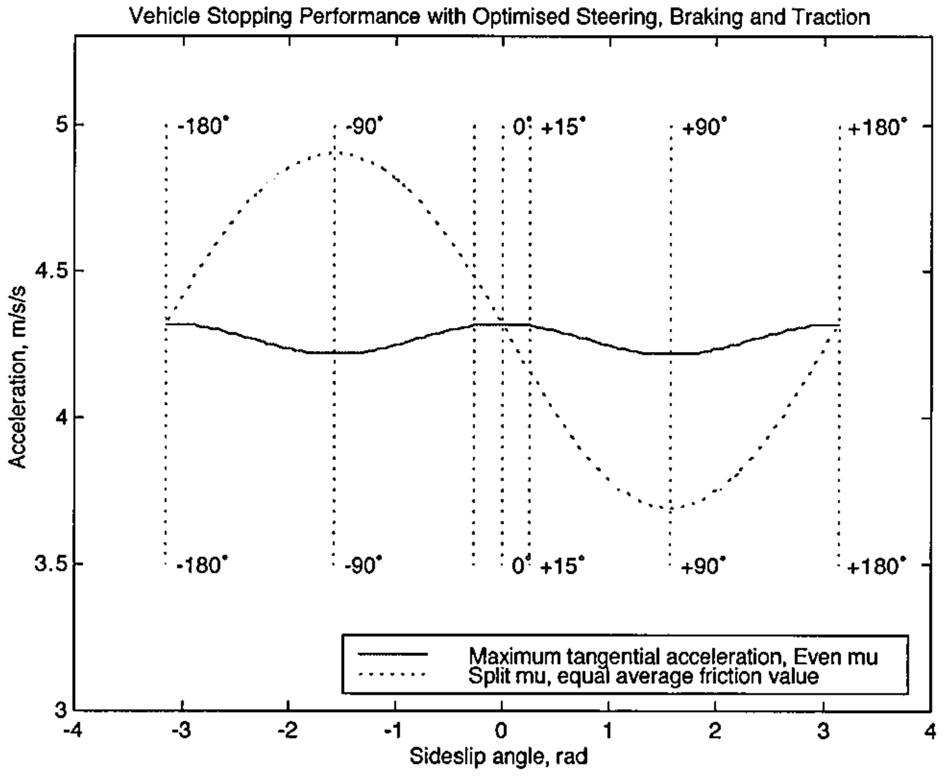

Figure 3.5

Vehicle acceleration/deceleration performance $\left(f = -{}^{P}a_x, \alpha_z = 0\right)$ **on a split-mu surface**

$M = 1400, h = 0.4, t_f = t_r = 0.7, b = 1.0, c = 1.7, \lambda = 1$

(i) even friction ('even-mu') $\left(\mu_{FL} = \mu_{FR} = \mu_{RL} = \mu_{RR} = 0.5\right)$

(ii) split friction ('split-mu') $\left(\mu_{FL} = \mu_{FR} = 0.05, \mu_{RL} = \mu_{RR} = 0.95,\right)$

In this case, it can be seen that if the vehicle is rotated such that the front tyre which is able to generate the greatest force (i.e. the tyre on the surface with the higher μ value) is positioned such that the line of action of that force is closer to the CG (and thus that force has a reduced yawing moment) then a greater deceleration can be sustained. Here, a $\approx$ 5% improvement in deceleration performance is achieved within the chosen 'realistic' bounds on sideslip angle.

Note: The result presented here has limited validity in the large sideslip range, as it has been assumed that the coefficient of friction at the tyre remains constant as the sideslip angle changes (i.e. is 'carried with the tyre'), so the cornering performance (90 degrees of sideslip relative to the acceleration vector) may not be analysed from this plot, since in reality this would place the tyres on different coefficients of friction, and this effect is not taken into account.

(iv) Braking or accelerating in a turn

The significant sensitivity to sideslip identified in the preceding analysis prompted the analysis of a more common situation where braking is required and the available frictional forces between left and right tracks differs. During braking in a turn, where the path-lateral acceleration ${}^{P}a_y$ must be maintained - the available friction at left and right wheel tracks differs due to the lateral load transfer, i.e. due to the reaction of the lateral acceleration across the vehicle track (about the vehicle x axis), assuming the sideslip remains within the practical bounds already mentioned.

In figure 3.6, the lateral acceleration of the vehicle ${}^{P}a_y$ has also been varied, and dual constraints have been applied that limit the braking performance – (i) that the lateral acceleration (and thus path curvature) must be maintained constant, and (ii) that there must be zero yaw acceleration $(\alpha_z = 0)$.

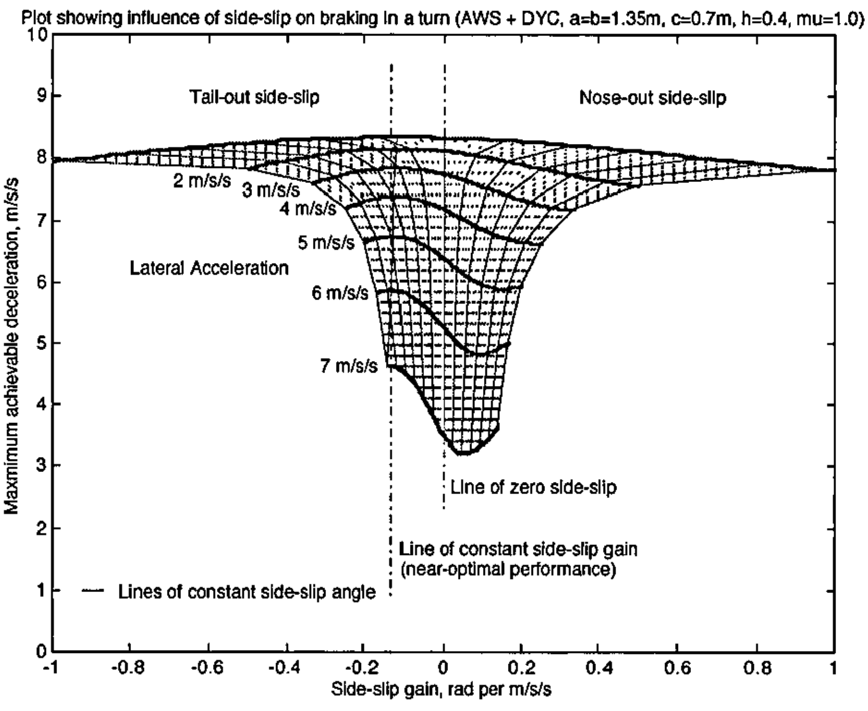

Figure 3.6

Performance of a vehicle during braking in a turn $\left(f = -{}^{P}a_x, \alpha_z = 0, a_y = a_{y_{demand}}\right)$

$$\mu_{FL} = \mu_{FR} = \mu_{RL} = \mu_{RR} = 1.0, M = 1400, h = 0.4, t_f = t_r = 0.7, b = c = 1.35, \lambda = 1$$

Considering that the result of this optimisation might be exploited in practice by implementing a controller with a constant target sideslip gain, $\frac{d\beta}{da_y}$ (i.e. a constant relationship between steady-state lateral acceleration and sideslip angle), the ordinate has been changed so that results are now plotted against the sideslip gain of the vehicle, instead of directly against the sideslip angle.

As with the above plots, there are two factors at work in defining the shape of the plot:

- ***the available friction (due to the evenness of the load distribution on the tyres).*** When the demand acceleration vector lies close to the longitudinal axis of the vehicle and the load is reacted across the long wheelbase rather than the narrow track, the load transfer is less, the available tyre forces are greater and thus the achievable acceleration is higher. Conversely, when the demand acceleration vector is close to the lateral axis, the performance is worse. Hence, at low lateral accelerations, performance is best at low nose-out sideslip, and at higher lateral accelerations, performance is best at higher nose-out sideslip. This is the influence which is seen even when the yaw moment constraint is removed;
- ***the usability of the available friction*** – if the tyres with the greater friction are positioned such that their lines of action for generation of the combined cornering and deceleration lie a long distance from the CG, then these will generate significant yaw moments. If these are not balanced by opposing moments generated by another tyre, then the performance will be poor as the force directions of all of the tyres must somehow be compromised in order to balance the yaw moment. This second influence on the performance is that effect which is observed only when the yaw moment is somehow constrained.

The result shows increasing sensitivity to the sideslip angle as the lateral acceleration increases, and shows a practically interesting result – that the optimal result across all decelerations lies very close to a ***constant, non-zero, speed-independent, sideslip gain*** $\partial\beta / \partial a_y$. This is the same characteristic that was shown to occur throughout the linear range of a vehicle with simple open-loop 4WS or AWS ($\delta_f = b / E, \delta_r = -c / E$), where changes in sideslip angle at the centre of mass are controlled by the cornering compliances of the tyres.

However, in actual fact, the optimal value of the sideslip gain is of opposite sign to that delivered by the vehicle with open-loop control, and is also much higher than is practically feasible, since it corresponds to a vehicle which exploits these factors by sideslipping almost to 90 degrees at high (but practically achievable) lateral acceleration values.

However, it shows clearly that vehicles with a strongly ***nose-out*** sideslip gain (that is, ***opposite*** to the high speed behaviour of conventional passive vehicles, and the greater the better) will be capable of stopping more rapidly during turning when all control over tyre slip is available.

It should be noted that for the opposite case of improvement of ***acceleration*** in a turn performance, sideslip of ***opposite*** sign would be required.

However, making such rapid changes of sideslip angle (for instance, when the driver switches from acceleration to braking) places additional demands on the tyres in transient conditions.

Assuming it is found that the tyre force demands required to rotate the vehicle in sideslip are significant, this result suggests that since ***braking capability*** is almost certainly more important than acceleration capability [Blank, 2000], a nose-out sideslip gain would appear to be a preferable target - at least for a vehicle with a controller that has full authority over the tyre forces.

3.4: Concluding Remarks

It has been seen that, as expected, the need to maintain yaw moments within reasonable bounds always limits the (cornering or braking) acceleration performance of a vehicle, when compared with the optimum that would be achievable if yaw control were not required.

In the simplest case of even-mu braking or acceleration, it has been seen that there is little sensitivity of the maximum performance acceleration to the sideslip angle, irrespective of whether yaw motion is constrained.

When yaw moments are unconstrained, the lateral acceleration (cornering) performance exhibits sensitivity to small sideslip ***only*** if the centre of mass is non-central (regardless of the roll stiffness distribution). This effect is due to there being a component of the rotated acceleration vector that leads to an improvement of the evenness of the vertical load distribution, such that the vehicle with a rearward centre of mass is improved by nose-out sideslip, and conversely a vehicle with a forward centre of mass would be improved by tail-out sideslip;

When yaw moments are constrained, this sensitivity becomes more significant due to the fact that the heavily loaded outer tyres move forwards with tail-out sideslip and thus increase the turn-in yaw moment (or vice versa) - therefore, nose-out sideslip benefits the performance of the unbalanced (rearward CG) vehicle even more.

Therefore, when improvement of the lateral acceleration performance requires more turn-in moment (e.g. as at the limit of a limit-under-steering vehicle, where maximised tyre forces would tend to straighten the vehicle), more tail-out sideslip is beneficial. Conversely, when more turn-out ('stabilising') moment is required, (e.g. as at the limit of a limit-over-steering vehicle), more nose-out sideslip is beneficial.

On split-mu surfaces, braking performance becomes highly sensitive to sideslip angle, with the front of the vehicle shifted towards the low friction improving the performance. The scenario of braking in a turn, where the outer wheels are more heavily loaded, shows a very similar sensitivity, especially at high lateral acceleration. The optimal sideslip angle to maximise longitudinal acceleration performance along the same path, therefore, is nose-out during acceleration, and tail-out during braking.

In all cases, the optimum sideslip is in the opposite sense from the sense the vehicle would naturally turn if the maximum acceleration was generated without yaw moment constraint. Therefore, to ensure that optimal accelerations are generated in conditions where yaw control is required, the controller must either (i) put the vehicle into the necessary sideslip state before the demand is applied (e.g. by sensing friction), or (ii) sacrifice some transient performance to correct the the sideslip corrected before the lateral acceleration is generated. Additionally, since the sideslip angle required for optimal acceleration performance is the opposite from that required for optimal braking performance, it is not possible to identify an 'optimal' sideslip that could be targeted in order to apriori ensure good performance in response to any subsequent longitudinal input.

All of the above analysis assumes full control authority over all of the in-plane forces. The sensitivity to sideslip might be quite different if only the steering (path-lateral) forces could be controlled, if drive torque of DYC authority were limited, or if rear steering were not available. Situations of limited actuator authority are not considered here.

Chapter 4
Energy Consumption

When the driver's demand is within the envelope of capability of the vehicle, it is desirable to minimise the total energy dissipated per unit time, and thus optimise the fuel, tyre and brake consumption of the vehicle. The intent of this section is to investigate the influence of the vehicle's sideslip trajectory in both steady-state and transient cornering (and how the available actuation is used to achieve this) on the total energy consumption of the vehicle. The hypothesis investigated in this chapter is H2.

The objective of the exercises in this Chapter is therefore first to determine the combination of controls that minimises the power required to precisely follow a given target, such that the influence of (i) sideslip angle and (ii) the accelerations required to follow a sideslip trajectory may be understood, without a poorly chosen combination of controls or a poor controller making any confounding contribution to the result. Instead, since the available controls are always optimised, the result will always be the most efficient that is achievable within the applied constraints. Those constraints may include the vehicle maintaining a particular sideslip angle, or generating a certain lateral and yaw acceleration in order to follow a particular sideslip trajectory.

The energy that is continually dissipated by a vehicle comprises contributions due to:

- Aerodynamic Drag [Gillespie, 1992; Various, 1993]
- Tyre Rolling Resistance [Various, 1993]
- Gearbox, Differential and Bearing Friction [Various, 1993]
- Tyre In-Plane (frictional) Forces [Frey, 1995]
- Dissipation in controlled Brakes or Differential(s)

This dissipated energy may either be replaced by the engine, or the knietic energy of the vehicle may reduce, depending on the constraints applied. Energy losses which occur inside a particular engine while it generates the required mechanical power are also neglected, such that the results will not be influenced by the characteristics of any individual powertrain.

4.1: Choice of Model

The model used thoughout this chapter is a yaw plane model similar to that used in the previous chapter. However, rather than directly identifying the tyre forces, the combination of controls that generates the necessary tyre force is identified. This is because there may be more than one combination of controls that is able to generate the same tyre force, and each control combination may dissipate a different amount of energy in doing so. Since the goal is to identify the most efficient combination of controls, it is important to allow the optimiser the freedom to choose the combination of controls.

Once again, roll dynamic motion and load transfer due to a shift in the centre of mass are neglected, and an inertia-less quasi-static model of wheel rotation is employed. This model assumes that the force demanded of the tyre (i.e. the sum of the brake, drive and differential torques below) are balanced by the immediately delivery of a longitudinal tyre force ${}^{W}F_{x_k}$ of a magnitude that generates an equal and opposite moment on the wheel:

$$\left. {}^{W}F_{x_k} = \frac{\left(T_{brake_k} + T_{drive_k} + T_{diff_k}\right)}{R_k} \right\} \quad k = FL, FR, RL, RR$$

where

$$\left. T_{drive_k} = R_{d_k} \cdot T_{engine} \right\} \quad k = FL, FR, RL, RR$$

$$T_{diff_{FL}} = T_{diff_c} - T_{diff_f}$$

$$T_{diff_{FR}} = T_{diff_c} + T_{diff_f}$$

$$T_{diff_{RL}} = T_{diff_c} - T_{diff_r}$$

$$T_{diff_{RR}} = -T_{diff_c} + T_{diff_r}$$

with

$$R_{d_{FL}} = R_{d_c} \cdot \left(1 - R_{d_f}\right)$$

$$R_{d_{FR}} = R_{d_c} \cdot R_{d_f}$$

$$R_{d_{RL}} = \left(1 - R_{d_c}\right) \cdot \left(1 - R_{d_r}\right)$$

$$R_{d_{RR}} = \left(1 - R_{d_c}\right) \cdot R_{d_r}$$

It is assumed that the wheel and tyre instantaneously adopt the correct slip ratio s_k and the associated angular velocity w_k that is necessary for the tyre to deliver the required longitudinal force ${}^{W}F_{x_k}$.

The necessary slip ratio is determined by inverting the tyre model. In the case of the linear tyre model, this is straightforward:

$$s_k = -\frac{{}^{W}F_{x_k}}{C_{s_k}}$$

In the case of the non-linear tyre model, this inversion is more difficult to perform analytically. Therefore, it is effected by (i) adding the four longitudinal slips to the list of parameters which are to be varied by the optimisation, such that the slip also is optimised, and (ii) simultaneously introducing additional constraints that specify the relationship that is required between longitudinal force and slip. In other words, the model of longitudinal force generation becomes an additional equality constraint equation for each tyre:

$$\left.{}^{W}F_{x_k} - F_x\left(\alpha_k, s_k, F_{z_k}\right) = 0\right\} \quad k = FL, FR, RL, RR$$

Note: There will be values of the controls for which the balancing force has a magnitude that is too large to be delivered by the tyre. Therefore, with the nonlinear tyre model, there will be values of the demand for which the constraints cannot be satisfied, and the optimisation will fail.

The tyre forces arising from the selected combination of controls are initially computed in the wheel co-ordinate system. As mentioned above, two different models of the forces generated relative to the wheel are used in the analysis: the linear tyre model, and the nonlinear, Pacejka tyre model. Both tyre models are presented in full in Chapter 2.

These forces generated by the tyres are then transferred to the vehicle co-ordinate system by means of a rotation through the steer angle:

$$\left.\begin{aligned} {}^{V}F_x &= {}^{W}F_{x_k}\cos(\delta_k) - {}^{W}F_{y_k}\sin(\delta_k) \\ {}^{V}F_y &= {}^{W}F_{x_k}\sin(\delta_k) + {}^{W}F_{y_k}\cos(\delta_k) \end{aligned}\right\} \quad k = FL, FR, RL, RR$$

From the forces in the vehicle coordinate system, the accelerations in the vehicle coordinate system can be found by a simple application of Newton's second law:

$$^{V}a_x = \frac{1}{M}\sum_{k=1}^{4} {^{V}F_{x_k}}$$
$$^{V}a_y = \frac{1}{M}\sum_{k=1}^{4} {^{V}F_{y_k}}$$

and from these accelerations, the translational accelerations relative to the path may be found.

$$^{P}a_x = {^{V}a_x}\cos(\beta) + {^{V}a_y}\sin(\beta)$$
$$^{P}a_y = -{^{V}a_x}\sin(\beta) + {^{V}a_y}\cos(\beta)$$

These are the accelerations which will be specified using constraints:

$$^{P}a_x = {^{P}a_{x_{demand}}}$$
$$^{P}a_y = {^{P}a_{y_{demand}}}$$

Also of relevance in this analysis are the velocities of the tyre contact patches (influenced by the vehicle speed and sideslip) since these influence the slips and thus steer angles that are required to generate the necessary force. In the analyses which follow the vehicle velocity ^{P}U and the sideslip angle β are fixed at the outset, such that the velocities at the centre of mass in vehicle co-ordinates are:

$$\begin{aligned} ^{V}U &= {^{P}U}\cos(\beta) - {^{P}V}\sin(\beta) \\ &= {^{P}U}\cos(\beta) \\ ^{V}V &= {^{P}U}\sin(\beta) + {^{P}V}\cos(\beta) \\ &= {^{P}U}\sin(\beta) \end{aligned}$$

From these velocities and the vehicle yaw rate, r, it is possible to identify the inplane velocity vector at each tyre contact patch:

$$^{V}V_{FL} = {^{V}V_{FR}} = {^{V}V} + br$$
$$^{V}V_{RL} = {^{V}V_{RR}} = {^{V}V} - cr$$
$$^{V}U_{FL} = {^{V}U_{RL}} = {^{V}U} + tr$$
$$^{V}U_{FR} = {^{V}U_{RR}} = {^{V}U} - tr$$

The slip velocities computed in vehicle-fixed coordinates may be transformed into wheel-fixed coordinates by rotating them through the steer angle, δ:

$$\left.\begin{aligned} ^{W}U_k &= {^{V}U_k}\cos(\delta_k) + {^{V}V_k}\sin(\delta_k) \\ ^{W}V_k &= -{^{V}U_k}\sin(\delta_k) + {^{V}V_k}\cos(\delta_k) \end{aligned}\right\} \quad k = FL, FR, RL, RR$$

These velocities appear in the energy dissipation computations which follow. The wheel angular velocities are computed from the slip ratios, s_k, which is defined according to the SAE standard:

$$w_k = \left.\frac{{}^{W}U_k(s_k - 1)}{R_k}\right\} \quad k = FL, FR, RL, RR$$

and since a kinematic driveline is assumed (see Chapter 2.13), these velocities determine the angular velocity of the engine (or rather, the gearbox output shaft, since components upstream of this are not modelled):

$$w_{engine} = \sum_{k=1}^{4} w_k \cdot R_{d_k}$$

$$w_{diff_r} = w_{RR} - w_{RL}$$

$$w_{diff_f} = w_{FR} - w_{FL}$$

Note: Depending on the analysis, the steer angles δ_k, as with the other parameters of the model, such as the sideslip angle, β and the brakes torques T_{brake_k} may either be fixed (for instance, set to zero to represent the rear wheels of a 2WS vehicle) or may be free parameters that are iterated by the optimiser. Regardless of this, with the exception of the switch from linear to nonlinear tyres, the model remains the same in every analysis in this Chapter.

4.2: Analysis Method

The combination of controls that is necessary to achieve a certain performance with minimum energy consumption is computed using ***the same*** constrained optimisation routine that was applied in Chapter 3. In this case, however, the vehicle model is more complicated because it is necessary to identify the precise combination of steer angles, brake and drive torques that lead to a particular tyre force, such that the total energy dissipated may be computed.

Parameters are automatically varied in order to achieve this optimisation, and the subset of controllable parameters for each optimisation may be chosen from the set of:

- Four brake torques $(T_{brake_k}, k = FL, FR, RL, RR)$
- Three final drive ratios $(R_{d_f}, R_{d_c}, R_{d_r})$
- Four steer angles $(\delta_k, k = FL, FR, RL, RR)$

- Engine torque $\left(T_{engine}\right)$
- Three active differential torques $\left(T_{diff_f}, T_{diff_c}, T_{diff_r}\right)$
- Body sideslip angle (β)

Alternatively, any of these parameters may be fixed – for instance final drive ratios may be specified to apportion engine torque to simulate conventional FWD, RWD or 4WD vehicles with uncontrolled differentials, or the sideslip angle may be specified, to allow an analysis of the effect of its variation. Alternatively, the sideslip angle may be free but the rear steer angle constrained, such that the result from a passively steered vehicle is obtained.

Additional inequality constraints are introduced to ensure that:

- unphysical, energy-introducing 'brake' forces which actually act in the same sense as the wheel rotation (and thus accelerate it) are prevented, i.e:

  $$\left. T_{brake_k}\omega_k < 0 \right\} \quad k = FL, FR, RL, RR$$

- driveline torque distributions properly represent the proportion of drive torque that is directed to one output shaft:

  $$\left. 0 < R_{d_k} < 1 \right\} \quad k = f, r, c$$

- vehicle sideslip remains within 'reasonable' bounds:

  $$-\beta_{reasonable} < \beta < \beta_{reasonable}$$

- steer angles remain within practical steering lock limits:

  $$\left. -\delta_{full-lock} < \delta_k < \delta_{full-lock} \right\} \quad k = FL, FR, RL, RR$$

Equality constraints are employed as in Chapter 3, to ensure that the required accelerations (${}^P a_x$, ${}^P a_y$, α_z) are generated. Where non-linear tyre models are employed, equality constraints also ensure that the tyre model is adhered to. In all cases, wheel angular acceleration in spin is neglected - it is assumed that the wheel remains near equilibrium about its spin axis.

Energy Flow

In this model, the only available source of power is the vehicle engine. That power may be dissipated in the tyres and brakes or in the air (due to viscous drag), or may contribute to an increase in the total kinetic energy of the vehicle. Since energy stored in the vehicle might be recovered at a later date, it is the energy which is truly ***dissipated*** that is minimised in order to determine the combination of controls which is most efficient.

The energy input or extracted from the vehicle at each point is computed by multiplying the externally applied force or torque by the velocity or angular velocity:

(i) Engine:

$$P_{engine} = w_{engine} \cdot T_{engine}$$

This term is normally positive (energy input) except where 'engine braking' is being utilised. Note that since losses in geartrains are not of interest here, these are omitted and P_{engine} is assumed to be the net power output from the engine after such losses have been decucted.

(ii) Controlled, Passive Differentials:

$$P_{diff_f} = w_{diff_f} \cdot T_{diff_f}$$

$$P_{diff_r} = w_{diff_r} \cdot T_{diff_r}$$

$$P_{diff_c} = w_{diff_c} \cdot T_{diff_c}$$

These terms are always negative, since it is assumed that there is no power source in the differential, though energy may be dissipated by a single controlled clutch in order to allow the differential to generate yaw moments.

(iii) Aerodynamics:

$$P_{aero} = {}^{V}F_{y,aero} \cdot {}^{V}V + {}^{V}F_{x,aero} \cdot {}^{V}U + M_{z,aero} \cdot r$$

(iv) Brakes:

$$\left. P_{brake_k} = w_k \cdot T_{brake_k} \right\} \quad k = 1,2,3,4$$

These terms are always negative, since brake forces always oppose the rotation of the wheel.

(v) Tyre Contact Patches (always negative, energy dissipation):

$$\left. \begin{aligned} P_{tyre,x_k} &= {}^{W}F_{x_k} \cdot \left({}^{W}U_k + w_k \cdot r_k \right) \\ P_{tyre,y_k} &= {}^{W}F_{y_k} \cdot {}^{W}V_k \end{aligned} \right\} \quad k = 1,2,3,4$$

Therefore, the total energy dissipated in this vehicle model is:

$$P_{diss} = P_{diffs} + P_{aero} + P_{brakes} + P_{tyres,x} + P_{tyres,y}$$

where

$$P_{brakes} = \sum_{k=1}^{4} P_{brake_k}$$
$$P_{tyres,x} = \sum_{k=1}^{4} P_{tyre,x_k}$$
$$P_{tyres,y} = \sum_{k=1}^{4} P_{tyre,y_k}$$
$$P_{diffs} = P_{diff_f} + P_{diff_r} + P_{diff_c}$$

In each case, the total ***dissipated*** power, P_{diss} is minimised by iteration of the vector of the available controls in a direction that ensures that P_{diss} is continually reduced without violating any of the constraints. In order to speed the optimisation, there are small tolerances on constraint violations, and once changes in P_{diss} fall below a specified, very small change in energy, the optimisation is halted.

The same calculation of energy flows presented above is additionally employed to ensure that the model behaved in an energy-conserving manner at all times, i.e. that:

$$P_{diss} + P_{engine} + P_{KE} = 0$$

since the model employed contains no elements that are able to store potential energy.

The power that is converted to kinetic energy, P_{KE} is determined from:

$$\begin{aligned} P_{KE} &= \frac{\partial}{\partial t}\left(\tfrac{1}{2}MV^2 + \tfrac{1}{2}MU^2 + \tfrac{1}{2}I_{zz}r^2\right) \\ &= M\left(V\dot{V} + U\dot{U} + k^2 r\dot{r}\right) \end{aligned}$$

This check on conversaiton of energy brings confidence that the models have been implemented correctly.

4.3: Results and Discussion

In the first instance, the basic influence of sideslip angle, β on the energy dissipation during steady-state turning was determined.

The Influence of sideslip

Figure 4.5 shows the total power dissipated unrecoverably (in the brakes, tyres and air) during a 0.6g turn at 20 m/s, and how this varies with vehicle sideslip angle for a typical passenger car. The available actuators are, employed in the least energy consuming manner, such that P_{diss} is minimised at each point on the plot. The parameters selected represent nominal values for a typical passenger car, and are taken from Crolla [Crolla, 1996] and the Bosch Automotive Handbook [Various, 1993]. The sensitivity to the vehicle parameters is not explicitly studied here, but it was confirmed that the form of the result remained the same with different parameter sets.

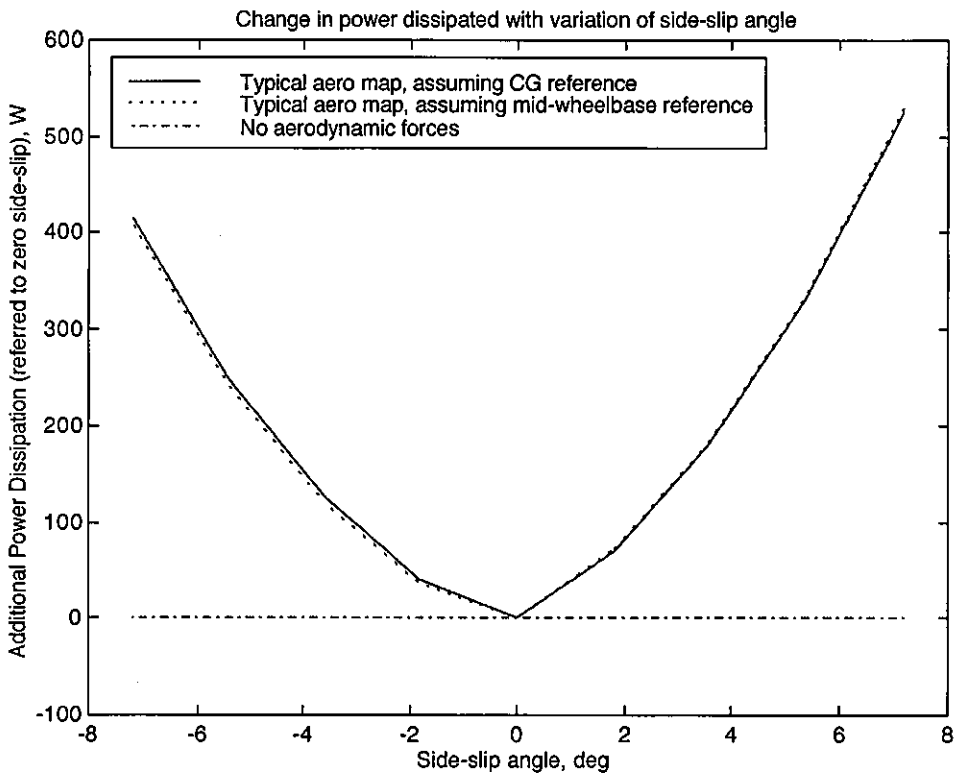

Figure 4.5
***Change* in power (J/sec) dissipated with change in sideslip angle relative to offset baseline; baseline energy dissipated at zero side-slip = 3230 W**

$$M = 1008, I_{zz} = 1031, b = 1.234, c = 1.022, t_f = t_r = 0.7, g = 9.81,$$

$$C_{\alpha_f} = 117440, C_{\alpha_r} = 144930, C_{s_f} = 352320, C_{s_r} = 434790,$$

$$A = 2, \rho_a = 1.225, C_D|_{\beta=0} = 0.3, C_S|_{\beta=0} = 2.3, C_{YM}|_{\beta=0} = 0.8$$

It can be seen that the optimal result is close to (but not exactly) zero sideslip. For typical vehicle shapes, $C_S|_{\beta=0}$ is positive, which means that aerodynamic forces make a positive contribution to the lateral force when the sideslip angle is negative (i.e. tail-out), thus reducing the work done by the tyres. However, the $C_{YM}|_{\beta=0}$ term is also important since any yaw moment generated by aerodynamics must be counteracted by the tyres, potentially either increasing or reducing the energy dissipated in the tyre contact patches.

The energy dissipated is plotted with and without the aerodynamic contribution, since this shows clearly that even at this relatively low speed, the dominant component in the variation of dissipaion with sideslip is due to the aerodynamic drag. Changes in energy losses in the tyres as the sideslip angle is changed can be seen to be effectively negligible in comparison.

The two very similar curves shown indicate how the results differ depending on the treatment of yaw motion in modelling the aerodynamic forces. Most aerodynamic data is presented against sideslip angle relative to the oncoming flow. However, when the vehicle is in a turn, this sideslip angle varies with position along the vehicle's longitudinal axis. The solid line shows the result if the sideslip angle is assumed to be measured at the vehicle CG; the dotted shows the result if it is measured at the mid-wheelbase point, which is the usual aerodynamic reference. For this typical passenger car, there is a significant difference in the locations of these points, and it can be seen that the change of reference point has little influence on the result.

Optimal Choice of Actuators

Further optimisations were performed in order to understand the relative energy cost of AWS versus DYC for the generation of yawing moments. Since DYC alone is unable to generate a lateral acceleration, the generation of a yaw moment is the only fair comparison of the energy consumption of the two alternative actuation methods.

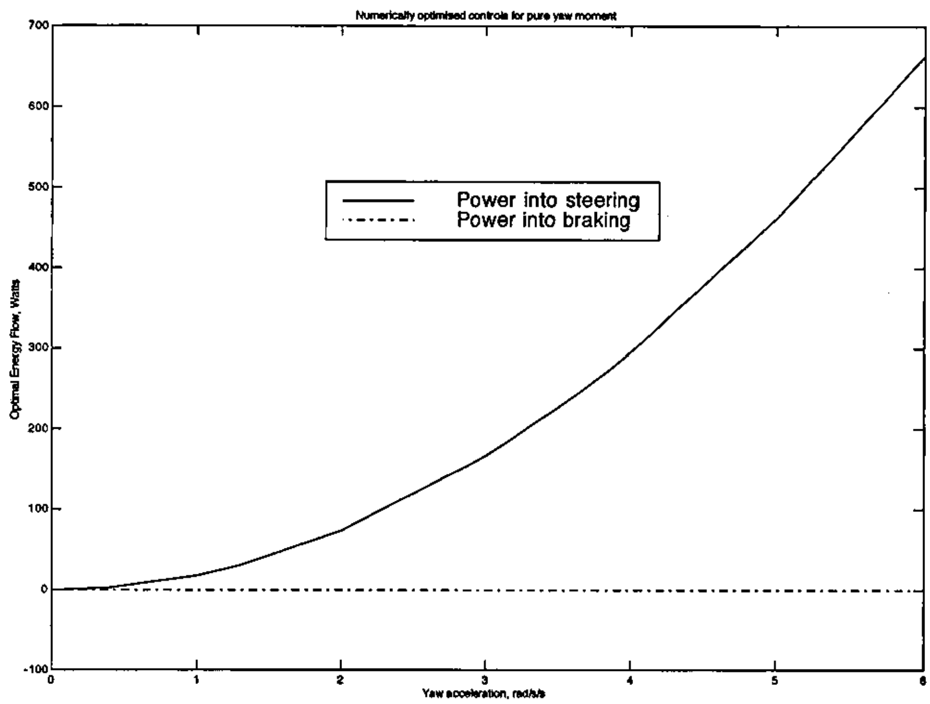

Figure 4.4
Optimal Energy Flow for yaw moment generation
(non-linear model, linear tyres, aerodynamic forces removed for clarity)

$$b = c = k = 1.35, t_f = t_r = 1.4, M = 1400,$$
$$C_{s_f} = C_{s_r} = C_{\alpha_f} = C_{\alpha_r} = 70000,$$
$$U = 20, r = 0, {}^P a_y = 0, {}^P a_x = 0$$

Figure 4.4 shows a typical result from a numerical optimisation to find the optimal controls to apply to a non-linear vehicle model in order to generate a pure yawing moment from a straight-line condition. Figure 4.4 clearly shows that the least energy-consuming solutions identified by numerical optimisation involve effectively no use of DYC.

This shows that for a typical vehicle, DYC consumes many time more energy than AWS for generating the same yaw moment unless front and rear tyre slip angles are of the order of one radian or greater. Such slip angles are impractical - if not impossible - to prescribe, and they imply tyres which are slipping at many times the angle where the peak lateral force would be generated. It is concluded, therefore, that DYC would never be chosen over AWS control on grounds of energy consumption. The same conclusion applies regardless of the vehicle speed and steer angle, since the speed-dependence and steer-angle dependence of the energy cost is the same for both controls.

For this reason, in the following Chapters, there will be a strong focus on developing a transient response that is 'compatible' in friction demand with the envelope of capability of an AWS vehicle, such that DYC need not be used except when absolutely required - to extend the envelope of capability of the vehicle once the authority of AWS has been exhausted.

This also shows that if a vehicle is to be driven for an extended period outside of the envelope of capbility of AWS, then alternatives to DYC that are able to adjust the balance of the vehicle without ***continually*** dissipating large amounts of energy should be considered. Such systems include active warp control, which uses active anti-roll bars, or active suspension actuators to modify the diagonal weight jacking of the vehicle and consequently modify the shape of the envelope. Additionally, for vehicles with a high centre of mass and short wheelbase, it may be possible to influence the limit balance by controlling the longitudinal acceleration, and if the vehicle is four-wheel-drive and the driver is accelerating, it may be possible to shift the drive torque distribution between front and rear axles. These alternatives are not discussed in detail in this thesis.

However, one should be clear that the use of DYC in the linear region of the vehicle cannot be completely ruled out, since DYC control offers both (i) fast response (ii) excellent linearity and (iii) established methods for prevention of high slip due to excessive demand. It is suggested, therefore, that DYC could reasonably be used at low to moderate lateral accelerations, for making fine or short-term corrections to the vehicle state.

Instantaneous Power Dissipation

Now that the influence of sideslip angle and actuator choice have been understood, the focus will be shifted to the influence of the lateral and yaw acceleration demands, since the relationship between these demands can be influenced though the choice of the transient sideslip trajectory.

In order to identify ideal trajectories for the transient case, an optimisation of instantaneous power dissipation during a transient maneuver was used. In figure 4.4, results were plotted to show the variation of power with increasing yaw acceleration and lateral acceleration.

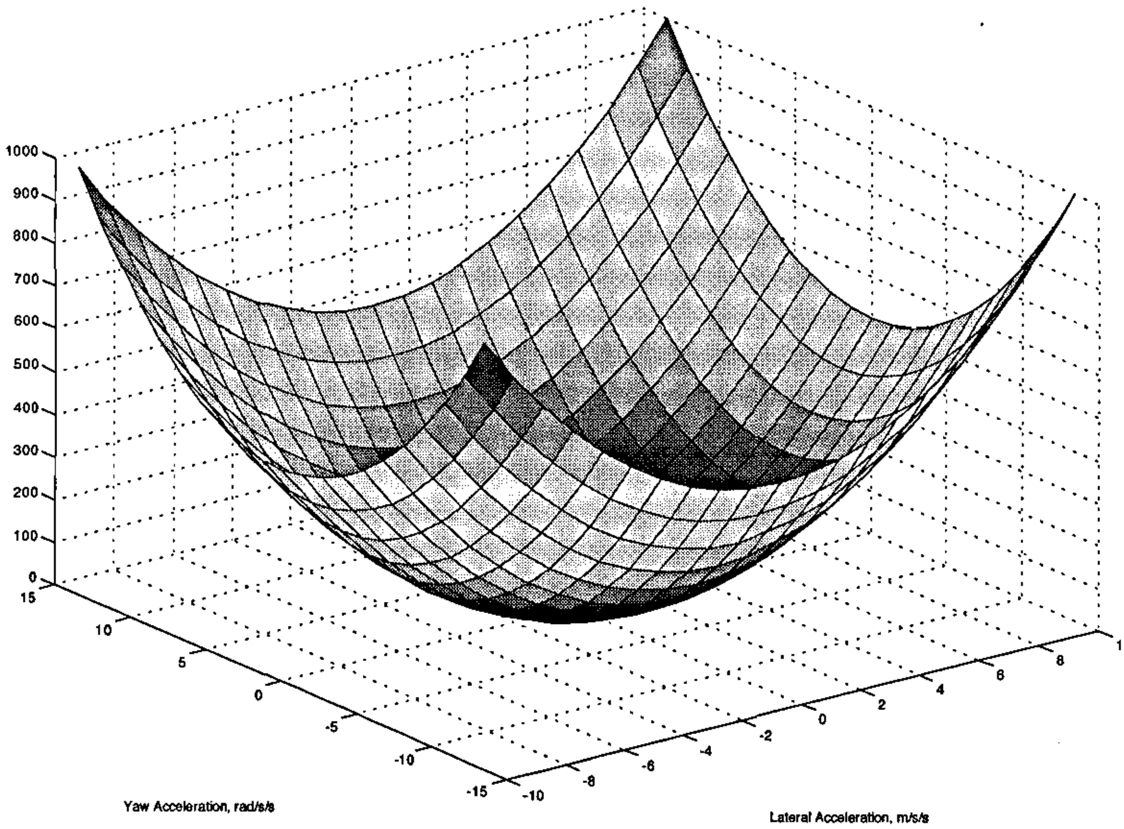

Figure 4.4: Power Dissipation - Linearly Neutral Steering Vehicle

$\left(M = 1000, b = c = 1.35, k = 1.0, C_{\alpha_f} = 100000, C_{\alpha_r} = 100000\right)$

Contours of Constant Power in a_y-α_z space

It is well understood that the least energy-consuming strategies follow a contour of constant power in response to a step change in demand, since the energy dissipation increases with the square of the control action, and performance increases only linearly. Therefore, for a given lateral acceleration target (e.g. prescribed by a step change in steer input), constant power dissipation is optimal, since a period of higher control action, followed be a period of lower control action would always lead to greater energy dissipation when integrated over the whole transient.

For this reason, the contours of constant power dissipation were identified, for several cases (figures 4.5-4.7). It is proposed that the least energy consuming transient trajectory would follow a contour of constant power dissipation.

Figure 4.5 to 4.7 show the contours of constant power dissipation in the plane of lateral acceleration versus yaw acceleration, for (i) a linearly neutral steering vehicle ($bC_{\alpha_f} - cC_{\alpha_r} = 0$), (ii) a linearly under-steering vehicle ($bC_{\alpha_f} - cC_{\alpha_r} < 0$), and (iii) a linearly over-steering vehicle ($bC_{\alpha_f} - cC_{\alpha_r} > 0$).

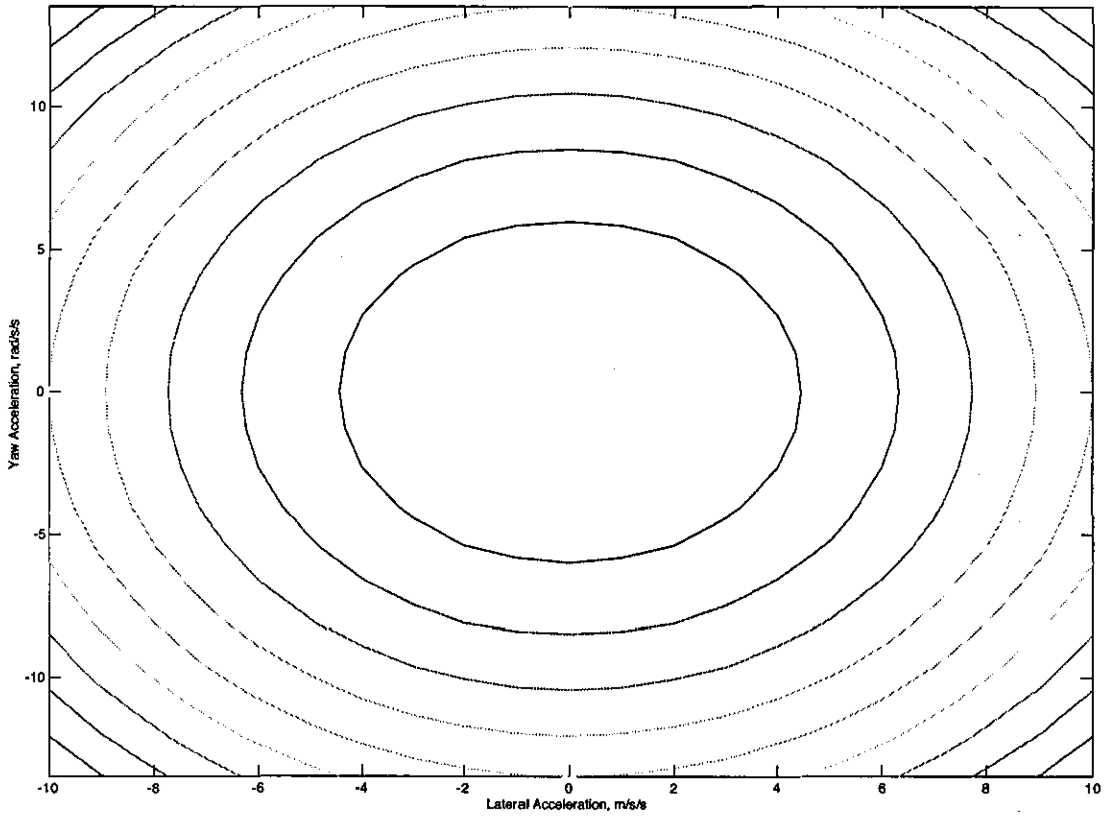

Figure 4.5: Contours of Constant Power Dissipation (Linearly Neutral-Steering Vehicle)

$$\left(M = 1000, b = c = 1.35, k = 1.0, C_{\alpha_f} = 100000, C_{\alpha_r} = 100000\right)$$

Note: In this case, the term ***linearly*** under-steering refers to the behaviour of the vehicle around straight-line driving, i.e. where the tyre cornering stiffnesses remain approximately linear. This is in sharp contrast with 'limit under-steering', which refers to the balance of forces acting on the vehicle around the maximum lateral acceleration, where the tyre behaviour is highly non-linear.

It can be seen that the basic shape of the contours, especially for the neutral-steer vehicle, matches the contours from a single tyre.

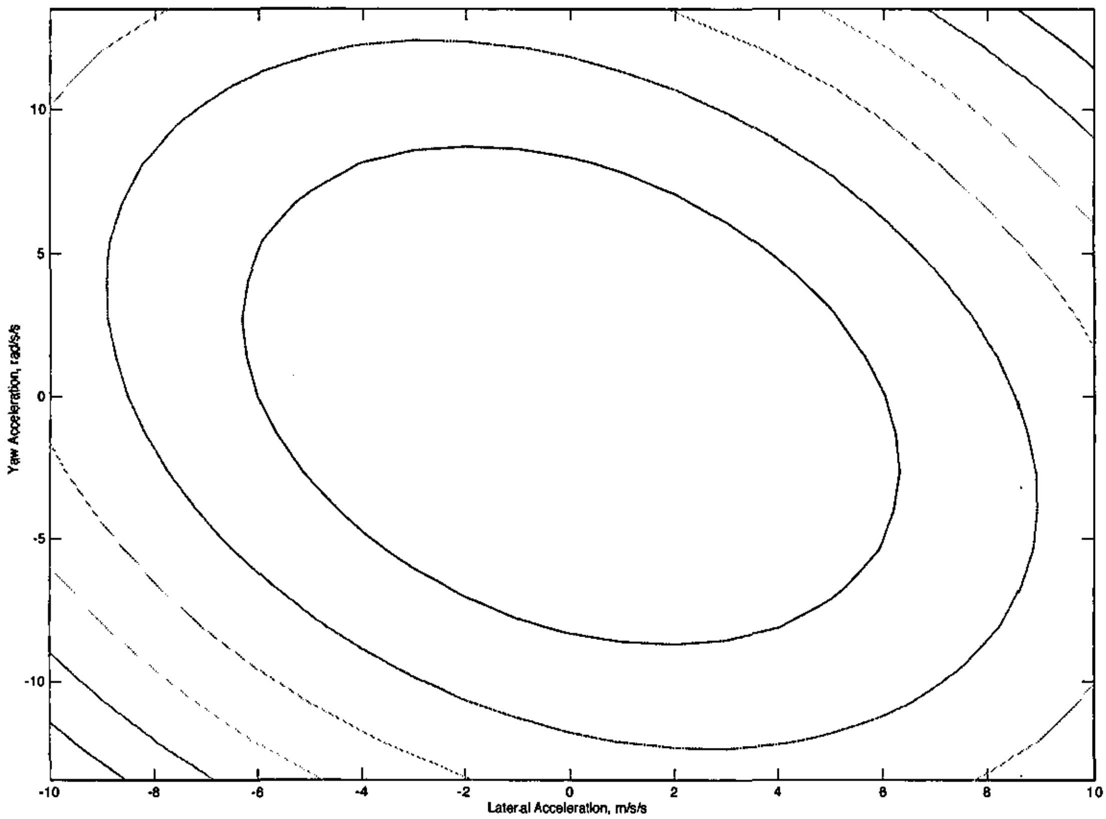

Figure 4.6: Contours of Constant Power Dissipation
Linearly Under-steering Vehicle

$$\left(M = 1000, b = 1.5, c = 1.2, k = 1.0, C_{\alpha_f} = 80000, C_{\alpha_r} = 120000\right)$$

A simplification of the energy consumption model that assumes AWS only and pure-lateral forces generated by the tyres yields an analytical expression for the power dissipated that shows clearly the dependence on the linear handling characteristics of the vehicle. Assuming a bicycle model (equal forces at each front tyre) and neglecting aerodynamic effects, the energy dissipated in the tyres is:

$$\begin{aligned} P &= P_f + P_r \\ &= {}^W F_{y_f} \, {}^W V_f + {}^W F_{y_r} \, {}^W V_r \end{aligned}$$

The lateral velocities at the tyre contact patches, V_f and V_r are related to the slip angles of the tyres, which in turn are related to the force.

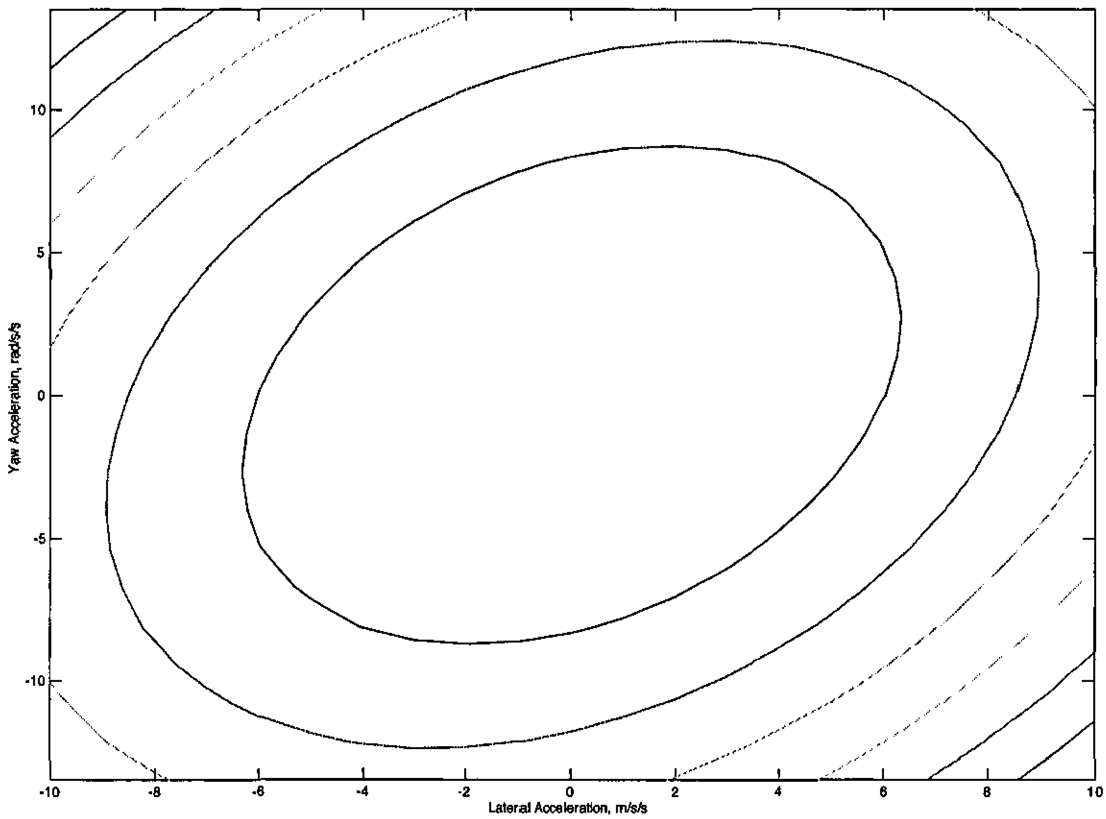

Figure 4.7: Contours of Constant Power Dissipation
Linearly Over-steering Vehicle

$$\left(M = 1000, b = 1.2, c = 1.5, k = 1.0, C_{\alpha_f} = 120000, C_{\alpha_r} = 80000\right)$$

Assuming small angles,

$$\alpha_f = \tan^{-1}\left(\frac{{}^{W}V_f}{{}^{W}U_f}\right) \approx \frac{{}^{W}V_f}{{}^{V}U} \qquad \alpha_r = \tan^{-1}\left(\frac{{}^{W}V_r}{{}^{W}U_r}\right) \approx \frac{{}^{W}V_r}{{}^{V}U}$$

$${}^{W}F_{y_f} = -C_{\alpha_f}\alpha_f \qquad {}^{W}F_{y_r} = -C_{\alpha_r}\alpha_r$$

Rearranging and substituting for V_f and V_r,

$$\begin{aligned} P &= F_{y_f}V_f + F_{y_r}V_r \\ &= U\left(F_{y_f}\alpha_f + F_{y_r}\alpha_r\right) \\ &= -U\left(\frac{F_{y_f}^2}{C_{\alpha_f}} + \frac{F_{y_r}^2}{C_{\alpha_r}}\right) \end{aligned}$$

The lateral forces may be related, via the vehicle inertia, to the chosen vehicle trajectory in $a_y - \alpha_z$ space:

$$\alpha_z = \frac{1}{Mk^2}\left(F_{y_f} b - F_{y_r} c\right)$$
$$a_y = \frac{1}{M}\left(F_{y_f} + F_{y_r}\right)$$

Putting these equations into matrix form and inverting yields:

$$\begin{bmatrix} \alpha_z \\ a_y \end{bmatrix} = \frac{1}{M}\begin{bmatrix} \frac{b}{k^2} & \frac{-c}{k^2} \\ 1 & 1 \end{bmatrix}\begin{bmatrix} F_{y_f} \\ F_{y_r} \end{bmatrix}$$

$$\begin{bmatrix} F_{y_f} \\ F_{y_r} \end{bmatrix} = \frac{M}{E}\begin{bmatrix} k^2 & c \\ -k^2 & b \end{bmatrix}\begin{bmatrix} \alpha_z \\ a_y \end{bmatrix}$$

such that:

$$\begin{aligned} P &= -U\left(\frac{F_{y_f}^2}{C_{\alpha_f}} + \frac{F_{y_r}^2}{C_{\alpha_r}}\right) \\ &= -\frac{UM^2}{E^2}\left(\frac{\left(\alpha_z k^2 + a_y c\right)^2}{C_{\alpha_f}} + \frac{\left(a_y b - \alpha_z k^2\right)^2}{C_{\alpha_r}}\right) \\ &= -\frac{UM^2\left(C_2 a_y^2 - 2k^2 C_1 a_y \alpha_z + k^4 C_0 \alpha_z^2\right)}{E^2 C_{\alpha_f} C_{\alpha_r}} \end{aligned}$$

where the zeroth, first and second-moment cornering stiffnesses, C_0, C_1 and C_2 are fundamental properties of the vehicle, defined [Dixon, 1995] as:

$$C_0 = C_{\alpha_f} + C_{\alpha_r}$$
$$C_1 = bC_{\alpha_f} - cC_{\alpha_r}$$
$$C_2 = b^2 C_{\alpha_f} + c^2 C_{\alpha_r}$$

Note that the vehicle states do not appear in the result, since for an AWS vehicle, changes in the states may always be compensated for by changes in the steer angles. For a given force to be generated, the same slip is required, irrespective of the current vehicle states.

Since each term in P is divided by the product of the cornering stiffnesses, the power generally reduces with increasing cornering stiffnesses. This is expected, since increasing cornering stiffness reduces the lateral velocity that is required to generate a given force.

The relationship between the front and rear cornering stiffness and the vehicle geometry, characterised by C_0, C_1 and C_2, then governs the shape of the function.

The cross-term which skews the diagram is proportional to the first-moment cornering stiffness, or the fundamental linear stability parameter of the vehicle [Dixon, 1995], such that linearly neutral steer vehicles exhibit an unskewed plot (see above), linearly under-steer vehicles are skewed in one direction, and linearly over-steer vehicles in the other.

It is perhaps surprising to note that it is the zeroth moment cornering stiffness C_0 that contributes to the increase of power loss with yaw acceleration, and the second moment cornering stiffness C_2 that contributes to the increase of power loss with lateral acceleration.

The above expression for the energy dissipated is useful since it indicates the influence of the fundamental parameters on the energy consumption of the vehicle (though, as described above, it is additionally possible to influence the energy consumption through the choice of transient response trajectory, since this determines the instantaneous a_y and α_z demands).

It is considered that it is most important to reduce the energy consumption of the vehicle at lower lateral accelerations, since this comprises the majority of typical vehicle driving conditions. In such situations the above expression for the power loss (where small angles have been assumed) remains approximately valid.

It is considered less important to optimise energy consumption at very high (near-limit) lateral acceleration, because it such conditions occur rarely and energy consumption is therefore likely to be considered much less important than assuring obstacle avoidance performance, controllability and yaw stability.

4.4: Concluding Remarks

When minimum energy consumption is the only concern, individual brake intervention (i.e. DYC-by-brake) is not used until the capabilities of the steering are exhausted. This is confirmed by the fact that brakes are never used when a linear tyre model is employed, and by analytical calculations indicating that DYC only becomes the more efficient method for generating a yawing moment once lateral slip angles are of the order of one radian or greater.

According to established models of aerodynamic force generation, the optimum sideslip for minimisation of aerodynamic drag in turning is not zero (neither at the centre of mass nor at the aerodynamic reference point at mid-wheelbase), but is dependent upon the aerodynamic coefficients of the vehicle. Also, during turning, each point on the vehicle has a different velocity vector and thus a different sideslip angle, so there is some ambiguity as to what constitutes 'zero aerodynamic sideslip'. However, variations in the chosen reference point on the vehicle only have been shown to have only a minor influence on the result.

The contours of constant energy dissipation in the vehicle tyres are approximately (but not exactly) elliptical, and are scaled according to the zeroth and second-moment cornering stiffnesses of the vehicle, C_0 and C_2. As C_2/C_0 increases, lateral acceleration becomes relatively more expensive, and as C_2/C_0 reduces, yaw accelerations become relatively more expensive. This is because the term C_2 increases the sensitivity of the vehicle yaw response to equal and opposite changes in slip angle, and the term C_0 increases the sensitivity of the lateral acceleration response to equal changes in slip angle. Since the same accelerations may be generated for lower slip angles as these parameters increase, this has a direct effect on the energy consumption.

Additionally, the contours are skewed by linear under-steer or over-steer according to the first-moment cornering stiffness of the vehicle C_1, such that when the vehicle is linearly over-steering, generating a yaw moment and a lateral acceleration of the same sign becomes less expensive (in energy consumption terms) than generating a yaw moment and an acceleration of opposite sign.

Chapter 5: Identification of Tyre Force Demands (Frequency Domain)

In this section, linear modelling is employed to determine the lateral tyre forces that are required to maintain a particular sideslip target whilst simultaneously maneuvering the vehicle so that it precisely follows a path with changing curvature. The hypothesis being investigated here is H3.

Since a frequency domain analysis is to be performed, all modelling in this section is purely linear. Therefore, it must be assumed at the outset that the geometric non-linearities have a second-order influence (which is reasonable only if the sideslip angle is small). Non-linearities in tyre behaviour are largely irrelevant in this analysis since it is the force demand that is being identified mathematically, not the slip required for the tyre to deliver that force, nor the feasibility of delivering the force on any particular road surface.

In the analysis of the results, it is assumed that provided sufficient friction is available, then a vehicle dynamics controller would be able to deliver the demanded force (by whatever strategy for inversion of the tyre model, which is not considered here). Therefore, the purpose of the analysis is simply to investigate the magnitudes of the in-plane frictional forces F_y that must be available from the tyres if the target transient path curvature is to be precisely followed. From the magnitudes of these forces, conclusions are drawn about the appropriateness of the particular sideslip target which was enforced.

Constant speed is assumed and two constraints on the vehicle motion are introduced. These are: (i) precise sideslip control according to the target, and (ii) precise path following (according to an oscillatory demand). Both are rigidly enforced such that the front and rear lateral tyre forces F_{y_f} and F_{y_r} are explicitly determined. The resulting tyre force demands are then expressed in a ***frequency response function***, where the input is the amplitude and frequency of the desired path curvature (or, equivalently, lateral acceleration, since $a_y = U^2\rho$, and the forward speed, U, is assumed constant).

5.1: Choice of Model

All models used here are purely linear. Therefore, constant speed is assumed and all of the linearisations (of the geometry, and of the tyres) described in Chapter 2 are adopted.

Simple yaw plane models without tyre relaxation are utilised in the first instance, since the goal is simply to understand the order of magnitude of the influence that sideslip control has on the tyre force demands.

It was observed during the studies of the previous chapter that brake forces are never used when minimum energy consumption is required, such that it is anticipated that DYC control would only be used outside the linear regime (or perhaps very briefly during a transient). For this reason, and for reasons of simplicity, it is assumed in this and the following chapter that steering controls (AWS) alone are available, and DYC is not.

The equations of motion then become:

$$a_y = \dot{V} + Ur = \frac{F_{y_f} + F_{y_r}}{M}$$
$$\alpha_z = \dot{r} = \frac{bF_{y_f} - cF_{y_r}}{I_{zz}}$$

Note: no distinction is made regarding the difference between path-normal and vehicle-lateral acceleration here, since the vehicle model is linear, and constant speed is assumed. Thus:

$$\begin{aligned} {}^{P}a_x &= {}^{V}a_x \cos(\beta) + {}^{V}a_y \sin(\beta) \\ &\approx 0 \\ {}^{P}a_y &= -{}^{V}a_x \sin(\beta) + {}^{V}a_y \cos(\beta) \\ &\approx {}^{V}a_y \end{aligned}$$

Such that ${}^{P}a_y \approx {}^{V}a_y$ and is denoted simply a_y.

In all cases, it is assumed that the front steer angle is controlled in order that the required force is delivered, and the necessary steer angle is not of interest. However, the responses of 2WS vehicles are compared with those of AWS vehicles, such that a model of force generation at an uncontrolled rear axle is required:

$$F_{y_r} = -C_{\alpha_r}\alpha_r$$

with the linearised dependence of slip angle on the vehicle states being:

$$\alpha_r = \frac{V - cr}{U} - \delta_r$$

This linear set of equations describing the vehicle dynamics model is augmented with constraints, requiring that:

(i) path curvature, or lateral acceleration response is precisely equal to the (filtered) demand:

$$^P a_y(\omega) = \frac{1}{1+0.2s} {}^P a_{y_{demand}};$$

(ii) sideslip is controlled according to the selected strategy for rear wheel steering - for instance,

(a) passive 2WS vehicle $(\delta_r = 0)$;

(b) zero sideslip 4WS or AWS $({}^V V = 0, {}^V \beta = 0)$;

(c) fixed motion centre $({}^V V + dr = 0)$.

The front and rear lateral axle forces (F_{y_f} and F_{y_r}), the sideslip, V and yaw rate r are then each explicitly determined as a transfer function (or equivalently, a 'frequency response function') from the 'input' lateral acceleration demand.

This yields the following transfer functions relating the tyre forces to the lateral acceleration which is generated (where s is the Laplace operator):

(a) passive 2WS vehicle $(\delta_r = 0)$;

$$F_{y_f} = \frac{a_y M\left(c^2 C_{\alpha_r} s + c C_{\alpha_r} U + k^2 s\left(C_{\alpha_r} + MsU\right)\right)}{c^2 C_{\alpha_r} s + c C_{\alpha_r} U + k^2 M s^2 U + b C_{\alpha_r}(cs + U)};$$

$$F_{y_r} = \frac{a_y C_{\alpha_r} M\left(-k^2 s + b(cs + U)\right)}{c^2 C_{\alpha_r} s + c C_{\alpha_r} U + k^2 M s^2 U + b C_{\alpha_r}(cs + U)}$$

(b) zero sideslip 4WS or AWS $({}^V V = 0, {}^V \beta = 0)$;

$$F_{y_f} = \frac{a_y M\left(k^2 s + cU\right)}{(b+c)U}; \quad F_{y_r} = \frac{a_y M\left(-k^2 s + bU\right)}{(b+c)U}$$

(c) fixed motion centre $({}^V V + dr = 0)$

$$F_{y_f} = \frac{a_y M\left(cds - k^2 s - cU\right)}{(b+c)(ds-U)}; \quad F_{y_r} = \frac{a_y M\left(bds + k^2 s - bU\right)}{(b+c)(ds-U)}$$

5.2: Analysis Method

For the centres of mass of two different vehicles to follow the same path, their forward speeds and lateral accelerations (or path curvatures) must be equal. Thus, in the following analyses, the required lateral acceleration $a_y(\omega)$ was employed as the input, approximating the driver demand.

In order to account for the limited bandwidth of a human driver, a flat spectrum of possible sinusional demands was filtered through a first-order time lag with a time constant of 0.032s (i.e. a corner frequency of 5Hz):

$$a_y(\omega) = \frac{1}{1+0.032s} a_{y_{demand}}$$

This was selected such that the demand spectrum corresponds to one which might realistically occur during a relatively fast turn-in or obstacle avoidance maneuver. The filter is introduced in order to give a more realistic impression of the likely force demand at high frequency, since it is related both to the driver demand and the vehicle dynamics, with very high frequency behaviour of the vehicle being largely irrelevant, since the driver would not attempt to control this.

Setting the Laplace operator $s = j\omega$ in the transfer function yields the ***frequency response function*** (FRF). This represents the complex ratio of the amplitude of the output $F_{y_f}(\omega)$ or $F_{y_r}(\omega)$ to the input $a_{y_{demand}}(\omega)$, at the angular frequency of $\omega = 2\pi f$. The magnitude of the FRF is of primary interest, since it indicates the magnitude of the sinusoidal tyre forces that are required in order to generate the demand lateral acceleration at the centre of mass.

The force demands plotted in the following section are non-dimensionalised, so that the plots which follow present the force that is required for following a sinusiodal path at a given frequency or wavenumber, compared with the force that is required to follow the same curvature in steady-state. These quantities are described as the (complex) 'proportion utilisation' of the steady-state front and rear tyre force, denoted p_f and p_r, where:

$$p_f(\omega) = \frac{F_{y_f}(\omega)}{F_{y_f}(0)}$$

$$p_r(\omega) = \frac{F_{y_r}(\omega)}{F_{y_r}(0)}$$

5.3: Results and Discussion

For an initial investigation, frequency responses were used to investigate the tyre lateral force (and therefore friction) demands of a zero-sideslip four wheel steer (4WS) vehicle, and to compare these with the demands of a passive vehicle with similar parameters in executing the same maneuver.

The results in figures 5.1 and 5.2 show clearly that the zero-sideslip strategy requires greater front ***and*** rear tyre force demands at high frequency. Thus, where the driver input contains high frequencies, such as in emergency obstacle avoidance, it seems possible that the vehicle would perform perform poorly if zero-sideslip were enforced for high frequencies - either saturating the tyres, or failing to properly track one or other of (a) the demanded path or (b) the target sideslip.

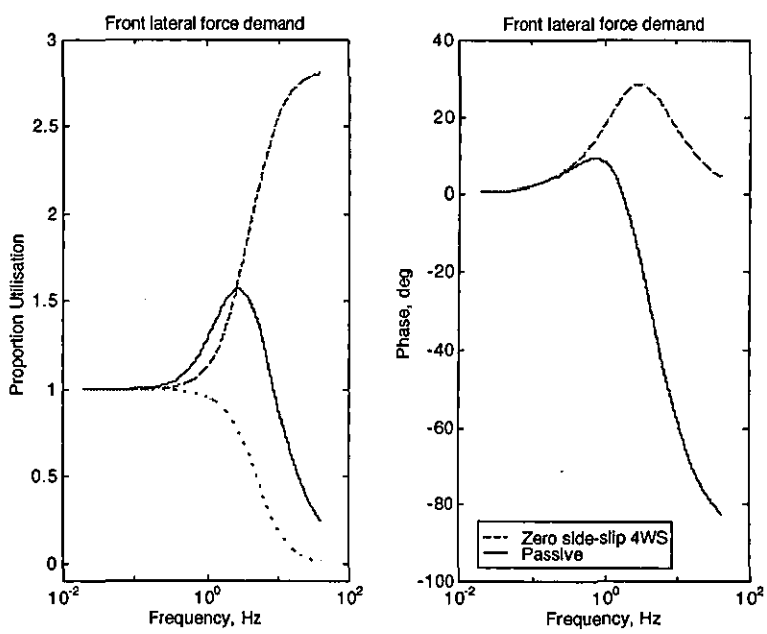

Figure 5.1

Proportion front tyre force utilisation $p_f(\omega) = \dfrac{F_{y_f}(\omega)}{F_{y_f}(0)}$

AWS, zero-sideslip (dashed lines); 2WS (solid lines);
reference particle (filtered flat spectrum)

$\left(M = 1008, I_{zz} = 1031, b = 1.234, c = 1.022, U = 10, C_{\alpha_r} = 144930\right)$

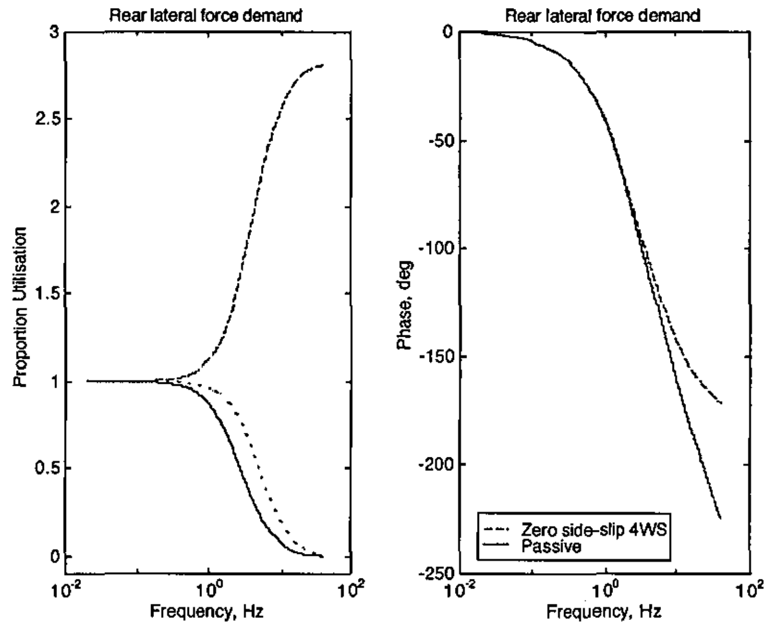

Figure 5.2

Proportion rear tyre force utilisation $p_r(\omega) = \dfrac{F_{y_r}(\omega)}{F_{y_r}(0)}$

AWS, zero-sideslip (dashed lines); 2WS (solid lines)
reference particle (filtered flat spectrum)

$$\left(M = 1008, I_{zz} = 1031, b = 1.234, c = 1.022, U = 10, C_{\alpha_r} = 144930\right)$$

Effect of motion centre location

In the next analysis, the influence of varying the motion centre location was considered. The hypothesis here is that the location of the motion centre may have an influence on the magnitude of the yaw motion of the vehicle and thus on the yaw moment demand. For the most basic yaw plane model, we have:

$$a_y = U^2\rho = \dot{V} + Ur$$

Applying the constraint of a fixed motion centre (constant d with sideslip $V + dr = 0$), such that $\dot{V} + d\dot{r} = 0$, we can identify the magnitude of the yaw rate r that is required to follow a path of curvature ρ and simultaneously satisfy the sideslip constraint:

$$\begin{aligned} |r| &= \left|\frac{U^2\rho}{U - dj\omega}\right| \\ &= \frac{U\rho}{\sqrt{1 + d\lambda^2}} \end{aligned}$$

where λ is the wave-number of the sinusoidal path:

$$\lambda = \frac{\omega}{U}$$

It can be seen from this result that a ***maximum*** of yaw rate demand (and thus also of yaw acceleration demand α_z) with respect to d occurs at a value of $d\lambda = 0$ - in other words, at zero sideslip. As the motion centre location, d increases ***either*** in the positive or negative direction (i.e. either nose-out of tail-out sideslip), the yaw rate and yaw acceleration demand reduces. The form of the curve can be seen in the plot below, where both the motion centre and ***frequency***, $f = \frac{\omega}{2\pi} = \frac{\lambda U}{2\pi}$ of the path curvature have been varied, with constant forward speed, U and constant curvature amplitude, ρ:

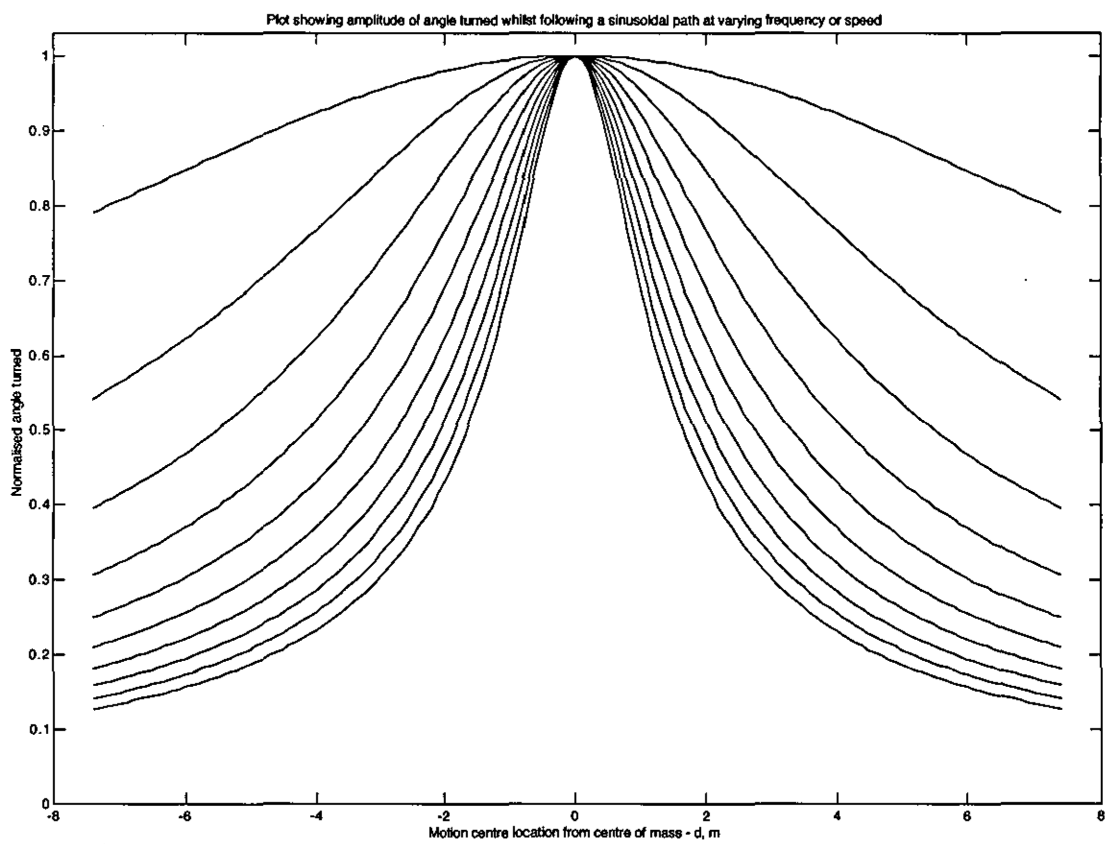

Figure 5.4
Angle θ turned by the vehicle in following a sinusoidal path, normalised to the angle turned by the zero sideslip vehicle on the same path (upper lines correspond to lower input frequencies f)
$(U = 20, \rho = 2, f = 0.3, 0.6, 0.9, 1.2, 1.5, 1.8, 2.1, 2.4, 2.7, 3.0)$

This result would appear to suggest that zero sideslip is the worst possible choice in terms of friction demand. However, this demonstration alone does not prove that the front and/or rear friction demand is highest at zero sideslip since as the motion centre is moved away from zero sideslip, the yaw moment demand moves further ***into phase*** with the lateral force demand)

The friction demand is actually a combination of the lateral force demand and yaw rate demand and the phasing between them. Therefore, whether or not zero sideslip is truly a bad choice (i.e. for arbitrary transient maneuvering) is not immediately clear from looking at frequency-domain plots and considering purely sinusoidal motions, as the phase and the relative magnitudes of each frequency that form the total transient will have a significant influence on the time-history. For this reason, the time domain demands for a sudden change in curvature are identified in the following chapter.

5.4: Limitations of Frequency Domain Modelling and Analysis

Where linear models are used for handling analysis, lateral forces are always assumed to act directly laterally to the vehicle path. Therefore, drive torques must be assumed to be acting to counteract any significant induced drag due to the fact that tyre slip angles are required for a force to be generated and the resulting force occurs in the plane of the slipping wheel (see Chaper 2). Also, the position of the application point (and thus the moment) of the lateral forces is assumed not to vary with the sideslip angle.

The error these assumptions introduce depends upon the cornering compliances of the tyres and the magnitude of the demand and vehicle sideslip angle response, respectively.

Also, the approach presented here can be considered either to be testing the appropriateness of the path for the vehicle, ***or*** the appropriateness of the vehicle to the path which must be followed.

In reality the optimum realistic path is certainly related to the vehicle dynamics, since it is rare that very precise path following is required, such that where the tyre force demands for a given path curvature have peaks at certain frequencies, it may be acceptable for those frequencies to be filtered out of the target path.

5.5: Concluding Remarks

It has been seen that the enforcement of zero sideslip at high frequency yields very large tyre force demands which could not be delivered except for the very smallest of sinusoidal input amplitudes. It is concluded, therefore, that a controller which attempted to satisfy a sudden lateral acceleration demand and simultaneously maintain zero sideslip would always fail in at least one of those objectives.

If this conflict is corrected by simply filtering the path curvature (or lateral acceleration) demand, then the appropriate filtering must consider the vehicle dynamics (due to the observed frequency dependence of the vehicle lateral acceleration response).

In the approaches presented here, no account is taken of the absolute limit on the available frictional forces, and when a high demand occurs for a short period of time, it is unclear where the vehicle's failure to satisfy that demand (due to tyre saturation) would significantly impair the performance.

The largest amplitude in global yaw rotation, yaw rate and yaw acceleration occurs when the motion centre is fixed at the centre of mass (i.e. when zero sideslip is imposed), regardless of vehicle speed and freqeuncy of demand. Since the maximum with respect to motion centre location occurs at zero sideslip, small changes in the motion centre location around zero sideslip yield little reduction in the magnitude of the resulting yaw motion. However, the magnitude of the yaw motion is more sensitive to the motion centre location at higher frequency.

Chapter 6: Identification of Tyre Force Demands (Time Domain)

As already mentioned, the frequency domain approach of Chapter 5 does not predict the transient variation of the tyre forces during maneuvering - unless the maneuver happens to involve following a pure sinusoid!

This chapter continues to investigate hypothesis H3, by investigating whether the enforcement of zero sideslip has a sifgnificant influence on the time-domain tyre force demands.

In this Chapter, the ***same*** frequency response functions identified in the previous Chapter:

(a) passive 2WS vehicle $(\delta_r = 0)$;

$$F_{y_f} = \frac{a_y M\left(c^2 C_{\alpha_r} s + c C_{\alpha_r} U + k^2 s\left(C_{\alpha_r} + MsU\right)\right)}{c^2 C_{\alpha_r} s + c C_{\alpha_r} U + k^2 M s^2 U + b C_{\alpha_r}(cs + U)};$$

$$F_{y_r} = \frac{a_y C_{\alpha_r} M\left(-k^2 s + b(cs + U)\right)}{c^2 C_{\alpha_r} s + c C_{\alpha_r} U + k^2 M s^2 U + b C_{\alpha_r}(cs + U)}$$

(b) zero sideslip 4WS or AWS $\left({}^V V = 0, {}^V \beta = 0\right)$;

$$F_{y_f} = \frac{a_y M\left(k^2 s + cU\right)}{(b + c)U}; \quad F_{y_r} = \frac{a_y M\left(-k^2 s + bU\right)}{(b + c)U}$$

are used in order to determine the transient tyre forces $F_{y_f}(t)$ and $F_{y_r}(t)$ required to follow a time-dependent path curvature $\rho(t)$ (or lateral acceleration, $a_y(t)$) by means of ***Fourier and Inverse Fourier Transforms***.

6.1: Analysis Method

The approach of using Fourier and Inverse Fourier Transforms was selected over direct integration of the equations of motion for this analysis, due to the fact that it is the inverse response (rather than the usual 'forward response') of the model which is being analysed. When a causal (physical) system is inverted prior to analysis, the response usually becomes ***acausal*** - in other words, the impulse response of the inverted system may begin before $t = 0$ (indicating, for instance, that the 'output' steering angles or forces occur ***before*** the 'input' lateral acceleration is applied). Such system descriptions are clearly unsuitable for direct integration in the time domain and are not unphysical, since for example a driver must always steer in advance of any curve 'demand'.

The time-domain variation of the tyre forces required to track a particular curvature demand may, however, still be identified from the frequency response function. This is preformed by recalling the standard result that convolution in the time domain is equivalent to multiplication in the frequency domain [Franklin, 1988], and applying this process to a discretised input. Since the time response is equal to the convolution of the impulse response of the system with the input:

$$\underline{F}_{y_f}(t) = \underline{h}_{F_{y_f}/a_y}(t) * \underline{a}_y(t)$$
$$\underline{F}_{y_r}(t) = \underline{h}_{F_{y_r}/a_y}(t) * \underline{a}_y(t)$$

a discretisation of the outputs of interest, $\underline{F}_{y_f}(t)$ and $\underline{F}_{y_r}(t)$ may be determined by taking the Discrete Fourier Transform of the input, yielding a Fourier Series:

$$\underline{A}_y^*(f) = \Im\{\underline{a}_y(t)\} \ ,$$

which gives the outputs as a function of frequency by multiplication of the input spectrum and frequency response:

$$\underline{F}_{y_f}^*(f) = \underline{H}_{F_{y_f}/a_y}^*(f) \cdot \underline{A}_y^*(f); \quad F_{y_r}^*(f) = H_{F_{y_r}/a_y}^*(f) \cdot A_y^*(f)$$

where $\underline{H}^*(f)$ is the complex frequency response function (equal to the transfer function determined in the previous chapter, at equally spaced frequencies $f = \omega/2\pi$, with the fundamental frequency $f_0 = 1/T$, T being the time duration of the input and output) and computing the discretised output by taking the ***Inverse*** Discrete Fourier Transform of the resulting Fourier Series:

$$\underline{F}_{y_f}(t) = \Im^{-1}\{\underline{F}_{y_f}^*(f)\}; \quad \underline{F}_{y_r}(t) = \Im^{-1}\{\underline{F}_{y_r}^*(f)\}$$

6.2: Results and Discussion

Inversion of Vehicle Dynamics Models

For an initial investigation into the feasibility of direct inversion of vehicle handling models prior to comparison of 2WS and AWS, some simple yaw-plane vehicle dynamics models were inverted, such that the steer angle $\delta(t)$ required to follow a given lateral acceleration $a_y(t)$ was identified.

In this case, the procedure followed was that described above, but with the input $a_y^*(f) = \Im\{a_y(t)\}$, the system transfer function, $H^*(f) = \dfrac{\delta^*(f)}{a_y^*(f)}$ and the output $\delta(t) = \Im^{-1}\{\delta^*(f)\}$.

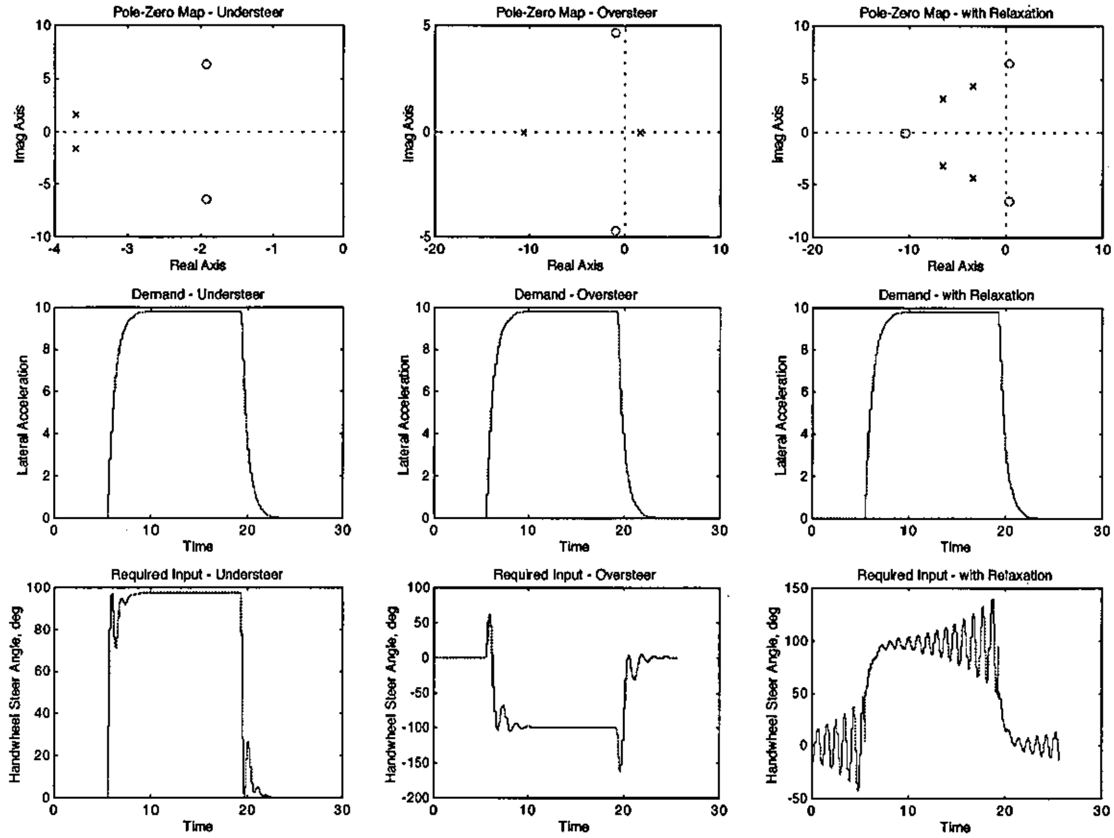

(i) **(ii)** **(iii)**

Figure 6.1

(a) pole-zero map (x = pole, o = zero),

(b) demand acceleration time-histories, $a_y(t)$,

and (c) necessary (front) steer angle time-histories, $\delta_f(t)$

for a three yaw-plane vehicle models.

In all cases: $M = 2045, I_{zz} = 5428, b = 1.488, c = 1.712, U = 20$

(i) linear under-steer, no tyre relaxation $\left(C_{\alpha_f} = 77850, C_{\alpha_r} = 76510\right)$

(ii) linear over-steer, no tyre relaxation $\left(C_{\alpha_f} = 155700, C_{\alpha_r} = 38255\right)$

(iii) linear over-steer as above, with tyre relaxation $\left(l_f = 2.0, l_r = 2.0\right)$

An inversion involves exchanging poles for zeros, such that models (such as the first two) with stable or unstable poles cause no problem, since those poles simply correspond to minimum-phase or non-minimum phase zeros in the inverted transfer function.

However, models such as the third (with tyre relaxation) that have non-minimum phase zeros do cause difficulties, since those non-minimum phase zeros map to unstable poles in the inversion. Therefore, the envelope of the control signals identified in the third case can be seen to be increasing with time due to the right-half-plane pole pair in the inverted transfer function, which corresponds to a ***dynamically unstable*** mode.

Interestingly, vehicles which are linearly statically unstable (i.e. linearly over-steering, even and driven above their critical speed [Gillespie, 1992]) may still be precisely controlled ***with a finite (bounded) steering input***, indicating that the linear stability of the underlying vehicle is not a fundamental problem for a vehicle dynamics controller, provided the plant can be identified and inverted.

However, limitations on what is fundamentally achievable by a controller will arise due to then eventual saturation of the controlling forces due to the limited available friction. Therefore, in the following section, the demands that path following places on the available friction are identified.

Tyre demands from inversion of 2WS and Zero Sideslip (ZSS) models

Bearing in mind the issue of relaxation lags (and acknowledging that alternative approaches may be necessary in order to deal with the issue of tyre relaxation, if an effective controller target is required), models ***without*** tyre relaxation were selected for the analysis in the following section. This is considered acceptable for the purposes of this exercise (if not for the development of a controller) since it is the distribution of the tyre force demands which is of interest here, rather than the slip or steer angles necessary to achieve them.

For the 2WS and ZSS yaw plane models, the lateral force demands were identified for a dual Heaviside ('step') function in the path curvature or lateral acceleration.

The lateral acceleration was applied as the input to the system transfer functions $\frac{F_{y_f}}{a_y}(s)$ and $\frac{F_{y_r}}{a_y}(s)$, and following the procedure described above to identify the time domain lateral force demands, $F_{y_f}(t)$ and $F_{y_r}(t)$.

The Inverse Fourier Transform of the required front and rear tyre forces, $F^{-1}\{F_{y_f}(f)\}$ and $F^{-1}\{F_{y_r}(f)\}$ was plotted in figure 6.2.

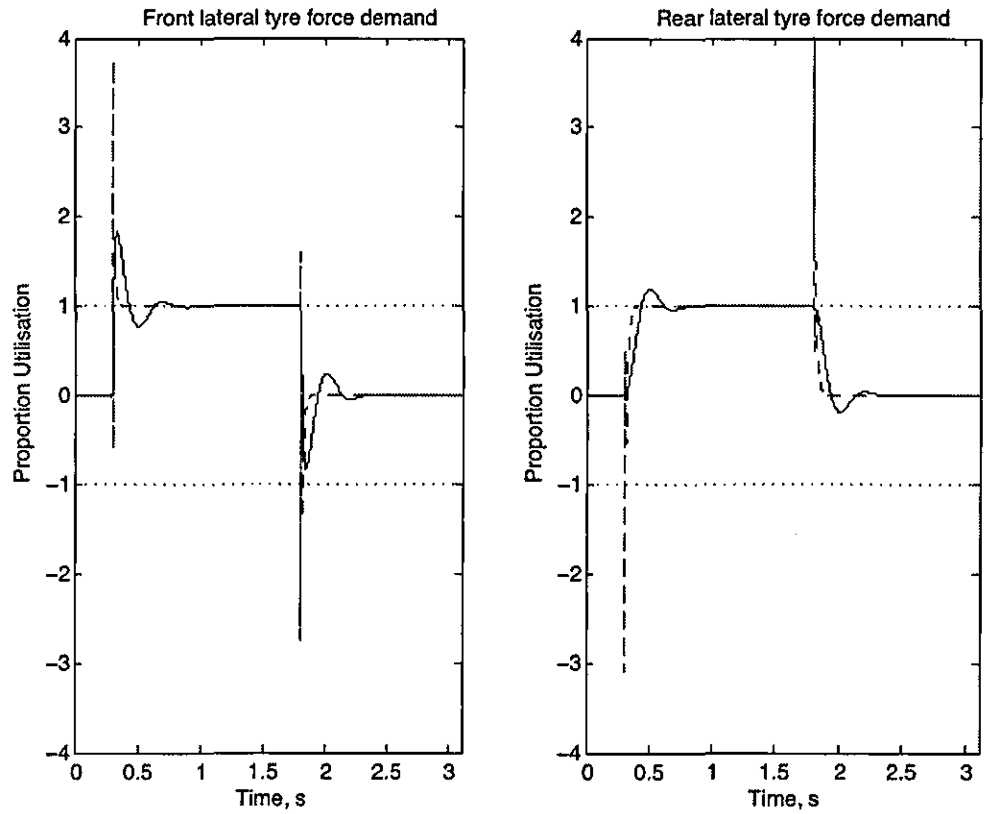

Figure 6.2
Transient tyre force demands
(yaw-plane model with centre CG, dual-step lateral acceleration demand, filtered at 5Hz)
solid line = 2WS; dashed line = ZSS 4WS

$$\left(M = 1008, I_{zz} = 1031, b = 1.234, c = 1.022, U = 20, C_{\alpha_r} = 144930\right)$$

From figure 6.2, it can be seen that the high tyre force demands which were observed to occur in the frequency domain for the ZSS vehicle do indeed have a significant influence on the tyre forces required to follow a step change in lateral acceleration (or, equivalently, a step in path curvature). If the corner frequency of the input filter frequency is increased (such that the demand becomes more immediate), the magnitude of the initial tyre force demand becomes extremely large. As the filter frequency is reduced, the transient lateral acceleration (obstacle avoidance) performance of the vehicle is clearly impaired.

Note that the 2WS vehicle with nominal rear tyre cornering stiffnesses, whose tyre force requirements are overlaid, is required to follow the same path as the ZSS vehicle, and does so with much lower peak tyre forces.

Since the available friction is always hard-limited, there are, therefore, levels of available friction for which the 2WS vehicle (or a 4WS/AWS vehicle controlled to the same sideslip) could complete the maneuver successfully whilst also maintaining sideslip control, whereas the ZSS vehicle would not be able to both follow the path and maintain the sideslip target, since the high instantaneous demands would exceed the available friction.

Inversion of multi-input (4WS/AWS) models

For a 4WS/AWS vehicle, where both front and rear lateral axle forces may be controlled, the non-minimum phase zeros disappear from the system transfer functions. Since it has been shown above that both the front and rear tyre force demands to track a given sideslip target may be identified, it is proposed that (for a 4WS or AWS vehicle), the necessary lateral slip and steer angle time-histories could be identified from the force demands.

The plots shown in figure 6.3 show examples of the tyre slip angle time-histories $\alpha_f(t)$ and $\alpha_r(t)$ that are required to deliver a filtered step in lateral force, as the filter frequency is progressively increased such that the input becomes more demanding. The filter employed is a simple first-order time lag.

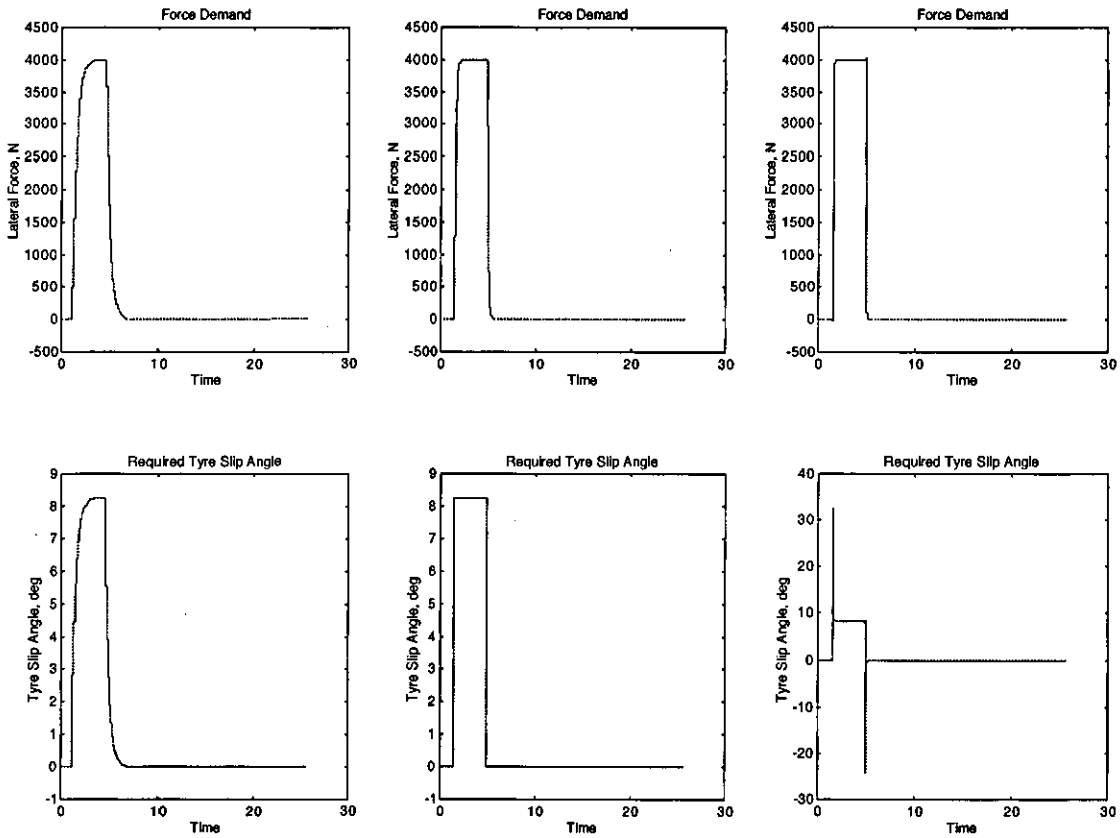

(i) (ii) (iii)

Figure 6.3

Examples of tyre slip required to precisely satisfy steps in force demand, with (i) 3x longer, (ii) equal and (iii) 3x shorter demand lag, compared with the tyre relaxation lag

The feasibility of such an inversion is considered important, because obstacle avoidance maneuvers typically require a rapid buildup of lateral acceleration and thus of lateral tyre force. Since such a force buildup would typically be required to occur much more quickly than the response of the vehicle would occur, such a time-history of the slip angle would need to be supplied primarily by a similar time-history in steer angle. Clearly making such rapid changes in steer angle is impossible, so this was identified as a further potential restriction on the optimal obstacle-avoidance performance. This restriction is discussed in more detail in Chapter 8, where all of the factors that limit transient obstacle avoidance (or turn-in) performance are identified ***analytically***.

6.3: Limitations of Linear Modelling and Analysis

In all of the above analysis, linear models are employed, and lateral forces are assumed to be directed laterally to the vehicle. Since sideslip angles are assumed small, the same force is assumed to act laterally to the path. In addition, the position of the application point (and thus the moment) of the lateral forces does not vary with the sideslip angle. Apart from the modelling assumptions which must be made, the approach unavoidably tests both the path and the vehicle simultaneously. In reality the optimum ***realistic*** path is related to the vehicle dynamics, or alternatively the vehicle dynamics need to be tuned to give the desired transient path curvature. Appropriate choice of transient path curvature demand should really be made with reference to the dynamic capability (and typical transient response) of the vehicle.

For some vehicles there exists a frequency at which the vehicle responds in yaw and sideslip in such a manner that the resulting lateral acceleration is ***always*** zero. If the demand included ***any*** curvature at this frequency, then it would be impossible for the vehicle to follow that demand, regardless of the available friction.

In addition, in the approaches taken here, proper account is not taken of the hard limit which exists on the available tyre forces, and when a high demand is specified for a short period of time, it is unclear where the vehicle's failure to exactly satisfy that demand (due to tyre saturation) would - or would not - significantly impair the performance. Such effects can only be predicted by non-linear analyses.

These issues led to the development of the alternative, ***constrained*** method for assessing transient performance that is described in the following section.

6.4: Concluding Remarks

Zero sideslip 4WS/AWS versus 2WS

The enforcement of zero sideslip at high frequency yields transient spikes in the time-domain tyre force demand, that are much greater than the maximum tyre forces demanded by the sideslip behaviour of the typical 2WS vehicle.

Since the maximum frictional force is always limited, there will therefore certainly be maneuvers during which these demands cannot be satisfied - whenever the demand is large compared with the available friction, and the demand is rapidly changing.

It is expected, therefore, that a controller which attempts to satisfy a sudden lateral acceleration demand and simultaneously maintain sideslip control during an obstacle-avoidance maneuver or lane-change maneuver would be more likely to fail to meet its objective if it had a sideslip target of zero, compared with the alternative sideslip target of a 2WS vehicle.

It should be noted, however, that this conclusion applies only when strict trajectory-following is enforced. If the strict requirement of a fixed centre of rotation were relaxed at high frequency (i.e during sharp transients) then a different conclusion might be reached.

Chapter 7:
Identification of Ideal Transient Behaviour (by Linear Programming)

In the previous chapter, it was identified that the assessment of different vehicles against their ability to follow a specific transient path curvature demand is an imperfect approach, since vehicles with essentially very similar dynamic performance capability may 'find it difficult' to satisfy one demand (i.e. significant, or even infinite control activity may be required) whilst the same vehicle may "find it easy" to satisfy another very similar demand, depending upon whether the detail of the demand time-history is somehow well matched to the natural transient behaviour of the particular vehicle. In particular, it may be impossible for a vehicle to generate any component of lateral acceleration at certain frequencies, such that enforcing this as a demand and analysing the tyre forces which result leads to undue criticism of an otherwise capable vehicle.

A popular solution to this problem is to employ a 'cost function' on the outputs of interest, and apply feed-back control to minimise (though perhaps not zero) this cost using an approach known as LQR (Linear Quadratic Regulation). However, the LQR approach is only linear-optimal. This not only implies that the resulting control action is linear, but also that the control is optimal only when applied to a linear system. There is no way for the quadratic cost of an LQR controller to take account of the hard limits on tyre force which exist due to limited friction. Therefore, LQR controllers may demand more friction than is available from the tyres when an alternative solution might exist that would yield a similar 'cost' but using a feasible combination of tyre forces. Conversely, LQR may overlook the possibility of improving the dynamic performance by utilising ***more*** of the readily available friction, since friction utilisation is normally quadratically costed (as an attempt to prevent solutions such as that described above, where LQR makes excessive demands on the available friction).

Since LQR is sub-optimal when applied to the non-linear, hard-limited handling control problem, an alternative approach has been developed to allow identification of the control inputs which are truly optimal in this hard-limited sense, in an effort to ensure a a fairer comparison of the best achievable dynamic performance of vehicles with differing sideslip targets.

The outputs from this analysis correspond to the most extreme maneuver that is possible within a certain amount of available friction. It is hypothesised, however, that since the available forces and accelerations scale approximately according to the friction level, if the trajectory and control outputs from this analysis are simply scaled according to the demand, then whenever the demand is within the envelope of capability of the vehicle, then the vehicle should be able to satisfy that demand in the optimal manner.

The approach presented in this Chapter continues to employ simple linear models in an attempt both to gain understanding, reduce the parameter space and facilitate identification of a single, globally optimal solution. However, it does not enforce a precise path curvature (as in Chapters 3 to 6) nor does it arbitrarily cost friction utilisation and performance, as in LQR. Instead, this chapter uses Linear Programming to determine the optimal control inputs - within the constraints of the available friction - that maximise the path curvature as quickly as possible. The hypothesis being investigated here is H4:

It is proposed that with consideration given to the modelling assumptions, the resulting ***friction-force-optimal transient responses*** could later be used to identify a transfer function between demand and controller reference, such that the step response to a change in demand to a given lateral acceleration always makes optimal use of the friction that would exist were this lateral acceleration the limit of the vehicle.

7.1: Modelling the Vehicle and Limits

For use in Linear Programming analyses, all models must be linear. The detail of the modelling and the linearisations are presented in Chapter 2. Both simple yaw-plane models and models with a roll degree of freedom, tyre relaxation and suspension derivatives are utilised.

However, applying the objective of maximising lateral acceleration (or path curvature) to a purely linear model would always lead to an infinite response with infinite tyre force demands. For this reason, a constrained optimisation has been adopted, where the available friction and selected other system outputs, such as actuator forces and the available road are hard-limited. In other words, the actuator forces are constrained by means of inequality constraints.

These limits being ***hard*** facilitate fair comparison between vehicles or sideslip targets, since the optimal performance of every vehicle encroaches on each constraint by exactly the same amount - zero. Variable encroachment on softer constraints was found to be a problem when comparing vehicles whose performances had been optimised using unconstrained, non-linear optimisation techniques such as Generalised Optimal Control [Hendrikx, 1996].

The use of linear models to model the dynamics yields another significant advantage – that it is possible to express (and solve) the problem in a manner (dynamic Linear Programming) that ensures that a single optimum exists. This ensures that the effects of fundamental vehicle parameters can be explored, with confidence that changes in the optimal performances identified numerically are not strongly dependent upon non-linear tyre properties, or characteristics of non-linear solution procedures.

The restriction to linear constraints is ***not*** actually a highly restrictive one. The bounds may be functions of many states of the system, such that, for instance, the constraint on the maximum lateral tyre force may depend upon the instantaneous vertical load on the tyre, upon the longitudinal force which is being generated; and upon the camber angle. Each individual constraint must always be linear in the states, but it is possible to represent certain classes of nonlinear constraint with multiple linear constraints, and thereby partition off any concave region of the solution space. It turns out that the representation of the ellipse of friction of a tyre, and the non-linear variation of the size and shape of this ellipse with changes in the vertical load on the tyre, is a class of constraint which is able to be represented without restriction, since the solution space is convex.

Note: In representing non-linear constraints in this approximate way, it is advisable to bear in mind that the solution of a linear programming problem always lies at the intersection of two constraints – such that it is wise to choose the linear approximation such that all of the possible solutions (that is the intersections of the lines) lie exactly on the non-linear saturation or constraint function being approximated (e.g. on the boundary of the ellipse).

7.2: Analysis Method

7.2.1: Optimisation Objective

The optimisation objective is to identify the best transient performance that is achievable by a particular vehicle in given road conditions - i.e. what the controller would need to achieve to be considered optimal - and to understand what governs that performance, apart from the effectiveness of the control strategy.

Definition of Ideal Transient Behaviour

The use of an optimisation approach such as Linear Programming to identify the best-case vehicle obstacle avoidance performance requires that some ***scalar metric(s)*** be defined against which to maximise and/or rate the vehicle performance. Since optimal physical performance is the focus of this thesis, metrics were developed which maximise the turn-in/obstacle-avoidance performance and allow a comparison between the transient performance of a vehicle and the path followed by an 'ideal' vehicle (i.e. particle).

First metric of transient turn-in or obstacle-avoidance performance: lateral velocity 'shift' Δv_y

The first metric of transient handling performance that is used in this section, which is described as the 'lateral velocity shift', is identified from the time-variation of the difference between the transient lateral acceleration time-history of the vehicle, $a_y(t)$ and its final value $a_y(\infty) = a_{y_{ss}}$, where an immediate step to $a_y(\infty) = a_{y_{ss}}$ is assumed to represent the step-response behaviour of an 'equivalent' vehicle with an 'ideal' (immediate) transient response:

$$\Delta a_y(t) = a_y(t) - a_{y_{ss}}$$

Note that here, 'equivalent' implies that the vehicles have the same steady-state lateral acceleration limit, $a_y(\infty) = a_{y_{ss}}$.

The time-integral of this difference in the lateral accelerations gives the evolution of the lateral velocity 'shift' $\Delta v_y(t)$ (which is the relative velocity between the two vehicles):

$$\Delta v_y(t) = \int_0^t \Delta a_y(t) dt = \int_0^t a_y(t) - a_{y_{ss}} dt$$

whose final value $\Delta v_y(\infty)$ provides the first scalar metric of transient handling performance, $\Delta v_{y_{ss}}$.

$$\Delta v_{y_{ss}} = \Delta v_y(\infty)$$

Alternative expressions of the first metric:

(i) lateral acceleration delay time, t_{lag}

This metric may also be expressed as the 'lateral acceleration delay', since the velocity shift occurs due to there being a time delay in the development of the lateral acceleration, $a_y(t)$.

The evolution of the effective time lag, $t_{lag}(t)$, may be identified as

$$t_{lag}(t) = \int_0^t \frac{a_y(t) - a_{y_{ss}}}{a_{y_{ss}}} dt = \frac{\Delta v_y(t)}{a_{y_{ss}}}$$

and the value of the metric $t_{lag_{ss}}$ is therefore:

$$t_{lag_{ss}} = t_{lag}(\infty) = \int_0^\infty \frac{a_y(t) - a_{y_{ss}}}{a_{y_{ss}}} dt = \frac{\Delta v_y(\infty)}{a_{y_{ss}}} = \frac{\Delta v_{y_{ss}}}{a_{y_{ss}}}$$

It will be seen later that this alternative expression of the first metric has the advantage that it is ***independent*** of the magnitude of available frictional forces $\hat{F}_f$ and $\hat{F}_r$, and thus in some sense independent of the available friction μ. Additionally, when the response is either a pure time lag of τ seconds, or a first-order time lag with a time constant of τ, the metric $t_{lag_{ss}}$ is ***equal*** to that time delay, τ.

Alternative expressions of the first metric:

(ii) shift in angle turned, $\Delta\theta$

The first metric may also be expressed as the shift in angle turned by the velocity vector of the vehicle, or the shift in angle turned by the path.

The evolution of this quantity, $\theta(t)$, may be identified from the integral of the path curvature:

$$\begin{aligned}
\Delta\theta(t) &= \int_0^{s(t)} \Delta\rho(s)ds \\
&= \int_0^t \Delta\rho(t)\frac{ds}{dt}dt \\
&= U\int_0^t \rho(t) - \rho_{ss}\,dt \\
&= \frac{1}{U}\int_0^t a_y(t) - a_{y_{ss}}dt \\
&= \frac{\Delta v_y(t)}{U}
\end{aligned}$$

and the associated scalar metric of performance $\Delta\theta_{ss}$ is again the final value of this quantity, $\Delta\theta(\infty)$:

$$\Delta\theta_{ss} = \Delta\theta(\infty)$$

Second metric: lateral displacement 'shift', Δd_y

The second metric of transient handling performance, known as the 'lateral displacement shift', is identified from the time-variation of the difference between the time-history of the quantity $\Delta v_y(t)$ and its final value $\Delta v_y(\infty) = \Delta v_{y_{ss}}$.

$$\Delta\Delta v_y(t) = \Delta v_y(t) - \Delta v_{ss}(t)$$

the time-integral of this gives the evolution of the lateral displacement 'shift' $\Delta d_y(t)$

$$\Delta d_y(t) = \int_0^t \Delta\Delta v_y(t)dt = \int_0^t \Delta v_y(t) - \Delta v_{ss}(t)dt$$

whose final value $\Delta d_y(\infty)$ provides the second scalar metric of transient handling performance, $\Delta d_{y_{ss}}$.

$$\Delta d_{y_{ss}} = \Delta d_y(\infty)$$

Relative importance of each metric

In adopting these shifts as metrics of obstacle avoidance performance, it has been assumed that the transient is sufficiently short compared with the time-to-impact that the effect is approximately the same as if the entire shift (both displacement and rate of change of displacement) developed immediately at $t = 0$.

Therefore, the lateral displacement performance of the vehicle compared with the reference (ideal) vehicle is being modelled (approximated) as:

$$\Delta d_{approx}(t) \approx \Delta d_{y_{ss}} + \Delta v_{y_{ss}} t$$

Therefore, for short time-to-impact, only the lateral displacement term is of any importance; for long time-to-impact, the velocity term becomes the most important (since the sensitivity of the modelled displacement difference, Δd_{approx} to these parameters is

$$\frac{\partial \Delta d_{approx}}{\partial \Delta d_{y_{ss}}}(t) = 1$$

and

$$\frac{\partial \Delta d_{approx}}{\partial \Delta v_{y_{ss}}}(t) = t$$

respectively).

In truth, of course, the whole displacement time-history is the best measure of the performance, and the approximate model Δd_{approx} is likely to be equal to this at large t, but in significant error at small time-to-impact (i.e. during the transient), but it was desired to simplify the influence of the transient for the sake of understanding the influence of parameters and control targets in a generic manner when the time-to-impact is not known.

7.2.2: Expression as a problem in Linear Programming

In this chapter, the technique of *Linear Programming* is applied in a novel way that give new insights into optimal control of vehicle handling dynamics, where it is used to determine the optimal driver and controller input time-histories, assuming simplified and discretised representations of the optimisation target, the controller capabilities and the system dynamics.

The use of Linear Programming in problems of identifying optimal control input for a vehicle is not new [Kimbrough, 1992] although using it in a dynamic (rather than instantaneous) sense may indeed be new.

The primary focus in applying this technique in this work is in the identification of optimal control behaviour for emergency obstacle avoidance, in other words, what must a controller do in order to transition to as high a path curvature as possible, as soon as possible.

It is recognised that in such a situation, the vehicle behaviour would always enter highly non-linear regions of the tyres, but it is reiterated that the objective of the work is to increase understanding, not to accurately simulate any specific vehicle. Although the vehicle speed also changes during such maneuvers, Alleyne [Alleyne, 1997] concurs with the assumption that during emergency obstacle avoidance, the body-fixed longitudinal velocity will not decrease significantly, such that the eigenvalues of the response don't change much (except due to tyre saturation), and the linear model remains reasonably valid.

Limitations of other approaches

Classical linear model based techniques for identification of appropriate control (such as LQR) often require that the assumption be made that the system dynamics remain linear throughout an unbounded operating range, such that any physical limitations on the values of the states (and the associated possible loss of accurate control) may not be considered. This limitation was evident, for instance when inverse linear models of vehicle handling behaviour were used to solve precise path-following problems such as in Chapter 5 and 6, because differences in transient dynamic characteristics mean that a path that is realistically appropriate for one vehicle to follow may be significantly different from that which is appropriate for another. This problem often results in tyre force or steer rate demands which are instantaneously higher than those which are feasible, because the input time-history is constrained to be such that the path is followed perfectly and the exceedance of physical limits is not taken into account [Karnopp, 1991].

Conversely, the more complex (non-linear system model) approaches may represent properly and without restriction, all of the details of the behaviour of a non-linear system, including saturation and constraints. However, massive computational effort is generally required in order to perform optimisation on a system of any complexity, and in addition are subject to the problem of finding results which are only locally optimum. Non-linear model-based approaches which are less susceptible to this (not insignificant) problem, such as those described as "simulated annealing", generally require even greater computational effort, and no approach is able to guarantee to find a global minimum in all circumstances [Press, 1992]. This leads to significant uncertainty regarding whether general conclusions can be drawn from trends in 'optimal' results. In addition, the non-linear model invariably requires the identification of many parameters, such that at the concept level it is inappropriate, as it is desired to develop strategies which are not sensitive to the details of the vehicle (or system) design.

The variant of Linear Programming used here employs a linearised and time-discretised model of the system under consideration, but constrains, as required, certain of the states or outputs of this linear system to remain within certain bounds - either for the whole duration of the simulation, or for a subset of time instants.

Definition of the Available Inputs In Discrete-Time

The vehicle system under consideration may respond to multiple control inputs (e.g. steer angles, direct yaw control moments, active differential controls, brake or throttle) at any single time instant. For identification of the optimal input time-histories by Linear Programming, the input(s) are represented in discrete-time, such that:

$\underline{x}$ is a vector of the amplitudes of a train of impulses,
representing the sampled inputs applied to each control.

For example,

$\underline{x} = \left[\underline{F}_{y_f}\right]$ or $\underline{x} = \left[\underline{\delta}_f\right]$ for a 2WS vehicle with no DYC;

$\underline{x} = \begin{bmatrix} \underline{F}_{y_f} \\ \underline{F}_{y_r} \end{bmatrix}$ or $\underline{x} = \begin{bmatrix} \underline{\delta}_f \\ \underline{\delta}_r \end{bmatrix}$ for a 4WS/AWS vehicle with no DYC;

$$\underline{x} = \begin{bmatrix} \underline{F}_{y_f} \\ \underline{F}_{y_r} \\ \underline{M}_{z_f} \\ \underline{M}_{z_r} \end{bmatrix} \text{ or } \underline{x} = \begin{bmatrix} \underline{\delta}_f \\ \underline{\delta}_r \\ \underline{\Delta F}_{x_f} \\ \underline{\Delta F}_{x_r} \end{bmatrix} \text{ for a 4WS/AWS vehicle with front and rear DYC.}$$

such that the number of elements of the vector $\underline{x}$ is equal to the sum of the number of control inputs multiplied by the number of time instants of the input. In the simulations presented here, it is assumed that all controls are available at all time instants.

Definition of Outputs to be Constrained

The relationship between this input vector (set of concatenated discrete-time-histories) and each output vector time-history to be constrained is defined by a matrix $\underline{\underline{A}}$, such that

$$\underline{y} = \underline{\underline{A}}\underline{x}$$

or

$$\begin{bmatrix} \underline{y}_1 \\ \cdots \\ \underline{y}_n \end{bmatrix} = \begin{bmatrix} \underline{A}_1 \\ \cdots \\ \underline{A}_n \end{bmatrix} \underline{x}$$

where

$\underline{x}$ is the vector of the amplitudes of the ***input*** impulse train

$\underline{y}$ is the concatenation of the vectors of the amplitudes of the ***output*** impulse trains

Note that the lengths of the $\underline{x}$, $\underline{y}_i$ and $\underline{y}$ vectors may differ. This is useful, for instance, if it is desired to constrain the output states after the input signal ends or reaches steady-state - in this case, the vector $\underline{x}$ need only be as long as the transient input, but the vector $\underline{y}_i$ could be longer, in order to capture change in the system response ***after*** the transient input is applied. Also, the outputs to be constrained in $\underline{y}$ - for instance, representing vehicle position may be required to be constrained only at certain time instants, corresponding to certain forward distances traveled - for instance, to represent the boundaries of a straight section of road before a turn.

The values of the elements of the matrix $\underline{\underline{A}}$ are determined from the discrete-time transfer functions between the inputs $\underline{x}$ and outputs $\underline{y}$. The $\underline{\underline{A}}$ matrix essentially becomes a staggered set of discrete-time impulse responses between each input and output of the system, such that each output becomes a sum of an appropriately weighted set of such staggered impulse responses.

Determination of the System Response Matrix $\underline{\underline{A}}$

In continuous-time, the transfer functions from one of the controls $f(s)$ to one of the outputs $g(s)$ of a continuous time system may be expressed (as discussed in Chapters 5 and 6) in the form:

$$\frac{g}{f}(s)=\frac{\sum_{q=0}^{Z} n_q s^q}{\sum_{p=0}^{P} d_p s^p}$$

For example, for a ***second-order*** system (such as the simplest yaw plane vehicle dynamics models), the transfer function between each input-output pair may be described using 6 coefficients, describing the poles and zeros of the transfer function:

$$\frac{g}{f}(s)=\frac{n_2 s^2+n_1 s+n_0}{d_2 s^2+d_1 s+d_0}$$

The transfer functions between the controls and the outputs to be constrained (which, in most analyses, include at least the tyre forces, g_2 and g_3) must be identified, as must those corresponding to other other outputs of interest.

These continuous-time transfer functions, derived by Laplace transformation, e.g.

$$\frac{g_2}{g_1}(s) \quad \frac{g_3}{g_1}(s)$$

are formed, then z-transforms are taken:

$$\frac{g_2}{g_1}(z) \quad \frac{g_3}{g_1}(z)$$

and these are then transformed into difference equations of the following form (again using the example of a second-order system):

$$g_2(k)=a_1 g_1(k)+a_2 g_1(k-1)+a_3 g_1(k-2)+a_4 g_2(k-1)+a_5 g_2(k-2)$$
$$g_3(k)=b_1 g_1(k)+b_2 g_1(k-1)+b_3 g_1(k-2)+b_4 g_3(k-1)+b_5 g_3(k-2)$$

where the final two terms refer to the values of the output (g_2 or g_3 respectively above), over the previous two time steps.

The coefficients (a_n, b_n) in these equations may be determined by discretisation of the identified continuous-time transfer functions - for example, by making the backward difference (or 'first order hold') approximation to differentiation:

$$\frac{\partial}{\partial t}x(t) \approx \frac{x(k)-x(k-1)}{T}$$
$$\frac{\partial^2}{\partial t^2}x(t) \approx \frac{x(k)-2x(k-1)+x(k-2)}{T^2}$$

Note that this approximation is reasonable only if the time step, T is kept small compared with the bandwidth of the system under investigation.

Alternative strategies such as Tustin's "bilinear transform" are available, and reduce the error introduced by discretisation, especially if relatively large time steps are to be used, though these approaches generally yield a higher order z-transform, or a difference equation with a greater number of terms, which then demands a little more processing time since the size of the matrix increases by one with each increase in the order of the z-transform.

Usually, the time step, T, needs to be of the order of ten to twenty times the bandwidth of the system [Franklin, 1988], such that it is important to understand the dynamics (i.e. the eigenvalues, or pole locations) of the system being modelled (where the magnitude of the largest eigenvalue is a good indicator of the bandwidth of the system).

These difference equations, once formed, may used to determine the elements of the matrix $\underline{\underline{A}}$, yielding outputs including those required to be constrained. This results in a matrix that expresses the discrete-time history of the output tyre forces ($\underline{\underline{A}}\underline{x}$) as a discrete-time convolution involving impulse response of the system from each control input, x to the tyre force.

Specification of the objective function, $\underline{f}$ for Linear Programming

Finally, for the LP problem to be complete, the scalar objective function ("functional") to be ***minimised*** must be specified in the form:

$$O = \underline{f}^T \underline{x}$$

where $\underline{f}$ is a vector of weightings on each of the samples of the input time-history(s), $\underline{x}$.

For problems of the form discussed here, where it is desired to optimise the transient response of a system, it is normally desired to maximise the final value of an output which has been discrete-time integrated over a finite period, as an approximation to the infinite-time integral. For instance, it may be desired to maximise either the integrated path curvature (which is related to the path-lateral velocity achieved relative to the initial path, or the angle turned by the velocity vector), or the double-integrated path curvature (which is related to the achieved path-lateral displacement of the vehicle).

Thus, for LP type optimisations, it is the final value of some output time-history vector $\underline{y}_i = \underline{\underline{A}}_i \underline{x}$, which is of interest, where the $\underline{\underline{A}}_i$ matrix is derived by discretisation of the system transfer function, including the necessary integrator(s), as discussed above. The final value of the output $\underline{y}_i$ may then be identified from the final row of this $\underline{\underline{A}}_i$ matrix, and this row becomes the vector $\underline{f}$ that specifies the objective function. The total time of the simulation is set to be sufficient that the final value is approximately equal to the steady-state (infinite-time) value.

Available Controls (Inputs) for Vehicle Dynamics Control

The choice of whether steer angle or axle lateral force is represented by the values of the input time-history $\underline{x}$ is arbitrary, as each is (dynamically) linearly related to the other. In fact, the inputs considered in the following analyses include:

- Front (AWS, or driver) steer angle or lateral force
- Rear (4WS, AWS or driver) steer angle or lateral force
- Front axle DYC moment (by brakes and engine or by active differentials)
- Rear axle DYC moment (by brakes and engine or by active differentials)

Each analysis may include more than one input.

Constraints on the Vehicle Dynamics

Sets of time-dependent constraints in the form

$$\underline{\underline{A}}_i \underline{x} \leq \underline{b}$$

indicating a discretisation of the continuous-time constraint

$$i(t) \leq b(t)$$

where $i(t)$ is a system response that linearly related to the input $x(t)$, i.e.

$$i(t) = h_i(t) * x(t)$$

These constraints may be used to express, for instance:

- that the sum of the front and the sum of the rear tyre forces (which will be linearly related to the steer angle and/or DYC force inputs) must not exceed the frictional limit for those axles;
- that the vehicle position (which again is linearly related to the input) must not stray outside given boundaries;
- that the driver must not act until a certain time instant (i.e. the the input must be zero);
- that body sideslip or steer angles and rates are bounded to practical limits.

Tyre Force Constraints

In the simplest case, where only steering is available, and the maximum tyre force is considered to be constant and independent of the vertical load on the tyre, the lateral tyre forces are constrained to remain below a limiting value b (and also to remain greater than $-b$) at all time instants of the simulation. This requires four subsets of constraint equations expressing each of the following:

$$\begin{array}{ll} F_{y_f}(t) \le \hat{F}_{y_f} & F_{y_r}(t) \le \hat{F}_{y_r} \\ -F_{y_f}(t) \le \hat{F}_{y_f} & -F_{y_r}(t) \le \hat{F}_{y_r} \end{array}$$

Since each of these forces is time-dependent, and the constraint equations are required to apply at all time instants, these equations become (in the simplest case, where the available friction is a constant):

$$\begin{array}{ll} \underline{\underline{A}}_{F_{yf}} \underline{x} \le \underline{\hat{F}}_{yf} & \underline{\underline{A}}_{F_{yr}} \underline{x} \le \underline{\hat{F}}_{yr} \\ -\underline{\underline{A}}_{F_{yf}} \underline{x} \le \underline{\hat{F}}_{yf} & -\underline{\underline{A}}_{F_{yr}} \underline{x} \le \underline{\hat{F}}_{yr} \end{array}$$

These constraint equations, when combined with the simple displacement-maximising objective function described above, yield a complete LP problem.

However, it should be noted that (i) each of these constraints results in one LP constraint equation ***for each time instant*** and (ii) extending the actuation to include longitudinal force control (and thus an approximation of the ellipse of friction) or enhancing the tyre model to include vertical load or camber dependence further increases the number of necessary constraints.

Dynamic Behaviour Constraints (e.g. constant motion centre location)

Equality constraints may also be introduced, in order to maintain desired relationships between the states. For instance, a constant (or time-varying) motion position might be enforced by adding the dual inequalities

$$\underline{\underline{A}}_v\,\underline{x} + d\underline{\underline{A}}_r\,\underline{x} \leq \underline{0}, -\underline{\underline{A}}_v\,\underline{x} - d\underline{\underline{A}}_r\,\underline{x} \leq \underline{0}$$

This is an alternative to introducing the dynamic constraints in the form of modified system transfer functions, since each equality constraint effectively removes one state from the system.

Road Geometry Constraints

It is also possible, at limited cost, to introduce additional constraints on the displacement states in order to approximate the road geometry. Then, for instance, it is possible to determine the ideal input time-history for turning the idealised vehicle around a corner, where the driver may apply some input prior to the apex, but must not cut the corner, and must not move the vehicle too wide (in order to increase the radius). It is anticipated that such solutions may be of interest in motor racing applications.

Solution Method

LP solutions are computed by the well-known ***revised simplex*** method, which reduces demands on memory [Press, 1992]. Since the solution identified is always the global optimum, the details of the particular solution approach which was used are not considered important and not discussed here. The reader is referred to the literature for a full description of the approach.

Note: The solution time depends strongly upon the ability for a discretisation of the model to express the dynamic behaviour without the need for very small time steps, so the removal of high frequency poles is desirable. The optimisation code used for these analyses was therefore augmented with a pre-filter to detect dominant low frequency poles and delete the associated high frequency poles that are insignificant to the results.

7.3: Results and Discussion

(i) Optimal Response and Sideslip with 4WS or AWS

The first goal of the Linear Programming analysis was to attempt to directly identify the controls $F_{y_f}(t)$ and $F_{y_r}(t)$ and sideslip behaviour required for optimal turn-in of a 4WS or AWS vehicle.

However, with the objective function described above, it was found that the problem was actually underdetermined, and that the Linear Programming result was simply to maintain the lateral forces from both front and rear axles at their peak values for all time, such that the sideslip increased terminally (in the tail-out direction for limit-over-steering vehicles, in the nose-out direction for limit-under-steering vehicles).

Clearly this result is of no practical use and of highly questionable validity as the sideslip becomes large - note the infeasible values of sideslip velocity which are reached in Figure 7.2, indicating that the modelled vehicle has in fact gained energy due to error caused by linear modelling assumptions.

This first trial, therefore, identified some areas where caution must be exercised in expression of the problem Linear Programming.

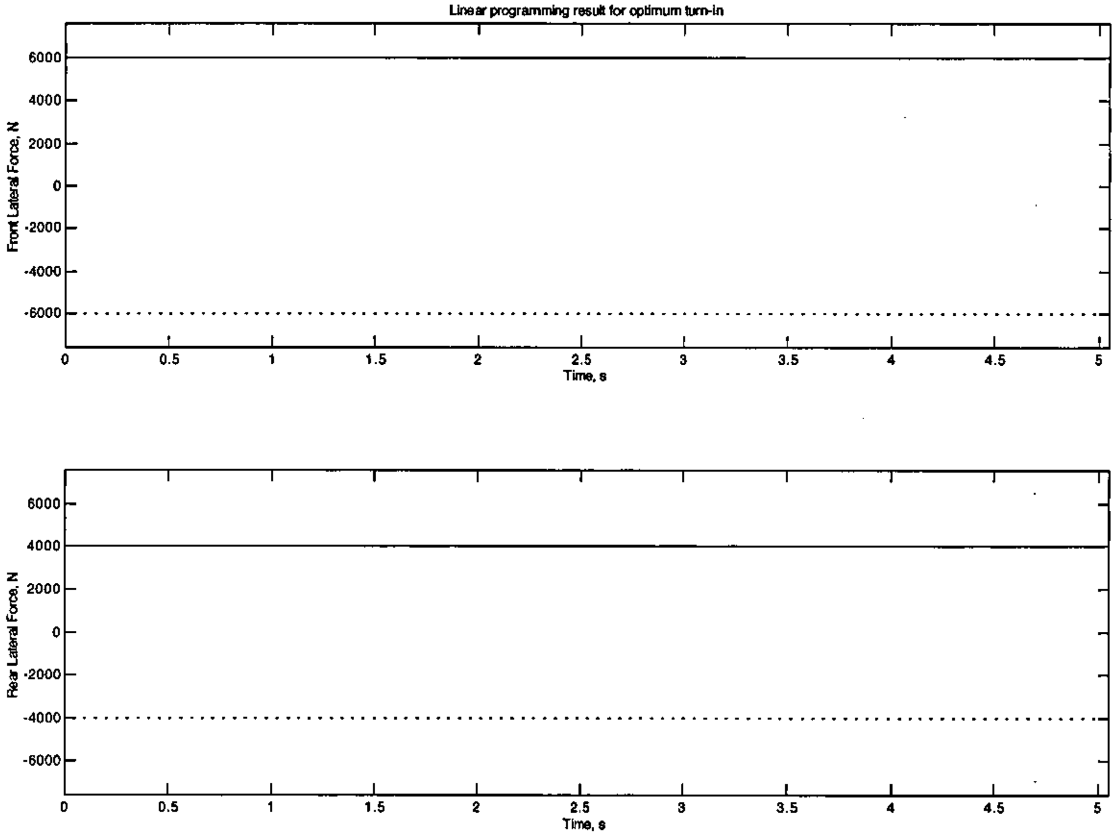

Figure 7.1

Controls $\left(F_{y_f}(t), F_{y_r}(t)\right)$ for 'optimal' turn-in of a 4WS or AWS vehicle with no sideslip constraint

$$\left(\hat{F}_{y_f} = 6000, \hat{F}_{y_r} = 4000\right)$$

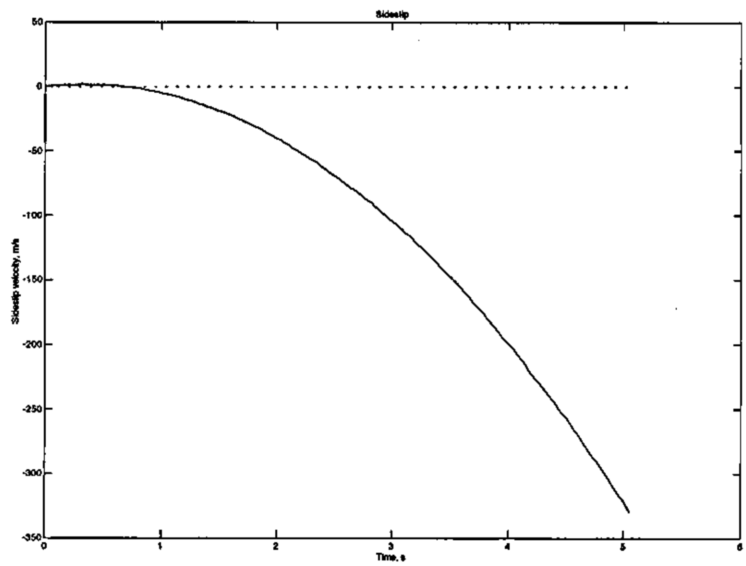

Figure 7.2

Terminally increasing sideslip response $V(t)$ resulting from 'optimal' turn-in of a 4WS or AWS vehicle without any sideslip constraint

$$\left(\hat{F}_{y_f} = 6000, \hat{F}_{y_r} = 4000, b = c = k = 1.35, M = 1000\right)$$

The vehicle shown in figures 7.1 and 7.2 has a limit-over-steering balance, since

$$\frac{b\hat{F}_{y_f}}{c\hat{F}_{y_r}}\left(=\frac{3}{2}\right) > 1$$

and therefore the terminal sideslip occurred in the tail-out direction that is the common direction in which statically unstable, over-steering passive vehicles would spin. For a limit-under-steer vehicle, the terminal sideslip occurs in the opposite ('anti-spin') direction.

(ii) Optimal turn-in of a 2WS vehicle model (3 cases)

Case I: Limit Under-steer, sufficiently damped rear tyre force/slip

Figure 7.3 shows the optimal force lateral tyre force rear input where the vehicle model has sufficient limit under-steer and rear tyre force/slip damping that the rear slip and force do not overshoot the maximum during the transient phase (such that the constraint on the rear tyre force is not violated). Note that the dotted line at a rear lateral tyre force of 5500N is shown for reference only; this is not an active constraint.

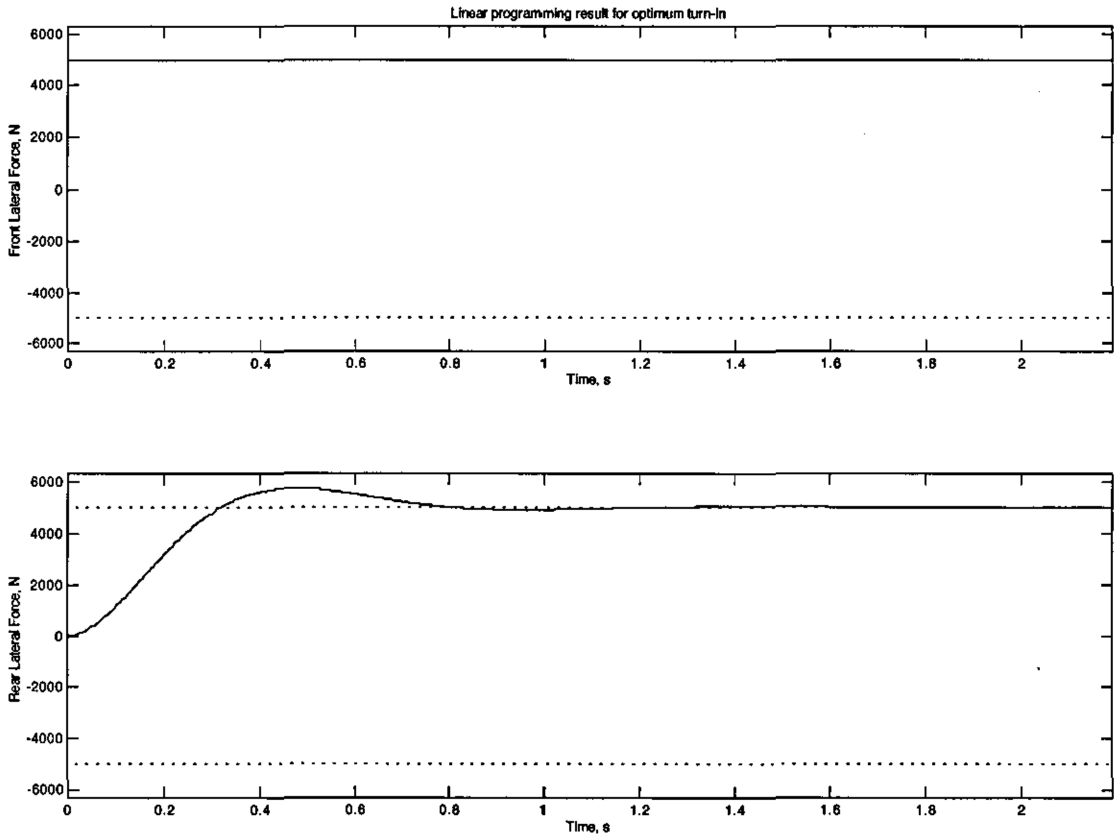

Figure 7.3

Controls $\left(F_{y_f}(t), F_{y_r}(t)\right)$ for optimal turn-in of a 2WS vehicle with a limit-under-steer balance (i.e. $F_{y_r}(t) \le \hat{F}_{y_r}$ for $F_{y_f}(t) = \hat{F}_{y_f}$)

$$\left(\hat{F}_{y_f} = 5000, \hat{F}_{y_r} >> 6000, b = c = k = 1.35, M = 1000, C_{\alpha_r} = 80000\right)$$

Case II: Limit Under-steer, insufficiently damped rear tyre force/slip

In the next plot, the same vehicle dynamics have been preserved, but the available rear tyre force has been reduced such level of limit under-steer has been reduced, from strongly under-steering, to that of a limit-neutral-steer vehicle,

$$\frac{b\hat{F}_{y_f}}{c\hat{F}_{y_r}} = 1$$

such that the overshoot in the rear tyre force response would exceed the available friction at the rear tyres. Note that the overshoot where $F_{y_r}(t) > 5000$ which occurred at 0.32 seconds in figure 7.3 no longer occurs in figure 7.4. Instead, the violation of the constraint that $F_{y_r}(t) < \hat{F}_{y_r}$ (which was allowed to occur in figure 7.3) is prevented by a last-minute, preemptive 'opposite-lock' correction at the front axle.

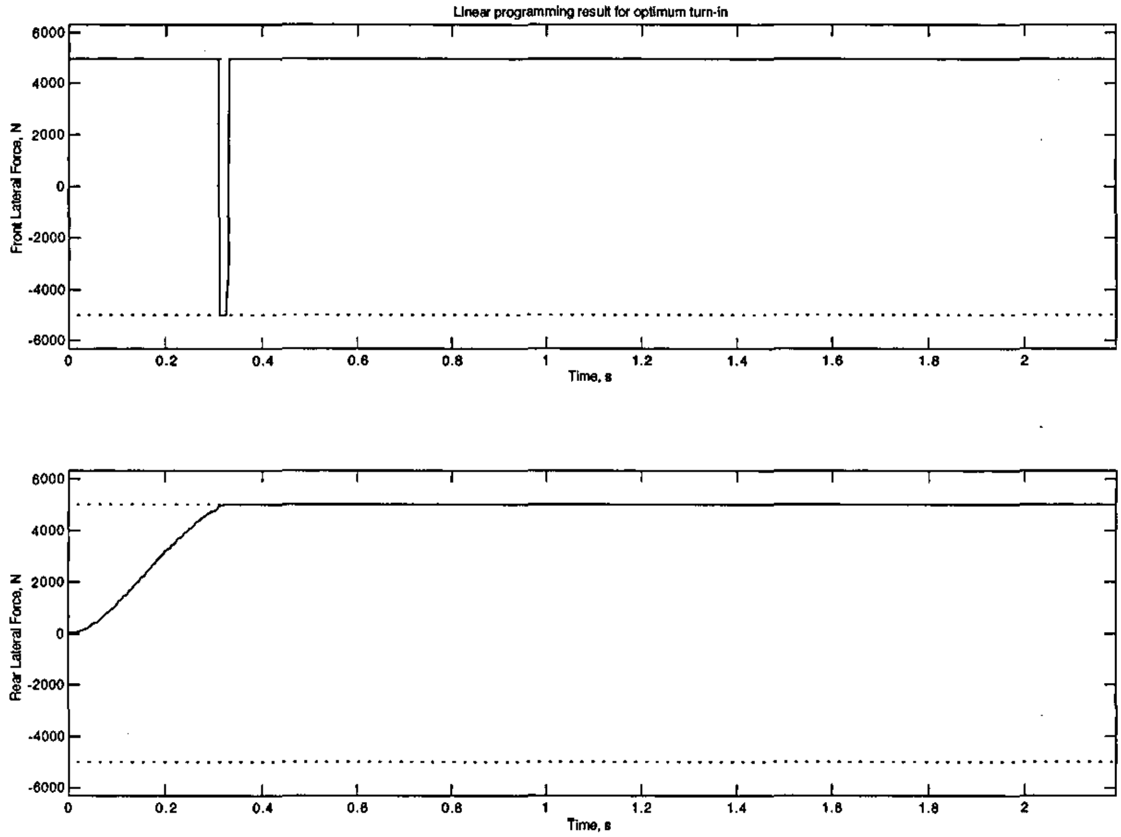

Figure 7.4

Controls $\left(F_{y_f}(t), F_{y_r}(t)\right)$ for Optimal Turn-In of a Limit-Neutral-Steer Vehicle with rear tyre slip/force response that is insufficiently damped

$\left(\hat{F}_{y_f} = 5000, \hat{F}_{y_r} = 5000, b = c = k = 1.35, M = 1000, C_{\alpha_r} = 80000\right)$

Case III: Limit Over-steer

Figure 7.5 shows the optimal controls for turn-in of a typical limit-over-steer vehicle, and figure 7.6 shows the sideslip response. This vehicle exhibits behaviour similar to the previous case where the vehicle was limit under-steer, except that on reaching steady-state, it is the front lateral force which must be compromised rather than the rear in order to maintain the limiting steady-state lateral acceleration.

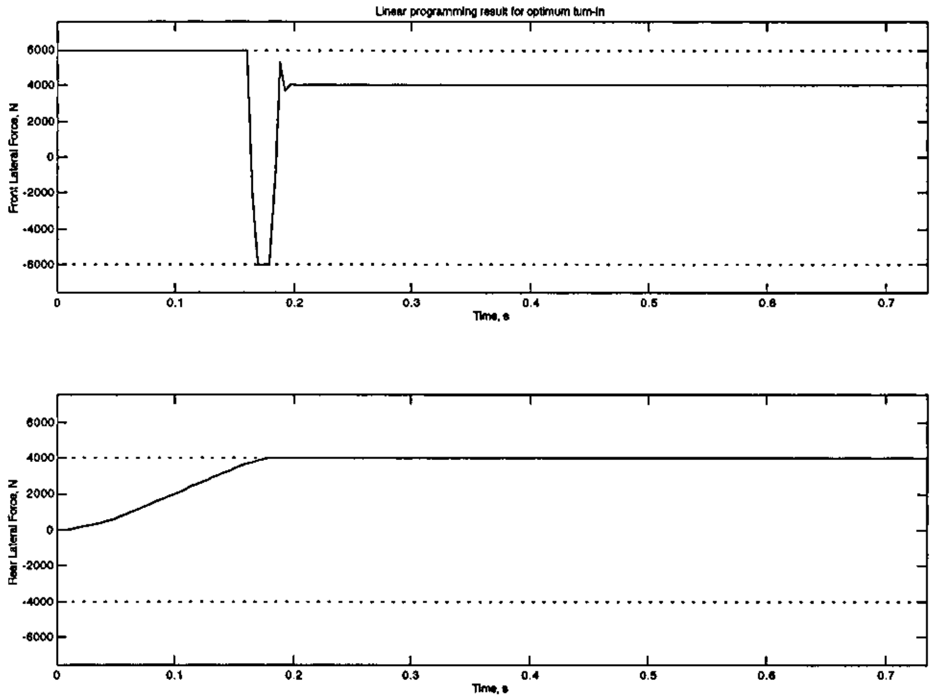

Figure 7.5

Controls $\left(F_{y_f}(t), F_{y_r}(t)\right)$ for Optimal Turn-In of a Limit-Over-Steer 2WS Vehicle

$$\left(\hat{F}_{y_f} = 6000, \hat{F}_{y_r} = 4000, b = c = k = 1.35, M = 1000, C_{\alpha_r} = 150000, U = 20\right)$$

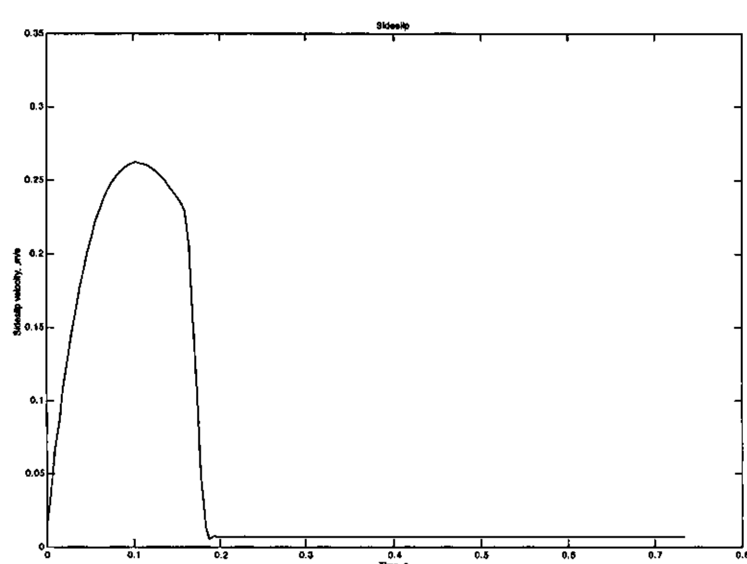

Figure 7.6

Sideslip velocity, $V(t)$ for Optimal Turn-In of a Limit-Over-Steer 2WS Vehicle

$$\left(\hat{F}_{y_f} = 5000, \hat{F}_{y_r} = 5000, b = c = k = 1.35, M = 1000, C_{\alpha_r} = 80000\right)$$

Summary - 2WS (or 4WS with controlled sideslip) Results

It was observed that for vehicles with front steer input only, the optimal control time-histories are always of a bang-bang nature (i.e. oscillating between the constraints), and always follow one of the following patterns:

- an immediate step input to $F_{y_f}(t) = \hat{F}_{y_f}$ for all $t > 0$, for a limit under-steer vehicle where such an input does not cause an overshoot in rear tyre force/slip that violates the imposed constraint of $F_{y_r}(t) \le \hat{F}_{y_r}$;
- an immediate step to $F_{y_f}(t) = \hat{F}_{y_f}$ at $t = 0$ followed by a brief period of full opposite lock, $F_{y_f}(t) = -\hat{F}_{y_f}$, for a vehicle that has a less well damped rear lateral tyre slip/force response such that the constraint $F_{y_r}(t) \le \hat{F}_{y_r}$ is hit during the transient;
- the same an immediate step followed by a brief period of opposite lock, followed by a return to a lower value of $F_{y_f}(t) = \frac{c}{b}\hat{F}_{y_r}$ in the steady-state in order to maintain the limiting steady-state lateral acceleration, in the case a vehicle that is limit over-steer.

(iii) Varying Motion Centre Location (4WS or AWS)

In the following analysis, the optimal turn-in of a 4WS or AWS vehicle, with rear tyre force control to ensure a fixed motion centre, has been identified. All of the plots in figures 7.7 and 7.8 show the results for $d = -2.0, -1.5, -1.0, -0.5, 0.0, 0.5, 1.0, 1.5, 2.0$.

In order to distinguish the value of d corresponding to each trace on the following plots, note that the steady-state sideslip $V = -\frac{d}{r}$. Therefore, traces with larger positive values of steady-state sideslip correspond to large negative values of d. The sideslip is shown in each group of plots.

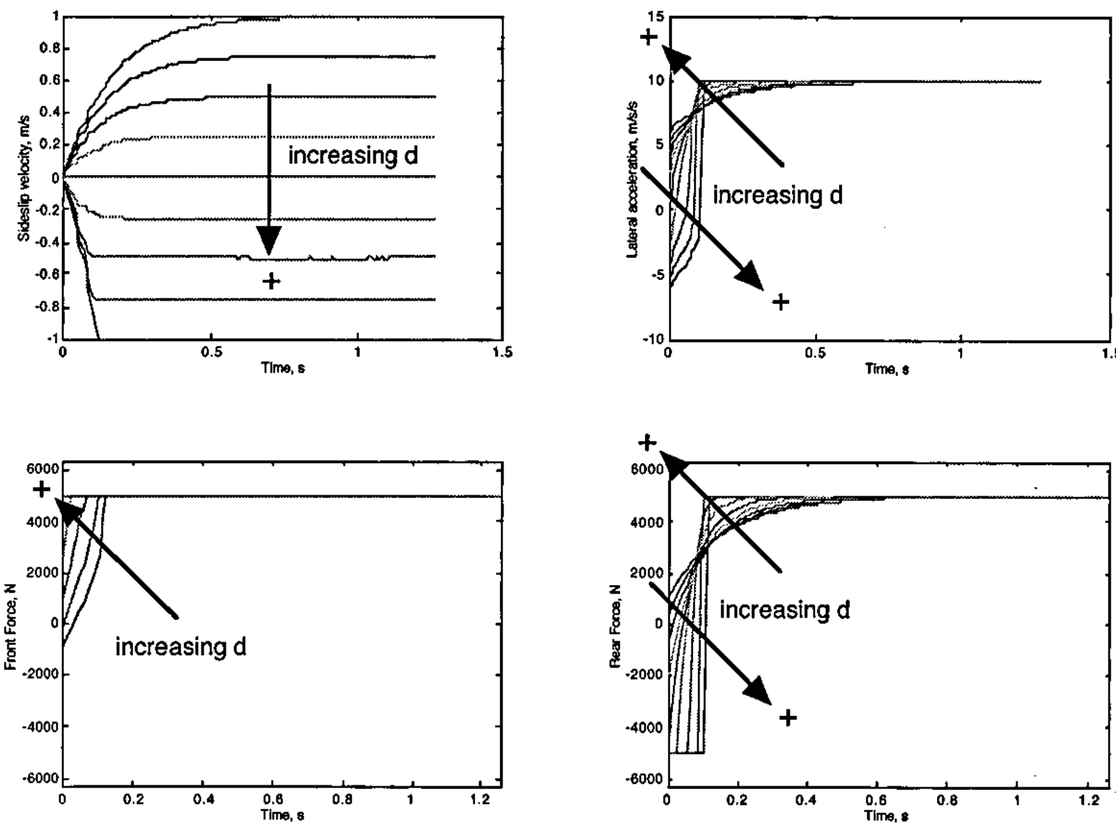

Figure 7.7

sideslip, $V(t)$, lateral acceleration, $a_y(t)$ and controls $F_{y_f}(t)$ and $F_{y_r}(t)$

for optimal turn-in with 4WS/AWS and fixed motion centre location

$$\left(\hat{F}_{y_f} = 5000, \hat{F}_{y_r} = 5000, b = c = k = 1.35, M = 1000, U = 20\right)$$

$$\left(d = -2.0, -1.5, -1.0, -0.5, 0.0, 0.5, 1.0, 1.5, 2.0\right)$$

It can be observed from figure 7.7 that:

- the motion centre location d, as expected, governs the steady-state sideslip velocity, V_{ss}, with positive values of d, i.e. motion centres behind the centre of mass, yielding negative steady-state sideslip, since the response is subject to the constraint that $V_{ss} + dr_{ss} = 0$ and the steady-state yaw rate $r_{ss} = \frac{a_{y_{ss}}}{U}$ is unaffected by the sideslip target;
- for the more ***rearward*** motion centres, i.e. for large negative d (in the case of this limit-neutral-steer vehicle, for any $d \leq 0$), the optimal front lateral force time-history is simply $F_{y_f}(t) = \hat{F}_{y_f}$. For such values of d, the front lateral force combines with a rear lateral tyre force that is equal to a step plus a first order time lag, to give a total lateral acceleration response which is also a step plus a first order time lag.

- for the more ***forward*** motion centres, i.e. for small d, the optimal front lateral force time-history includes initial portions where $F_{y_f}(t) < \hat{F}_{y_f}$. Since the objective is both to generate lateral acceleration and yaw rate, and the control F_{y_f} always contributes positively to both (since $\frac{\partial a_y}{\partial F_{y_f}} = \frac{1}{M}$ and $\frac{\partial \alpha_z}{\partial F_{y_f}} = \frac{b}{Mk^2}$), it is clear that the control time-histories for these vehicles have been compromised by the constraint that d remain small. Therefore, they are constrained-optimal (i.e. optimal ***only*** whilst the constraint that $V + dr = 0$ is imposed).

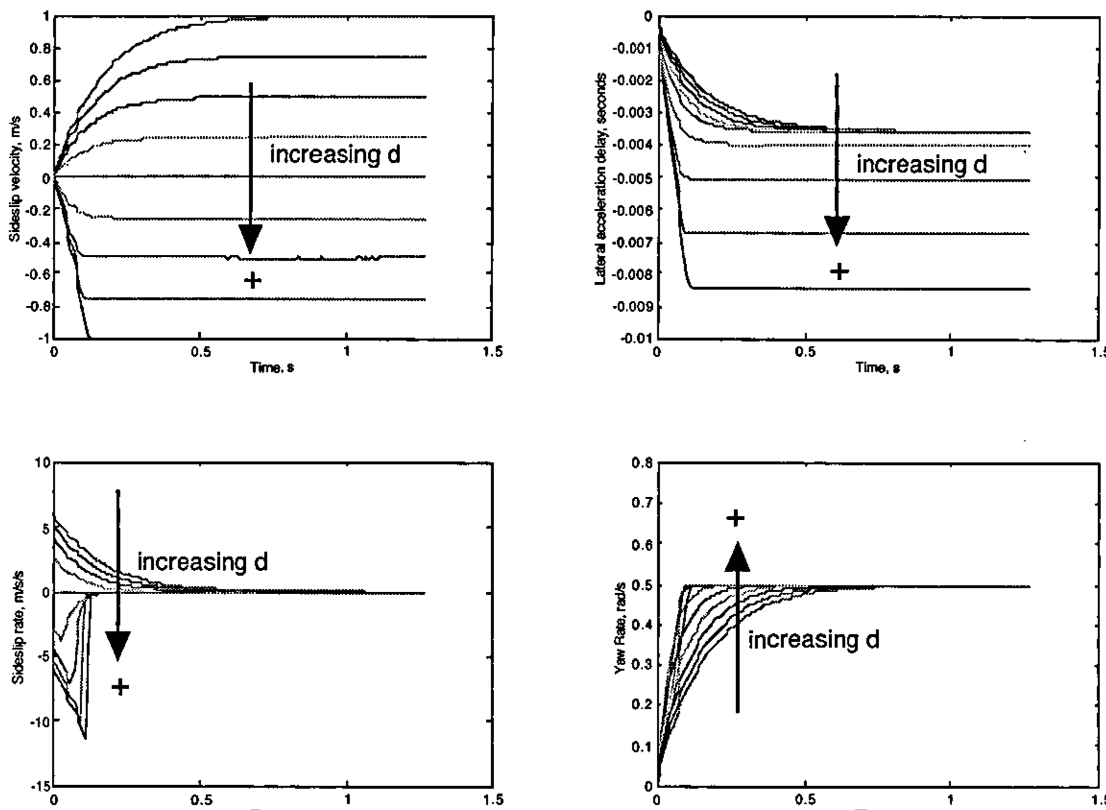

Figure 7.8

sideslip, $V(t)$, lateral acceleration delay, $t_{lag}(t)$,

sideslip rate $\dot{V}(t)$ and yaw rate $\dot{r}$

for optimal turn-in with 4WS/AWS and fixed motion centre location

$\left(\hat{F}_{y_f} = 5000, \hat{F}_{y_r} = 5000, b = c = k = 1.35, M = 1000, U = 20\right)$

$(d = -2.0, -1.5, -1.0, -0.5, 0.0, 0.5, 1.0, 1.5, 2.0)$

Figure 7.8 shows further details of the optimal response of the same, limit-neutral-steer 4WS/AWS vehicle for varying motion centre. In the lower two plots, it can be observed that for the vehicle whose transient performance is not inhibited by the sideslip constraint, the response in yaw rate, sideslip rate and thus sideslip are smooth, and that both of the fundamental handling states, V and r, have the form of a ***first order time lag.***

Also, the plot of the performance metric t_{lag} shows a fascinating result. It appears that the effective delay to the lateral acceleration, t_{lag}, is ***invariant*** with respect to the choice of motion centre location, provided the motion centre is sufficiently far ***rearward***, i.e. $d < d_{crit}$, wherever the constrained-optimal control $F_{y_f}(t) = \hat{F}_{y_f}$.

For the limit-neutral-steer vehicle shown here, it appears that $d_{crit} \approx 0$. This will be investigated further later in this thesis, with a view to gaining an understanding of the influence of vehicle parameters on the values of both t_{lag} and d_{crit}.

(iv) Influence of Actuator Limits

It has been observed that many of the solutions for optimal turn-in require a sudden step in at least the front (and sometimes also the rear) tyre force. Since the dynamics of the vehicle are slow compared with the dynamics of the steering, it is assumed that this step in slip angle would need to be taken care of by making a step in steer angle in order to effect the necessary slip, and clearly an instantaneous change in steer angle, nor steer velocity is possible. In order to demonstrate that this may be taken into account in a LP analysis, constraints were imposed that place upper limits on the moment which may be applied to the wheel by the steering system. The wheel is modelled as a simple rotational inertia, and thus the maximum steer angular acceleration of the wheel is limited by the limiting moment.

The optimal result for a limit-under-steering 2WS vehicle is shown in figure 7.9 below.

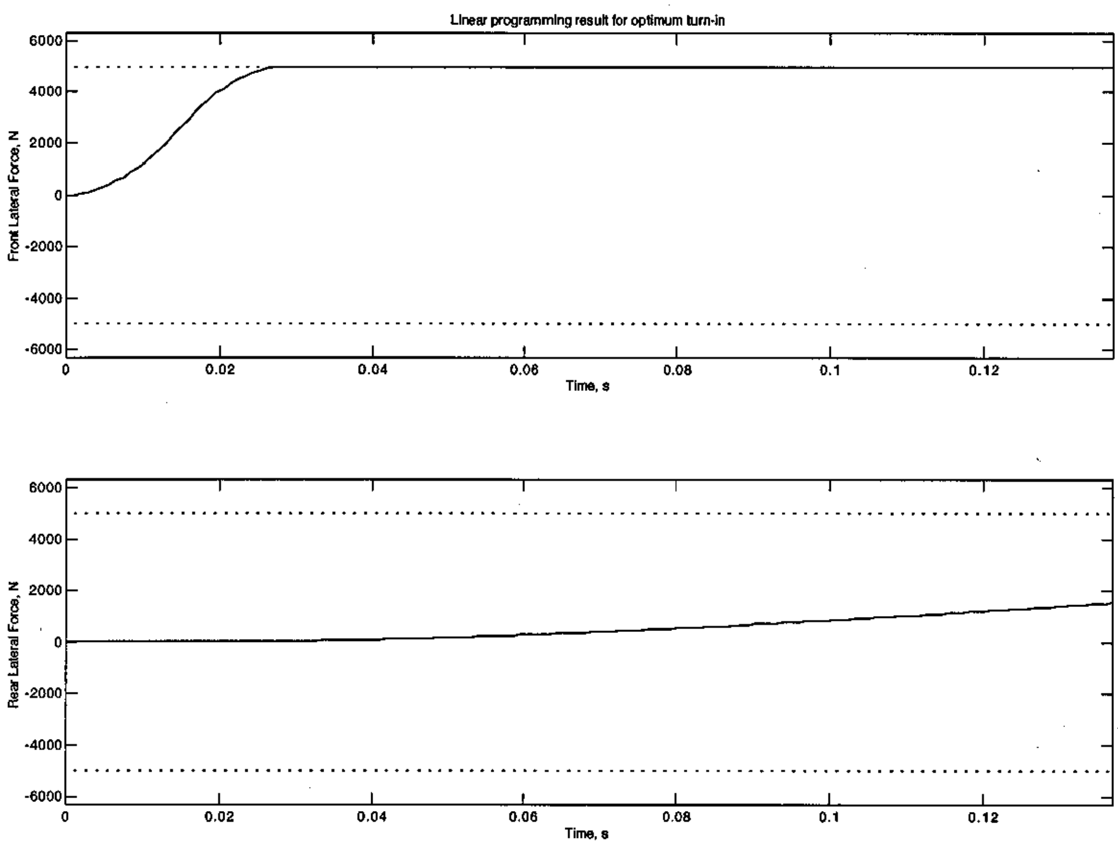

Figure 7.9
Optimal response of a vehicle with hard limits on steering system moment (for illustration only)

7.4: Possible Extensions, and Fundamental Limitations

Increasing Problem Complexity

The computational effort required in the solution of a Linear Programming problem increases with the number of constraint equations. In vehicle handling problems, the specification of the limit of available tyre friction at each time instant forms the majority of the constraints. Thus, if the number of tyre force constraints can be reduced, the solution time is significantly improved.

The use of a bicycle handling model can help in this respect – by lumping both tyres of a given axle together, and modelling the frictional limit of the whole axle with respect to the lateral (and longitudinal) load transfer, the number of necessary constraints is halved. However, if truly optimal solutions are required for vehicles with separate control of dual-wheel (whole axle) braking and single-wheel braking or traction (active differential control or independent brake control) then a separate set of constraints is required for each wheel on the axle. A bicycle (or tricycle) model may be satisfactory provided only one of the two (i.e. ***either*** net braking, or equal and opposite braking) is available for a particular axle (as the left and right longitudinal tyre force ***magnitudes*** are then equal, and both sides may be constrained by a single equation, or a single tyre model - even if lateral load transfer is to be considered).

Extension to Longitudinal Dynamics

It is also possible to maximise approximations of the first or second infinite-time integrals of the path curvature, for models which include longitudinal dynamics (and thus, perhaps a change of forward speed, where the path curvature is approximated to second order as:

$$\rho_a(t) = \frac{a_y(t)}{U_i^2} - \frac{2U_c(t)a_y(t)}{U_i^3}$$

The solution of such problems is facilitated by the extension of the Linear Programming method to ***Quadratic Programming***.

Such an extension is considered worthwhile for future studies, since it is known that most drivers brake prior to steering when attempting to avoid obstacles, and it has also been shown that the optimal input for obstacle avoidance invariably involves a combination of braking and steering, and maximisation of the lateral acceleration at the expense of making zero speed reduction yields the best path for obstacle avoidance only in exceptional circumstances [Blank, 2000].

However, it should be noted that in further analysis of this problem by QP, the resulting performance will only be an approximation of the optimal achievable with combined steering and braking. There may, therefore, be alternative optimisation approaches that yield a more instructive result. The optimal control approach adopted by Blank, for instance (based on classical variational calculus [Weinstock, 1974]) yielded interesting results for a problem where braking was considered but the yaw degree of freedom of the vehicle was neglected (in order to determine the optimal combination of brake and cornering forces for a particle model). This approach could potentially be extended to consider the yaw degree of freedom, but such an extension is beyond the remit of this work.

Fundamental Limitations of LP

Having a linear cornering stiffness, these models by no means constitute a perfect representation of the non-linear behaviour of tyres in response to changes in slip, camber and normal load. However, if caution is applied in the interpretation of the results (such as if they are applied to vehicles where closed-loop control of the forces is applied) then such a constrained model can give a great deal of insight.

The technique has several fundamental restrictions:

i. the system must be assumed to behave in a linear manner throughout the whole of the "feasible region" of state-space between the constraints. This implies that linear programming is unable to represent, for instance, the change in system dynamics associated with the loss of tyre cornering stiffness that occurs when approaching the limit of available friction, or the change in system dynamics which occurs when forward speed changes during a maneuver;

ii. the constraints applied in Linear Programming are hard constraints and ***not*** just saturations, such that for instance the kinematic tyre slip is limited as the force is limited. This means that the 'optimal' result may, for instance, include corrective opposite-lock to prevent violation of a constraint, that then results in a poorer performance in situations where an equivalent real vehicle could perhaps have been driven (assuming sufficient driver skill) beyond the point of saturation. Such solutions are excluded by the Linear Programming approach;

iii. however, in cases where the all of the steer angles (and thus lateral tyre slips) are optimised (as in most analyses in this thesis), the constraint on slip does not become a constraint on the vehicle dynamic states - instead it is only a limit on the tyre forces that may be generated, and this is equivalent to a model of saturation;

iv. the additional time taken to reach the obstacle (due to either speed reduction or travelling along a less direct path) is not accounted for.

The technique also has two significant advantages:

i. the expression of the problem using linear equations and (perhaps non-linear) constraints always ensures that there exists a single, globally optimum result, and this improves understanding (and, in some cases, yields analytical results that give direct insight into the likely influence of funamental vehicle parameters such as the CG location and yaw inertia);

ii. the optimum may be determined with significantly reduced computational effort compared with most non-linear optimisation methods;

In addition, for this work, controllable steering is being considered in order allow considerable variation of the vehicle sideslip trajectory. When the rear steering may be controlled, the rear tyre slip angle is no longer directly coupled to the rear axle lateral velocity, so that the constraints on the vehicle's kinematic state mentioned above are removed. In addition, "linear" handling behaviour up to the vehicle's limit of adhesion is often considered a desirable target that is artificially introduced by many controllers.

Important Note: In all of the LP analysis which has been presented, no account is taken of the influence of transient lateral load transfer (LLT). If the transient LLT caused by the extreme transient causes the tyre capability to deteriorate significantly, then this sharp turn-in performance may be sub-optimal. Komatsu acknowledged this possibility, and showed that at least for his particular non-linear vehicle model with AWS control [Komatsu, 2000], that either the LLT or roll angle effect is important (since in his simulations, the same vehicle with an additional term for roll angle and roll angular velocity minimisation performed better in a lane-change maneuver).

7.5: Concluding Remarks

It was shown that it is possible to express the problem of friction-optimal turn-in of a linear vehicle model as a problem in Linear Programming, but that it is not in fact possible to directly identify any realistic 'optimal sideslip' behaviour, since depending on the vehicle characteristics, either terminal sideslip in the positive direction or terminal sideslip in the negative direction yields the optimal maximised lateral acceleration.

However, when some sideslip control is introduced, it became possible to compare different vehicles in a sense that takes very good account of the hard limits that friction imposes.

It was seen that for a sufficiently limit-under-steering or vehicle that is well damped in yaw, the optimal control input is an immediate step to maximum front lateral force. Also, it was observed that the delay to the lateral acceleration due to the transient appears to be invariant with respect to changes in the sideslip control - for instance, is the rear tyre cornering stiffness was varied, or the motion centre constraint of the 4WS vehicle was adjusted.

However, it was seen that in some circumstances, it was not possible to apply and hold the front lateral force at the maximum value.

Three cases of this were identified.

For the limit under-steering 2WS vehicle, this occurred when the rear axle slip (and directly proportional tyre force) were under-damped, or the level of limit under-steer was insufficient, such that during the transient response of the vehicle, the rear tyre force hit the constraint (where the vehicle is generating the absolute peak lateral acceleration) after a short time. It was then necessary to preemptively prevent a constraint violation by applying a short period of opposite-lock. As anticipated, whenever this action was necessary, the time delay due to the transient increased.

For the limit over-steering 2WS vehicle, the optimal transient input was similar, except that the steady-state front lateral force input was also compromised, in order to maintain the vehicle at the peak steady-state lateral acceleration.

For the 4WS or AWS vehicle with the constraint of a fixed motion centre imposed, there were combinations of motion centre and vehicle limit when the initial rear tyre force required to maintain the motion centre for $t > 0$ was simply too large to fit within the imposed constraints. Once again, this problem occurred when the vehicle was insufficiently limit under-steering, but in this case the rear tyre force immediately hit the maximum ***opposite-sense*** limit, limiting the front lateral force which could be applied in the early part of the transient.

In summary, it was found that the technique of Linear Programming yielded some qualitative new results worthy of further investigation. It was decided to use an analytical vehicle dynamics model to determine the response to a step front force input and thus to try to further understand (i) why the time lag remained invariant whenever the front lateral force was able to be held at the peak value, and (ii) which parameters which would influence constraint violation, preventing the front force from being applied or maintained.

Chapter 8
Further Mathematical Analysis

Results from Linear Programming analyses showed that when some form of sideslip control is enforced, there is ***always*** a time delay in the lateral acceleration response.

The results also showed that suprisingly, this delay is ***not*** a function of the steady-state sideslip angle or motion centre location, and that it was invariant with most of the vehicle parameters, even including the rear tyre cornering stiffness (subject to the condition that $F_{y_f}(t) = \hat{F}_{y_f}$ does not violate the imposed rear tyre force constraints).

In this section, some further mathematical analysis is undertaken in an attempt to explain these findings. This chapter attempts to answer hypothesis H4 in an analytical manner.

8.1: Limit 'Steering' Characteristics of Vehicles

For vehicles where only steering may be controlled (so that the yawing effect of any longitudinal forces is negligible), the limit cornering performance (that is, the maximum steady-state lateral acceleration or path curvature that can be generated) is always determined by the need to balance yawing moments (such that the vehicle turns to follow its path).

The exception to this rule is in the case of the notional 'perfectly balanced vehicle', where the available frictional forces from the front and rear axles are perfectly balanced about the mass centre. In this case, neglecting the natural self-aligning moments of the tyres, the maximum lateral forces available at each axle are related as:

$$\hat{F}_{y_f} b = \hat{F}_{y_r} c$$

and this ideal vehicle may be said to be '***limit neutral-steer***'. There exist two possible conditions for the more common, limit-unbalanced vehicle:

i) Limit under-steer, where

$$\hat{F}_{y_f} b < \hat{F}_{y_r} c$$

ii) Limit over-steer, where

$$\hat{F}_{y_f} b > \hat{F}_{y_r} c$$

In the analyses which follow, the optimal performance of each is determined. Here, the term "limit steer behaviour" (i.e. limit under-steer, or limit over-steer) is defined in terms of the absolute frictional forces which are available at the axles, ***not*** in terms of the non-linear tyre behaviour (instantaneous cornering stiffness) in the region where peak force is generated. It is the latter that is considered in many analyses of limit handling stability, though multiple definitions of 'under-steer' and 'over-steer' are used.

8.2: Limit Under-Steer, Well Damped Rear Tyre Slip

For a limit-under-steering vehicle without DYC, and with sufficient damping of the rear tyre slip (such that the availability of rear tyre force is never a limiting factor) - as Case I in Chapter 7, result (ii) - it has been observed that the optimal steady-state turn-in performance is achieved when the front axle lateral force is stepped immediately to the maximum value:

$$F_{y_f} = \hat{F}_{y_f} \quad t > t_{demand}$$

The rear tyre force will then build according to the dynamics of the vehicle.

In the following section, the resulting motion has been analysed for some example vehicles.

Example 1

For a 2WS vehicle modelled using the classical linearised bicycle model, the rear tyre force is simply:

$$F_{y_r} = -C_{\alpha_r} \alpha_r$$

where

$$\alpha_r = \tan^{-1}\left(\frac{V - cr}{U}\right) \approx \frac{V - cr}{U}$$

And the yaw-plane dynamics of the vehicle are controlled according to:

$$F_{y_f} + F_{y_r} = M\left(\dot{V} + Ur\right)$$

$$I_{zz}\dot{r} = bF_{y_f} - cF_{y_r}$$

The effective time-delay owing to these dynamics may be found. Assuming the front lateral force to rise as a step function, ignoring longitudinal components, and taking Laplace transforms of the equations of motion:

$$F_{y_f}(s) = \frac{1}{s}\hat{F}_{y_f}$$

$$F_{y_f} + F_{y_r} = M(Vs + Ur)$$

$$I_{zz}rs = bF_{y_f} - cF_{y_r}$$

we can determine expressions for the vehicle states (that is, the yaw rate r and sideslip velocity V):

$$V = \frac{bcC_{\alpha_r} + c^2C_{\alpha_r} - bMU^2 + k^2MUs}{Ms\left(cC_{\alpha_r}U + k^2\left(C_{\alpha_r} + MUs\right)s + c^2C_{\alpha_r}s\right)}\hat{F}_{y_f}$$

$$r = \frac{cC_{\alpha_r} + b\left(C_{\alpha_r} + MUs\right)}{Ms\left(cC_{\alpha_r}U + k^2\left(C_{\alpha_r} + MUs\right)s + c^2C_{\alpha_r}s\right)}\hat{F}_{y_f}$$

and thus find the path-normal acceleration response:

$$\begin{aligned} a_{y_{passive}}(s) &= Vs + Ur \\ &= \left(\frac{(b+c)C_{\alpha_r}(cs+U) + k^2MUs^2}{Ms\left(cC_{\alpha_r}U + k^2\left(C_{\alpha_r} + MUs\right)s + c^2C_{\alpha_r}s\right)}\right)\hat{F}_{y_f} \end{aligned}$$

Note that the ***ideal*** transient response for this vehicle would be an immediate step to the steady-state limiting lateral acceleration (i.e. to the highest possible lateral acceleration at which yaw moments can still be balanced). For the idealised under-steering vehicle, this condition is where the rear tyre force is found from:

$$\hat{F}_{y_f}b = F_{y_r}c$$

It is therefore possible to determine the lateral acceleration that would ideally be achieved immediately:

$$a_{y_{ss}} = \frac{\hat{F}_{y_f}}{M}\left(1 + \frac{b}{c}\right)$$

Taking the arbitrary demand application time t_{demand} to be zero,

$$t_{lag} = \int_0^\infty \frac{a_{y_{ideal}}(t) - a_{y_{passive}}(t)}{a_{y_{ss}}} dt$$

which may be written using Laplace transforms, as:

$$t_{lag} = \lim_{t \to \infty} \left\{ L^{-1} \left\{ \frac{1}{s} \left(\frac{a_{y_{ideal}}(s) - a_{y_{passive}}(s)}{a_{y_{ss}}} \right) \right\} \right\}$$

$$= \lim_{t \to \infty} \left\{ L^{-1} \left\{ \frac{1}{s} \left(\frac{1}{s} - \frac{c(b+c)C_{\alpha_r}(cs+U) + ck^2MUs^2}{(b+c)s\left(cC_{\alpha_r}U + k^2\left(C_{\alpha_r} + MUs\right)s + c^2C_{\alpha_r}s\right)} \right) \right\} \right\}$$

According to the ***Final Value Theorem,***

$$\lim_{t \to \infty}\{x(t)\} = \lim_{s \to 0}\{sX(s)\} = \lim_{s \to 0}\{s \cdot L\{x(t)\}\}$$

so that

$$t_{lag} = \lim_{s \to 0} \left\{ \frac{a_{y_{ideal}}(s) - a_{y_{passive}}(s)}{a_{y_{ss}}} \right\}$$

$$= \lim_{s \to 0} \left\{ \frac{1}{s} - \frac{c(b+c)C_{\alpha_r}(cs+U) + ck^2MUs^2}{(b+c)s\left(cC_{\alpha_r}U + k^2\left(C_{\alpha_r} + MUs\right)s + c^2C_{\alpha_r}s\right)} \right\}$$

$$= \frac{k^2}{cU}$$

This result is simple and understandable in that lag time increases with yaw moment of inertia, but is perhaps surprising that it decreases at higher speed and is independent of tyre properties.

Example 2

As a second example, take a vehicle with an active rear steering system, running a control strategy that ensures zero sideslip at all times. Taking Laplace transforms, the equations of motion for zero sideslip:

$$F_{y_f} + F_{y_r} = MUr$$

$$I_{zz}rs = bF_{y_f} - cF_{y_r}$$

provide a constraint on the path-normal rear tyre force as a function of the front:

$$F_{y_r} = \frac{bU - k^2s}{cU + k^2s} F_{y_f}$$

Assuming the same (immediate step in front axle force) input as previously, such that

$$\begin{aligned} a_{y_{tss}}(s) &= \left(1 + \frac{bU - k^2 s}{cU + k^2 s}\right)\frac{1}{Ms}\hat{F}_{y_f} \\ &= \left(\frac{c + b}{cU + k^2 s}\right)\frac{U}{Ms}\hat{F}_{y_f} \end{aligned}$$

and again

$$a_{y_{ss}} = \frac{\hat{F}_{y_f}}{M}\left(1 + \frac{b}{c}\right)$$

so

$$a_{y_{ideal}}(s) = \frac{\hat{F}_{y_f}}{Ms}\left(1 + \frac{b}{c}\right)$$

Once again, we can compute the transient response time lag:

$$\begin{aligned} t_{lag} &= \lim_{s \to 0}\left\{\frac{a_{y_{ideal}}(s) - a_{y_{passive}}(s)}{a_{y_{ss}}}\right\} \\ &= \lim_{s \to 0}\left\{\frac{\frac{\hat{F}_{y_f}}{Ms}\left(1 + \frac{b}{c}\right) - \left(\frac{c + b}{cU + k^2 s}\right)\frac{U}{Ms}\hat{F}_{y_f}}{\frac{\hat{F}_{y_f}}{M}\left(1 + \frac{b}{c}\right)}\right\} \\ &= \lim_{s \to 0}\left\{\frac{k^2}{cU + k^2 s}\right\} \\ &= \frac{k^2}{cU} \end{aligned}$$

In other words - subject to the assumption that the rear tyre force does not overshoot, such that the input $F_{y_f}(t) = \hat{F}_{y_f}(t)$ may be applied without violating the rear tyre force constraint - then we see the same result irrespective of the tyre properties, axle steering kinematics or rear-steering based sideslip control strategy. Thus, we also see the same result irrespective of the steady-state sideslip angle which is reached. This is an important result when considering alternative steady-state sideslip targets for an active rear steering system.

Calculation of the time delay by yaw impulse

The reason for this surprising result is clear if the problem is considered in terms of ***yaw impulse***. For a vehicle to reach the correct steady-state yaw rate,

$$r_{ss} = \frac{a_{y_{ss}}}{U}$$

its angular momentum in yaw must be changed, such that a certain yaw impulse must be provided during the transient phase. This impulse may be provided early, late, or progressively, according to the vehicle dynamics, but the total impulse that will ultimately be provided by the time the vehicle reaches steady-state, is equal to the necessary change in its angular momentum:

$$\begin{aligned} H &= I_{zz}\Delta r \\ &= Mk^2 r_{ss} \end{aligned}$$

The total yaw impulse is the infinite-time integral of the yaw moment

$$M_z = F_{y_f} b - F_{y_r} c$$

If the front axle force is assumed to be a step to the maximum force, and the steady-state yaw rate is that corresponding to the vehicle limit, then the yaw impulse becomes a constraint on the infinite-time integral of the rear tyre force

$$\begin{aligned} H &= \int_{t_{demand}}^{\infty} M_z(t)dt \\ Mk^2 r_{ss} &= \int_{t_{demand}}^{\infty} \left(F_{y_f}(t)b - F_{y_r}(t)c\right)dt \\ \frac{Mk^2}{U} a_{y_{ss}} &= \int_{t_{demand}}^{\infty} \left(\hat{F}_{y_f} b - F_{y_r}(t)c\right)dt \\ \frac{k^2}{U}\hat{F}_{y_f}\left(\frac{b+c}{c}\right) &= b\int_{t_{demand}}^{\infty} \hat{F}_{y_f} dt - c\int_{t_{demand}}^{\infty} F_{y_r}(t)dt \\ \int_{t_{demand}}^{\infty} \frac{F_{y_r}(t)}{\hat{F}_{y_f}} dt &= \frac{b}{c}\int_{t_{demand}}^{\infty} dt - \frac{k^2}{U}(b+c) \end{aligned}$$

If the expression for the transient response time lag is expanded, it can be seen that the term on the left appears:

$$
\begin{aligned}
t_{lag} &= \int_0^{\infty} \frac{a_{y_{ideal}}(t) - a_{y_{vehicle}}(t)}{a_{y_{ss}}} dt \\
&= \int_0^{\infty} \frac{\frac{\hat{F}_{y_f}}{M}\left(1+\frac{b}{c}\right) - \frac{\hat{F}_{y_f}}{M} - \frac{F_{y_r}(t)}{M}}{\frac{\hat{F}_{y_f}}{M}\left(1+\frac{b}{c}\right)} dt \\
&= \left(\frac{b}{b+c}\right)\int_0^{\infty} dt - \left(\frac{c}{b+c}\right)\int_0^{\infty}\frac{F_{y_r}(t)}{\hat{F}_{y_f}} dt
\end{aligned}
$$

Substituting the infinite-time integral from above, we have:

$$
t_{lag} = \frac{k^2}{cU}
$$

In other words, the requirement to find the same steady-state yaw rate (and thus for the time-infinite integral of the yaw moment to be invariant with changes in the tyre, suspension or steering controller) in itself defines the value of this performance metric.

In addition, higher order effects, such as tyre relaxation and roll dynamics, can also be shown to have no influence on this result.

However, this result applies ***only*** to vehicles:

i. that are limit under-steering (or neutral-steering, but not over-steering),
ii. without any yaw moment provided by a difference in longitudinal tyre forces,
iii. whose controller or passive dynamics ensure that the rear tyre forces are not saturated during the transient phase
iv. whose tyre vertical load control is such that the friction available from each axle does not significantly change during the maneuver

Note 1: This result is valid even for the 'perfectly balanced' neutral-steer vehicle (neutral steer being the limiting case of very little under-steer). In other words, in terms of transient response, effective use cannot be made of all of the rear tyre force. During the transient, therefore, a limit-over-steering vehicle has the potential to perform better, since the need during this period is for large front axle tyre forces.

Note 2: The literature suggests [Hac, 2002] that a time-lag which is 'consistent' with respect to the forward velocity of the vehicle is ideal. This is at odds with the physics of the turn-in process, which demonstrates that the lower limit on the time lag reduces (as 1/U) with the speed of the vehicle. Therefore, if an attempt is made to ensure that the time-lag remain consistent, the obstacle avoidance performance of the vehicle will certainly be sub-optimal at high speed, and the target may not be feasible at low speed.

Limitations on the validity of $t_{lag} = \frac{k^2}{cU}$

Since external conditions may cause the balance of the vehicle to change, it is next necessary to consider what happens if the strict conditions for validity of the result that

$$t_{lag} = \frac{k^2}{cU}$$

are violated, i.e. if the vehicle is not sufficiently limit-under-steering. For instance:

- What would the time lag be if the vehicle were limit over-steering?
- What happens if the rear axle is insufficiently damped and becomes saturated at some point during the transient turn-in phase?

8.3: Limit Over-Steer, Well Damped Rear Tyre Slip

For a vehicle with an over-steering limit balance, the optimal control signals (i.e. the forces, compared to the limit) were observed to differ from those for the limit-under-steering vehicle - see Case III in Chapter 7, result (ii). In this case, the ***rear*** tyre force must be maintained at its peak value in steady-state, and at some point the front force must be compromised in order to maintain the yaw moment balance required for steady-state motion at the maximum steady-state lateral acceleration.

As in the above derivation for the limit-under-steering vehicle, the yaw impulse required to achieve the necessary change in yaw rate may be employed to determine the turn-in time delay.

For a change in yaw rate of Δr, the required impulse is:

$$H_{req} = I_{zz} \cdot \Delta r$$

The necessary yaw impulse to transition from straight line driving to a given steady-state lateral acceleration, is:

$$\Delta r = \frac{a_{y_{ss}}}{U}$$

For the over-steering vehicle, the maximum steady-state lateral acceleration is

$$a_{y_{ss}} = \frac{F_{y_{f_{ss}}} + \hat{F}_{y_r}}{M}$$

where the steady-state value of the front lateral force, $F_{y_{f_{ss}}}$, is chosen to precisely oppose the yaw moment generated by the maximised rear tyre force:

$$F_{y_{f_{ss}}} = \hat{F}_{y_r} \frac{c}{b}$$

If, for simplicity, it is assumed that the maximum possible yaw moment is applied constantly throughout the transient phase, then the computation of the time delay is simplified. This maximum achievable yaw moment occurs when the tyre forces are maximised, in opposition to each other:

$$\hat{M}_z = \hat{F}_{y_f} b + \hat{F}_{y_r} c$$

This yaw moment must then be applied for a time period t_{trans}, which lasts until the necessary yaw impulse has been applied:

$$\int_0^{t_{trans}} \hat{M}_z dt = H_{req}$$

The time for which this constant moment must be applied may be determined very simply:

$$t_{trans} = \frac{H_{req}}{\hat{M}_z}$$

Therefore,

$$\begin{aligned} t_{lag} &= \int_0^{\infty} \frac{a_{y_{ideal}}(t) - a_{y_{vehicle}}(t)}{a_{y_{ss}}} dt \\ &= \int_0^{t_{trans}} \frac{a_{y_{ss}}(t) - a_{y_{trans}}(t)}{a_{y_{ss}}} dt \\ &= t_{trans} \cdot \frac{a_{y_{ss}} - a_{y_{trans}}}{a_{y_{ss}}} \end{aligned}$$

with, for the over-steering vehicle with the maximum yaw moment applied, during the transient phase,

$$a_{y_{trans}} = \frac{\left(\hat{F}_{y_f} - \hat{F}_{y_r}\right)}{M}$$

and from above,

$$\begin{aligned} a_{y_{ss}} &= \frac{F_{y_{f_{ss}}} + \hat{F}_{y_r}}{M} \\ &= \frac{\hat{F}_{y_r}}{M}\left(1 - \frac{c}{b}\right) \end{aligned}$$

$$\begin{aligned} t_{trans} &= \frac{G_{req}}{\hat{M}_z} \\ &= \frac{I_{zz} \cdot a_{y_{ss}}}{\left(\hat{F}_{y_f} b + \hat{F}_{y_r} c\right)U} \end{aligned}$$

thus

$$
\begin{aligned}
t_{lag} &= t_{trans} \cdot \frac{a_{y_{ss}} - a_{y_{trans}}}{a_{y_{ss}}} \\
&= \left(\frac{I_{zz}}{\left(\hat{F}_{y_f} b + \hat{F}_{y_r} c\right) U} \right) \cdot \left(\frac{\hat{F}_{y_r}}{M}\left(1 + \frac{c}{b}\right) - \frac{\left(\hat{F}_{y_f} + \hat{F}_{y_r}\right)}{M} \right) \\
&= \frac{2k^2}{cU\left(1 + \frac{b}{c}\frac{\hat{F}_{y_f}}{\hat{F}_{y_r}}\right)}
\end{aligned}
$$

For the limit-NS vehicle, which is perfectly balanced in the steady-state,

$$\frac{b}{c}\frac{\hat{F}_{y_f}}{\hat{F}_{y_r}} = 1.0$$

and the result collapses to the previously derived result of:

$$t_{lag} = \frac{k^2}{cU}$$

And hence the result is in agreement with that from the previous derivation for the case of a limit-neutral-steering vehicle, which is a limiting case for both under-steer and over-steer.

The Response of Limit-Over-Steering Vehicles

For limit over-steering vehicles,

$$\frac{b}{c}\frac{\hat{F}_{y_f}}{\hat{F}_{y_r}} > 1.0$$

always holds. Therefore, the time lag for an over-steering vehicle,

$$t_{lag,os} < \frac{k^2}{cU}$$

and this time lag becomes shorter with increasing limit over-steer. In contrast, the time lag for an under-steering vehicle,

$$t_{lag,us} = \frac{k^2}{cU}$$

is not a function of the level of limit under-steer.

For a given level of limit-unbalance, therefore, a vehicle that is unbalanced in the direction of over-steer is theoretically capable of faster turn-in (and thus better transient lateral acceleration performance) than the vehicle which is unbalanced in the direction of limit under-steer.

8.4: Transient Rear Slip or Force Saturation

Results from 2WS vehicles analysed at the beginning of the previous chapter suggest that in cases where the yaw damping of the vehicle is insufficient, the rear axle may saturate during optimal transient turn-in - see Case II in Chapter 7, result (ii) - and in these cases, the front steering control input needs to include a brief period of ***opposite-lock*** (where the lateral force provided by the front axle is briefly reversed in direction). This action serves to 'check' the rear axle slip before it becomes excessive.

The delay caused to the lateral acceleration response due to this period of opposite-lock may be computed by considering the negative yaw impulse which is applied to the vehicle by this action when applied during a right-turn, where the truly optimal transient front force input is $F_{y_f}(t)=\hat{F}_{y_f}$. Whilst opposite-lock is applied, $F_{y_f}(t)=-\hat{F}_{y_f}$, such that the change in front tyre force is $\Delta F_{y_f}(t)=-2\hat{F}_{y_f}$ throughout this period. The change in yaw angular momentum H_z due to the integral effect of this change in front tyre force during the period of front axle opposite-lock, t_f, is

$$\begin{aligned}\Delta G_f &= b\int_0^{t_f}\Delta F_{y_f}(t)dt\\ &= -2b\hat{F}_{y_f}t_f\end{aligned}$$

Since the same steady-state yaw rate (i.e. the same yaw angular momentum) must eventually be reached, this negative yaw impulse must be offset by an equal and opposite (positive) yaw impulse provided by a change $\Delta F_{y_r}(t)$ in the rear tyre force in response to the opposite-lock correction at the front:

$$\Delta G_r = -c\int_0^{t_r}\Delta F_{y_r}dt$$

In other words, the change in the impulse provided by the rear tyres must be:

$$\Delta G_{r,OL}+\Delta G_{f,OL}=0$$

therefore, the integral effect of the change in rear tyre force,

$$\int_0^{t_r}\Delta F_{y_r}dt=-2\frac{b}{c}\hat{F}_{y_f}t_f$$

The influence of this correction on the lateral acceleration time lag

$$t_{lag} = \int_0^{\infty} \frac{a_{y_{ideal}}(t) - a_{y_{vehicle}}(t)}{a_{y_{ss}}} dt$$

is

$$\begin{aligned}\Delta t_{lag} &= \int_0^{t} \frac{\Delta a_{y_{vehicle}}(t)}{a_{y_{ss}}} dt \\ &= \frac{1}{Ma_{y_{ss}}}\left(\int_0^{t_f} \Delta F_{y_f}(t)dt + \int_0^{t_r} \Delta F_{y_r}(t)dt\right)\end{aligned}$$

(with terms due to the change in front tyre force and the change in rear tyre force). Substituting the integrals of the changes in tyre force from above, we find that this simplifies to:

$$\begin{aligned}\Delta t_{lag} &= \left(\frac{2t_f}{a_{y_{ss}}}\right)\frac{\hat{F}_{y_f}}{M}\left(1+\frac{b}{c}\right) \\ &= 2t_f\end{aligned}$$

In other words, any opposite-lock correction ***extends*** the turn-in time delay by twice the duration for which the opposite-lock $\left(F_{y_f}(t) = -\hat{F}_{y_f}\right)$ corrective steering is applied. (Note that this is intuitively logical, since a correction of ***half*** the magnitude $\left(\Delta F_{y_f}(t) = -\hat{F}_{y_f}\right)$ would be equivalent to zeroing the force force input for that duration $\left(F_{y_f}(t) = 0\right)$ - equivalent (in terms of this time lag) to simply ***delaying*** the initial steering input by the same time).

Therefore, for time-optimal turn-in behaviour (that is, a zero value of the t_f term), the vehicle requires some minimum level of damping on the rear axle slip, in order to ensure that high values of rear axle slip are not reached during the transient phase. This is because it has been seen that optimal turn-in performance is achieved when rear tyre force or steering control (regardless of whether it be active or passive) allows rapid maximisation and maintenance of maximum front lateral tyre force.

Note: The same correction to the time lag applies to both limit under- and over-steering vehicles whenever the transient response of the vehicle is such that opposite lock is required to prevent the rear tyre force from overshooting the peak value during the turn-in phase.

8.5: Lateral Displacement due to Rear Lateral Force

Additionally, it was observed in the results of the Linear Programming optimisations that differences in the timing of the rear tyre force buildup (i.e. whether the yaw moment was generated early or later) has relatively little influence on the lateral motion of the front of the vehicle during the transient (provided the front lateral force input remained the same).

It will be shown that this is due to the inertial response of the vehicle to lateral forces applied at the rear axle.

Centre of Percussion

The ***centre of percussion*** [Den Hartog, 1984] with respect to forces applied laterally at the rear axle is located at a longitudinal position (i.e. a distance in x from the centre of mass) of:

$$d_{COP,r} = \frac{k^2}{c}$$

The ***centre of percussion*** is effectively the 'instantaneous centre of acceleration', or the position on the body which experiences zero acceleration in response to a force applied at a particular position on the body (in this case the rear axle).

In 2D (e.g. in pure yaw plane dynamics), a body will accelerate both in translation (according to $F = Ma_G$) and in rotation (according to $Fr = Mk^2\alpha$) in response to a single force applied at a distance r from the mass centre, G.

If the force is applied along one cartesian coordinate direction (such as the lateral, vehicle y axis), then the magnitude of the acceleration will vary along the orthogonal coordinate direction (e.g. along the longitudinal, vehicle x axis). By simple linear summation, the total acceleration at a point d along this orthogonal axis will be:

$$a_d = a_G + d\alpha$$

If d is selected such that $a_d = 0$, then the point d becomes ***the centre of percussion with respect to forces applied at*** r. It is straightforward to manipulate these relations to show that

$$d_{COP} = -\frac{k^2}{r}$$

Therefore, for a force applied laterally at the rear axle of a vehicle ($r = -c$),

$$d_{COP,r} = \frac{k^2}{c}$$

and for a force applied laterally at the front axle ($r = b$),

$$d_{COP,f} = -\frac{k^2}{b}.$$

This means that in response to lateral forces applied at the rear axle location, the vehicle accelerates about the point $d_{COP,r} = \frac{k^2}{c}$, which is typically close to the front of the vehicle. Therefore, application of lateral rear tyre forces such as those provided by rear steering, has little effect on the lateral motion of points near the front of the vehicle.

The conclusion from this is that transient rear steering control (and the effect this has on sideslip) has little influence on the time-history of the behaviour of the front of the vehicle during transient turn-in.

One caveat to this, however, is that the level of yaw damping provided determines the need for opposite-lock later in the turn-in phase, and changes in sideslip motion may influence the driver's ability to control the vehicle [Hac, 2002].

8.6: Time Delays Introduced By Actuator Limits

It was shown in Chapter 4 that for a vehicle to generate a step in lateral tyre force, a step change in tyre slip angle is required, and that in the presence of relaxation, a transient slip ***beyond*** the target slip angle is required. Since the vehicle dynamic response to step changes in force is relatively slow, if a rapid turn-in response is required, then the majority of this change in slip angle must be provided by a change in steer angle.

Since wheels have mass and inertia, instantaneous changes in steering angle are impossible, and this also applies to changes in steering velocity. Therefore, the maximum moment that the steering system is able to impart to the wheel, and consequently the fastest possible time-response of the steer angle, will have a significant influence on the optimal response of the vehicle, given that the optimal turn-in behaviour of the vehicle ***without*** such a constraint on steering system moments always involves an immediate step to the slip angle which generates the maximum lateral force from the front tyres.

In order to assess the magnitude of this influence, and thus the relative importance of fast actuation, the time lag associated with making a step change in front steer angle has been estimated. It is assumed that the maximum actuator force or moment (be this a driver, an electric actuator or a hydraulic actuator) and thus the second derivative of change of steer angle $\hat{\ddot{\delta}}$ is approximately ***constant*** (and not, for instance, dependent upon time, steer angle or rate). For a change in steer angle of $\Delta\delta$ with $\dot{\delta}(0) = \Delta\dot{\delta}(0) = 0$ and $\dot{\delta}(t_f) = \Delta\dot{\delta}(t_f) = 0$, the optimal steering angular acceleration within this constraint is:

$$\ddot{\delta}(t) = \begin{cases} \hat{\ddot{\delta}} & 0 < t < \frac{t_f}{2} \\ -\hat{\ddot{\delta}} & \frac{t_f}{2} < t < t_f \end{cases}$$

such that the optimal steering angular velocity time-history becomes:

$$\begin{aligned} \dot{\delta}(t) &= \int_0^t \ddot{\delta}dt \\ &= \begin{cases} \int_0^t \hat{\ddot{\delta}}dt & 0 < t < \frac{t_f}{2} \\ \int_0^{\frac{t_f}{2}} \hat{\ddot{\delta}}dt - \int_{\frac{t_f}{2}}^t \hat{\ddot{\delta}}dt & \frac{t_f}{2} < t < t_f \end{cases} \\ &= \begin{cases} \hat{\ddot{\delta}}t & 0 < t < \frac{t_f}{2} \\ \hat{\ddot{\delta}}(t_f - t) & \frac{t_f}{2} < t < t_f \end{cases} \end{aligned}$$

and optimal the steering displacement time-history is therefore:

$$\delta(t) = \int_0^t \dot{\delta} dt$$

$$= \begin{cases} \displaystyle\int_0^t \hat{\ddot{\delta}} t dt & 0 < t < \dfrac{t_f}{2} \\ \displaystyle\int_0^{\frac{t_f}{2}} \hat{\ddot{\delta}} t dt - \int_{\frac{t_f}{2}}^t \hat{\ddot{\delta}}(t_f - t) dt & \dfrac{t_f}{2} < t < t_f \end{cases}$$

$$= \begin{cases} \left[\dfrac{1}{2}\hat{\ddot{\delta}} t^2\right]_0^t & 0 < t < \dfrac{t_f}{2} \\ \left[\dfrac{1}{2}\hat{\ddot{\delta}} t^2\right]_0^{\frac{t_f}{2}} - \left[\hat{\ddot{\delta}}(t_f t - t^2)\right]_{\frac{t_f}{2}}^t & \dfrac{t_f}{2} < t < t_f \end{cases}$$

$$= \hat{\ddot{\delta}} \begin{cases} \dfrac{1}{2} t^2 & 0 < t < \dfrac{t_f}{2} \\ \dfrac{3t_f^2}{8} + t^2 - t_f t & \dfrac{t_f}{2} < t < t_f \end{cases}$$

thus the final steer angle,

$$\delta(t_f) = \Delta\delta = \frac{3\hat{\ddot{\delta}} t_f^2}{8}$$

such that the time taken to achieve the required steer angle change $\Delta\delta$ is:

$$t_f = \sqrt{\frac{8}{3}\frac{\Delta\delta}{\hat{\ddot{\delta}}}}$$

and the effect on the turn-in time delay t_{lag} is half of this:

$$\Delta t_{lag} = \frac{t_f}{2} = \sqrt{\frac{2}{3}\frac{\Delta\delta}{\hat{\ddot{\delta}}}}$$

which should serve as an approximation of the influence of the actuator lag on the optimal time-response.

Note that some sideslip targets, such as zero sideslip ***also*** demand a fast response from the ***rear*** steering, since the optimal turn-in response requires immediate generation of rear lateral force. However, sufficient sideslip control (with an alternative sideslip target) can normally be provided with much slower changes in the rear steer angle (see the examples of 2WS vehicle responses in Chapter 5). Since making fast changes of steer angle might be costly (due to the additional actuator capacity required), this factor should also be considered when the sideslip target is selected. It can also be seen that, if the time delay due to the rear steer actuator limits is large compared with that due to the vehicle dynamics, then this will delay the generation of the front lateral force and thus directly increase the time lag discussed previously.

8.7: Concluding Remarks

It has been shown that the constant time delay which was observed in the results from Linear Programming analyses is due to fact that the application of rear tyre force in the direction of the turn must always be delayed in order to allow the vehicle to acquire sufficient yaw momentum.

Analytical expressions for the time delay were derived, and showed that the lag is dependent only on inertial properties of the vehicle, not on tyre, suspension or steering system influences.

The time delay was shown to increase in inverse proportion to the vehicle speed, since the yaw rate necessary for steady-state cornering at a given lateral acceleration also reduces linearly with speed.

It was shown, however that a caveat to this is that the delay is increased according to lags in the front steering actuator, and/or by any need to reduce front steering input to prevent violation of the rear tyre slip constraint.

The results derived assume that the available tyre friction is independent of the vertical load on the tyre, and that the lateral forces always act lateral to the vehicle such that there are no yawing moments introduced by longitudinal force components.

Chapter 9:
The Transient Handling Envelope

In this chapter, the constraints on the controls that are imposed by the limited available friction are analysed in a graphical manner that shows the transient handling 'envelope' of the vehicle. It will be seen that this alternative analysis provides further insight into the problem of appropriate motion centre selection.

It was shown in the previous chapter that whenever the driver demands a sudden change in lateral acceleration, the delivery of this lateral acceleration must be traded off against asserting the desired directional (yaw/sideslip) control, since the same frictional forces must provide both the in-plane translational accelerations (a_x and a_y) and the yaw acceleration (α_z) to turn the vehicle.

It was observed that the coupling between a_y and α_z introduces a minimum time delay into the lateral acceleration response of the vehicle, and that for simple models of vehicle capability, this minimum delay is straightforward to identify. However, it was also shown that both this time delay and the motion of the front of the vehicle, is largely insensitive to the sideslip control that is exercised during the transient phase.

The caveat to this is that the buildup of the rear tyre force must be sufficiently rapid that the rear tyre slip (and force) do not saturate, since this demands a reduction or reversal of the front axle force (known as 'opposite lock'). It has been shown that opposite-lock contributes directly to an increase in the minimum response time of the vehicle.

In this section, an alternative (graphical) view of the constraints imposed by limited friction is presented as the ***instantaneous handling envelope*** of the vehicle. In the following chapter, it is then shown that certain motion centres are more compatible with the shape of the handling envelope than others, if time-optimal turn-in (with no tyre saturation) is required. The goal of this chapter, in combination with Chapter 10, is to address hypothesis H4 in a more intuitive manner.

9.1: Simplified Modelling of the Vehicle Envelope

Since simple control strategies are generally desired (such that the strategy and software can be shown to be clearly robust), and the vehicle dynamics controller is unlikely to have knowledge of the detailed non-linear contact mechanics of the tyre, this section shows how ***simple models*** of the vehicle could be used to determine the likely available a_x, a_y and α_z in a given dynamic situation, such that the demands for these can be traded appropriately.

It will be seen that, as in the LP analysis undertaken in Chapter 4, some knowledge of the ***limit balance*** of the vehicle is required - either in advance of the maneuver, or during the maneuver - in order to identify the ***extent*** of the handling envelope.

However, when modelled to first order, certain characteristics of the handling envelope (such as the orientation of the edges of the handling envelope of a purely steered vehicle, when projected into a_y-α_z space), remain entirely ***independent*** of the limit capabilities of the vehicle (i.e. independent of the limit balance, available friction, tyre characteristics or suspension design). In the following chapter, it will be seen that this knowledge can be used to advantage in the selection of a more appropriate target trajectory for a vehicle dynamics controller, such that the controller, irrespective of the control strategy that is adopted, is more likely to be successful in tracking the reference.

Simple Modelling of the a_y-α_z Envelope

In the first analysis, the following influences are neglected:

- ***changes in braking*** (a constant deceleration a_x is assumed, such that the influence of the brake input on the available friction and tyre load distribution is neglected, or at least assumed constant)
- ***sideslip angle***, β (this is assumed zero - this is considered reasonable, since near-zero sideslip is likely to be the controller target anyway, and the influence of sideslip is second order, through the tyre-dependent vertical load sensitivity of the tyres)
- ***lateral load transfer*** (a significant effect in many vehicles, that must be taken into consideration prior to implementation, but whose influence is again highly dependent upon the vertical load sensitivity of the tyres [Milliken, 1995])
- ***any limit on the authority of DYC*** (such as limited brake pressure, friction or fundamental limitations on the mechanism for moment generation, such as if it is provided only by restricting relative motion inside the

differential)

With the above assumptions, the envelopes of AWS vehicles, with and without DYC, are as shown on the following pages. This set of assumptions simplifies the compuatation of an approximate envelope for the vehicle, since (i) equal lateral forces $F_{y_L} = F_{y_R}$, and equal and opposite longitudinal forces $F_{x_L} = -F_{x_R}$ are available from both tyres on the same axle, (ii) lateral and longitudinal forces act in the vehicle axis directions.

The envelope of an AWS vehicle

With the assumptions of zero lateral load transfer and zero sideslip, the computation of the envelope of a steered vehicle is straightforward. Since no longitudinal forces can be generated, the constraints for the AWS envelope computation are:

$$F_{x_f} = F_{x_r} = 0$$

$$-\hat{F}_{y_f} < F_{y_f} < \hat{F}_{y_f}$$

$$-\hat{F}_{y_r} < F_{y_r} < \hat{F}_{y_r}$$

Four points can immediately be found which correspond to (a) the maximum and minimum yaw moment and (b) maximum and minimum lateral acceleration. These are clearly four points on the boundary of the envelope.

Between these points, solutions which lie on the boundary of the envelope always lie on at least one constraint. This is clear, because if neither lateral force was at its maximum value, then it would be possible to change the lateral forces in order to effect a change in the acceleration vector in ***any*** direction in $a_y - \alpha_z$ space, such that this could never be a point on the boundary.

Therefore, alternative solutions are found by varying one of the controls over its full range whilst the other remains fixed at one of its limits, such that the four edges of the envelope are defined by:

(i) $F_{y_r} = \hat{F}_{y_r}$, $-\hat{F}_{y_f} < F_{y_f} < \hat{F}_{y_f}$

(ii) $F_{y_r} = -\hat{F}_{y_r}$, $-\hat{F}_{y_f} < F_{y_f} < \hat{F}_{y_f}$

(iii) $F_{y_r} = \hat{F}_{y_r}$, $-\hat{F}_{y_r} < F_{y_r} < \hat{F}_{y_r}$

(iv) $F_{y_r} = -\hat{F}_{y_r}$, $-\hat{F}_{y_r} < F_{y_r} < \hat{F}_{y_r}$

The envelope of a vehicle with AWS and DYC

For an AWS vehicle with DYC, the boundary of the envelope is more complex, since the constraints must be expanded to cater for the coupling between the maximum magnitudes of the lateral and longitudinal forces:

$$\left.\left(\frac{F_{x_k}}{\hat{F}_{x_k}}\right)^2 + \left(\frac{F_{y_k}}{\hat{F}_{y_k}}\right)^2 < 1\right\} \quad k = FL, FR, RL, RR$$

However, the two points where the lateral acceleration is maximised are not changed by the availability of longitudinal force control, since the maximum lateral acceleration is always generated by the maximum lateral forces (and therefore zero longitudinal force).

Between these limits, there are an infinity of combinations of F_{y_f} and F_{y_r} that may be chosen to generate the same lateral acceleration a_y. If we express the requirement for a particular lateral acceleration as a constraint that fixes one of the forces as a function of the other - for instance:

$$F_{y_r} = Ma_y - F_{y_f}$$

then we may vary F_{y_f}, determine the associated $F_{y_r} = Ma_y - F_{y_f}$, and consequently identify the maximum and minimum ***longitudinal*** forces F_{x_f} and F_{x_r} that may be generated by the friction which remains available at each axle.

If we express the total yaw moment M_z as a function of F_{y_f} (with the associated F_{x_f} being identified using the knowledge that either a maximum or minimum F_{x_f} is required in order to find the extremity of the envelope, together with the defined constraints on the available tyre friction), then we may determine an expression for the total yaw moment as a function of the distribution of the lateral forces between the front and rear axles.

Therefore, it is possible to find the value of F_{y_f} that maximises (and that which minimises, towards minus infinity) the ***total*** yaw moment and note the associated values of F_{y_r}, F_{x_f} and F_{x_r} that yield the maximum yaw moment for a given lateral acceleration.

If the lateral acceleration a_y is varied in the interval between the lower limit $-\hat{a}_y$ and the upper limit $\hat{a}_y$, we can therefore find both the upper (maximum α_y) and lower (minimum α_z) limits of the envelope as a function of a_y.

Iteration procedure and convergence tolerance

For every lateral acceleration point between the minimum and maximum values, it is required to find the values $\hat{F}_{y_f}$ and $\breve{F}_{y_f}$ of F_{y_f} which in turn maximise and minimise the total yaw moment:

$$\hat{M}_z = \hat{F}_{y_f} b - F_{y_r}\left(\hat{F}_{y_f}\right)c + D_f F_{x_f}\left(\hat{F}_{y_f}\right)t_f + D_r F_{x_r}\left(F_{y_r}\left(\hat{F}_{y_f}\right)\right)t_r$$
$$\breve{M}_z = \hat{F}_{y_f} b - F_{y_r}\left(\breve{F}_{y_f}\right)c - D_f F_{x_f}\left(\breve{F}_{y_f}\right)t_f - D_r F_{x_r}\left(F_{y_r}\left(\breve{F}_{y_f}\right)\right)t_r$$

where $D_f, D_r \in \{0,1\}$ indicating whether or not DYC control is available at that axle;

$$F_{y_r}\left(F_{y_f}\right) = Ma_y - F_{y_f}$$

in order to maintain the required lateral acceleration, and

$$F_{x_f}\left(F_{y_f}\right) = \hat{F}_{x_f}\sqrt{\left(1 - \frac{F_{y_f}^{\ 2}}{\hat{F}_{y_f}^{\ 2}}\right)}$$

$$F_{x_r}\left(F_{y_r}\left(F_{y_f}\right)\right) = \hat{F}_{x_r}\sqrt{\left(1 - \frac{F_{y_r}\left(F_{y_f}\right)^2}{\hat{F}_{y_r}^{\ 2}}\right)}$$

in order to ensure that the maximum possible DYC moments are generated by each axle as F_{y_f} is varied.

Note the choice of positive or negative signs on the DYC moments in the equations for $\hat{M}_z$ and $\breve{M}_z$ according to whether the maximum or minimum yaw moment is required.

In other words, it is necessary to find the roots of:

$$\frac{\partial \hat{M}_z\left(F_{y_f}\right)}{\partial F_{y_f}} = 0 \qquad \text{to find the maximum yaw moment}$$

$$\frac{\partial \breve{M}_z\left(F_{y_f}\right)}{\partial F_{y_f}} = 0 \qquad \text{to find the minimum yaw moment}$$

These roots are found by repeated Newton-Raphson iteration:

$$\hat{F}'_{y_f} = \hat{F}_{y_f} - \frac{\dfrac{\partial \hat{M}_z\left(F_{y_f}\right)}{\partial F_{y_f}}}{\dfrac{\partial^2 \hat{M}_z\left(F_{y_f}\right)}{\partial F_{y_f}^2}}$$

$$\breve{F}'_{y_f} = \breve{F}_{y_f} - \frac{\dfrac{\partial \breve{M}_z\left(F_{y_f}\right)}{\partial F_{y_f}}}{\dfrac{\partial^2 \breve{M}_z\left(F_{y_f}\right)}{\partial F_{y_f}^2}}$$

This iteration is assumed to have converged when the change $\left|\breve{F}'_{y_f} - \breve{F}_{y_f}\right|$ that occurred is less than $10^{-6}\hat{F}_{y_f}$. It was found that the iteration converged extremely rapidly.

The optimal values $\hat{F}_{y_f}$ and $\breve{F}_{y_f}$ are used to construct the upper and lower limits of the envelope, $\hat{\alpha}_z\left(a_y\right)$ and $\breve{\alpha}_z\left(a_y\right)$ which are shown in the following section, where they are employed in order to find the bounds of the transient handling capability of the vehicle.

On later plots, the yaw moment generated by the optimal lateral forces $\left(\hat{F}_{y_f},\hat{F}_{y_r}\right)$ and $\left(\breve{F}_{y_f},\breve{F}_{y_r}\right)$ alone is also shown, in order to indicate the capability of a vehicle with lateral forces modulated for optimal performance with DYC, when DYC is not to be used (for instance, for efficiency reasons).

9.2: Results and Discussion

In figure 9.1, it can be seen that for the limit US and limit NS AWS-only vehicles, the limiting performance for rapid turn in to the limiting lateral acceleration requires a linear relationship for the tradeoff between yaw moment and lateral acceleration targets.

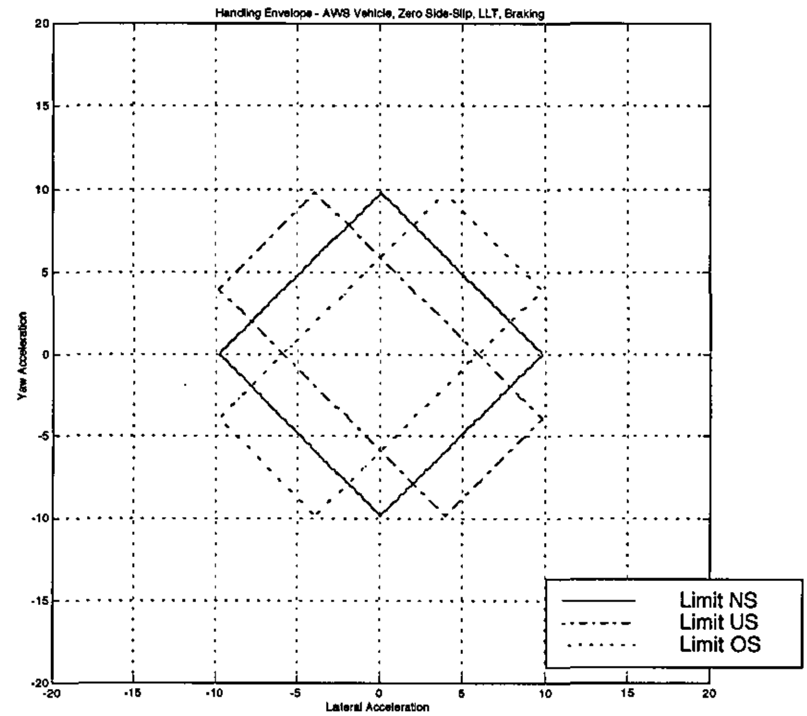

Figure 9.1

Handling envelope to first order - AWS vehicle with no DYC $\left(D_f = D_r = 0\right)$

(i) limit neutral-steer (NS) $\left(\hat{F}_{y_f} = 4905, \hat{F}_{y_r} = 4905\right)$

(ii) limit under-steer (US) $\left(\hat{F}_{y_f} = 2943, \hat{F}_{y_r} = 6867\right)$

(iii) limit over-steer (OS) $\left(\hat{F}_{y_f} = 6867, \hat{F}_{y_r} = 2943\right)$

(inall cases, $b = c = 1.35, k = 1.61, M = 1000$)

The four edges of the diagram, from top-right, through bottom-right, bottom-left and top-left, correspond to (i) $F_{y_f} = \hat{F}_{y_f}$, (ii) $F_{y_r} = \hat{F}_{y_r}$, (iii), $F_{y_f} = -\hat{F}_{y_f}$, (iv) $F_{y_r} = -\hat{F}_{y_r}$, each with the other axle lateral force being varied.

The resulting diamond-shaped envelope is in contrast to the typically presented plot of the tradeoff between a_x and a_y, often known as the 'g-g diagram', which usually has the form of a clipped ellipse.

From this diagram, it can clearly be seen that for the unbalanced (US or OS) vehicles, the highest lateral acceleration is achievable only when a nonzero yaw moment can be tolerated. Since this is rarely the case in practice, the limiting performance in most conditions tends to be close to the limiting ***steady-state*** performance. It can be seen from where the plots cross the x (a_y) axis (at $\alpha_z = 0$), that the influence of limit under-steer or over-steer is to significantly compromise the steady-sate cornering performance, despite the fact that the size of the envelope remains similar. Also, it can be seen that at the point of maximum lateral acceleration, the yawing moment created by a limit-over-steering vehicle is in the turn-in (unstable) direction, whereas that created by the limit-under-steering vehicle is in the turn-out (stabilising) direction.

One further point of significant interest is that the ***slopes*** of the edges of the envelope:

$$m = \frac{d\alpha_z}{da_y}$$

may be determined analytically. For the AWS vehicle, these accelerations vary only with the axle lateral forces:

$$\frac{d\alpha_z}{da_y} = \frac{\partial \alpha_z}{\partial F_{y_f}} \frac{\partial F_{y_f}}{\partial a_y} + \frac{\partial \alpha_z}{\partial F_{y_r}} \frac{\partial F_{y_r}}{\partial a_y}$$

For the top-right and bottom-left edges, where the front lateral force is held constant,

$$\begin{aligned}
\frac{d\alpha_z}{da_y} &= \frac{\partial \alpha_z}{\partial F_{y_r}} \frac{\partial F_{y_r}}{\partial a_y} \\
&= \frac{\partial\left(\dfrac{bF_{y_f} + cF_{y_r}}{Mk^2}\right)}{\partial F_{y_r}} \cdot \frac{\partial F_{y_r}}{\partial\left(\dfrac{F_{y_f} + F_{y_r}}{M}\right)} \\
&= -\frac{c}{k^2}
\end{aligned}$$

and for the top-left and bottom-right edges, where the rear lateral force is held constant,

$$\begin{aligned}\frac{d\alpha_z}{da_y} &= \frac{\partial \alpha_z}{\partial F_{y_f}} \frac{\partial F_{y_f}}{\partial a_y} \\ &= \frac{\partial\left(\dfrac{bF_{y_f} - cF_{y_r}}{Mk^2}\right)}{\partial F_{y_f}} \cdot \frac{\partial F_{y_f}}{\partial\left(\dfrac{F_{y_f} + F_{y_r}}{M}\right)} \\ &= \frac{b}{k^2}\end{aligned}$$

Therefore, although the extent of the diagram varies according to the available friction (and thus road conditions, tyre load and pressure etc.), the limit capability of the vehicle remains consistent in terms of the relationship between the lateral and yaw accelerations that may be generated.

For instance, since the optimal strategy for obstacle avoidance, identified in the previous section, was identified to be the set of possible responses where $F_{y_f} = \pm\hat{F}_{y_f}$, we can now see that any force-optimal response would need to satisfy $\frac{d\alpha_z}{da_y} = -\frac{c}{k^2}$ at all times during a transient obstacle-avoidance maneuver.

Since the form of optimal yaw-sideslip trajectory is therefore ***independent*** of the available friction, it is concluded that on-line estimation of the available tyre friction is ***not required*** in order to determine the optimal handling transfer function for a vehicle. This is considered to be a critical new result in terms of optimal dynamics control of AWS vehicles.

AWS vehicles with DYC provided by the unsaturated axle (common)

It can be seen from figures 9.2 and 9.3 that the provision of DYC using the longitudinal forces available at the unsaturated axle expands the vehicle envelope significantly, notably by allowing significantly greater (both positive and negative) yaw accelerations to be generated for the same lateral acceleration, and significantly improving the steady-state performance.

In the case of the US vehicle, since the most common strategy of ***rear axle DYC*** is applied in order to help the vehicle to turn in, the top right edge of the diagram (i.e. the line of optimal performance) becomes non-linear. This is due to the fact that along this line of optimality, a range of different rear lateral forces are available. Each allows a certain amount of DYC moment to be applied, and that available moment is determined by the elliptical nature of the tyre's circle of friction. Therefore, the force-optimal turn-in for such a vehicle requires a ***non-linear*** $a_y^P - \alpha_z$ trajectory to be targeted.

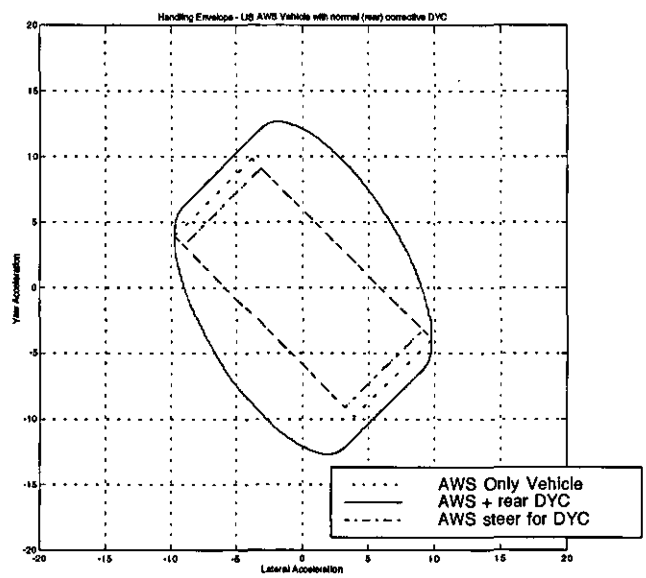

Figure 9.2

US AWS with normal (rear) corrective DYC $\left(D_f = 0, D_r = 1\right)$

$$\left(\hat{F}_{y_f} = 2943, \hat{F}_{y_r} = 6867, \hat{F}_{x_r} = 6867, b = c = 1.35, k = 1.61, M = 1000\right)$$

In the case of the over-steering vehicle, the top edge of the diagram from the base AWS vehicle is displaced vertically, indicating that a much faster turn-in response is achievable when DYC is employed. The dashed line indicates the necessary lateral forces to be generated by steering, in order that sufficient force remains available for the DYC to work optimally. It can be seen that naturally, only the front axle lateral force must be compromised.

In addition, it can be seen that this necessary compromise is precisely that which allows the combination of steering and DYC forces to generate the maximum turn-in yaw moment, which is when the total force from each of the front tyres acts at 90 degrees to a line from the contact patch through the vehicle CG.

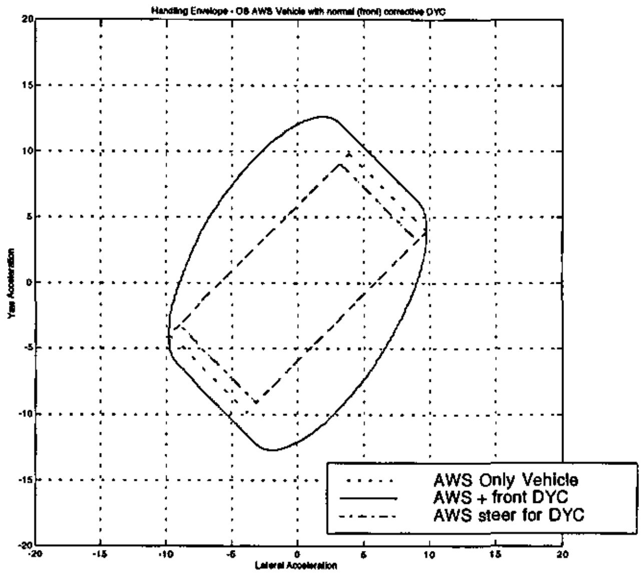

Figure 9.3

OS AWS with normal (front) corrective DYC $\left(D_f = 1, D_r = 0\right)$

$$\left(\hat{F}_{y_f} = 6867, \hat{F}_{x_f} = 6867, \hat{F}_{y_r} = 2943, b = c = 1.35, k = 1.61, M = 1000\right)$$

AWS vehicles with DYC provided by the saturated axle (uncommon)

It has been mentioned in the literature that DYC has an added benefit in that it is able to work even when the axle is completely saturated. In such circumstances, even if the steering cannot be controlled (or if controlling it generates no change in lateral force), the DYC input can increase the longitudinal slip, and thus rotate the total slip vector in a more favourable direction. Although such an increase in the magnitude of the combined slip is not energy-optimal, it may be useful in stabilising the vehicle when there is no better solution.

Additionally, if an integrated control strategy is able to recognise the need to leave some force available for use longitudinally as DYC, then the benefit can be gained at the same time as generating peak tyre force and consuming less energy.

This situation is shown in figures 9.4 and 9.5.

For the under-steering vehicle with only front DYC available, it may seem unnatural to compromise the front lateral force for any reason. However, since generating the maximum turn-in moment is what improves the maximum possible lateral acceleration (allowing the rear tyres to generate more lateral force), it can be seen (above) that compromising that front axle force does indeed allow a greater lateral acceleration to be generated, regardless of the desired yaw acceleration. Once again, with front DYC only being used, the line of optimal turn-in behaviour remains linear and is simply displaced.

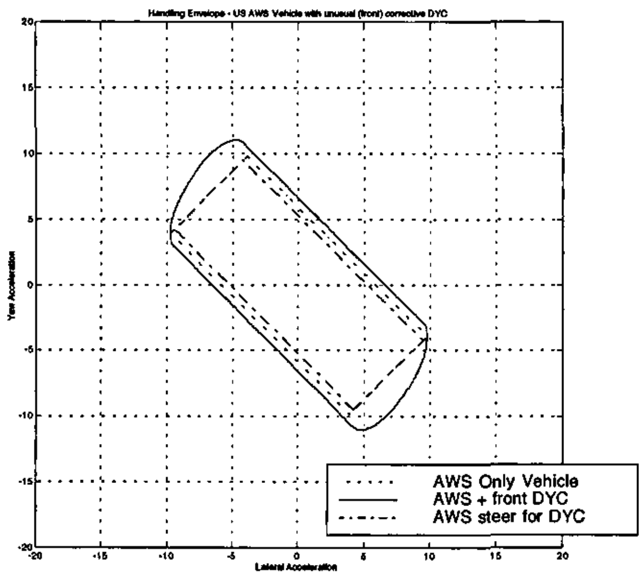

Figure 9.4

Handling Envelope of US vehicle with unusual (front) corrective DYC $\left(D_f = 1, D_r = 0\right)$

$$\left(\hat{F}_{y_f} = 2943, \hat{F}_{x_f} = 2943, \hat{F}_{y_r} = 6867, b = c = 1.35, k = 1.61, M = 1000\right)$$

The dot-dashed line ('AWS steer for DYC') again shows the forces and accelerations generated by the steering when the steering is compromised to ***allow*** for optimal DYC. It can be shown that the necessary compromise is that which allows the maximum yaw moment about the CG to be generated, i.e. when the total in-plane tyre force vector acts perpendicular to a line that runs through both (a) the projection of the vehicle CG onto the ground and (b) the tyre contact patch.

It can also be seen that the maximum lateral acceleration (irrespective of yaw moment) demands the maximum lateral tyre forces, but as the lateral acceleration demand is reduced when there is yaw moment demand (in either sense), this reduction in lateral acceleration is effected by reducing only the front tyre force, such that the yaw moment introduced by DYC is achieved as soon as possible.

The same effect can be seen for the over-steering vehicle, although whilst the line of optimum stabilisation behaviour (maximum yaw moment for a lateral acceleration in the opposite sense) is displaced linearly, the line of force-optimal turn-in behaviour once again becomes non-linear due to the use of rear DYC.

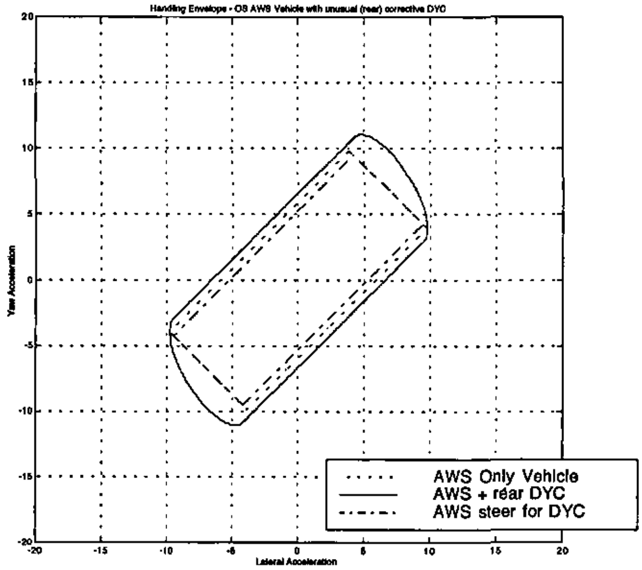

Figure 9.5

Handling Envelope of OS vehicle with unusual (rear) corrective DYC $\left(D_f = 0, D_r = 1\right)$

$$\left(\hat{F}_{y_f} = 6867, \hat{F}_{y_r} = 2943, \hat{F}_{x_r} = 2943, b = c = 1.35, k = 1.61, M = 1000\right)$$

Perhaps surprisingly, the envelope in both of these cases is significantly extended. Additionally, the use of DYC on an axle which is saturating laterally may have benefits for control. Referring to typical lateral force against lateral and longitudinal slip surface plots, it can be seen that as the longitudinal slip is increased, the lateral force characteristic begins to lose it's 'overshoot'. Since it is the negative cornering stiffness portion of this curve that causes particular difficulty in achieving robust control, there may therefore be a second benefit of applying DYC at the saturating axle.

AWS vehicles with dual-axle ('full') DYC

In the following plots, it has been assumed that both front and rear-axle DYC is available, and that each is used optimally. In other words, it is assumed that all forces lie on the ellipse of friction, and for a given lateral acceleration, the ratio of front to rear DYC usage is optimised in order to generate the highest possible lateral acceleration.

Note that the envelope of the full DYC car is not equal to the union of the envelopes of the front DYC and rear DYC cars; it is significantly ***larger***, particularly in the region around peak yaw moment generation (at low lateral acceleration), where a vehicle with DYC applied at a single axle must compromise the lateral acceleration in order to generate the desired high yaw acceleration, but the vehicle with dual-axle DYC is able to generate equal and opposite changes in lateral acceleration whilst generating an increase in yaw moment. Note that there are very significant performance gains, over either of the previously discussed single-axle DYC performances.

In the plots below, the steering (lateral) forces required to allow optimal exploitation of DYC are also shown (the innermost contour).

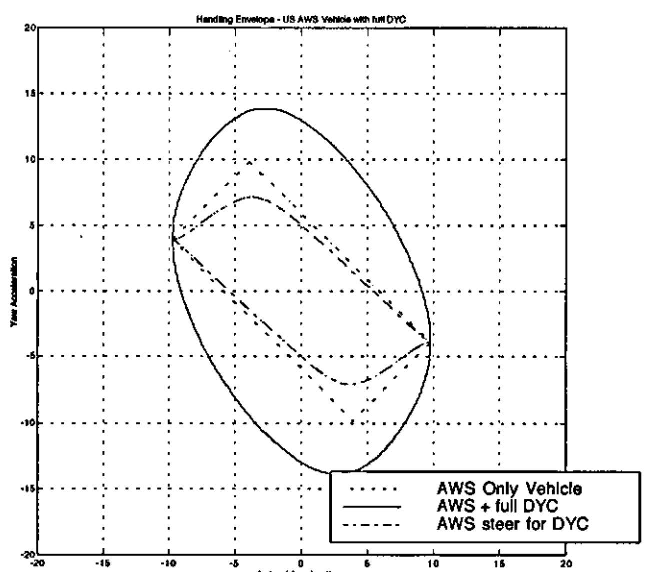

Figure 9.5

US AWS with Full DYC $\left(D_f = D_r = 1\right)$

$$\left(\hat{F}_{y_f} = 2943, \hat{F}_{x_f} = 2943, \hat{F}_{y_r} = 6867, \hat{F}_{x_r} = 6867, b = c = 1.35, k = 1.61, M = 1000\right)$$

Here, it is clear that both axles must compromise the lateral forces which are generated in order to leave some friction available for generation of the optimal DYC moment.

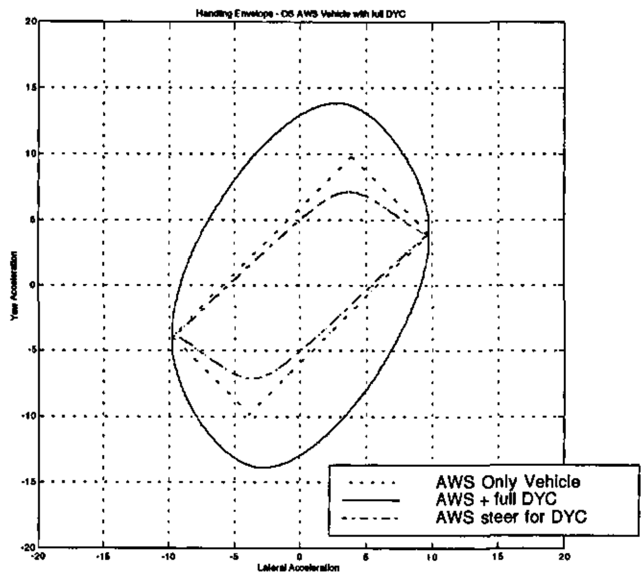

Figure 9.6

OS AWS with Full DYC $\left(D_f = D_r = 1\right)$

$$\left(\hat{F}_{y_f} = 6867, \hat{F}_{x_f} = 6867, \hat{F}_{y_r} = 2943, \hat{F}_{x_r} = 2943, b = c = 1.35, k = 1.61, M = 1000\right)$$

In figure 9.7, it can be seen that in the same sense that the full DYC performance is not equal to the union of the front-DYC-only and rear-DYC-only performances, so the steering angle (or force) compromises necessary to ***facilitate*** the optimal performance are not the same, except at the point where the other axle is generating zero lateral force, or maximum DYC (i.e. in the middle of each side of the above diagram). It would seem that it is optimal to compromise the lateral force at each axle a little, rather than compromise one a lot. This is clearly the case when the initial compromise is considered, since a small loss of lateral force at each axle contributes a significant yaw moment, but this process is subject to 'diminishing returns' as the lateral force is reduced further. For that reason, the maximum yaw moment is generated by compromising the lateral force at each axle a little.

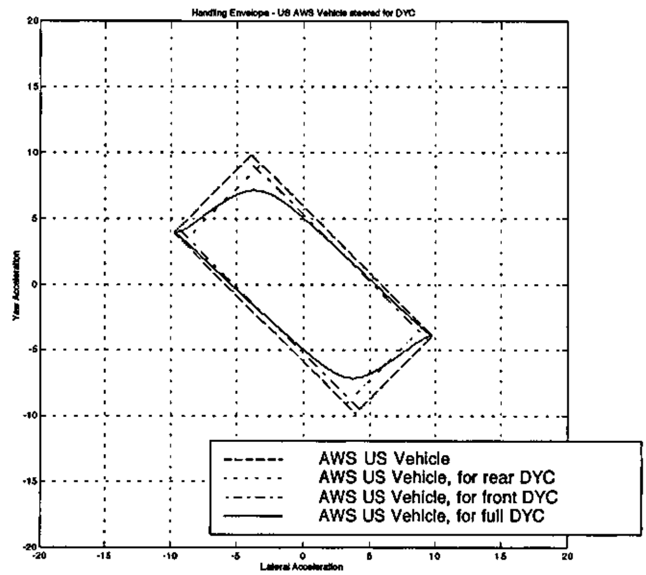

Figure 9.7

Necessary lateral force modulation to allow force-optimal DYC (US vehicle)

(i) AWS only $\left(D_f = D_r = 0\right)$

(ii) Rear DYC only $\left(D_f = 0, D_r = 1\right)$

(ii) Front DYC only $\left(D_f = 1, D_r = 0\right)$

(ii) Full DYC $\left(D_f = D_r = 1\right)$

$$\left(\hat{F}_{y_f} = 2943, \hat{F}_{x_f} = 2943, \hat{F}_{y_r} = 6867, \hat{F}_{x_r} = 6867, b = c = 1.35, k = 1.61, M = 1000\right)$$

Energy-conserving performance

The similarity of shape between the constant power contour and the envelope of the vehicle with full DYC is an interesting one. This suggests that it might be possible to have the transient response of a vehicle follow an optimally energy conserving contour (usually using only AWS, since it was shown that any use of DYC is inefficient) and to have the same kinematic behaviour delivered to the driver right up to the vehicle limit, by using DYC as necessary (whenever the AWS envelope was breached).

It is also interesting also to consider how the shape of the envelopes would change if the DYC moments were to be generated only by the (more efficient) ***controlled differentials***. A controlled differential is able to generate moments only in the direction that opposes the relative wheel rotation. If the assumption is made that the longitudinal tyre slip characteristic is linear, then the only contribution to the difference in wheel and half shaft speeds comes from the vehicle yaw rate. Therefore, for a positive yaw rate, the controlled differential would only be able to increase the yaw acceleration in the ***negative*** sense, and vice versa. Since generating DYC moments by means of an active differential consumes less energy than doing so by brake control, a vehicle with both actuators could prefer the active differential whenever it has authority. The maximum moment that the controlled differential is able to deliver would also be limited by the longitudinal tyre slip stiffness, since the maximum the differential could do is lock, generating equal and opposite slip in proportion to the yaw rate. This indicates a speed-dependence in the envelope of authority of the controlled differential - for a given lateral acceleration, at higher speed, the yaw rate is lower since ${}^{P}a_y = Ur$ and thus the slip and yaw moment which can be generated is lower.

9.3: Limitations

Load transfer between the tyres has not been included in this simple modelling, and as discussed, can be of significant importance, especially for short, narrow vehicles with a high centre of mass and particularly 'load-***insensitive*** tyres' [Milliken, 1995] (where the limiting performance of the tyre increases proportionally with the load, approximately according to the basic friction relation of $\hat{F} = \mu N$).

For vehicles with significant sensitivity to load transfer, an improved model is required. The sensitivity of the available tyre forces to load changes usually lies somewhere between the two limiting conditions of (i) $\hat{F} = \mu N$ ('load-insensitive tyres') and (ii) $\hat{F} = constant$ (the 'load-sensitive' tyres). Based on experimental data, it may be possible to identify a nominal load sensitivity model, or to include on-line identification of load model in the controller. Without data, some nominal condition midway between these extremes would perhaps be the optimal assumption. However, such a model should certainly be developed and validated in order to assure more precise force-optimality of control strategies developed based on these envelope models, before they are applied in practice.

The effect of load transfer due to longitudinal acceleration a_x would always be to make the vehicle more over-steering during braking (by increasing the load on the front tyres, and reducing the load on the rear) and more under-steer during acceleration. In cornering, net effect of load transfer would be to shrink the envelope towards high lateral acceleration, 'rounding the points' of the envelope. The distribution of load transfer between front and rear axles is also important, since this could cause the shape of the envelope to become either more 'under-steering' or more 'over-steering' at high lateral acceleration. This effect is neglected here, since is is hypothesised that the notional 'optimal vehicle' (with active control applied) would probably be designed with a chassis that had the optimal 'limit-neutral' behaviour (since the active controller could assure the necessary stability).

A further effect that warrants consideration is transient over-steer. The load transfer (roll-resisting moment) distribution need not be constant during the transient phase. Since an over-steering balance is optimal only during turn-in, a rearward biased distribution of transient load transfer (created, for instance, by a higher level of damping or damper inertia in the rear suspension) can improve the turn-in performance without impairing the steady-state. If the sideslip trajectory can be chosen such that the yaw acceleration demand occurs when there is significant roll velocity (i.e. yaw acceleration in phase with roll velocity), then significant performance benefit could be derived from this. In addition, this strategy may be appropriate for limitation of roll excitation, since the lateral acceleration would then be out of phase with the roll velocity, thus minimising the energy transferred to the roll mode. Since there are potential performance gains derivable from this, it is proposed that also in this sense, the choice of handling (motion centre) reference should be integrated with the suspension design.

9.4: Concluding Remarks

Very simple models, simply relating tyre forces to accelerations, have been utilised to identify the shapes of the transient handling envelopes of vehicles fitted with different combinations of actuators. Accelerations were selected rather than total forces or moments, because this permits the ***kinematics*** of handling maneuvers to be considered in terms of their usage of the envelope.

Additionally this showed some interesting properties of the envelope of the AWS vehicle - that the slopes of the boundaries are dependent only upon inertial properties of the vehicle, and not on the available tyre friction. However, this conclusion is subject to the restriction that changes in tyre friction with respect to changes in tyre load must be assumed negligible.

As DYC was introduced to the AWS vehicle, it was shown that:

- the handling envelope of all vehicles is significantly expanded in size by the introduction of DYC;
- when DYC is applied at a given axle, the straight-line $a_y - \alpha_z$ limit of the underlying AWS vehicle becomes convex nonlinear;
- when DYC is applied at ***either*** axle of an unbalanced vehicle, the ***steady-state*** limit is increased over the pure AWS vehicle;
- the envelope is still significantly extended in all directions, even when the DYC is available only on the less capable axle;
- the envelope of a vehicle with both front and rear DYC is ***larger*** than the union of the envelopes of the vehicle with front DYC only and the vehicle with rear DYC only;
- the notable difference between full DYC and (front DYC ∪ rear DYC) occurs at low lateral accelerations, where full DYC vehicles are able to generate much higher yaw accelerations;
- the shape of the full DYC ***envelope*** for a vehicle with a particular ***limit*** balance is very similar to the shape of the constant ***power*** contour of a vehicle with a particular ***linear*** balance;
- front DYC increases the shape of the envelope in the more under-steer direction, and rear DYC more in the over-steer direction;
- DYC significantly increases the yaw accelerations which may be generated at high (or limit) lateral acceleration;

Chapter 10: Optimal Target Trajectories

10.1: Objective

In Chapter 6 (Transient Demand Analysis, Time Domain), it was shown that making an arbitrary choice of reference trajectory and applying hard control to this trajectory can lead to transient peaks in tyre force demand. Such transients are certainly inefficient (since applying half the force for twice the time is always more energy efficient) but also may not be feasible when the level of demand is relatively high compared with the limit, or if the demand is rapidly changing.

In Chapter 7 (Optimal Target Identification by Linear Programming), the optimal inputs within the constraints enforced by the available friction were identified, and it was shown that the requirement for optimality of turn-in performance (at least in terms of the defined, equivalent metrics of lateral acceleration delay, t_{lag} and lateral velocity offset, v_{lat}) leaves some freedom over the rear tyre force control during the transient.

It was also shown that certain sideslip responses, such as zero rear steer with a low rear tyre cornering stiffness, or 4WS/AWS with a fixed motion centre at a location $d < d_{crit}$, could lead to sub-optimal performances (i.e. $F_{y_f}(t) \neq \hat{F}_{y_f}$). However, the value of d_{crit} and its dependence on the vehicle parameters was not identified, due to the numerical nature of the analysis. In addition, it was also observed from numerical analyses that the metric of lateral ***displacement*** offset, d_{lat} was also rather insensitive to the rear tyre force control.

In Chapter 8 (Further Mathematical Analysis), this was shown to be due to the fact that (i) the first-order metric of obstacle avoidance performance is insensitive to the sideslip control strategy, since it is influenced only by the steady-state yaw rate demand (which is in turn defined by the kinematics of turning), and (ii) the lateral acceleration of the ***front*** of the vehicle, throughout the transient and steady-state phases, is largely ***insensitive*** to the rear lateral tyre force, F_{y_r}, since the ***centre of percussion*** [Den Hartog, 1984] of the vehicle with respect to forces applied laterally at the rear axle, is normally very close to the front of the vehicle. It was, however, shown that it is necessary for the rear tyre force (and slip angle) to have a minimum level of damping if a phase of highly sub-optimal opposite-lock is to be avoided.

In the preceding chapter, another view of the tyre-friction constraints on optimal transient handling was provided, in the form of the envelope of vehicle capability.

In this chapter, the compatibility between these envelopes and the possible response trajectories in a_y-α_z space is considered in further detail. The set of trajectories which are completely compatible with envelope of the vehicle (and thus allow the driver to make optimal utilisation of the available friction) are described here as 'force-optimal'.

In particular, the typical second order behaviour of 2WS vehicles is compared with the first-order responses of zero sideslip (ZSS) and fixed motion centre vehicles, and which have the apparent benefit that they always satisfy the need to avoid transient overshoots in the rear tyre slip or force.

10.2: Optimal transient response

When the magnitude of the acceleration demand is lower than the available friction is able to provide, it would, in theory, be possible to deliver the desired new acceleration almost instantaneously, since the remaining friction could then be used for subsequent (delayed) generation of the yaw moments necessary to eventually find the steady state.

However, if the demand is approaching the limit of the vehicle, the constraints on the maximum available tyre forces mean that the same tyre friction (that may be used purely for generation of lateral acceleration in the steady-state) must then be shared between generation of yaw moment and lateral acceleration during the transient phase.

Therefore, since consistent handling behaviour is normally considered desirable [Furukawa, 1989; Komatsu, 2000], it is proposed that a vehicle dynamics controller should maintain a consistent, linear transfer function. Since the same transfer function must then be appropriate at high friction demand/utilisation as well as at low, it is suggested that the trajectories associated with steps to the maximum capability of the vehicle must fit neatly inside the identified handling envelope of the vehicle, ensuring 'force-optimal' turn-in behaviour when the demand is stepped to the limiting value.

The criterion of force-optimality or energy-optimality determines how the ***magnitude*** of the a_y and α_z demands should vary throughout the transient phase (i.e. to follow either a contour of optimal friction utilisation, with $F_{y_f}(t) = \hat{F}_{y_f}$ throughout the transient when the limit lateral acceleration is demanded, or to follow a contour of constant power if minimum energy consumption is desired).

However, in the case of either target (or a compromise of the two), the position ***along*** this contour remains to some extent free, since it is governed by the rear lateral tyre force, or the desired relationship between yaw rate and lateral acceleration - i.e. the sideslip, or the variation of the motion centre location.

10.3: The second-order responses of a 2WS vehicle

The lateral dynamics of a passive vehicle (the motions controlled by the in-plane tyre forces) are typically dominated by a second order pole pair [Dixon, 1995]. Therefore, in response to a step input in lateral demand, an overshoot of the sideslip and yaw rate, and thus of the lateral acceleration and tyre slips is possible.

It was shown in Chapter 5 that a certain minimum of damping is required if the need for opposite-lock during turn-in is to be avoided. The sensitivity of the yaw damping to the yaw inertia, $I_{zz} = Mk^2$ is analysed here. This parameter was chosen because it is known that by repackaging a passenger car, changes in k can be achieved relatively easily.

By inspection of the transfer function between the front force input and output quantities of interest, such as, for example, the lateral acceleration of the vehicle:

$$\frac{a_y}{F_{y_f}}(s) = \frac{c^2 C_{\alpha_r} s + c C_{\alpha_r} U + k^2 M s^2 U + b C_{\alpha_r}(cs + U)}{M\left(c^2 C_{\alpha_r} s + k^2 s\left(C_{\alpha_r} + MUs\right) + c C_{\alpha_r} U\right)}$$

it can be seen that all of these transfer functions exhibit the same second order pole pair. This is expected, since the poles (natural frequencies and damping ratios, or eigenvalues) are a property of the system, rather than of any particular output quantity.

Rearranging the denominator of any of these transfer functions into a polynomial in the Laplace operator s, we have the following:

$$\begin{aligned} D_{2WS} &= c^2 C_{\alpha_r} s + k^2 s\left(C_{\alpha_r} + MUs\right) + c C_{\alpha_r} U \\ &= \left(c^2 + k^2\right) C_{\alpha_r} s + k^2 MUs^2 + c C_{\alpha_r} U \end{aligned}$$

Comparing this with the denominator (pole pair, or characteristic equation) of the classical single degree of freedom system,

$$D_{SDOF} = m_{eff}s^2 + c_{eff}s + k_{eff}$$

it is possible to draw analogy between the terms in the transfer function of the vehicle:

$$m_{eff} = k^2 MU$$
$$c_{eff} = \left(k^2 + c^2\right)C_{\alpha_r}$$
$$k_{eff} = cC_{\alpha_r}U$$

where

m_{eff} is the effective mass;

c_{eff} is the effictive damping, and

k_{eff} is the effective stiffness

such that the effective damping ratio may be found:

$$\begin{aligned}\zeta_{eff} &= \frac{c_{eff}}{2m_{eff}\omega_{n,eff}} \\ &= \frac{\left(k^2 + c^2\right)C_{\alpha_r}}{2k^2 MU\sqrt{\frac{cC_{\alpha_r}U}{k^2 MU}}} \\ &= \frac{\left(k^2 + c^2\right)}{2kU}\sqrt{\frac{C_{\alpha_r}}{cM}}\end{aligned}$$

Note: The damping ratio, being a property of the pole pair, is also a property of the system, ***not*** of a specific output of the system, such that the same damping ratio applies to the response of the sideslip angle, the rear tyre slip angle, and all other outputs that might be considered.

The dependence of the damping ratio on the rear axle cornering stiffness, the mass and the vehicle speed is clear. Note that the front axle cornering stiffness is ***not*** involved, since it has been assumed that the driver or controller controls the lateral force, rather than the steer angle.

However, the dependence upon both k and c is quadratic. To find out at what values of k the maxima or minima occur, we take the partial derivative with respect to k:

$$\frac{\partial \zeta_{eff}}{\partial k} = \frac{\left(k^2 - c^2\right)}{2ck^2 U}\sqrt{\frac{cC_{\alpha_r}}{M}}$$

It can be seen that an extremum with respect to k occurs at $k = c$. By analysing the second derivative, it can be seen that this extremum is in fact a ***minimum*** of damping ratio. Referring to typical data from subjectively tuned vehicles, we find that cars that are deemed to 'handle well' [Crolla, 1996] tend to approximately ***satisfy*** $k = c$. Since k is generally relatively easy to vary, it must be concluded that this was for some reason deemed desirable handling behaviour.

This appears contradict the results of the optimal turn-in analysis from Chapter 7 at the further analyses which follows, both of which suggest that for optimal transient response (at least for obstacle avoidance), a certain level of yaw damping is required.

However, it should be remembered that these vehicles are entirely passive and therefore have no form of continuously acting closed-loop limit balance control (such as, for instance, active vertical load control, direct yaw control or longitudinal acceleration control). Therefore, the excitation of the sideslip angle by the driver may be one of the only mechanisms (apart from acceleration or deceleration), by which the stability and thus the performance of the vehicle can be controlled (noting that neutral stability is required for optimal steady-state limit handling).

For a vehicle that is fitted with a robust handling controller that is able to ensure both stability and optimal handling performance (implying a limit-neutral underlying vehicle), the possibility for the driver to excite sideslip becomes unnecessary. In addition, despite the fact that pure physics implies that turn-in of a near-neutrally balanced vehicle would only ever saturate the front axle, the literature (and manufacturers attempts to solve problems of handling with front-axle DYC) suggests that it is more common for drivers to get into trouble with saturation of the rear axle. The reason for this can only be that they tend to excite excessive transient slip in the rear axle, due to the fact that the vehicle behaves as an under-damped second order system.

In summary, such a design may be appropriate for a vehicle without any from of balance control (i.e. no DYC, active differentials or active warp control), but is clearly sub-optimal in terms of both ease of control and obstacle avoidance performance, since the critical metric (that is, damping in response to torque- or force-input) is strongly sub-optimal. In effect, in this vehicle design, the variation of the front tyre slip and force is the mechanism by which yaw damping is provided. Therefore, to control the vehicle, effectively, some "opposite-lock" (or at least opposite-force) is required.

Therefore, it is proposed that for vehicles with some form of limit balance control, the damping in response to front lateral force (or steering torque) inputs should be increased, by transient control of rear steering, DYC or active differentials.

10.4: Reduction of dynamics to first order

The dominant poles affecting yaw and sideslip motion are second order for a typical 2WS, uncontrolled (passive) vehicle in response to inputs at the front axle.

However, with the application of control (subject to the caveat of there being sufficient control authority available to meet the target) - even if the vehicle is linearly unstable, and regardless of tyre cornering stiffnesses - it has been shown in Chapters 4 and 5 that the response can be controlled to follow to an arbitrary, predefined response. Typically, either a first- [Koresawa, 1994] or second-order [Abe, 1999] response is proposed.

Since the possibilities for second and higher order responses are extremely wide ranging, and since optimisations conducted previously suggest a first-order response may be appropriate for controlled vehicles, this section analyses the advantages and disadvantages of various different first-order targets (i.e. alternative motion centre locations). Any change to second-order target will be considered a refinement of the fundamental first-order strategy.

As described previously, a first-order target implies a fixed motion centre. The motion centre location may be related to a_y and α_z, or to the applied forces, based upon the kinematics of turning:

$$a_y = \dot{V} + Ur$$

Since the motion centre location, d has been defined according to:

$$V + dr = 0$$

this may be differentiated to identify $\dot{V}$ in terms of d and $\dot{d}$:

$$\dot{V} + \dot{d}r + d\dot{r} = 0$$

where $\dot{r} = \alpha_z$.

Substituting this into the equation for basic kinematics of turning, we have:

$$a_y = Ur - (\dot{d}r + d\alpha_z)$$

or, for fixed motion centre (i.e. first-order motion in yaw),

$$a_y = Ur - d\alpha_z$$

such that the lateral acceleration must be linearly related to the yaw acceleration, according to a slope defined by d, and with an offset according to the current yaw rate of the vehicle, r (or more precisely, according to associated the steady-state lateral acceleration, $a_{y_{ss}} = Ur$, that must be generated in order to convert the current yaw rate into a ***steady-state*** cornering condition).

Zero sideslip

'Zero sideslip' (minimisation of sideslip, or sideslip rate at the centre of mass) is the specific target that is commonly found in the literature. The successful satisfaction of zero sideslip implies a fixed motion centre ***coincident with the centre of mass*** of the vehicle (except at low speed, where such a strategy can become inconvenient for maneuvering);

If force-optimality requires that response must 'snap' to the peak front force, it might be considered that this necessarily leads to a non-smooth discontinuous lateral acceleration time-history. However, this is not the case. In fact, the step to peak front force can be made with a simultaneous step to the same, equal and opposite rear tyre force, such that the lateral acceleration is initially zero. This is what occurs when the constraint of zero sideslip is imposed.

A 'fixed motion centre'

When a control strategy describes a fixed motion centre [Koresawa, 1994], care should be taken to identify whether the author implies a motion centre that is fixed (i) during the transient and/or (ii) with respect to changes in vehicle speed.

Koresawa [Koresawa, 1994] proposes that the motion centre be maintained at constant value at all times (i.e. irrespective of the vehicle speed, and during transient maneuvering). The net result of this is that the geometry of the vehicle path as viewed from overhead becomes invariant with the vehicle speed. In other words, the sideslip ***angle***, β at a given location along a fixed path is proportional to the path curvature, and unrelated to the vehicle speed.

Substituting the steady-state values:

$$r = U\rho$$
$$V = U\beta$$

then for speed-independent geometry of turning,

$$U(\beta + d_{PMC}\rho) = 0$$
$$\therefore \beta = -d_{PMC}\rho$$

Note: The popular target of zero sideslip may also be achieved simply by setting d to zero, such that the 'perceived motion centre' becomes the centre of mass and zero side-slip is achieved.

A motion centre that is fixed during transient maneuvering yields optimal responses that are first-order in both the yaw rate and the now nonzero sideslip (angle, or velocity). However, in contrast to zero sideslip, the ***lateral acceleration at the centre of mass is no longer exactly in phase with the yaw rate*** - in fact, the lateral acceleration could theoretically be discontinuous (which the yaw rate can never be), since it comprises a step input of some magnitude, followed by a first order time lag to the steady-state value.

However, critically, it can also be shown that the vehicle response (that is, the yaw rate, sideslip and even the load transfer) may remain ***first-order*** even if the initial lateral acceleration is ***nonzero*** (as for nonzero sideslip targets). This confirms that the desirable conditions presented above may be achieved for motion centres that are not at the vehicle centre of mass.

However, any motion centre that is not coincident with the mass centre clearly violates one of the reasons that zero sideslip has been proposed as the target - the fact that drivers supposedly are better able to control a vehicle if 'the lateral acceleration' responds exactly in phase with the yaw rate. However, if the lateral acceleration were measured (or 'sensed' by a driver) at ***that*** position instead of at the centre of mass, then it is found that this is indeed in phase with the yaw rate.

As mentioned in the literature survey, it is hypothesised that it is actually the lateral acceleration somewhere near the driver's location that the driver is sensitive to, such that then locating the driver and motion centre close together, rather than locating the motion centre at the centre of mass, might be what is required for easy control - ***if*** (though this is certainly unproven, and strongly doubted by the author), the driver was expressing a preference for the yaw-plane ***kinematics*** of zero side-slip motion.

It has been shown that for a fixed motion centre location, the relationship between the lateral and yaw accelerations must be:

$$a_y = Ur - d\alpha_z$$

If this line of constraint is overlaid on the handling envelope of the vehicle, it can be seen how the combination of lateral and yaw acceleration must be chosen in order to satisfy the maintenance of a fixed motion centre. On the following diagrams, these lines may be overlaid according to possible values of the current yaw rate, r, or 'steady-state lateral acceleration', $a_{y_{ss}} = Ur$, which is be the lateral acceleration that would be maintained as the steady-state if the $\alpha_z = 0$ (i.e. maintain-steady-state) point were selected. In other words, $a_y = a_{y_{ss}} = Ur$ at the intersection of the ***line of constant motion centre*** and the horizontal (a_y) axis.

It should be noted that the asymptotic slopes of the constraint line, for the most forward ($d_{PMC} = \infty$) and the most rearward ($d_{PMC} = -\infty$) motion centres both have the same (zero) slope. For this limiting value of the motion centre, the vehicle delivers pure sideslip and no yaw motion. Whilst such a value may be seen briefly during a transient (provided the vehicle response is higher than first order), it is clearly impractical for a consistent motion centre target.

However, it can also be seen that certain motion centre locations are not force-optimal for some AWS vehicles, since they require that the vehicle have a certain ***minimum level of limit-under-steer*** if the initial motion centre is to lie both (i) inside the envelope and (ii) on the line of maximum front tyre force (required for optimal obstacle avoidance). For instance, if the ay-az trajectories required for ***zero sideslip*** are overlaid onto the envelope of the ***neutral-steer*** vehicle, and the lateral acceleration demand is stepped between zero and the limiting lateral accelerations, a trajectory of the form shown in figure 10.1 is traced.

In other words, for this vehicle, whilst the steady-state value of the demand could be satisfied, ***the transient demand could not.*** Alternatively, if the vehicle exhibited sufficient under-steer that the trajectories remained within the envelope, the trajectory traced is that shown in figure 10.2.

Clearly, for this particular (very strongly limit-under-steering) vehicle, such a trajectory ***is*** force-optimal (although there may be others which are also force-optimal). However, it is well known (and discussed previously) that excessive limit under-steer impairs the steady-state lateral acceleration performance of the vehicle. Therefore, motion centres such as this, which demand significant limit under-steer in order that they do not saturate the tyres during transients, must be considered sub-optimal.

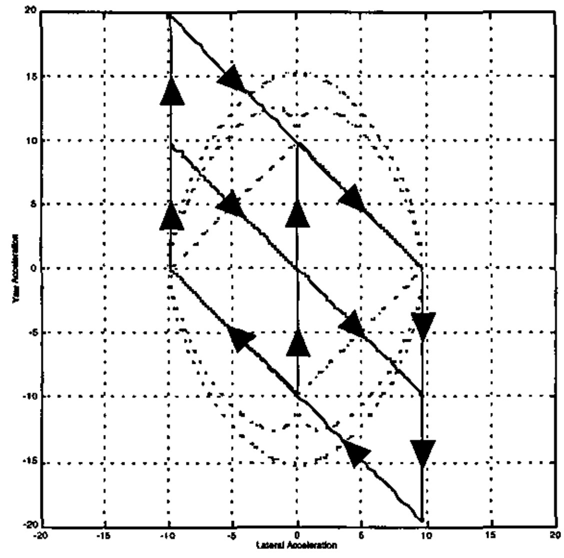

Figure 10.1
solid line = lateral-yaw acceleration trajectory
for constant motion centre at $d = 0$ (zero sideslip);
dotted line = envelope of NS vehicle

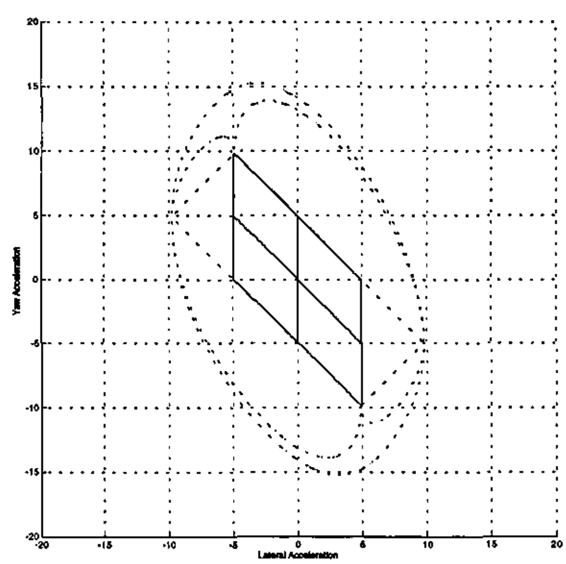

Figure 10.2
solid line = lateral-yaw acceleration trajectories
for constant motion centre at $d = 0$ (zero sideslip);
dotted line = envelope the 'compatible' US vehicle

This is consistent with the findings from Linear Programming analyses presented in Chapter 6, that 4WS or AWS vehicles conformed to the defined criteria for optimal handling onloy if they had sufficiently ***rearward*** motion centres $d < d_{crit}$, such that they allowed maximisation of the front axle lateral force $F_{y_f}(t) = \hat{F}_{y_f}$ and thus exhibited the same lateral acceleration delay t_{lag} behaviour as 2WS vehicles, with t_{lag} being invariant with sideslip control (i.e. rear tyre force control, or motion centre location). However, for $d > d_{crit}$, the front force input became sub-optimal $\left(F_{y_f}(t) \neq \hat{F}_{y_f}\right)$ and thus the response was subject to an increase in the time-delay, with the compromise of front lateral force, and hence the time delay worsening as d became larger.

Derivation of d_{crit}

It can be seen that the most forward motion centre that is acceptable (in the sense of optimal friction-usage) for a vehicle with a given level of under-steer is that which places the initial lateral and yaw accelerations at the vertex of the envelope where $F_{y_f} = \hat{F}_{y_f}$ and $F_{y_r} = -\hat{F}_{y_r}$, i.e. the point of ***maximum yaw moment*** generation for that vehicle. At the instant of turn-in, the yaw rate $r = 0$ and thus from the kinematic relation $a_y = Ur - d\alpha_z$ that was previously identified for a fixed motion centre location, we have :

$$a_y = -d\alpha_z$$

thus, for maximum (positive) yaw moment and a fixed motion centre at the critical location where $d = d_{crit}$, we have:

$$\frac{\hat{F}_{y_f} - \hat{F}_{y_r}}{M} = -d_{crit}\frac{b\hat{F}_{y_f} + c\hat{F}_{y_r}}{Mk^2}$$

thus the relationship between acceptable motion centre position and the vehicle limit balance is the following:

$$d_{crit} = -\frac{\hat{F}_{y_f} - \hat{F}_{y_r}}{b\hat{F}_{y_f} + c\hat{F}_{y_r}}k^2 = -\frac{k^2}{b}\frac{\left(1 - \dfrac{\hat{F}_{y_r}}{\hat{F}_{y_f}}\right)}{\left(1 + \dfrac{c}{b}\dfrac{\hat{F}_{y_r}}{\hat{F}_{y_f}}\right)}$$

Note: These occurrences of transient saturation of the rear tyres may be a less significant problem if the driver's inputs are slow, if the driver doesn't driver at the limit, if the vehicle has some form of DYC or active differentials (see the larger envelope of the DYC vehicle in figure 7.1, which almost accommodates the worst-case transient associated with the zero-sideslip constraint). So for such vehicles or drivers, or vehicles which must be strongly under-steering for some other reason, it may be acceptable to allow a more forward motion centre.

A Motion Centre Fixed At $d = -\frac{k^2}{b}$?

It was shown in Chapter 9 that the slope of the top left and bottom right edges of the envelope is always equal to:

$$\frac{d\alpha_z}{da_y} = \frac{b}{k^2}$$

For fixed motion centre we have a relationship of $a_y = -d\alpha_z$ for the initial response when $r = 0$, such that initially, $\frac{d\alpha_z}{da_y} = -\frac{1}{d}$.

Therefore, if it were desired that the initial a_y-α_z trajectory step in parallel with this top left edge of the diagram - thus generating the maximum yaw moment that could never saturate the rear tyres due to transient excitation - then a motion centre at the location

$$d = -\frac{k^2}{b}$$

would be required. The a_y-α_z trajectory for such a motion centre is shown in figure 10.3.

It is clear that for all limit-steer conditions, this target (targeting which precisely does not require a knowledge of the available friction; only of the centre of percussion of the vehicle with respect to front tyre forces) yields a response that is ***force-optimal for all vehicles, in both the transient and steady-state conditions.***

It can be observed that this condition is achieved when the initial value of F_{y_r} (and thus also the rear steer angle, δ_r) during a step input is zero, and that the motion centre is equal to the centre of percussion of a standard 2WS (front-steer-only) vehicle. This is the reason why, when, for instance, the lateral acceleration demand is suddenly reduced from the limiting lateral acceleration, the rear tyres are not suddenly subject to very large force demands - although the front steer angle is immediately reduced, in fact, the initial ***rear*** steer angle remains the same, and with the reduction of the front lateral force, the rear tyre force progressively diminishes to the new steady-state value.

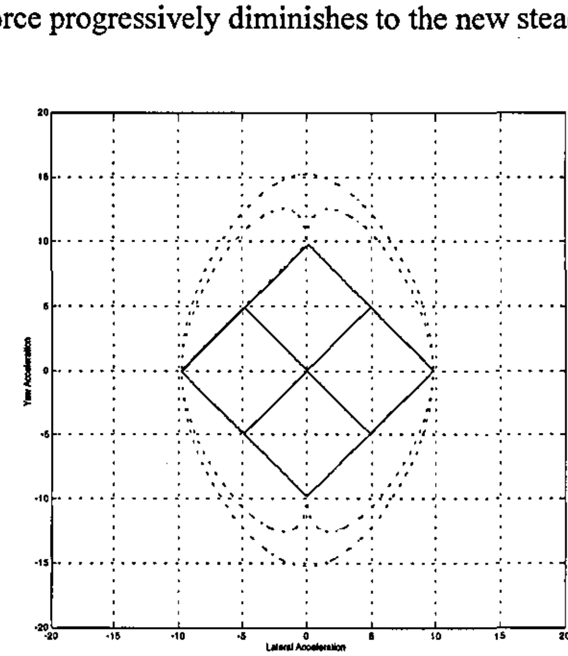

Figure 10.3
solid line = lateral and yaw acceleration trajectories
for constant motion centre at $d = -\frac{k^2}{b}$
dotted line = envelope of a limit NS vehicle

However, there is apparently a downside to this choice of motion centre. For a vehicle that is limit-over-steer, the lateral acceleration rises higher during the transient but then falls to a lower value in the steady-state. This is ***perhaps*** an undesirable characteristic, since the response during the transient may mislead the driver into estimating that there is more friction available than is truly the case (and since the transient begins by applying only front lateral force, the steady-state limit is completely unknown). Whether or not this is truly a problem remains a matter for further research. However, if DYC by brake or active differential were employed to increase the limit performance of OS vehicles, this problem would be avoided (see the shape of the envelopes for vehicles with DYC, in Chapter 6).

Confirmation of transient behaviour

In figure 10.4, the time-history of the rear lateral axle force is shown for the two motion centre locations discussed above, for an emergency maneuver where the front lateral tyre force is suddenly maximised, then suddenly reversed.

The intention is to show the difference in the transient rear tyre force usage, between the 2WS, zero side-slip and the 'optimised motion centre' (OMC) case, where

$$d = -\frac{k^2}{b}$$

Once again, the response is plotted for a 'perfectly controlled' vehicle, where the necessary forces to satisfy the target are assumed to be delivered by the controller at exactly the correct time, in order to remove any possible controller influences.

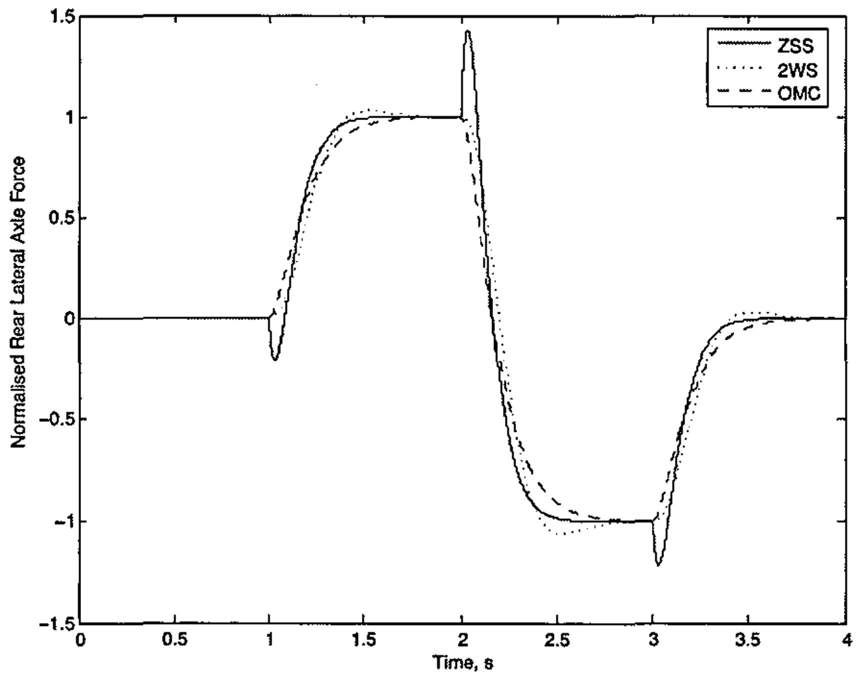

Figure 10.4
Normalised lateral rear axle force time-histories
for baseline (2WS)
and two alternative motion centres for AWS (ZSS, $d = 0$ and OMC, $d = -\frac{k^2}{b}$)

$$\left(M = 1000, I_{zz} = 1350, b = 1.35, c = 1.35, U = 20, C_{\alpha_r} = 100000\right)$$

It can be seen from the plot that the behaviour for the 2WS and OMC cases is not dissimilar (though a fixed motion centre such as the OMC case provides a first-order vehicle yaw response). The zero side-slip case, however, clearly demands a significantly greater lateral force from the rear axle, and extremely high rates of change of those tyre forces, which places a much greater demand on the rear steering system.

10.5: Concluding Remarks

It has been shown that certain reference state trajectories, such as the first-order response, with a fixed motion centre at:

$$d = -\frac{k^2}{b})$$

allows the optimal turn-in performance identified in the previous chapter, ***and*** remains a reasonable and achievable target ***regardless*** of the limit balance, such that a controller does not require information about the current balance of the vehicle in order to determine a reference trajectory to follow for a given change in lateral acceleration demand. In this case, friction identification may be unnecessary, and a consistent handling response could be delivered to the driver regardless of the road surface or limit balance of the vehicle.

Conversely, it has also been shown that the commonly adopted target of zero sideslip does not meet this criterion, and makes very large demands of the rear tyre forces, such that a significant margin of ***limit under-steer is required*** if a vehicle is to be successfully controlled to a zero sideslip target in situations where a significant portion of the available friction is being utilised and the driver applies rapidly changing inputs.

Motion centre targets ahead of the centre of mass ($d > 0$, such as the steady-state motion centre of a typical 2WS vehicle at high speed) require an even greater margin of under-steer if they are to be maintained, such that care must be taken when designing a controller that attempts to maintain a first-order response (fixed motion centre) and employs the steady-state behaviour of the passive vehicle as its reference.

Where such a target is attempted by a vehicle with control provided by DYC by braking, the expanded envelope of the vehicle (compared with the pure AWS) is such that maintaining such a motion centre could be possible, provided there is a short time lag in the demand. When a fixed motion centre target is enforced, the vehicle would sometimes be forced to employ DYC to deliver a faster response than would be achievable by the passive vehicle, at the expense of the dissipation of some energy by the brakes. Vehicles with DYC provided by active differentials would be able to track the motion centre on turn-out, but would be subject to the same problems as steered vehicles on turn-in.

However, if the vehicle were purely AWS, then without sufficient limit-under-steer, it would be *impossible* for the controller to track the reference. The conclusion of the author, therefore, is that motion centre targets ahead of the centre of percussion of the front axle, i.e.

$$d > -\frac{k^2}{b}$$

(which is always true for zero side-slip) either (i) cannot be maintained at all times, or (ii) place excessive demands on the limit balance of the vehicle, such that the limit cornering performance is compromised, or (iii) introduce very long delays into the transient response of the vehicle, with the delay increasing as the vehicle was driven at increasing lateral acceleration. Interestingly, for the notionally optimal, limit-neutral-steering AWS vehicle cornering at the limiting steady-state lateral acceleration, if this motion centre is rigidly enforced by the controller, than it would be ***impossible*** for the vehicle to ever reduce its lateral acceleration! Clearly controllers prioritising such a motion centre target would have a tendency to 'trap' vehicles at high lateral accelerations.

Conversely, the alternative motion centre at the centre of percussion of the front axle (yielding nose-out sideslip in all circumstances) is able to be tracked regardless of the limit balance of the vehicle, and without compromising the ability of the vehicle to generate an optimal turn-in performance. For vehicles with rear steering control, therefore, this is proposed as a more appropriate sideslip target. Interestingly, it is also the ***initial*** motion centre location of any passive, 2WS vehicle.

For vehicles without rear steering control - for instance, with DYC only (whose envelopes were not studied here), it is anticipated that this would not be an appropriate target, since it would reduce the lateral force generation of the rear tyres even more than the zero sideslip target which was shown to be sub-optimal for such a vehicle by Abe and Wang. If a motion centre that is fixed in the transient is desired for those vehicles, then the value which must be selected is the expected steady-state value, such that no DYC control is applied in the steady-state until the rear tyres begin to saturate.

Chapter 11
Synthesis and Conclusions

In Chapter 1, it was observed that zero sideslip is widely targeted in the literature, and the reasons given are usually either (i) to ensure a good lane-change performance and human subjective rating, and (ii) to ensure that sideslip does not induce a change in the stability as the lateral acceleration increases. However, it was not clear if the reason for zero sideslip leading to good lane-change performances was simply the elimination of the increasing destabilising moment or some human preference for zero sideslip kinematic motion. However, it is simple to show that if the motion centre of the vehicle is able to be controlled to any arbitrary location, then it is impossible for the driver to sense the location of the centre of mass from the motion of the vehicle, such that the latter possibility can be ruled out. Other authors suggest that minimisation of the sideslip at the driver gives the vehicle a neutral feel. It was also shown that it is possible to form a quadratic cost function to minimise sideslip ***rate*** at any arbitrary location along the vehicle x axis, and that this potentially removes the need for sideslip estimation, even if nonzero sideslip is desired. However, it is not known whether it is the low frequency or the high frequency sideslip motion (or both) must be removed in order to ensure good human control performance. It was also shown (see Chapter 3) that a ***consistent*** sideslip-induced destabilisation with lateral acceleration requires a motion centre located a distance from the centre of mass that is proportional to the square of the vehicle speed. It was also shown that a simple mechanical 4WS system that tracks zero sideslip at low lateral acceleration is able to provide this speed-consistency (if not lateral acceleration-consistency) of vehicle balance.

It was seen in Chapter 1 that rear steering control is required if any significant change in steady-state sideslip angle (compared with the natural sideslip of the vehicle) is required, since the use of DYC to generate a continuous opposing moment is extremely inefficient (in both friction utilisation and energy). However, it was also seen that many authors found difficultly in implementing successful rear steering control. Feed-forward systems were shown to perform poorly in the non-linear regions, and feedback strategies were frequently shown to worsen the vehicle stability in critical conditions. Other authors did report success when modern control techniques were applied but so far there appears to be insufficient evidence to be confident that robust and effective steering control (and thus precise sideslip angle control) is feasible. The trend in the literature appears to be away from zero sideslip by steering control, towards model following (i.e. near-natural sideslip angle) by DYC instead. In other words, the trend appears to be towards the use of brake actuation, rather than sideslip, to control stability.

In Chapter 3, the effect of sideslip on the steady-state lateral acceleration performance of vehicles (through the changes in the tyre locations relative to the path) was studied, and the increase of destabilising yaw moment with increasing 'tail-out' sideslip that was mentioned in the literature - was confirmed. It was shown that tail-out sideslip increases the destabilising yaw moment at the limit due to (i) the effect of the acceleration vector direction on tyre loading and further (ii) due to lateral load transfer and the heavily loaded tyres moving forwards. This suggests that the natural tail-out sideslip of 2WS vehicles might provide some benefit for excessively stable, limit under-steering vehicles.

Additionally, it was shown that nonzero sideslip could improve performance in split-mu braking, but that the sideslip angle adjustment would require either friction sensing or a brief sacrifice of deceleration in order to correct sideslip during the transient. It was also shown that nonzero sideslip could improve acceleration or braking in a turn, even for a vehicle with the centre of mass located exactly mid-wheelbase. However, the optimal sideslip angle was shown to be opposite sense in acceleration than in braking.

In Chapter 4, energy-efficiency was considered, and it was shown that for a typical passenger vehicle, there is little change in the instantaneous efficiency as sideslip angle is varied, provided the controls are optimised. At high speed, aerodynamic effects dominated the energy dissipation, and a small nonzero sideslip angle was shown to be optimally efficient in turning, since the sideslip generally leads to an additional lateral force which reduces the demands on the tyres .

The same constrained optimisation that identified the optimal controls for steady-state was used to identify the shape of the contours of constant power dissipation against lateral and yaw acceleration. It was shown that these contours are approximately elliptical in shape, regardless of the available controls. It was also demonstrated that the DYC brake control was never used while the tyre model remained linear - only when reaching vehicle limit when the tyre became highly saturated. It was therefore concluded that in the linear regime of the vehicle, and under the above assumptions, maneuvering should be controlled by steering forces alone, and an analytical expression was derived for the power dissipation in the tyres of an AWS vehicle, as the lateral and yaw acceleration were varied. This showed clearly that the contours scale with the zeroth and second moment cornering stiffnesses C_0 and C_2 and are skewed by the linear stability (under-steer/over-steer) term C_1.

In Chapters 5 and 6, transients were considered in more detail, by identifying the friction requirements for tracking a certain sideslip. The analysis was first conducted in the frequency domain, and then (by Inverse Fourier Transform) in the time domain, and this showed that certain sideslip constraints require very high tyre forces at high frequency. Chapter 6 showed that these high forces are also predicted in time domain analyses, leading to an inefficient (or perhaps infeasible) target trajectory unless the demands on the vehicle (i) are small compared with the available friction, and (ii) are applied slowly (in truth, slowly compared with k^2/cU). It was also shown that the zero sideslip strategy leads to the greatest yawing motion (angle, rate and acceleration) of the vehicle during sinusoidal path following, with either a forward or rearward shift in motion centre reducing the yaw motion equally.

In Chapter 7, Linear Programming was used to identify the optimal time-variation of the controls for the limiting transient maneuver within the hard constraints enforced by the available friction. It was shown that for a limit under-steering vehicle, the optimal control input is an immediate step to the maximum front lateral force, and that for many vehicles, the minimum lateral acceleration delay that is induced by the need to delay the rear tyre forces in order to control yaw motion was completely insensitive to the sideslip control. The conclusion from this is that some freedom in sideslip control is available even if optimal obstacle avoidance performance is required. However, it was also shown that certain sideslip responses (e.g. 2WS with very low yaw damping, or zero sideslip) can lead to violation of the rear tyre force constraints at some point during the transient, and that this in turn means that the front lateral force must be reduced, directly extending the response time delay. It was also noted that the lateral acceleration time-history of points near the front of the vehicle was highly insensitive to changes in the rear tyre force control.

In Chapter 8, armed with knowledge of the form of the optimal control input, the minimum lateral acceleration time delay was calculated analytically. It was shown that for the limit under-steering vehicle, the delay depends only on geometry and inertia. Conversely, it was shown that increasing the levels of limit over-steer reduces the time delay, and that any delay to the front force application (e.g. due to actuator lags or a need for opposite-lock introduced by the dynamics) directly increases the time delay, equivalent to delaying the input. Additionally, the fact that the lateral acceleration, velocity and displacement of the ***front*** of the vehicle was highly insensitive to the rear force was shown to be due to the centre of percussion for rear lateral forces being located very near the front of the vehicle, such that rear lateral forces cause typical vehicles to approximately rotate about the front end. The conclusion from this is that the path followed by the front of the vehicle (and thus the obstacle avoidance performance) is primarily governed by the applied ***front*** lateral force (including whether it must be compromised in order to control the yaw motion).

In Chapter 9, the shapes of transient handling envelopes were computed from some simple vehicle dynamics models, such that further insight could be gained into why certain (forward) motion centres caused a need for the front tyre force to be compromised during the transient. Newton-Raphson iteration was used to identify the roots of the derivative of yaw moment and thus the optimal force directions (i.e. lateral-longitudinal sharing of the friction) for maximum performance when DYC was available. It was noted that the envelopes of the vehicle with DYC match very closely the elliptical shape of the constant power contours plotted earlier, provided the limit balance of the vehicle approximately matches the linear balance. Therefore, it was concluded that it would be possible to determine a transient response that was energy-efficient in the linear regime, and also friction-efficient near the limit, by employing DYC in critical conditions.

In Chapter 10, the trajectories followed by the vehicle in tracking a particular motion centre and stepping from one limiting lateral acceleration to the other were identified. From the shape of the envelope, the critical motion centre location, forward of which friction-optimal turn-in is compromised - was identified. Also, a further possible area of breach of the AWS envelope by some motion centres was identified - when the steer angle is ***reduced*** from the limit. For any strategy which has an initial motion centre ahead of the centre of percussion for front lateral forces, such a steer reduction was shown to demand an ***increase*** in rear lateral tyre forces. When the vehicle is near the limit, this may be infeasible.

At this point it is necessary to consider these results in the context of everyday driving. It is unlikely that such peaks in transient tyre forces would be observed during normal driving, since the frequency of steering inputs is usually very low. In these situations, the improved consistency of balance provided by zero side-slip four-wheel-steering may be more important than a minor increase in transient demand. However, in emergency obstacle avoidance conditions, the ability of the vehicle to respond to the drivers demands without saturating the rear tyres may be more important.

The three major conclusions of the work are the following:

1. The target of zero side-slip has been adopted many times in the literature. However, it was shown in this work that zero side-slip cannot be preferred by the driver for purely kinematic reasons, since zero side-slip at the CG implies non-zero sideslip elsewhere along the longitudinal axis of the vehicle, and a human driver would be not be able to sense the CG location in order to specifically prefer zero side-slip at this location. However, the change in the plan-view geometry that occurs with any increase in tail-out sideslip directly leads to a change in the vehicle stability, due to an immediate increase in the turn-in moment, if the same tyre slip angles and thus lateral forces are maintained. This builds on the results of Shibahata who concluded that increasing sideslip leads to a reduction in stability due to its direct influence on rear tyre saturation if no steering correction is made, and this provides further motivation for targeting zero side-slip in steady-state.

2. It was also shown that a very simple AWS system that steers both axles to provide zero side-slip at low speed can lead to some benefits in limit conditions, since it eliminates the speed-dependence of the vehicle sideslip and stability that is inherent in 2WS configurations. This would allow the vehicle dynamicist to control the vehicle stability consistently throught the speed range, using the well understood mechanisms of compliance-steer/camber, roll-steer/camber and lateral load transfer distribution, each of which provides some control on handling stability that is directly related to steady-state lateral acceleration.

3. Tracking zero side-slip in transients leads to over-working of the rear tyres in transients. For transient conditions, a better choice of motion centre is the centre of percussion of the vehicle with respect to lateral forces applied at the front axle. This choice of motion centre completely eradicates the peaks in tyre force demand that otherwise occur during sudden transients, and should therefore ease the task of the

controller. Such a MC simultaneously also provides equal obstacle avoidance capability (since this was shown analytically to be independent of rear steering) and it has the additional benefit of improving the smoothness of lateral load transfer, by having the vehicle generate more lateral acceleration earlier in the transient. This result, when combined with point 1 above, suggests that a first-order response may not be the ideal target - an initial motion centre at the above-mentioned centre of percussion is preferred, but a steady-state motion centre at zero is desired for consistent stability. Since a first order response necessitates a fixed motion centre, a second or higher order yaw response is required if both of these targets are to be satisfied.

Glossary

Nomenclature

- An uppercase, ***left superscript*** indicates the coordinate system in which the quantity is expressed (i.e. vehicle, V, wheel, W, aerodynamic, A or path, P)
- An ***uppercase final subscript*** (e.g. PP in $F_{x_{PP}}$ or $\underline{F}_{PP}$) indicates that the quantity refers to an individual wheel or tyre (i.e. FL, FR, RL or RR)
- A ***lowercase final subscript*** (e.g. p in w_p) indicates that the quantity refers to a particular axle or differential
- An ***underline*** (i.e. $\underline{a}$ rather than a) indicates a vector quantity.
- A double ***underline*** (e.g. $\underline{\underline{a}}$) indicates a matrix quantity.
- A ***dot*** indicates a derivative with respect to time (i.e. $\dot{U} = \frac{dU}{dt}$).
- A ***hat*** indicates the maximum available value of the quantity when constraints are imposed (e.g. $\hat{F}_x$ typically indicates the maximum value of F_x that is available when limitations on the available friction are considered).
- A superscript ***star*** indicates discrete-time (i.e. sampling of a signal) when applied to a time-domain signal (e.g. $g^*(t)$) and indicates a complex amplitude when applied to a frequency-domain signal (e.g. $G(\omega)$).

Symbols

- $\underline{a}$ is the acceleration vector of the vehicle centre of mass
- a_q is the acceleration of the vehicle centre of mass in the q coordinate direction (i.e. x, y or z).
- b is the magnitude of the distance from the centre of gravity to the front axle of the vehicle (always positive).
- c is the magnitude of the distance from the centre of gravity to the rear axle of the vehicle (always positive), unless used as a subscript where it indicates a quantity which refers to the *centre* differential of the vehicle.
- d is the scalar distance in vehicle x from the centre of mass to the motion centre (MC), the point on the vehicle where the lateral velocity, $V + dr = 0$.
- f is the frequency in Hz (cycles per second), unless used as a subscript where it indicates a quantity which refers to the *front* axle of the vehicle.
- $F\{g^*(t)\}$ is the Discrete Fourier Transform $G(\omega)$ of the distrete-time (i.e. sampled) signal $g^*(t)$
- $F^{-1}\{G(\omega)\}$ is the Inverse Discrete Fourier Transform $g^*(t)$ of the complex spectrum $G(\omega)$
- F_{q_p} is the scalar magnitude of the force applied to the vehicle, in the q coordinate direction (i.e. x, y or z), by axle p (e.g. f or r).

- $F_{q_{PP}}$ is the scalar magnitude of the force applied to the vehicle, in the q coordinate direction (i.e. x, y or z), by the PP tyre (e.g. FL, FR, RL, RR).
- $\underline{F}_{PP}$ is the force vector applied to the vehicle by the PP tyre (e.g. FL, FR, RL, RR).
- $\underline{H}$ is the angular momentum vector of the vehicle
- l_f, l_r are the relaxation lengths of the front and rear tyres
- $L\{g(t)\}$ is the Laplace transform $G(s)$ of $g(t)$
- $\underline{L}$ is the linear momentum vector of the vehicle
- M is the total mass of the vehicle (sprung plus unsprung)
- M_{z_p} is the ***total*** direct yaw control (DYC) moment applied to the vehicle by axle p.
- $p_f, p_r(\omega)$ are the proportions of the steady-state lateral axle forces that are required to generate a sinusoidal lateral acceleration of the same magnitude at the angular freqeuncy ω
- t_{lag} is the net delay to the lateral acceleration of the vehicle when the demand is a step from straight-line driving to the limiting lateral acceleration.
- r is the yaw rate of the vehicle, unless used as a subscript where it indicates a quantity which refers to the *rear* axle of the vehicle.
- U is the forward velocity of the centre of mass (i.e. the speed of the vehicle)
- $v_y(x)$ is the lateral velocity at a distance x from the centre of mass
- v_f, v_r are the lateral velocities at the front and rear axles
- V is the sideslip velocity of the centre of mass
- $\underline{V} = \begin{bmatrix} U \\ V \\ W \end{bmatrix}$ is the velocity vector of the centre of mass
- α (e.g. α_f, α_r, α_{FL}) is the slip angle of the tyre (where $\tan(\alpha) = \frac{{}^W V}{{}^W U}$)
- α_z is the yaw angular acceleration. $\alpha_z = \dot{r}$.
- β is the sideslip angle of the vehicle (where $\tan(\beta) = \frac{{}^V V}{{}^V U}$).
- δ is the steer angle (the yaw angle of the wheel relative to the body)
- $\omega = 2\pi f$ is the angular frequency, in radians per second
- $\underline{\omega} = \begin{bmatrix} p \\ q \\ r \end{bmatrix}$ is the angular velocity vector of the centre of mass (in roll, pitch and yaw)

References

Abe, M. (1989). Handling Characteristics of Four Wheel Active Steering Vehicles over Full Maneuvering Range of Lateral and Longitudinal Accelerations. 11th IAVSD-Symposium, Kingston, Ontario, Swets & Zeitlinger.

Abe, M. (1999). "Vehicle dynamics and control for improving handling and active safety: from four-wheel steering to direct yaw moment control." Proceedings of the Institution of Mechanical Engineers **213 (Part K)**: 87-101.

Abe, M., Y. Kano, et al. (1999). Improvement of vehicle handling safety with vehicle sideslip control by direct yaw moment. International Association for Vehicle System Dynamics; Symposium, Pretoria, Swets & Zeitlinger.

Abe, M., N. Ohkubo, et al. (1996). "A Direct Yaw Moment Control for Improving Limit Performance of Vehicle Handling - Comparison and Cooperation with 4WS -." Vehicle System Dynamics Supplement (The Dynamics of Vehicles on Roads and on Tracks) **25**: 3-23.

Ahring, E. and M. Mitschke (1995). "Comparison of All-Wheel Steerings in the System Driver-Vehicle." Vehicle System Dynamics **24**: 283-298.

Allen, R. W., T. T. Myers, et al. (1993). "Vehicle Stability Considerations with Automatic and Four Wheel Steering Systems." SAE Transactions **102**(6): 2191.

Bakker, E., L. Nyborg, et al. (1987). "Tyre Modelling for User in Vehicle Dynamics Studies." SAE.

Bernard, J. E. and C. L. Clover (1996). "Tire Modeling for Low-Speed and High-Speed Calculations." Sae Transactions **104**(6, Pt1): 474-483.

Best, M. C. and T. J. Gordon (1998). Real-Time State Estimation of Vehicle Handling Dynamics Using an Adaptive Kalman Filter. AVEC '98, Nagoya, Japan.

Best, M. C., T. J. Gordon, et al. (2000). "An Extended Adaptive Kalman Filter for Real-time State Estimation of Vehicle Handling Dynamics." Vehicle System Dynamics **34**: 57-75.

Blaauw, G. J., H. Godthelp, et al. (1984). "Optimal Control Model Applications and Field Measurements with Respect to Car Driving." Vehicle System Dynamics **13**: 93-111.

Blank, M. and D. L. Margolis (2000). "Minimizing the Path Radius of Curvature for Collision Avoidance." Vehicle System Dynamics **33**: 183-201.

Cann, B. E., R. B. Hathaway, et al. (1995). "Critical Suspension Relationships and Their Influence on Transient Behavior of Performance Vehicles." SAE: 1880-1887.

Charek, L. T. and J. C. Huston (1984). "A New Dual Hitch Trailer Concept for Improved Stability and Reverse Maneuverability." SAE.

Crolla, D. (1996). An Introduction to Vehicle Dynamics.

Den Hartog, J. P. (1984). Mechanical Vibrations. New York, Dover.

Dixon, J. C. (1995). Tires, Suspension and Handling. Warrendale, PA, SAE International.

Dreyer, A. and H. D. Heitzer (1992). "Control Strategies for Active Chassis Systems with Respect to Road Friction." SAE Transactions **100**(6): 872.

Franklin, G. F., J. D. Powell, et al. (1988). Digital Control of Dynamic Systems, Addison-Wesley.

Frey, M., R. Gnadler, et al. (1995). "Examination of power loss at passenger car tyres." VDI Berichte **1224**: 101-129.

Fujioka, T. and K. Goda (1996). "Discrete Brush Tire Model for Calculating Tire Forces with Large Camber Angle." Vehicle System Dynamics **25**: 200-216.

Fukada, Y. (1998). Estimation of Vehicle Slip-angle with Combination Method of Model Observer and Direct Integration. AVEC '98, Nagoya, Japan, Society of Automotive Engineers of Japan.

Furukawa, Y. and M. Abe (1998). "Advanced Chassis Control Systems for Vehicle Handling and Active Safety." Vehicle System Dynamics **28**: 59-86.

Gadola, M., D. Vetturi, et al. (1996). "A Tool for lap Time Simulation." SAE: 153-157.

Gillespie, T. D. (1992). Fundamentals of vehicle dynamics. Warrendale, PA, Society of Automotive Engineers.

Gordon, T. J. and M. C. Best (1998). Stability Augmentation of Handling Dynamics for Uncertain Road Friction. 4th International Symposium on Advanced Vehicle Control 1998, Nagoya Congress Center, Nagoya Japan.

Hac, A. (2002). "Influence of Active Chassis Systems on Vehicle Propensity to Maneuver-Induced Rollovers." SAE.

Harty, D. (2003). "Brand-By-Wire: A Possibility?" SAE.

Hendrikx, J. P. M., T. J. J. Meijlink, et al. (1996). "Application of Optimal Control Theory to Inverse Simulation of Car Handling." Vehicle System Dynamics **26**: 449-461.

Higuchi, A. and H. B. Pacejka (1996). The Relaxation Length Concept at Large Wheel Slip and Camber. Tyre Models for Vehicle Dynamic Analysis. F. Boehm and H. P. Willumeit, Swets & Zeitlinger Bv. **27**: 50-64.

Higuchi, A. and Y. Saito (1992). Optimal Control of Four Wheel Steering Vehicle. AVEC '92.

Hirschberg, W. (1993). Tyre Force Computation Module DTIRE. 1st International Colloquium on Tyre Models for Vehicle Dynamics Analysis. H. B. Pacejka, Swets & Zeitlinger Bv. **21**: 167.

Horiuchi, S., K. Okada, et al. (1999). Effects of integrated control of active four wheel steering and individual wheel torque on vehicle handling and stability - A comparison of alternative control strategies. International Association for Vehicle System Dynamics; Symposium, Pretoria, Swets & Zeitlinger.

Huston, J. C. and D. B. Johnson (1979). "Relative Significance of Parameters Affecting Lateral Stability of Articulated Recreational Vehicles." SAE: 31-39.

Inagaki, S. (1994). Analysis in vehicle stability in critical cornering using phase-plane method. AVEC 94, Tsukuba.

Jun, C. (1998). "The Study of ABS control system with different control methods." AVEC '98: 623-628.

Kaminaga, M. and N. Genpei (1998). Vehicle Body Slip Angle Estimation Using an Adaptive Observer. AVEC '98, Nagoya, Japan, Society of Automotive Engineers of Japan.

Karnopp, D. (1991). "On Inverse Equations for Vehicle Dynamics." Vehicle System Dynamics **20**(6): 371-379.

Komatsu, A., T. J. Gordon, et al. (2000). 4WS Control of Handling Dynamics Using a Linear Optimal Reference Model. International symposium on advanced vehicle control; AVEC '2000, Ann Arbor, MI, University of Michigan.

Koresawa (1994). "Study on a Four Wheel Steering Vehicle Driven at an Objective Side Slip Angle." JSAE Review **15**: 45-51.

Leffler, H. (1995). "The Brake System of the New 7 Series BMW with Electronic Brake and Wheel Slip Control." SAE: 1482-1496.

Leffler, H. (1996). "Electronic Brake Management EBM - Prospects of an Integration of Brake System and Driving Stability Control." SAE: 1250-1262.

Legouis, T., A. Laneville, et al. (1987). "Vehicle/Pilot System Analysis: A New Approach Using Optimal Control With Delay." Vehicle System Dynamics **16**: 279-295.

Lin, Y. (1992). "Improving Vehicle Handling Performance by a Closed-Loop 4WS Driving Controller." SAE: 1447-1457.

MacAdam, C. C. and G. E. Johnson (1996). "Application of Elementary Neural Networks and Preview Sensors for Representing Driver Steering Control Behaviour." Vehicle System Dynamics **25**: 3-30.

Matsuo, Y., A. Okada, et al. (1993). "Intelligent Four-Wheel-Drive System." SAE: 1038-1045.

Milliken, W. F. and D. L. Milliken (1995). Race Car Vehicle Dynamics. Warrendale, PA, SAE International.

Nagai, M. (1989). Active Four-Wheel-Steering by Model Following Control. 11th IAVSD-Symposium, Kingston, Ontario, Swets & Zeitlinger.

Noronha, P. F. (1999). "A Robust Lumped-Parameter Tire Model Developed for Real-

Time Simulation." SAE Transactions **107**(6): 473-482.

Ono, E., S. Hosoe, et al. (1998). Theoretical Approach for Improving the Vehicle Robust Stability and Maneuverability by Active Front Wheel Steering Control. The Dynamics of Vehicles on Roads and on Tracks. L. Palkovics, Swets & Zeitlinger Bv. **29:** 748-753.

Palkovics, L., M. El-Gindy, et al. (1994). "Modelling of the cornering characteristics of tyres on an uneven road: a dynamic version of the 'Neuro-Tyre'." International Journal of Vehicle Design **15**(1 and 2): 189.

Pasterkamp, W. R. and H. B. Pacejka (1997). "The Tyre as a Sensor to Estimate Friction." Vehicle System Dynamics **27**: 409-422.

Press, W. H., B. P. Flannery, et al. (1992). Numerical Recipes in C, Cambridge.

Sakvoor, A. R. "Boundary Conditions on Models for Predicting Tyre to Road Traction." 178-185.

Sano, S., Y. Furukawa, et al. (1986). "Four Wheel Steering System with Rear Wheel Steer Angle Controlled as a Function of Steering Wheel Angle." SAE.

Sato, K., T. Goto, et al. (1998). A Study on a Lane Departure Warning System using a Steering Torque as a Warning Signal. AVEC '98, Nagoya, Japan, Society of Automotive Engineers of Japan.

Savkoor, A. R. (1993). Boundary Conditions on Models for Predicting Tyre to Road Traction. 1st International Colloquium on Tyre Models for Vehicle Dynamics Analysis. H. B. Pacejka, Swets & Zeitlinger Bv. **21:** 178.

Sayers, M. W. and D. Han (1996). "A Generic Multibody Vehicle Model for Simulating Handling and Braking." Vehicle System Dynamics **25**: 599-613.

Schieschke, R. and R. Hiemenz (1993). The Decisive Role the Quality of Tyre Approximation Plays in Vehicle Dynamics Simulations. 1st International Colloquium on Tyre Models for Vehicle Dynamics Analysis. H. B. Pacejka, Swets & Zeitlinger Bv. **21:** 156.

Seok Kang, J., J. Rak Yun, et al. (1997). "Elastokinematic Analysis and Optimization of Suspension Compliance Characteristics." SAE: 87-93.

Shimada, K. and Y. Shibahata (1994). "Comparison of Three Active Chassis Control Methods for Stabilizing Yaw Moments." Society of Automotive Engineers: 87-96.

Smith, M. C. (1995). "Achievable Dynamic Response for Automotive Active Suspensions." Vehicle System Dynamics **24**: 1-33.

Soma, H. and K. Hiramatsu (1995). "Dynamic Identification of Driver-Vehicle System Using AR-Method." Vehicle System Dynamics **24**: 263-282.

Sugai, M., H. Yamaguchi, et al. (1998). New Control Technique for Maximizing Braking Force on Antilock Braking System. AVEC '98, Nagoya, Japan, Society of Automotive Engineers of Japan.

Svendenius, J. and B. Wittenmark (2003). Review of Wheel Modeling and Friction Estimation. Lund, Lund Institute of Technology: 38.

Thomas, D. W., D. J. Segal, et al. (1996). "Analysis and Correlation using Lap Time Simulation-Dodge Stratus for the North American Touring Car Championship." SAE: 145-152.

Unknown (1992). Unknown. Car Design and Technology.

Various (1971). Computer Simulation of Watkins Glen Grand Prix Circuit Performance. New York, Cornell Aeronautical Laboratory, Inc: 24.

Various (1993). Automotive Handbook. Stuttgart, Robert Bosch GmbH.

Venhovens, P. J. T. and K. Naab (1998). Vehicle Dynamics Estimation Using Kalman Filters. AVEC '98, Nagoya, Japan.

Wade Allen, R. and T. J. Rosenthal (1994). "Requirements for Vehicle Dynamics Simulation Models." SAE: 1-20.

Wakamatsu, K., Y. Akuta, et al. (1997). "Adaptive Yaw Rate Feedback 4WS with Tire/Road Friction Coefficient Estimator." Vehicle System Dynamics **27**: 305-326.

Wang, Y., T. Morimoto, et al. (1993). Minimization of Side Slip Angle of Vehicles by Yaw Moment Control. Asia-Pacific Vibration Conference 1993, Kitakyushu.

Watari, A. and S. Iwamoto (1974). "Application of Sensitivity Analysis to Vehicle Dynamics." Vehicle System Dynamics **3**: 1-16.

Weinstock, R. (1974). Calculus of Variations. New York, Dover.

Yeh, T. J. and K. Youcef-Toumi (1998). "Adaptive Control of Nonlinear, Uncertain Systems Using Local Function Estimation." ASME Journal of Dynamic Systems, Measurement and Control **120**: 429-438.

Yoon, Y. S. and Y. G. Cho (1995). "Driver Model of Steering Based on Target Position and Orientation." SAE: 34-38.

Yoshioka, T., T. Adachi, et al. (1998). Application of Sliding-mode Control to Control Vehicle Stability. 4th International Symposium on Advanced Vehicle Control 1998, Nagoya Congress Center, Nagoya Japan.

Yuhara, N., J. Tajima, et al. (1999). "Steer-by-Wire-Oriented Steering System Design: Concept and Examination." Vehicle System Dynamics **33**(1999): 692-703.